Towards Immuno-profiling of Complex Biological Fluids in Patients Recovering from Major Surgery

---

Submitted by Stephanus Bernardus Jansen van Vuuren to the University of Exeter

as a thesis for the degree of Doctor of Philosophy in Biological Sciences

in June 2012

I certify that all material in this thesis which is not my own work has been identified and that no material has previously been submitted and approved for the award of a degree by this or any other University.

Signature: ……..

Dankie

Ma, Pa, Sussie en Dan

Abstract

The conventional biochemical diagnosis of disease using isolated blood biomarkers must be revisited by clinicians, replacing it with a multi-biomarker, personalised profile of human health. A label-free nanoparticle array technology, Liscar, has been developed. It is capable of performing rapid, multi-biomarker assays from complex biological samples which, if employed to assay the Complement cascade of the innate immune system, has the potential for a novel systemic profile of patient health.

An assay for IgG has been developed on the Liscar platform with a detection limit of 380 ± 100 ng/mL IgG in model sera. Furthermore, addition of a chaotropic agent to the complex sample is shown to improve the accuracy of the IgG assay. Competitive binding between nonspecific interfering proteins and specific target analytes (IgG) at the sensor surface is studied, and a quantitative mathematical model is developed to analyse the data, yielding evidence for the active displacement of albumin by IgG-antigen binding.

With a sensitive, accurate multi-biomarker detection platform, a systemic profile of patient health may be possible by examination of the Complement cascade. The Complement system can be activated by a variety of immunological challenges, causing large numbers of activation biomarkers to be produced quickly. Assays for three activation markers, C3d, TCC and Bb are developed, with detection limits of 0.864 ACS Units, 2.32 ng/ml and 54.7 ng/ml respectively.

Complement activation was tested in a prospective cohort study of 45 patients undergoing major abdominal surgery. Patient recovery was monitored from admission to ~60 hours postoperatively by Complement activation and consumption using C3d, TCC, Bb, C3 and C4 as biomarkers. A response profile was obtained for the entire cohort for C3 and C4 assays by normalising with respect to individual analyte levels on admission, against which individual responses are compared. 22% of patients in the study suffered postoperative complications, and 73% showed Complement activation by increased levels of C3d, as expected from the initial trauma of surgery. Expansion of the trial is needed to establish clinical significance and utility, especially in relation to the presymptomatic diagnosis of disease.

Acknowledgements, sincerely

I would like to thank my supervisor, Professor Andrew Shaw, as well as Dr Rouslan Olkhov, Dr Robert Parker and Dr Maxim Rooth for their continuous guidance and support throughout my PhD. This could in *no way ever* have been possible without you. Specific acknowledgement must go to Rouslan for writing the computer program used in Chapter 3 of this thesis, however he also deserves extra special thanks for his saint-like patience and willingness to explain the same things over and over, and over again. Thanks also to Tom Read and Lyndsey Penwill for their unrelenting joyfulness around the lab. Thank you also to Professor Paul Morgan, Dr Claire Harris and Dr Lana Hakobyan – you were exceptionally helpful on everything Complement. Thank you very much, Dr Yvonne Clements, for your help with the MSD instrument, and a huge thank you to all the staff at the RD&E Hospital who were so exceptionally helpful with everything during the CPOP trial.

Thanks very much to Dr Nick Walker for sticking out another 4 years at Exeter with me...

I'd also like to thank a number of people who have excelled in their roles as 'moral supporters' throughout the last four years. It is only because of their never-ending supply of cheer and encouragement that I have been able to get this far. I thank you from the very bottom of my heart. You are all wonderful people.

Tommy England, Michael Taylor, Rich Smith, James Seckel, Steve Humphrey.

Elly Mills, Anna Johns, Josh Stokes, Beth Durkin, Louise Parkin and Ben Hayes.

Emily Timmins, Aaron Summons, Jonny Eccles, Matthew Cuss, Faye Rodwell, Katie Carter, Alex Bramley, Gareth Campbell, Claire Lincoln, Libby Wilding, Becky Fox, Emma O'Hare and Nikki.

Table of Contents

Table of Abbreviations

aBSA	Anti Bovine Serum Albumin
ACS	Activated Complement Serum
AU	Arbitrary Units
BPH	Benign Prostatic Hyperplasia
BSA	Bovine Serum Albumin
C	Complement
C1-INH	C1 Inhibitor
CCD	Charge-coupled Device
CD46	Membrane Cofactor Protein
CPOP	Complement Procedure Outcome Predictor
CRP	C-reactive Protein
DNA	Deoxyribonucleic Acid
ECL	Electrochemiluminescence
EDC	1-ethyl-3-(3-dimethylpropyl)-carboiimide
EDTA	Ethylenediaminetetraacetic Acid
EIA	Enzyme Immunoassay
ELISA	Enzyme-linked Immunosorbent Assay
EWS	Early Warning System
fB	Factor B
FBR	Fibrinogen
fD	Factor D
FDA	US. Food and Drugs Administration
FPLC	Fast Protein Liquid Chromatography
HAIGG	Heat Aggregated IgG
HSA	Human Serum Albumin
IgG	Immunoglobulin G
k_a	Association Rate Constant
k_d	Dissociation Rate Constant
K_D	Affinity Constant
KTS	Knife to skin
LED	Light Emitting Diode
Liscar	Light Scattering Array Reader
MAC	Membrane Attack Complex
MBL	Mannose binding lectin
MCP	Membrane cofactor protein
MHDA	Mercaptohexadecanoic Acid
MSD	Meso Scale Discovery
MW	Molecular weight
NHS	N-hydroxysuccinimide
NICE	National Institute for Health and Clinical Excellence
NSB	Nonspecific Binding
OS	Optical Scaterring
PBS	Phosphate Buffered Saline
PCPT	Prostate Cancer Prevention Trial
PEG	Polyethylene glycol
PSA	Prostate Specific Antigen

R&D	Research and Development
RD&E	Royal Devon and Exeter
RI	Refractive Index
RIU	Refractive Index Units
RU	Response Units
SAM	Self Assembled Monolayer
SC5b-9	Terminal Complement Complex
SD	Standard Deviation
SIRS	Systemic Inflammatory Response Syndrome
SLE	Systemic Lupus Erythematosus
SPR	Surface Plasmon Resonance
TCC	Terminal Complement Complex

Table of Figures

Table of Tables

Chapter 1

Introduction

Conventional biochemical diagnosis of infection requires the detection of an infecting pathogen. An alternative approach could monitor the host's immune response to such a challenge, although its presence in the body may not necessarily lead to symptoms of illness. Most often the host's immune system mounts a response, either by the innate or adaptive immune systems without the need for medical intervention. Undoubtedly, however, the efficacy of each person's response has a different threshold regarding the level of infection required to trigger immunological activation, and the rate of response is a personalised measure of systemic health which could be profiled. Using a panel of biomarkers, such an approach would require a rapid diagnosis of disease, possibly at the point-of-care, coupled with an assessment of the state of a patient's immune system. The results could be combined to determine whether an intervention is necessary, and from the data the clinician could administer a more targeted treatment, based on the type of infection and immune response.

Only with this enhanced differential diagnosis of infection can the significant challenges facing medical science regarding the use and abuse of antibiotics, for example, be addressed. This is applicable not just for herd immunity or strata of patients, but perhaps even for individual patients – truly personalised medicine. There is a vast body of literature regarding the unnecessary intervention with antibiotics with an emphasis on the concern that bacteria are becoming resistant [1; 2]. This places a responsibility on the medical community to develop differential diagnosis methods, coupled with an assessment of the immunological state of the patient so that more targeted treatments can be given only when needed.

What is needed is a companion diagnostic to determine the state of a patient's immune system so that treatments may be prescribed to specifically accompany the body's defence mechanism. Companion diagnostics have been defined by the US. Food and Drugs Administration (FDA) as devices that provide essential information for the safe and effective use of a corresponding therapeutic product [3]. Ideally a companion diagnostic should be available for every disease state to support clinicians in their treatment of patients. Unfortunately, the development of these so-called companion diagnostics is difficult to achieve, and requires the co-operation of governments, funding bodies, pharmaceutical companies, universities and hospitals. It also requires an extended and expensive process that is subject to significant delays. A comparison with the Pharma R&D drug discovery timeline is presented by Pickl *et al* [4], reproduced in Figure 1.1, and displays the complexity of this process against the comparatively well-established progression for drug development. The research into companion diagnostics must be clinician led, with all other auxiliary parties working to facilitate the end point desired by the clinician for a successful clinical trial. If diagnostic tests are to be developed, coupled with immunological assessment, the approach has to be co-ordinated so that all bodies involved are working in harmony.

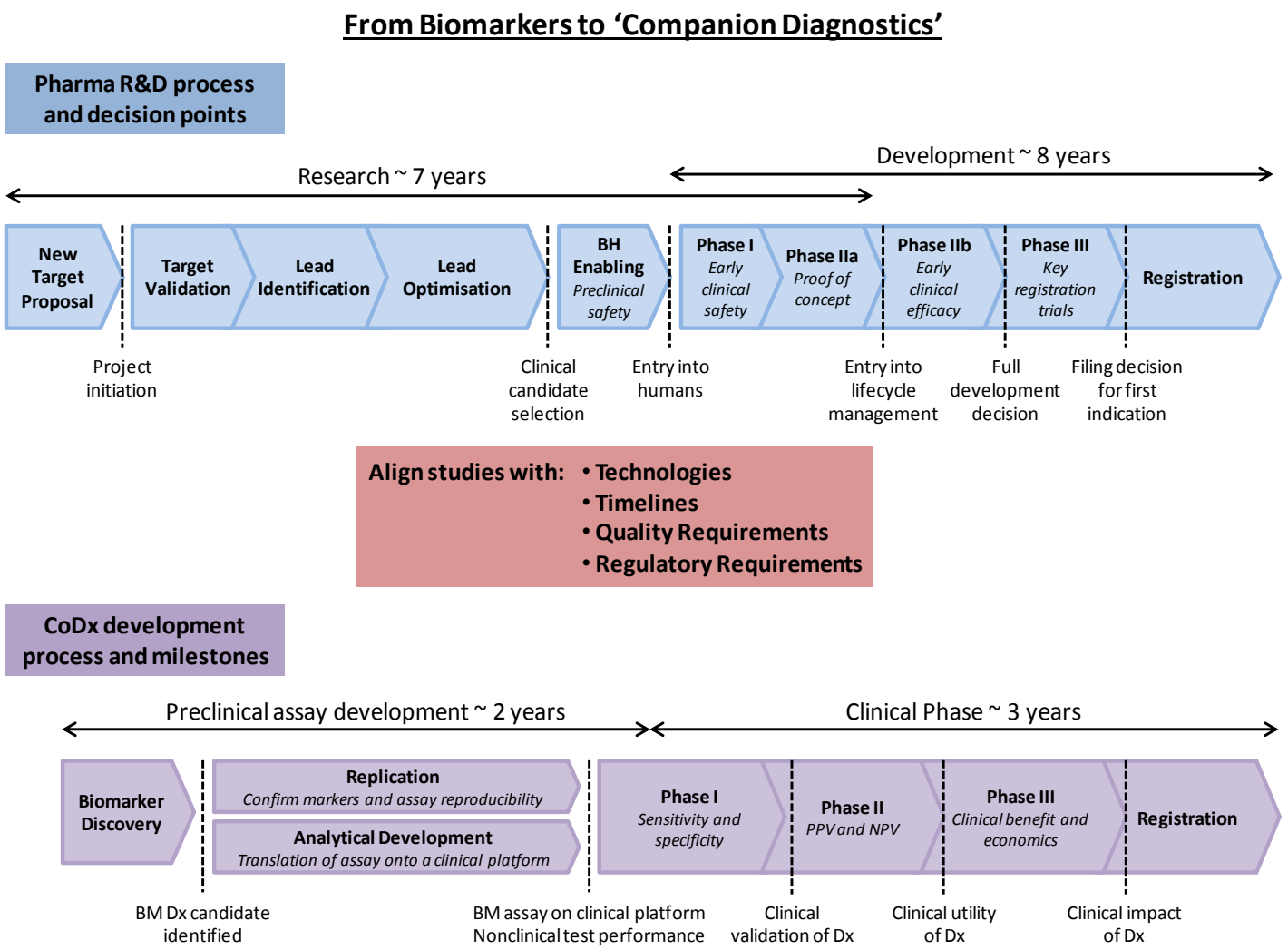

Figure 1.1. Comparison between companion diagnostic development aligned to the Pharma R&D new drug development process. Reproduced with permission from Pickl *et al* [4].

However the situation is not particularly straight forward; as a cautionary tale, the acceptance and clinical utility of the prostate cancer diagnostic, Prostate Specific Antigen (PSA) has been well documented and disputed [5]. It is therefore a good example of the difficulties encountered in the adoption of a companion diagnostic test, and will be considered here. In 1986, the United States Food and Drug Administration (FDA) approved PSA to monitor patients treated for prostate cancer, and in 1994 it became a diagnostic marker in its own right. However the threshold for PSA as a diagnostic of prostate cancer of ≥ 4 ng/ml in blood is heavily criticised, both for being too low and too high [5]. There is concern that this threshold has led to many diagnoses of prostate cancer in patients where their cancer may never have affected their lives had they not gone for the PSA test. It is sometimes argued that this 'low' threshold of PSA for diagnosis increases the test's sensitivity at the expense of its specificity, however, it has also been shown that prostate cancer is not that rare in patients with PSA levels <4ng/ml. Clinically, the 'positive' results from the test initiated a process whereby doctors make a decision based on a range of qualitative factors, whilst considering the level of PSA.

A large European study found prostate cancer in 21-25% of patients with PSA levels between 2-2.99ng/ml, and in 33% of patients with PSA in the range 3-3.99ng/ml [6]. Appropriately, recent thinking has concluded that a single cut-off for PSA is inappropriate, and that the number should be considered along with a range of other factors including race, age and hereditary presence of the disease, as done by the Prostate Cancer Prevention Trial (PCPT) calculator which can be found online [7]. A validation of the PCPT calculator was performed by Parekh *et al,* who found that the PCPT calculator produced an area under its receiver operating characteristic (ROC) curve of 65.5%, and even greater for African-American men at 80.0% [8]. However, given that this study compared a PSA-only analysis which gave an area under the ROC curve of 64%, the average result for the PCPT calculator is not significantly better, unless the patient is an African-American man. This gives some idea about the different, stratified

diagnosis approach that is becoming more commonplace, and is pointing the way to personalised medicine in the future.

Personalised medicine attempts to make a patient-specific diagnosis and treatment regimen taking into account all comorbidities, phenotype and genotype, prescribing patients with the right drug at the right time at the right dose: the next frontier in patient care. It is largely dominated by diagnosing and treating disease on the basis of genetic variations that have been found to contribute to human illness. Extending the genotype to the phenotype of a patient's systemic health, we postulate that the relationship between infecting disease and host immunity can also act as a personal marker for disease, and therefore treatments prescribed from such a diagnosis can also be tailored for the individual. Companion diagnostic tests can be developed to aid the clinician, either from a laboratory test or at the point-of-care. The logistics of performing the diagnostic test is dependent on a number of factors such as the nature of the sample being tested, the state of the patient and assay equipment mobility. Therefore it is important to involve the clinician on the development of such tests, so as to direct the development of the test to maximise clinical utility.

It is also possible that a panel of assays could be used as a single diagnostic test, such as interconnected proteins that form part of a biological system. An example of such a 'multivariate index assay' is OVA1, an FDA-approved panel assay consisting of 5 biomarkers and an algorithm [9] to help evaluate ovarian masses for the likelihood of cancer preoperatively. Development of such tests are likely to produce 'diagnostic values' from an algorithm based on a variety of data from each contributing assay and demographics, rather than absolute protein values. It is important that any complex analysis steps are removed, so that the factors contributing to the 'diagnostic value' can be entered and calculated by a computer, much like the online PSA calculator described above. It would therefore be

desirable to have a technology that would allow the screening of multiple biomarkers at the point-of-care, in order for clinicians to have such information readily available.

In light of these considerations, this thesis will focus on developing detection methods and high-throughput screening of blood biomarkers using optical techniques, namely Surface Plasmon Resonance (SPR), Optical Scattering (OS) and Electrochemiluminescence (ECL) to establish the feasibility of immune system profiling by measuring plasma proteins to observe the response of the Complement (C) cascade to the surgical trauma of major surgery. Thus, this thesis will ultimately investigate a well defined challenge to the immune system; the surgical insult and trauma following major abdominal surgery, and the recovery of the patient postoperatively.

Here, four key factors relating to biomarker detection from real samples are considered with a view to employing the biomarker for patient-health monitoring. The study performed in this thesis deals with the issue in two parts, first focusing on the general issues presented by real sample complexity for biomarker detection and analysis of label-free protein-protein binding studies from real biological samples. The second part of the thesis aims to develop immunologic biomarkers and implement those markers in a clinical trial to monitor patient recovery postoperatively. Specific focus will be on the kinetics of antibody-antigen interactions, the effect of nonspecific binding (NSB) on these interactions and ways to reduce the effects, and the Complement system, specifically its utility for monitoring the immunological state of the patient.

This Chapter will introduce each of the topics mentioned above, and elaborate on any techniques employed in the study, such as SPR, OS, and ECL. The C System will also be introduced, as it becomes the focus for the second part of the thesis for biomarker development and implementation. Finally, the assessment of a biomarker for diagnosis will be a discussed.

1.1 Biomarker Detection Techniques

Philipp Angenendt, from the German Cancer Research Center, has written that "the wide variety of different applications in which protein microarrays are employed … underlines the urgent need for technologies that are capable of high-throughput analysis of proteins and antibodies" [10]. Clearly there is also a very high commercial interest in such technologies. It is for these reasons that a great range of techniques have been employed to reach this common goal, including ELISA (enzyme-linked immunosorbent assay), immunoturbidimetric assays and ECL assays. Label-free SPR platforms have been commercialised and have been employed very successfully in detecting antibodies and antigens in simple buffer samples [11; 12]. Attempts have also been made to screen analytes from complex samples like whole serum [13], but with less success due to the problems posed by dealing with real biological samples.

1.1.1 Label-Free Biosensors

Surface Plasmon Resonance

The leaders in the field of label-free sensor technologies [14; 15; 16] are those based on continuous surface or particle plasmons. SPR is an optical phenomenon that permits the measurement of biomolecular interactions. SPR is observed when an incident beam of *p*-polarised light of a given wavelength strikes a thin metal surface at a given angle (the SPR angle) through a prism as shown by the Kretschmann configuration, Figure 1.2.

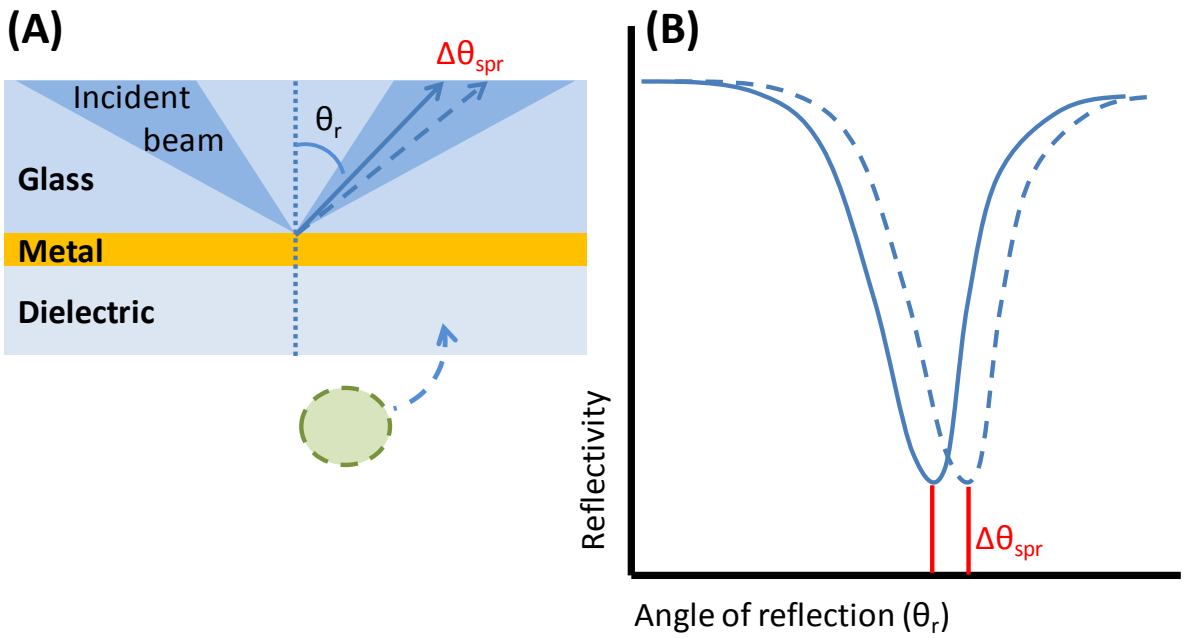

Figure 1.2. The Kretschmann configuration (A) of SPR, with the origin of the signal illustrated schematically (A) and (B).

The SPR angle is greater than the critical angle, but instead of complete total internal reflection, some of the energy is lost to the metal-dielectric interface exciting the surface plasmon, thereby causing a drop in reflectivity of the incident beam, with minimum reflectivity at the SPR angle (θ_{spr}). The local conditions at the metal-dielectric interface (for example RI) determine the SPR angle, and therefore any change in these properties will cause the angle to shift, $\Delta\theta_{spr}$, Figure 1.2.

Surface plasmons are waves that propagate along the interface between a conducting metal and a dielectric material. The plasmon resonance wave propagates parallel to the metal-dielectric interface [17; 18], the intensity of its associated optical electric field decaying exponentially with increasing distance from the metal surface [19]. The distance at which the intensity of the plasmon field decays to 1/e of its value at the interface is called the penetration depth. This plasmon field allows for the investigation of properties (crucially refractive index) of the medium up to approximately 200-300 nm [17; 20] away from the surface.

This property can be utilised in different ways by SPR sensors. The angle of incidence can be fixed in order to measure the change in resonant wavelength associated with ΔRI of the medium above the metal surface. Conversely, with fixed wavelength of the incoming light, a detector can monitor the SPR angle as the minimum in reflected light intensity profile, as done by SensiQ (Nomadics) and Biacore (Biacore AB) instruments. According to the equation:

$$\Delta\theta(\lambda) = c1\Delta n + c2\Delta d$$

Equation 1.1

the constants $c1$ and $c2$ relate the SPR angle at a given wavelength λ to the change in refractive index n at the surface and the change in thickness d of the surface layer [18]. The mass of biomolecules landing on the surface changes the local refractive index (RI) within the plasmon field from water (RI = 1.33 [21]) to protein (RI = 1.36-1.55 [22]), signifying that SPR sensor is a mass sensing device. This change alters the SPR angle, which is detected and generates the signal. In order for the sensor to be considered a biosensor, the surface must first be functionalised with a surface ligand, against which specific interactions with biomolecules can be observed.

The applications of conventional SPR are numerous and wide reaching. It is an excellent tool for evaluating macromolecules, equilibrium measurements, protein-protein kinetic analysis, and interrogation of mutant proteins. Studying small analytes can be problematic due to their small contribution to layer thickness on the sensor surface. The majority of existing platforms also have limitations for high throughput assays, as they provide only dual channel analysis, allowing for the interrogation of single protein-protein interactions only. However, more recent instruments such as the Biacore Flexchip does have label-free high throughput screening capabilities [23] [11], which further strengthens its viability as a biosensor.

Optical Scattering using Gold Nanoparticles

Optical scattering can also be used for the detection of biomolecules by the same principle of sensing ΔRI, generally employing nanoparticles in an array format. Such nanoparticle based biosensors are being developed to provide label-free, high throughput screening of biomarkers, using kinetic parameters as in conventional SPR to quantify target analytes in a given sample [24]. Noble metal nanoparticles exhibit a strong optical extinction in the visible region of the electromagnetic spectrum, which occurs when the incident photon frequency is in resonance with a localised surface plasmon mode in the conduction band of the nanoparticles. There is both a scatter and absorption element to the optical extinction displayed by the nanoparticles, however when the particles have a diameter >25 nm the scattering part dominates [24], allowing a photo camera to detect it. The size, shape and composition of the nanoparticles determine their optical properties, and therefore these can be altered and optimised by various nanoparticle production techniques. These optical properties can change in response to localised, biochemical binding events within the plasmon field of the particle, which normally penetrates ~20nm. This can be compared with a penetration depth of ~200-300 nm in conventional, continuous surface SPR [17; 20].

The implications of the difference in penetration depth between the two techniques are very important in terms of nonspecific binding. As the interaction of interest (protein-protein binding) happens on the continuous gold or nanoparticle surface, it is unnecessary, and even disadvantageous to have a sensor that probes well beyond the space in which this interaction takes place. In 'clean' experiments, where the sample contains one analyte only, this is not a problem, but for complex biological fluids or multi-analyte samples it can pose real difficulties. The greater sensing range of the continuous surface setup means that it is susceptible to large amounts of background noise caused by nonspecific constituents in a complex sample. The signal obtained is therefore largely dominated by nonspecific proteins entering the plasmon

field, whether binding to the surface or not, and therefore affects the interaction of interest. As the nanoparticle plasmon propagation distance is over ten times less than with continuous surface plasmons, it is far less susceptible to this passing, nonspecific protein noise, and therefore the signal obtained is more attributable to the specific interaction studied.

1.1.2 Chemically Labelled Biosensors

Enzyme Linked Immunosorbent Assay (ELISA)

The general ELISA principle was invented by Engvall and Perlmann [25] as an alternative to immunofluorescence and radioimmunoassay. They linked antibodies with enzymes, rather than fluorescent markers or isotopes. The principle was that a chromogenic of fluorogenic substrate could be degraded by the enzyme, yielding an amplification factor by way of colour change which enabled sensitive and accurate detection of the enzyme, and therefore also the antibody it is linked to.

There are several variations to the general ELISA technique, three of which will be detailed here. Firstly, the competitive ELISA test for a target antigen. Two tests are run in tandem, one where a known sample of the antigen plus unknown antigen sample is labelled with an enzyme and allowed to bind to antibody immobilised in the solid phase. The addition of substrate allows a comparison between the two tests, the offset in signal being attributed to the unknown antigen sample.

Secondly, the indirect method involves the passive absorption of antigen onto the solid phase, followed by the incubation of test sera containing the antibody to allow antibody-antigen binding. Washing then removes any unreacted serum components, after which an antiglobulin enzyme conjugate is added and incubated, allowing the antiglobulin to bind to the antibody-antigen complex. Finally, after washing, the enzyme substrate is added and produces a colour change which measures the amount of fixed conjugate, which is proportional to the amount of antibody in the test sample.

Finally, there is also the double antibody 'sandwich' technique. The solid phase is coated with antibody, which is then reacted with the test sample and binds any of its respective antigen present in the sample. After washing to remove excess sample constituents, an enzyme labelled antibody is added (called the reporter antibody), also specific to the target antigen. After further washing, the substrate is added producing a colour change proportional to the amount of reporter antibody present, and therefore the amount of antigen.

Electrochemiluminescence Assays

Electrochemiluminescence (ECL) involves the emission of light by a species that has taken part in an electron transfer reaction at an electrode surface [26]. When a voltage is applied to an electrode where an ECL luminophore such as $Ru(bpy)_3^{2+}$ (bpy = 2,2'-bipyridine) is present, light is emitted and collected on a very sensitive CCD camera which produces an ECL assay with very low detection limits for a target analyte ($\leq 10^{-13}$M) [27]. Therefore, ECL is a technique whereby radiative energy is produced from electrical energy by means of light emitting reactive intermediates from stable precursors at the surface of an electrode once a voltage is applied. In the excited state formed by the ECL reaction, an electron moves from the metal based $d\pi$ orbitals to ligand-based π^* orbitals, known as a metal-to-ligand charge-transfer (MLCT) transition [26]. After excitation, the electron undergoes intersystem crossing to the lowest state of the complex, from where fluorescence emission occurs [26]. The fluorescence intensity is then proportional to the ECL luminophore concentration, from which a calibration curve can be constructed for the quantification of analyte concentrations in samples.

ECL has been employed extensively in immunoassays and DNA analyses by using an ECL-active species as a label on biomolecules [27; 28; 29]. The high sensitivity of the assay and the use of CCD cameras allows ECL assays to be employed in the multi-well plate format with specific assays localised to each well. The technique's high sensitivity and selectivity has suited it well to commercial application, where various systems have been developed to detect a range of

important analytes. The Meso Scale Discovey (MSD) platform is one commercial implementation [30; 31]. MSD sell commercial assays for cytokines exploiting the unique sensitivity (~10 pM) and this platform is used extensively in biomarker detection in the research laboratory [32; 33]. It is not qualified for clinical practice, but its sensitivity and multiplex assay capabilities make it an attractive tool for use in high throughput sample testing [34; 35]

Practically, ELISA and ECL techniques are very similar, as the only difference of note is the label on the reporter antibody. Therefore conventional sandwich assays can also be performed by ECL, whereby an immobilised capture antibody fixes the target antigen, after which the labelled reporter antibody can bind to the analyte, generating the signal when a voltage is applied across the solid phase.

1.1.3 Other Labelled Detection Techniques

Immunoturbidimetric Assays

Immunoturbidimetric assays rely on the reduction of scattered light owing to aggregation of latex particles in suspension [36; 37]. The latex particles are functionalised with antibody, and in the presence of antigen aggregation is caused by the formation of antibody-antigen immune complexes. This aggregation increases the optical opacity of the suspension and reduces the amount of light that can travel through the suspension, and therefore the greater the concentration of antigen in a sample, the greater the aggregation. It is a simple technique that has been automated for high throughput screening of biomarkers, and has found application in clinical chemistry laboratories for CRP, C3, and C4 [38], used later in this thesis.

1.2 Handling Complex Biological Samples

Although many clinical assays have been developed to screen for biomarkers from biological samples, they have largely been limited to Immunoturbidimetric and ELISA. Nonspecific interference on the sensor by background proteins present in the sample is the single biggest

challenge to overcome if many of the detection platforms available, especially SPR, are to be employed successfully in a clinical setting.

Investigators in the field have devised a variety of solutions to the problems posed by nonspecific binding, focussing their efforts on adjusting both the detection platform sensor surface and the samples. Special surface chemistries have been developed for SPR platforms, and the addition of products to samples, such as the surfactant Tween 20, has become commonplace for SPR, OS, ECL and ELISA. In this section we explore some of the techniques used to screen biomarkers in biological samples, and then investigate some of the auxiliary techniques developed that deal with real biological sample complexity.

1.2.1 Surface Chemistry Development

The current gold standard for SPR sensor surfaces is the widely used[1] Biacore CM5 chip, which employs a carboxymethylated dextran surface on which ligands can be covalently immobilised by EDC/NHS[2] coupling chemistry. Carboxylic groups on the dextran surface react (first with EDC, then NHS) to form a semi stable NHS-ester, which can react with free amine groups on incoming proteins, forming an amide bond which covalently binds the protein to the surface. The CM5 chip allows for greater surface loading due to the three dimensional structure of the dextran layer. Proteins can diffuse through and into the layer, allowing for a greater density of molecules to be absorbed onto the surface. Finally, the CM5 chip also offers resistance to nonspecific binding due to its hydrophilicity. This combination of properties has made it the most widely used sensing chip for SPR studies worldwide.

Therefore efforts to reduce the effect of nonspecific binding have focussed on creating relatively inert hydrophilic sensor surfaces [39] that create a suitable environment for biomolecular reactions, similar to that of the CM5 chip.

[1] The current author estimates that there have been over 500 papers reporting work with the Biacore CM5 chip published in the first 6 months of 2012 alone.
[2] EDC = 1-ethyl-3-(3-dimethylpropyl)-carboiimide, NHS = N-hydroxysuccinimide

1.2.2 Sample Preparation Protocols

Ideally a diagnostic assay should be performed with minimum sample preparation, however the effect of nonspecific binding has forced many investigators to develop pre-treatment methods for biological samples so as to reduce the effect of nonspecific binding on the assay. Most simply, some studies have diluted the samples [40; 41] in order to reduce the concentration of nonspecific constituents in the sample. Obviously, this also reduces the concentration of the analyte present in the sample, and therefore it is an unsuitable method for use with analytes that are already low in concentration, such as the cytokines [42].

Some researchers have also shown that nonspecific binding could be reduced by heating the sample (serum) at 56^{o}C for 30 minutes [43]. Although this method is successful for reducing some of the effect of nonspecific binding (referred to as the 'Ingredients Effect' [43]), it is not a practically plausible solution in a clinical environment, and has obvious denaturation implications for the target analyte. The addition of some other ingredient to the sample that limits nonspecific binding would be preferred, as the time consumed by such a step would be negligible compared to a 30-minute heating step.

One such proposed ingredient is the chaotropic anion, thiocyanate (SCN^-). It has been reported that a final concentration in the sample of 100 mM thiocyante can eradicate any signal caused by nonspecific albumin interference [7]. It was demonstrated by the same principal investigator that thiocynate can also disrupt the interactions between living cells and macromolecules [44]. Thiocynate, a relatively large anion, has a very large entropy of hydration [45], and is therefore thought to modulate the structure of water surrounding macromolecules, and therefore disrupts the nonpolar effects that underpin protein-protein interactions. This allows the protein-specific interactions of antibodies and antigens to dominate over the general, nonspecific interactions between proteins.

1.2.3 Kinetic Analysis of Label-free, Protein-Protein Binding Studies

To obtain biologically meaningful data from label-free binding studies, the data must be analysed to extract kinetic rate constants, thereby allowing the determination of an unknown concentration of an analyte in a sample, or protein-protein binding interaction energies. This is needed for SPR to become clinically useful, so as to specifically determine the concentration of a biomarker in a given sample, and not just to determine whether it is present or not. The current standard for data analysis of kinetic binding studies using SPR is the 1:1 interaction model [46; 47], whereby a finite number of binding sites on the surface become occupied singly by individual analyte molecules without interaction between species on the surface. This model is acceptable for simple binding studies of protein pairs where there are no other species present, but the presence of high concentrations of nonspecific background proteins in real biological samples requires this model to be altered, as it no longer becomes an accurate description of the processes taking place.

The 1:1 adsorption model is the simplest adsorption isotherm, and is based on three assumptions. Firstly, the adsorption cannot exceed a monolayer. Secondly, the binding surface is uniform and all sites on it are equivalent. Finally, the occupation of neighbouring sites does not affect a given molecule's ability to adsorb to a particular site. The nonspecific proteins will undoubtedly have some effect on the specific binding interaction, and therefore the use of this model for complex sample analysis is unsuitable.

It is clear that if SPR is to become a successful biomarker detection platform from real biological samples, a different analytical approach is needed to take account of sample complexity, along with surface chemistry and sample handling developments.

1.3 Detecting Biomarkers in Clinical Samples: Monitoring Biological Systems

The primary function of biomarkers is to assist in the diagnosis of disease – to evaluate organ damage or dysfunction, or to monitor the state of progression of a disease and the

effectiveness of prescribed treatments. Biomarkers have been defined as 'molecules that indicate an alteration in physiology from normal' [48], and thus they can be used as companion diagnostics for certain physiological alterations. Trull *et al.* [49] have written that:

> *"a diagnostic test is one element of a process which begins with a clinical question; the ideal test is one which provides an unequivocal answer to the question and enables a decision to be made on what action must be taken next."*

Unfortunately no perfect biomarker exists; one which can provide an undisputed answer about a particular disease or immunological state, as evidenced by the prostate cancer biomarker, PSA, above. All biomarkers assays have a limited diagnostic performance, which should be taken into account by the clinician, who will use the test results as supporting evidence only as part of his ongoing investigation. The majority of biomarkers are single proteins, their abundance or deficiency signalling for a particular disease state or organ dysfunction. For example, there is a wealth of biomarkers available for the determination of kidney dysfunction and renal disease (creatinine, urea, urate, cystatin C), however they can all be influenced by a variety of factors including muscle mass, diet and tubular secretion. Could it be possible to treat an entire biological system as a biomarker instead of using single proteins, and in doing so negate much of the variability throughout a population for a single protein biomarker? Additionally, would such an approach also enable the biomarker development process to require a smaller number of patients in clinical trials? The premise is that, compared with individual protein biomarkers that can fluctuate immensely from patient to patient, the constituents of a biological system are interrelated, so although individual concentrations may differ, these relationships may remain more constant for a particular state of a biological system.

In terms on infection and immunity, several such biological systems exist; the activation of T-cells by cytokines, the acute phase response, blood clotting, and the C system, which will be the immunological system interrogated in this study.

1.3.1 The Complement System

The C system is a defence mechanism that is part of the innate mammalian immune system. It is comprised of over 30 plasma and cell surface proteins that form part of a 'cascade system', whereby the components activate one another in series [50]. The cascade can be activated by three effector pathways by antibody-antigen immune complexes, microbial cell surfaces and lectins. The primary aim of the C system is to cause cell lysis by formation of the membrane attack complex (MAC) [50], however it also has the secondary functions of inflammation [51] and opsonisation for phagocytosis [51]. Thus determination of C activation may imply a host response to an immunological challenge, such as a bacterial infection. The C cascade will be explored in more detail below, along with an introduction to its regulators.

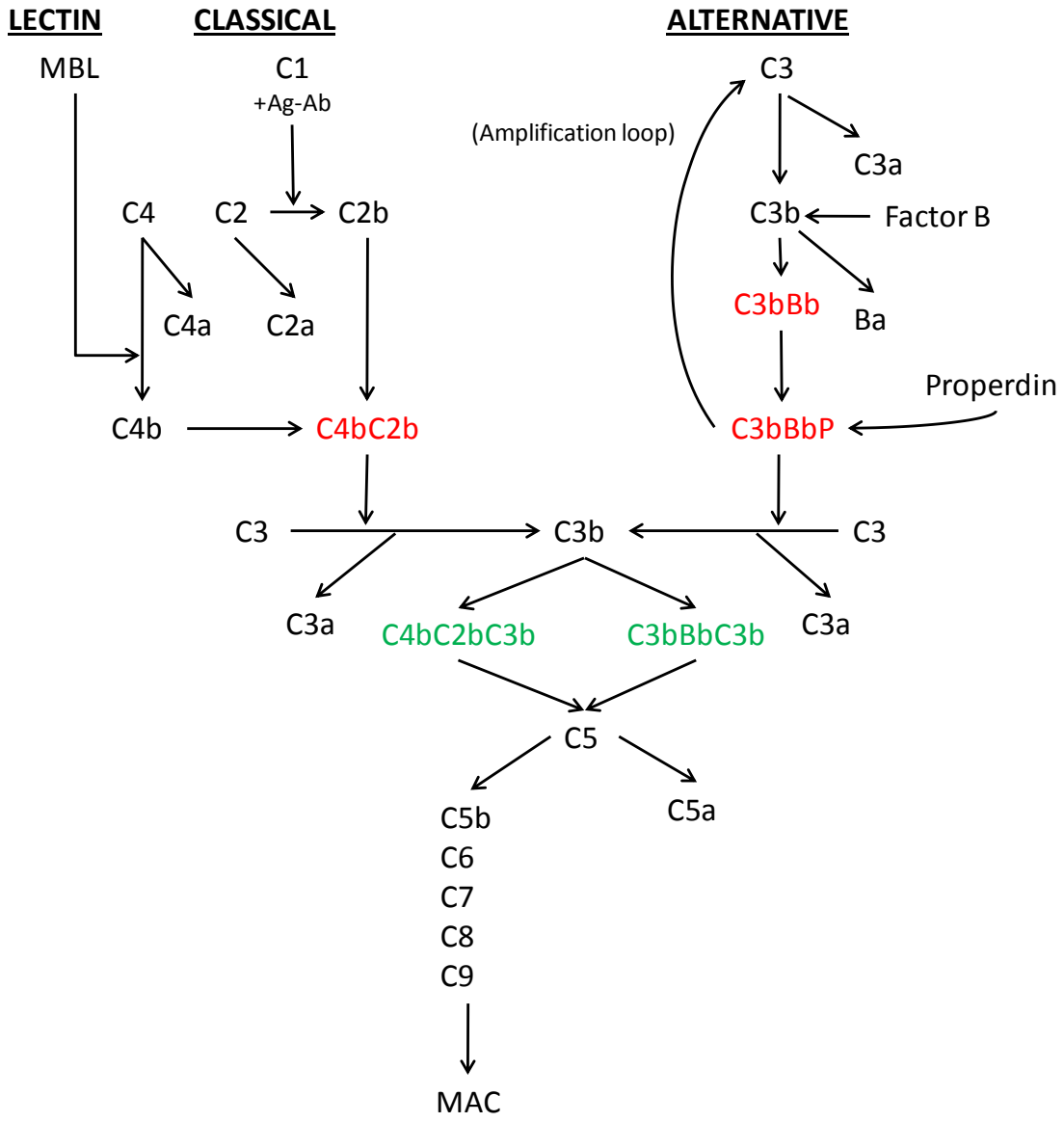

Figure 1.3. The C cascade, showing the three upper cascade pathways leading to the terminal pathway and ultimately MAC formation.

The Complement Cascade

The entire C cascade consists of three initiating pathways that lead to a fourth, lytic or terminal pathway. It is an enzymatic cascade based on positive feedback, and therefore once triggered it can be activated rapidly, quickly producing very large quantities of C activation products [52].

The Classical pathway, so-called because it was the first pathway discovered, is primarily triggered by antibody complexes formed from the interaction between antibodies and their

respective antigens [52]. The antibody-antigen complex creates a binding site for C1, a macromolecular component comprised of two C1r molecules, two C1s molecules, and one molecule of C1q, on which the binding site for the interaction with the antibody-antigen complex is found [53; 54]. The binding of C1q to the antibody-antigen complex causes a conformational change in C1r which then activates C1s [55; 56].

Before continuing, it should be noted here that the nomenclature for C components is determined by their order of discovery, and therefore the numerical sequence assigned to proteins does not follow the order of interactions. Also, in line with recent rationalisation of the nomenclature in the literature [57] regarding the C2 fragments, C2a and C2b, this investigation refers to the larger, protease fragment as C2b, and the smaller, nonproteolytic fragment as C2a by analogy with C3, C4 and C5 fragments.

Returning to the Classical pathway, the activated C1s cleaves C4 into C4a and C4b, the latter then binding to C2 before it is also cleaved by C1s into C2a and C2b. These reactions produce the Classical pathway C3 convertase, C4bC2b. This convertase can cleave C3 into C3a and C3b, the latter fragment initiating the amplification loop (discussed below), producing yet more C3b. The increased density of surface-deposited C3b gradually leads to a second convertase, C4dC2bC3b, which is the Classical pathway C5 convertase and initiates the Lytic pathway by cleaving C5 into C5b, the first molecule in the sequence to MAC formation, and C5a, a powerful anaphylatoxin [57; 58].

The Lectin pathway, an antibody-independent activation runs adjacent to the first part of the Classical pathway. This pathway is initiated by the Mannose Binding Lectin (MBL) which binds to mannose or N-acetyl glucosamine on the surface of micro-organisms. This binding event activates MBL-associated serine proteases (MASP), which in turn cleave C4 and C2 into their respective fragments. Following these cleavages the pathway continues as in the Classical pathway.

The third C activation pathway, the Alternative pathway, is another antibody-independent pathway that is activated by the presence of foreign surfaces. The Alternative pathway may be considered as two sub-pathways; the 'tick over' process and the amplification loop. It is commonly triggered by substances on microbial cell walls, especially molecules with repeating units, for example lipopolysaccharide or techoic acid, found in the cell walls of gram negative and gram positive bacteria respectively [59; 60]. The Alternative pathway is on constant standby, in a low-level activation state, said to 'tick over' slowly at cell surfaces. This 'tick over' process involves the spontaneous hydrolysis of a small fraction of C3 molecules into $C3_{H2O}$. The factor B (fB) protease then binds to $C3_{H2O}$ [57] (which has many of the properties of C3b), and the bound fB is cleaved enzymatically by Factor D (fD), generating an initial, soluble C3 convertase $C3_{H2O}Bb$ (here called the 'tick over' C3 convertase, as it is generated during 'tick-over' activation and not during the amplification loop) that can activate C by cleaving C3 into C3a and C3b.

It is this that allows for the enormous amplification potential of the alternative pathway, as upon cleavage of C3 a short-lived thioester moiety in C3b becomes exposed which can covalently attach to amine and carbohydrate groups on a foreign surface. The amplification continues uninterrupted on foreign cells, and is regulated on host cells, so as to not self harm. If foreign cells are not present, the C3b will be hydrolysed and the 'tick over' process will continue. However, if C3b does come into contact with an attacking micro-organism, the Alternative pathway can be amplified by the binding of C3b to fB, which is once again enzymatically cleaved by fD, yielding the Alternative pathway C3 convertase C3bBb. This convertase can be further stabilised by Properdin (C3bBbP) to prolong its activity. As in the Classical pathway, further deposition and gradual binding of C3b to this C3 convertase produces the C5 convertase C3bBbC3b, which can cleave C5 into C5a and C5b, initiating the Lytic pathway.

The Lytic, or terminal C pathway is the final part of the C cascade, and culminates in the production of the Terminal Complement Complex (TCC), also known as C5b-9_n or MAC. In terms of host defence, TCC is assembled at the surface of the target cell after C5b associates with C6 and C7, the intermediate complex inserting itself into the cell wall. Once inserted further association with C8 and several molecules of C9 forms a lytic pore, through which cell lysis can occur. The nomenclature for the soluble form of TCC is SC5b-9 [61], which is formed when the formation of TCC is intercepted by S Protein binding to the C5b-7 [62] complex before it is inserted. The assembly of soluble TCC continues, however the lytic functionality of the protein is lost.

Regulation of Complement

Effective regulation of C is imperative to avoid the C system attacking the host's own cells. Several proteases in the Classical and Lectin pathways are regulated by C1 esterase inhibitor (C1-INH), as well as two additional Lectin pathway modulators namely sMAP and MAP-1, both nonproteolytic splice products of the *MASP2* and *MASP1/3* genes respectively. These regulators seem to compete with MASPs for binding to MBL and ficolins. In-solution activation of the Alternative pathway is regulated by Factor H (fH) [57], which acts mainly on C3 by competitively removing Bb from C3bBb, or by acting as a cofactor to Factor I (fI) [57] in the degradation of C3b. A similar regulator, C4-binding protein (C4BP) is found in the Classical pathway, which has analogous effects on the Classical pathway convertases. Crucially fH and C4BP also contribute to self recognition by engaging in host-specific surface patterns such as sialic acid or glycosaminoglycans.

In self defence, most human cells also present C convertase regulators that act as cofactors for fI, such as CR1 and membrane cofactor protein (MCP or CD46), or as decay accelerators, such as CR1 or decay-accelerating factor (DAF, or CD55). The anaphylatoxins C3a and C5a are also

regulated by carboxypeptidase-N, which quickly converts both molecules into their respective desarginated forms.

Complement System Utility

The multiple activation pathways and cascade kinetics suggest that the C system may be used to detect indirectly an immune system challenge by monitoring its level of activity. During 'tick over', concentrations of C activation fragments will be low compared with when it is activated. Therefore, detection of high concentrations of these markers will indicate a C response, and if pathway specific activation could be determined, it might lead to the differential diagnosis of disease based on what is known about the specific triggers of each pathway. If C fragments could be detected in blood or urine samples, it could provide useful biochemical information to a clinician for assessment of a patient's immunological state, which may lead to better disease diagnosis and patient care.

1.4 Assessing Biomarkers for Diagnosis

In order to use a complex mechanism such as the C system as a diagnostic biomarker, whatever metric calculated to determine a particular diagnosis (as with OVA1 above) will still need to pass the same rigorous statistical tests to determine its validity as a good biomarker. In light of this, consideration should be given to the question of what makes a good diagnostic biomarker, and how it becomes a statistically acceptable companion diagnostic.

C-Reactive Protein (CRP) is an extensively assayed biomarker in hospital laboratory blood tests, and is a marker for the acute phase response. CRP is indicative of inflammation and is triggered by cytokines, part of the innate mammalian immune system. It is a pentraxin protein with a variety of well known functions [63] – it binds to the C polysaccharide of some streptococcal cell walls, promotes phagocytosis and is believed to activate C through the Classical pathway. As a result of this it has been described by some as a 'primitive antibody molecule' [64]. CRP is a useful biomarker in that it varies over three orders of magnitude in concentration during

activation, returning to its initial value when the acute phase response ends. Its concentration can range from an average of 0.8mg/L to >500 mg/L [63] during a severe acute phase response, for example inflammation after severe tissue damage as a result of surgery [65; 66]. This means that it is easy to distinguish CRP levels between healthy individuals and individuals undergoing an acute phase response to an immunological challenge. General elevated levels of CRP are also seen in individuals with rheumatoid arthritis [67] and SLE [68].

CRP is therefore a general marker for the acute phase response, but elevated systemic levels are also seen for certain permanent conditions. Attention should be given here to the mechanism of the acute phase response, and its helpfulness in providing such diagnostic markers. The acute phase response is a systemic, nonspecific physiological and biochemical response 'to most forms of tissue damage, infection, inflammation and malignant neoplasia.' [63]. The initial trigger of the acute phase response may be localised, but the cytokines that originate at the site of pathology triggers further protein synthesis and the wider acute phase response. After a single stimulus, such as a surgical insult, CRP is synthesised rapidly, and reaches a peak after approximately 48 hours, after which it is cleared with a half-life of ~19 hours for both healthy and diseased individuals [63]. The use of CRP for subsequent patient monitoring following the single stimulus event is problematic, as a prolonged synthesis process produces elevated CRP levels long after the event that caused it happened. Therefore any further stimulating event, such as a bacterial infection, would be masked by the initial CRP production for a significant period of time.

However it is not only CRP that poses problems for diagnosis. Often single biomarkers are not enough for a clinician to make a confident, evidence-based diagnosis. This is the case with Prostate Specific Antigen (PSA), introduced above. PSA acts as an indicator of tumour growth, specifically prostate cancer [5], however it can also suggest benign conditions such as prostatitis [69] (inflammation of the prostate gland) or benign prostatic hyperplasia (BPH) [70].

PSA is produced in the prostate gland, and is normally present at low levels in healthy men. Elevated levels of the protein cannot distinguish between cancer and benign conditions, however the level of PSA concentration in the blood is considered by the clinician when ordering further examination. The lower limit for cancer diagnosis based on PSA level was altered after a study in 2004 by Thompson *et al* [71]. Previously PSA levels below 4ng/mL were considered normal, however in this study prostate cancer was diagnosed in 15.2% of men with a PSA level below 4ng/mL. Furthermore, in 15% of these men, (2.3% overall) had high grade cancers.

By contrast, another routinely used biomarker is Troponin I for the diagnosis of acute myocardial infarction [72], as well as a range of other cardiac-related diseases such as chronic ischemic heart disease [73] and unstable angina [74]. A helpful contrast can be drawn with Troponin T which is also used to help diagnose acute myocardial infarction [72]. It has a 94% sensitivity towards myocardial infarction, however it has a lower specificity relating to this disease than Troponin I. This illustrates two key requirements for a good biomarker; sensitivity and specificity, and in the case of PSA, sensible cut-offs for these requirements. By contrast, total PSA has 60% specificity and 70% sensitivity for the diagnosis of prostate cancer [75].

Sensitivity and Specificity

The sensitivity of a given biomarker in relation to its predictive value is defined as the proportion of true positives correctly identified as such whereas the specificity of a biomarker is defined as the proportion of true negatives it correctly predicted as such [76; 77]. The number for sensitivity of a given biomarker is obtained by dividing the number of true positives by the number of true positives plus the number of false negatives. In the case of disease diagnosis, this therefore translates as the probability of a positive result given that the patient is in fact ill. It is not the quality of the assay for the biomarker, but rather the immune response that will dictate whether this parameter renders an assay useful or not. If, for a given

target analyte, the immune response to a particular compromise drastically changes the level of the analyte (as is the case with CRP), then the biomarker has a better chance of being sufficiently sensitive, as distribution of CRP concentrations between healthy and inflamed patients will vary greatly. If, on the other hand, the levels of an analyte are barely different between healthy and diseased individuals, it is unlikely that the marker will ever succeed as a clinical biomarker for disease, as it will not be able to discriminate between healthy and diseased. The number for specificity can be obtained by dividing the number of true negatives by the number of true negatives plus false positives.

Specificity and sensitivity can also be used to describe the quality of an assay, where specificity relates to the ability of the assay to isolate and detect one particular analyte, and the sensitivity of the assay is its detection limit – usually the level of background signal plus two standard deviations.

The Perfect Biomarker

In conclusion, a good biomarker for disease should display good sensitivity and specificity. It will be disease discriminating, achieved by exhibiting a large rise or fall in concentration between healthy and diseased states. This will enable lower false positive and false negative diagnosis rates to be achieved, which will give the clinician confidence in the assay. Ideally the marker should also respond rapidly to the host's immunological state, and therefore be an intimate marker of a patient's condition at a given time.

1.5 Aims and Objectives

This thesis aims to employ the C system as a companion diagnostic for postoperative, hospital acquired infection, and as a metric with which to measure postoperative patient recovery. This requires developing a set of assays that collectively produce a snapshot of the C system at a given time, thereby using the C system as a biomarker to measure the host's immunological response. The hypothesis is tested in a clinical trial, correlating C activation and consumption

with infection and patient recovery. Initially, some challenges are addressed regarding the general handling and screening of real biological samples, namely nonspecific binding, and the analysis of data generated from complex samples. This part of the investigation is largely performed using the in-house optical scattering instrument, Liscar, which generates binding curves of interactions between macromolecules, label-free. The second part of the investigation employs the Meso Scale Discovery (MSD) ECL platform in order to develop assays for various components of the C system in order to monitor C activation. These assays are utilised in a clinical trial to monitor perioperative C activation in all patients in order to assess the efficacy of the C system as an indicator of systemic health

.

Chapter 2

Assay Development in Complex Media: Chaotropes and Biophotonic Nanoparticle Array Sensors

2.1 Introduction

From the perspectives of the hospital patient, the medical professional and the healthcare investor, there is an obvious need for a fast, multiple-biomarker biosensor that is capable of disease diagnosis from whole blood or serum at the point-of-care. Such a device will enable physicians to provide significantly better care to the hospital patients by 'personalising' each course of treatment based on the feedback that such a diagnostic instrument would provide.

As mentioned previously, single biomarker studies and tests have been performed on Prostate Specific Antigen (PSA) to diagnose prostate cancer, for example [12], and have yielded consequent advantages for the diagnosis of the respective diseases. In order to achieve success with such studies, one must overcome the significant challenge of detecting low concentrations of the target biomarker against large protein background concentrations [42]. For example human serum albumin has a concentration range of 35 – 50 mg ml^{-1} [78] throughout a population of healthy and diseased patients. Albumin, a negative acute phase reactant [79], is currently being investigated as a potential biomarker for disease progression and mortality in conjunction with other serum proteins [80; 81; 82]. There is also the remainder of the blood proteome to consider, and the final goal must be to detect, selectively, individual target biomarkers against background proteins that might be as much as ten orders or magnitude more concentrated, as is the case between the cytokines and albumin [42].

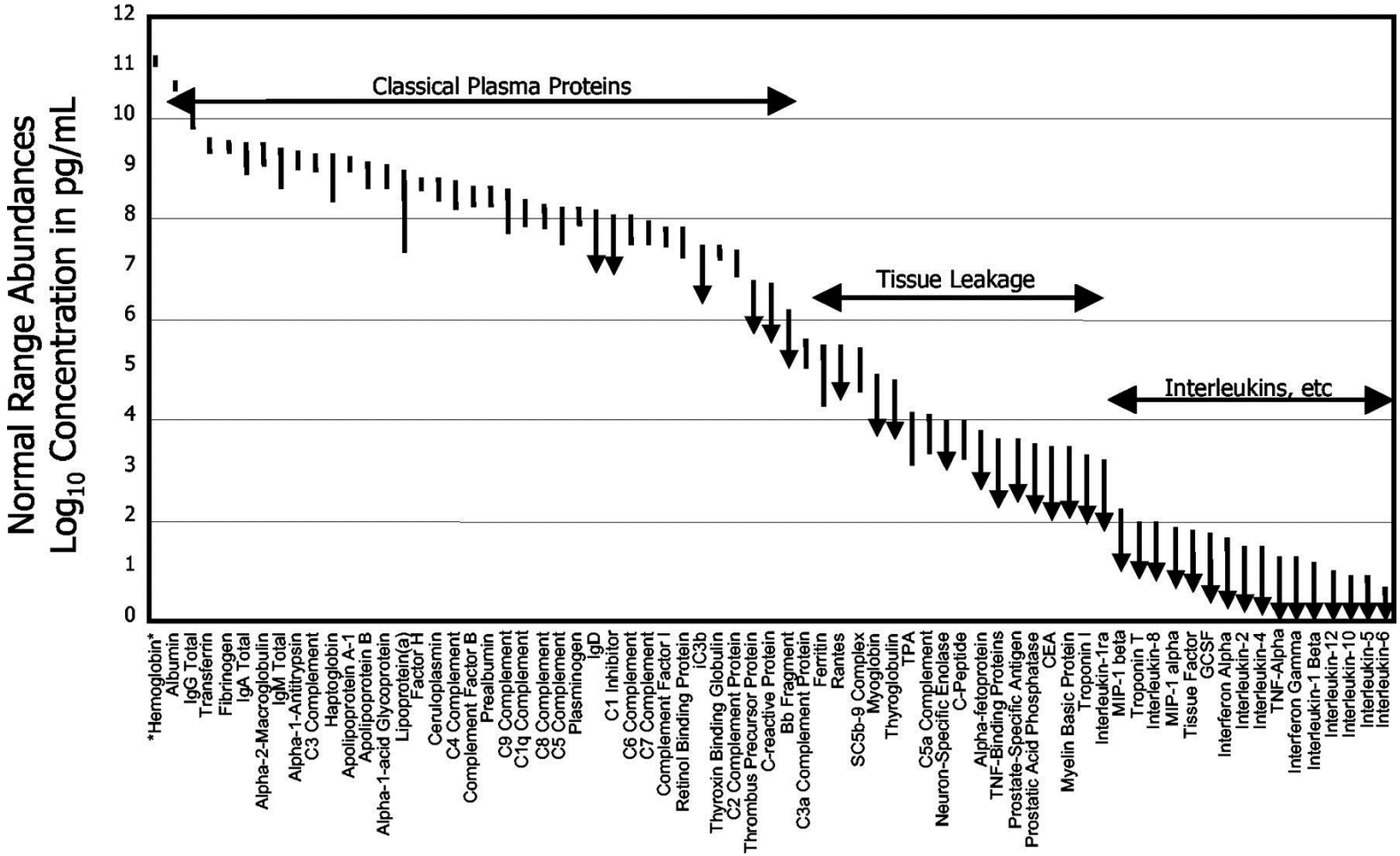

Figure 2.1. Reference intervals for 70 protein analytes in human plasma. Reproduced with permission from Anderson *et al* [42]. Abundance is plotted on a log scale spanning 12 orders of magnitude. Where only an upper limit is quoted, the lower end of the interval line shows an arrowhead.

This is clearly illustrated by Figure 2.1, which shows the classical plasma proteins at a far greater concentration than the interleukins, and the nonspecific interference from the former will have to be overcome before a successful assay can be developed for the latter. Furthermore, an ideal diagnostic test should be performed label free at the point of care, ideally on whole blood or on a sample with minimal pre-test preparation.

A number of SPR platforms have been used to conduct label-free biomarker detection studies, however these studies have generally been limited to only one or two biomarkers per assay [40; 41; 83; 84]. The majority of the investigations have been performed using dual-channel, continuous surface SPR platforms. Some multi-analyte, array format SPR technologies have been developed to detect multiple biomarkers simultaneously [11; 85], including a nanoparticle array and a light scattering based immunoassay [20; 24; 86], described in section 2.2.1. However, all SPR studies of complex fluids suffer from extreme nonspecific binding to the gold sensor surface owing to the intrinsic affinity that proteins have for gold.

This has presented a potent problem for all SPR investigators hoping to develop assays in complex fluids, and attempts have been made to alter the chemistry of the surface [87; 88], so as to deter nonspecific proteins whilst still allowing the target analyte to gain access to the surface target. If the surface chemistry is able to effectively deter nonspecific protein interactions, the investigator would be relieved of much of the background signal associated with nonspecific proteins. Also, considering the schematic in Figure 2.2, a biosensor that is only sensitive to changes close to the surface, as far as the binding reaction between antibody and antigen, would be relieved of much of the background noise associated with nonspecific proteins.

Therefore, regarding the problem presented by nonspecific binding, the nanoparticles have an advantage over continuous surfaces in that the sensing plasmon field is more localised on nanoparticles than on continuous surfaces [20]. This enables much of the “biological noise”

generated by nonspecific proteins to go unnoticed by the sensor, while still being capable of generating a signal from binding reactions close to the surface. The smaller sensing depth of the localised plasmons means that these sensors are less sensitive than continuous surface SPR sensors, however nonspecific background signal is precisely the feature we want to eliminate from our signal, which shows the advantage of using such particle-based sensors to detect antibodies in complex media such as delipidized serum [86].

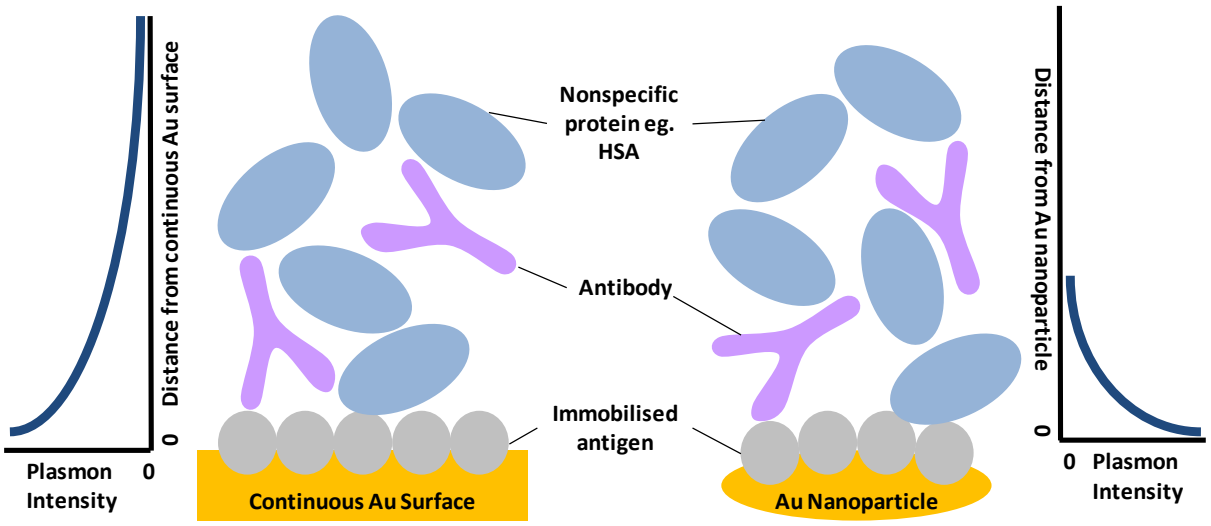

Figure 2.2. Schematic showing specific *vs* nonspecific binding on an SPR assay platform.

In this chapter, we address the problem of nonspecific binding and patient-to-patient albumin concentration variation that would affect directly the performance of a point of care sensor. We have performed a series of measurements on antibody-antigen reactions in model HSA-containing artificial serum solutions, using both continuous surface SPR and a nanoparticle-based plasmon sensor. The complexity of the detection serum is increased systematically; starting with the target analyte, IgG present in Phosphate Buffered Saline (PBS) solution, and then systematically increasing the concentration of the nonspecific binding species, Human Serum Albumin (HSA) to resemble physiological levels. We also examine the effect of the chaotrope KSCN on the antibody-antigen reaction, with and without HSA present.

2.1.1 Nonspecific binding

The high concentrations of nonspecific proteins and the significant variation over the normal range (35 – 50 mg ml^{-1} [78] for albumin) in patients causes problems for plasmon based immunokinetic assays, ELISA and immunoturbidimetric assays. The plasmon sensors are sensitive to two effects with increasing concentration of nonspecific binding protein as well as the concentration variation of the target analyte. Firstly, all plasmon-based sensors are essentially refractive index sensors, so changes in the total protein load in a patient's blood including any other changes will change the bulk refractive index. Secondly, nonspecific binding to the gold or modified gold sensor surface will compete with the target signal detection event. The bulk refractive index changes causes an immediate initial baseline offset and additional temporal changes are associated with nonspecific binding of proteins to the sensor surface. Crucially, there is a kinetic advantage in competition between specific and nonspecific binding: the antibody-antigen reactions generally have a very slow dissociation rate, characterised by the constant k_d, as well as a fast association rate with constant k_a, so that the antibody-antigen complex is more stable. Whereas the nonspecific proteins have a similar association rate but a much faster dissociation rate as the nonspecific protein-protein interaction it does not form a stable complex. An affinity constant K_D, can be calculated for each protein-protein interaction based on the ratio between the dissociation and association rates, k_d/k_a. The nonspecific binding association rate constant is typically 10^4 $M^{-1}s^{-1}$ which may be compared with the antibody association rate constant of 10^6 $M^{-1}s^{-1}$. For the dissociation rate constants, 10^{-2} s^{-1} compared with 10^{-4} s^{-1} respectively [86].

2.1.2 The Vroman Effect

Another phenomenon that requires consideration is that of the Vroman Effect [89; 90; 91; 92]. In the case where proteins have similar nonspecific association rates, a phenomenon called the Vroman effect takes place, whereby lighter proteins are displaced by heavier ones [93; 94; 95;

96]. In an experiment where IgG is the target analyte, this is not of great concern, as IgG has a large molecular weight (~150kDa), which is more than twice the weight of albumin at ~67kDa.

Therefore the kinetic factors, surface chemistry design and displacement properties of these proteins affect the overall sensitivity and accuracy of the assay.

2.1.3 Surface Control Proteins

In order to distinguish the specific antibody-antigen reaction from other nonspecific interactions taking place, control 'channels' are put in place where the specific epitope for the antibody being studied is absent. This allows the experimenter to distinguish between the nonspecific signal observed in the control channel and the specific signal that generates an offset in the antibody-specific channel. The concept of 'blocking' is also introduced, whereby another nonspecific protein is allowed to bind to the surface after the initial antigen immobilisation. This allows the surface to become completely covered in protein, and prevents any of the analyte sticking to the gold instead of the surface target, thereby providing a false signal. The target and control channels are therefore as similar as possible, save for the epitope specificity on the target protein for the analyte. A simple subtraction of the nonspecific channel signal from the specific channel signal will provide the data generated by the antibody-antigen reaction.

2.1.4 Reducing Nonspecific Binding

Several studies have been performed with the aim of lowering or eliminating the effect of nonspecific protein interactions, especially that of albumin. Efforts have included the addition of novel reagents [97], blocking agents [98] and tailored surface chemistries [99]. Other studies have also been performed on the addition of chaotropes and kosmotropes to the analyte medium, which is discussed further in section 2.1.6.

2.1.5 Protein Separation

Protein separation techniques include solubility methods, first performed successfully by Mörner in 1894 [100], who separated four components of lens protein using the differential solubility technique. Ultracentrifuge methods have also been employed successfully, relying on the principle that large molecules sediment in an ultracentrifugal field at a rate which is dependent on a number of factors, described by Svedberg [101] as

$$M = \frac{\mathrm{RTs}}{\mathrm{D}(1 - \rho \mathrm{v})}$$

Equation 2.1

where M equals molecular weight, R universal gas constant, T absolute temperature, s sedimentation velocity, D is the diffusion coefficient, v is the partial specific volume of the material in question, and ρ the density of the solution.

Electrophoresis is another quantitative and effective method for the separation of proteins. This technique became especially useful when performed on some support material, in addition to the demonstration of fractions when dyes were used, with the protein still remaining on the support, such as agar or starch. A development of this technique, immunoeletrophoresis, modified standard agar electrophoresis by identifying the protein fractions by the precipitin reaction which was made with antiserum placed in a trough cut placed in the agar parallel to the path of the electric current. Another technique for protein separation that has proved particularly successful is that of column separation, however it was only after the development of two cellulose-based ion exchangers that it became possible [102; 103]. 'Gel filtration' is another technique to spawn from column separation, whereby isolation of protein is achieved by the differential rate of diffusion in a dextran gel [104].

Unfortunately none of these techniques can be directly employed in an SPR-type experiment. What is needed instead is a method that restricts nonspecific interaction with the surfaces,

meanwhile allowing for the affinity between antibodies and antigens, so that these reactions can take place without interference from other proteins. This would be harder to achieve on a continuous surface SPR platform due to the greater sensing depth. Conversely, it could be particularly advantageous to particle sensors, and therefore the techniques mentioned in section 2.1.4 warrant further consideration, as they are the only realistic options available for on-sensor protein separation. A prepared surface that would favour specific binding only is the most desired solution, however addition of reagents to the analyte solution would also be a sensible, practical solution. For example urea and guanidine have been found to reversibly disrupt the tertiary structure of proteins, thereby reducing nonspecific binding, yet the mechanism for this is still unclear [105].

2.1.6 Protein Separation – Choatropes

Chaotropes are small molecules, such as the anion CNS^-, that exhibit stronger interactions with water than water with itself [106]. They are thought to surround proteins with a highly charged layer, altering the surface involved in protein-protein interactions [107; 108] by destabilising the salt bridges in protein-protein interactions via their effect of hydrogen bonding [109; 110]. There are many techniques available for separating plasma proteins for characterisation, including chromatography [111; 112; 113] and membrane separation techniques which can be used on biosensors [114]. Ionic and non-ionic surfactants have also been used to separate proteins, although not without complications: the proteins may become denatured, and surfactant micelles may form, therefore analysis below and above the critical micelle concentration and Krafft temperature needs to be considered [115]. Chaotrope molecules are also used in conjunction with surfactants to facilitate the separation of proteins in 2D gels [116]. Some success has come from employing chaotropes to separate proteins in solution when performing ELISA assays, where the question of specific and nonspecific binding competition was addressed [7].

2.1.7 Aims and Objectives

In this chapter we aim to determine the effect of nonspecific binding on continuous and nanoparticle based plasmon sensors, and also aim to mitigate its effect. This is achieved by doing a series of competitive binding experiments whereby a large protein background is introduced to a solution containing the analyte for a particular surface target. An antibody/antigen pair that is known to perform well in clean, buffer only experiments (aBSA-BSA) was selected for the specific binding reaction, and an abundant blood protein (HSA) was chosen as the nonspecific protein. The chaotrope KSCN is then added to the solution in large concentration, and its effect on the specific and nonspecific binding reactions studied.

2.2 Method

Given the advantages for analyte detection in complex fluids outlined in section 2.1.1, we have developed a nanoparticle based, light scattering array reader (Liscar) platform in order to perform multi-analyte detection studies. Nanoparticle seeds are printed in an array format on glass substrates and grown to larger 130nm truncated polyhedral structures to create bright light scattering centres. The arrays are illuminated in a total-internal-reflection configuration and the scattered light is monitored by a photo-camera in real time. The variation of scattered light in time for each functionalised array spot leads to an immune-kinetic assay whereby the kinetic response of a control assay is used to determine the concentration of the target analyte. In principle, the array setup allows for the concentrations of many different analytes to be determined simultaneously, however for current development and optimisation of the platform we have concentrated on understanding the assay characteristics for up to 8 species in a 96-spot array. The technical aim is to develop a point-of-care device for which no sample preparation is required, hence the emphasis on the challenge posed by nonspecific binding. Several proprietary buffers are used commercially within the blood sample collection containers, including chaotropes, and we are investigating their effect on the immuno-kinetic

assay. However, the primary cause of variation in blood samples is the effect of patient serum concentrations.

2.2.1 Experimental

The label-free binding studies were performed on two platforms: the commercially available continuous surface SensiQ Discovery SPR instrument from ICX Nomadics and the biophotonic particle plasmon Liscar instrument, developed in-house. The Liscar design has been discussed elsewhere [20; 86], however the current configuration employs an LED light source (Thorlabs, 660nm, 100mW) instead of the laser used previously. A schematic of the Liscar, including the fluidics system is shown in Figure 2.3a. A biophotonic sensor slide is prepared via a two-step process – firstly the fabrication of a gold nanoparticle array followed by functionalization with a target ligand.

Gold nanoparticle array fabrication

The gold nanoparticle array is manufactured by the chemical growth of small, ca.3 nm, gold nanoparticles that are spotted onto glass substrates in a 12×8 array format. Firstly a seed particle colloid by borohydride reduction of Au^{III} following the synthesis of Jana *et al* [117] to produce spherical seed gold particles with ca. 3 nm diameter. The seed solution is printed onto uncoated 25 mm × 25 mm glass slides in a 12 × 8 rectangular array using an inkjet printer (Arrayjet Aj100). The slides are left to dry for 2 hours at room temperature. The seed arrays then undergo a particle growth procedure to produce an array comprised of much larger individual nanoparticles. The grown nanoparticles take the shape of truncated polyhedra, and are approximately 130 nm in size [86]. The slides are completely immersed for 30 minutes in developing solutions containing: (i) 0.1 M CTAB, 2×10^{-4} $HAuCl_4$, and 4×10^{-4} M ascorbic acid and 2×10^{-6} M $AgNO_3$. The slides are then washed extensively in 18 MΩ deionised water to remove CTAB from the nanoparticle sureface. The slides are dried with nitrogen and stored at -4°C.

Protein Functionalisation

The nanoparticle arrays are then functionalized with the surface target proteins according to the array key in Figure 2.3(b). The slides are reinserted into the inkjet printer and 1 mg/mL protein solutions (in PBS) are printed precisely over the gold nanoparticle array according to a pre-determined functionalisation key, elaborated on in Section 2.2.3.

Protein binding measurements

The biophotonic sensor slide is installed into the Liscar and is equipped with a flow cell to enable kinetic protein-protein interaction assays to be recorded in real time by recording scattered light from the nanoparticles using a photo camera – incident light is scattered by the gold nanoparticles, and this scattering changes as proteins enter the plasmon field surrounding the nanoparticles. It is this change in scattered light that generates the signal. Therefore an individual kinetic trace can be recorded for each array spot, and in the case of this experiment, 24 array spot traces are averaged together per target surface protein.

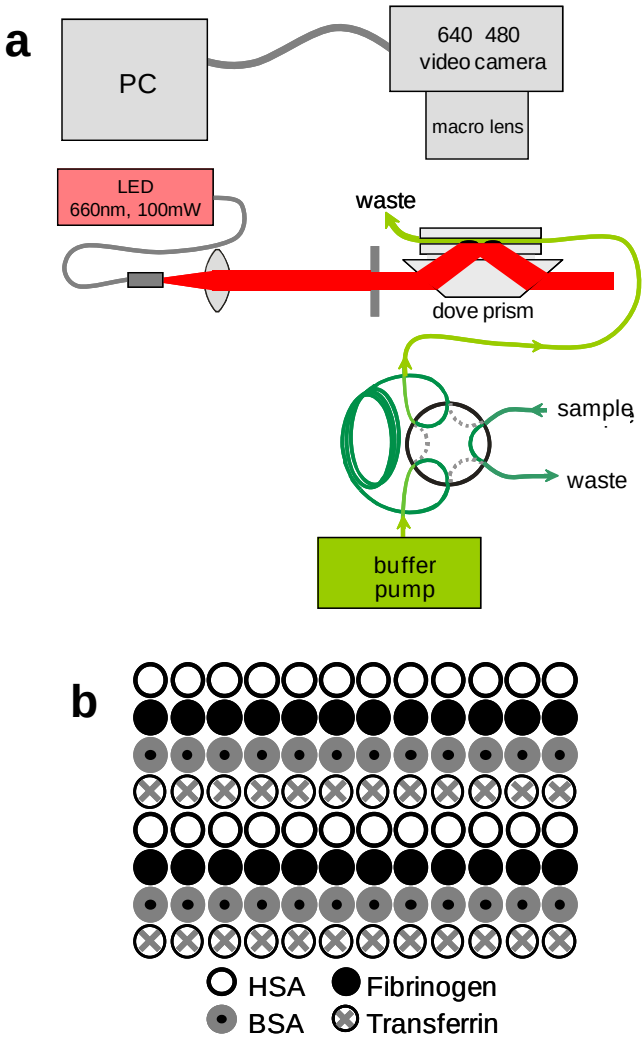

Figure 2.3. (a) Schematic of the Liscar instrument. (b) Protein functionalization array key.

Initially, a stable baseline is obtained for 5-10 min using a standard PBS running buffer, after which an antibody-containing analyte is injected over the protein functionalised surface for 15 min at a flow rate of 25µl min^{-1} (SensiQ) or 100 µl min^{-1} (Liscar) to ensure concentration limited kinetics [20]. The absolute response from the Liscar was calibrated for each set of 24 spots functionalised with the same protein, Figure 2.3b, by measuring the response to the buffer change from PBS to double concentrated PBS, corresponding to a change in bulk refractive index (RI) of 1.5×10^{-3} refractive index units (RIU); all data presented in the subsequent figures are presented as the change in RI, ΔRI. Similar calibrations were performed for both channels of the SensiQ SPR instrument where the sensitivity is typically 2×10^{-6} RIU.

2.2.2 Chemicals

N-(3-Dimethylaminopropyl)-N'-ethylcarbodiimide hydrochloride (EDC), N-hydroxysuccinimide (NHS), 16-mercaptohexadecanoic acid (MHDA), potassium thiocyanate (99%), bovine serum albumin (BSA) (98%), human fibrinogen (FBR) (60%, with 40% buffer salts; the protein content is >80% clottable FBR), human serum albumin (HSA) (>96%), and transferrin (98%) were obtained from Sigma-Aldrich; sheep polyclonal antibodies to BSA (aBSA, 23mg/ml, IgG fraction) were supplied by AbD Serotec UK; all solutions where prepared in 18 MΩ deionised water and protein solutions were prepared in standard phosphate buffered saline (PBS, 137 mM NaCl, 2.7 mM KCl, 10 mM Na_2HPO_4, and 1.5 mM, KH_2PO_4, pH 7.3) unless otherwise stated.

2.2.3 Sensor Surface Preparation

SensiQ SPR Surface

Proteins were immobilised on the two sensor channels of the SensiQ chip by peptide coupling between sensor surface carboxyl groups and free amine groups of the proteins. The two-channel gold surface of the SensiQ sensor chip surface for the SensiQ instrument has a 50 nm thick continuous gold surface which was first cleaned with 10 mM HCl solution followed by incubation in 10 mM 16-MHDA in ethanol for 15 hours, which forms a carboxyl-functionalised self assembled monolayer (SAM) on the sensor surface. The SAM carboxyl groups were activated with 0.05/0.25 M NHS/EDC aqueous solution, forming amine-reactive succinimide ester groups. Immediately after the activation step, 1 mg ml^{-1} solutions of BSA and transferrin in 10 mM sodium acetate buffer, pH4.9, were injected into channels one and two respectively at a flow rate of 5 µl min^{-1} for 45 minutes. Following the protein immobilization step, both surfaces were capped with 1 M ethanolamine, and after a 10 mM HCl wash the running buffer was then changed to PBS.

Liscar Particle Surface

The array format sensors were functionalized with proteins by spotting 1 mg ml^{-1} HSA, BSA, fibrinogen, and transferrin solutions in PBS directly over the nanoparticle containing array spots, according to the key on Figure 2.3(b). After 2 hour incubation the slides were washed with PBS and stored dry at 4^{o}C.

2.2.4 aBSA-BSA Binding Experiments

In order to simulate physiological conditions, and to compare those conditions to a 'clean' SPR experiment where only PBS is used as a buffer, a series of experiments were performed whereby the analyte, BSA, was detected both in the presence of high concentrations of HSA and in clean PBS buffer.

2.3 Results

Several series of experiments were performed to establish the interference effects of the HSA concentration on the immuno-kinetic assay accuracy for aBSA concentration measurements in model sera. The effect of added chaotrope was also investigated in an attempt to recover the accuracy of the assay; the experimental series are summarised in Table 2.1

Table 2.1. Summary of experiment series performed for on the Liscar and SensiQ platforms

Series	[aBSA]	[HSA]	[KSCN]	Liscar	SensiQ	Figure
A	varied 10-50 nM	-	-	+	-	Figure 2.9
B	fixed 30 or 50 nM	varied 100-450 nM	-	+	+	Figure 2.4, Figure 2.6
C	varied 10-50 nM	fixed 450 nM	-	+	-	Figure 2.7, Figure 2.9
D	varied 10-50 nM	-	fixed 150 mM	+	-	Figure 2.8, Figure 2.9
E	fixed 30 or 50 nM	varied 100-450 nM	fixed 150 mM	+	+	Figure 2.6
F	varied 10-50 nM	fixed 450 nM	fixed 150 mM	+	-	Figure 2.9

The aBSA-BSA binding kinetics were measured in pure PBS buffer acting as the control series. Further analyte solutions of 30 nM (SensiQ) and 50 nM (Liscar) aBSA with varying concentrations of HSA, were prepared in PBS and injected over the sensing surfaces of the SensiQ and Liscar platforms. Each injection lasted for 15 minutes and was followed by a 5 minute, 10 mM HCl regeneration step. Repeat injections were performed for each series to establish reproducibility. The order of injection of the analyte solutions of different HSA

concentration was randomised so as not to perform the experiment in a systematic manner. The aBSA immuno-kinetic assay was repeated with a fixed physiological concentration of HSA (450 µM). These experiments were performed in three series, A – C,:

A: The aBSA-BSA assay in PBS. This is the reference series with varying aBSA concentration from 10 to 50 nM, Figure 2.4 and Figure 2.9(b)

B: The aBSA-BSA assay with varying concentrations of HSA 0 – 450 µM, with fixed aBSA concentration, 30 nM (SensiQ) or 50 nM (Liscar), Figure 2.4 and Figure 2.6.

C: The aBSA assay was performed with fixed HSA concentration (450 µM), and varying concentrations, 10-50 nM, of aBSA. Figure 2.9 and Figure 2.8.

The effect of nonspecific binding was investigated by repeating experimental series A-C with fixed concentration of the chaotrope, KSCN, at 150 mM [7], series D-F:

D: The aBSA-BSA assay in PBS with 150 mM of chaotrope, analogous to Series A, Figure 2.8 and Figure 2.9.

E: The aBSA-BSA assay with varying concentrations of HSA 0 – 450 µM, with 150 mM KSCN, analogous to Series B, Figure 2.6.

F: The aBSA assay was performed with fixed HSA concentration (450 µM), and varying concentrations, 10-50 nM, of aBSA.with 150 mM KSCN, analogous to Series C, Figure 2.10 and Figure 2.9

The series A-F were performed on the Liscar platform with B and E repeated on the SensiQ.

Table 2.1 summarizes the conditions of each experiment and the figures presenting the corresponding data.

2.4 Discussion

The principal objective of this investigation is to interrogate the effect of varying concentrations of HSA that reflect physiological conditions on an immunokinetic assay for aBSA. Further to this we investigate the effect of the Chaotrope, KSCN on the aBSA assay in the presence of HSA. The maximum used HSA concentration of 450 μM roughly corresponds to the lower limit of clinical albumin concentration range expected clinically, 30 – 50 gL^{-1} [78]. Potential applications of the Liscar technology for the high throughput measurement of blood protein concentrations requires an understanding of the effect by the background blood proteome, as seen in Figure 2.4. It may be the case that HSA should be assayed simultaneously with the target analyte assays in order to accurately determine the concentration of the target analyte in whole blood or serum – aBSA in the present case. The arrays used in this experiment employed a 24-spot averaged fibrinogen control 'channel', Figure 2.3(b), to act as a nonspecific binding channel that is also sensitive to variations in light intensity and wavelength, both of which cause variations in the scattered light that generates our signal, and therefore add noise to the experiment. In addition, the normalisation of the averaged signal from the target spots against the fibrinogen control channel removes the effect of the large bulk RI change. ΔRI due to varying [HSA] in PBS is determined using the fibrinogen control and the absolute RI shift calculated for each of the model serum solutions, plotted in Figure 2.5. Although the data appear to present a complex, non-linear variation with concentration, a simple linear relation, r^2 = 0.94, satisfactorily describes a first measure (within experimental error) of the bulk composition of the patient's serum.

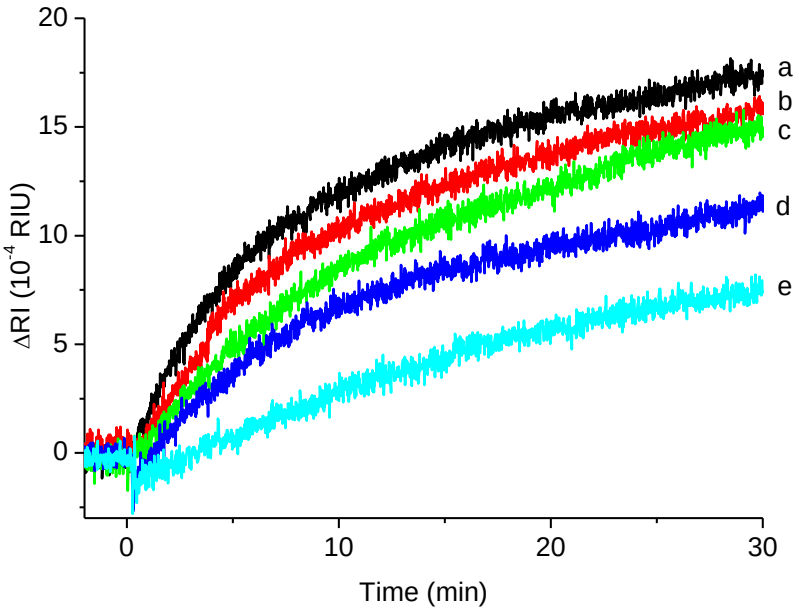

Figure 2.4. aBSA-BSA assay with varying concentrations of HSA; (a) 0 µM, (b) 100 µM, (c) 200 µM, (d) 300 µM, (e) 450 µM

The response detected from the sensor surface reflects the complex kinetics from an amalgamation of processes, including the co-adsorption of HSA and aBSA to the surface and various displacement reactions, including the Vroman effect [95]. A detailed analysis of the competing process is beyond the scope of this paper; here we present an empirical analysis that might form the basis for a simple interrogation algorithm for a point-of-care instrument based on the Liscar. The antibody immuno-kinetic response based on the Langmuir adsorption equation [86].

$$\theta = \frac{\vartheta}{\vartheta_m} = \frac{k_a[P]}{k_a[P]+k_d}\left(1-\exp\left(-\left(k_a[P]+k_d\right)t\right)\right)$$

Equation 2.2

where θ is the surface coverage (a fraction of the occupied binding sites, ϑ, to maximum binding sites, ϑ_m); $[P]$ is the concentration of antibody in solution; and k_a and k_d are the adsorption and desorption rate constants, respectively; and t is time. Since the present data

show that on the experimental scale k_d « k_a[P] for antibody-antigen reactions, the equation may be simplified into:

$$\vartheta \approx \vartheta_m\left(1-\exp\left(-k_a[P]t\right)\right)$$

Equation 2.3

where ϑ refers to the experimental observable, namely change in scattering brightness and ϑ_m corresponds to the maximum brightness change when complete coverage of the available active sites on the surface is achieved. Each recorded transient curve was fitted to this single exponential expression. k_a is therefore the observed association constant derived from the data fit to Equation 2.3.

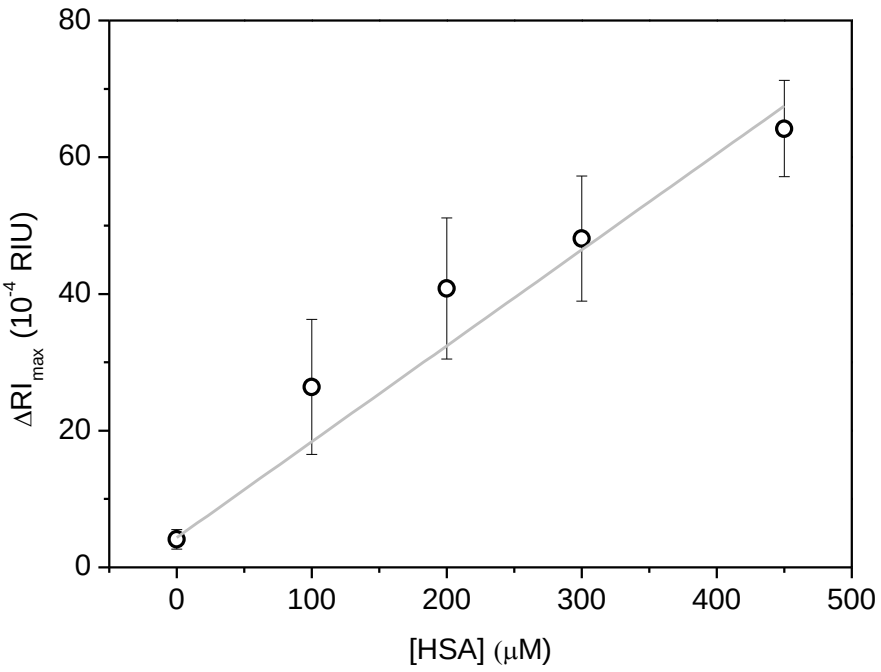

Figure 2.5. Variation of bulk ΔRI determined from the fibrinogen control spot responses to analyte samples containing 0-450 μM HSA (r^2=0.98)

The simple model contains the same assumptions as the Langmuir adsorption isotherm, notably the antibody interacting with its antigen on the surface but neglecting the interactions between antibodies at the surface or the interference from any other proteins fouling the

surface or the reduction in the rate of association as a result of diffusion through a viscous medium. Taking these into account the derived k_a and ϑ_m shall not be perceived as true kinetic constants for aBSA-BSA interaction but rather as effective/empirical factors describing the complex system of reactions in a most simple practical form. Moreover, a significant degree of correlation between k_a and ϑ_m may be removed by forming a single $\vartheta_m k_a$ parameter [86] which is used to discuss the effects of nonspecific protein binding and presence of chaotrope on specific response due to aBSA-BSA interaction. The $\vartheta_m k_a$ parameter is used to describe the data as it describes more accurately the processes occurring at the surfaces, namely bulk refractive index change, ϑ_m, and antibody-antigen binding, k_a.

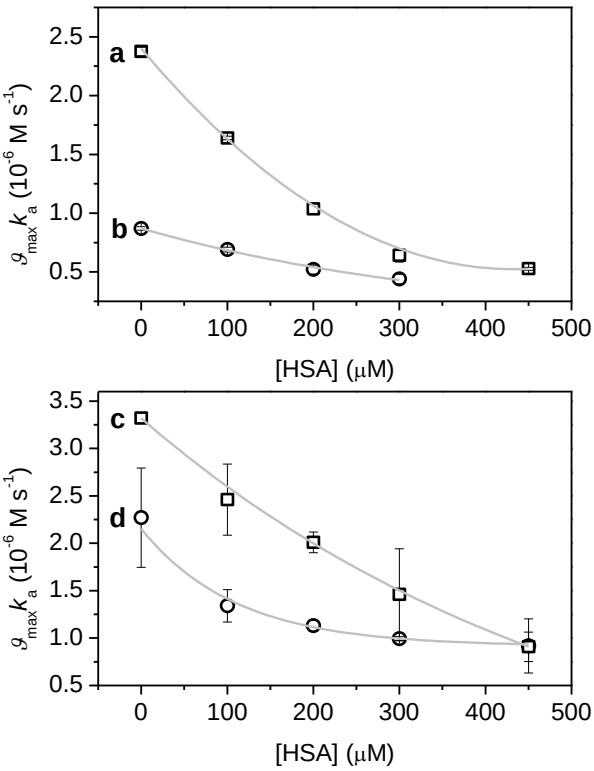

Figure 2.6. Dependence of $\vartheta_m k_a$ on concentrations of HSA in the analyte; a) SensiQ, 30 nM aBSA; (b) SensiQ, 150 mM KSCN, 30 nM aBSA; (c) Liscar, 50 nM aBSA; (d) Liscar, 150 mM KSCN, 50 aBSA

Using the $\vartheta_m k_a$ analysis, calibration curves for the concentration may be derived for the SensiQ and Liscar platforms, Figure 2.6. The curves show a significant difference between the particle

and continuous gold surfaces and the effect of the chaotrope on both platforms. The limiting $\vartheta_m k_a$ value for the continuous surface is 40% smaller than for the nanoparticle surface and with a smaller dynamic range for the assay. The effect of the chaotrope is more pronounced: on the SensiQ platform the value of $\vartheta_m k_a$ is reduced by one third with the addition of the 150 mM chaotrope which further reduced the dynamic range of the assay to 25% of the initial value and hence reducing the sensitivity. However, with the nanoparticle surface the dynamic range of the assay is only reduced to 60% of its original value. The variation in the performance of the Liscar platform in part depends on the variations during the printing process which dominates the error in the signal.

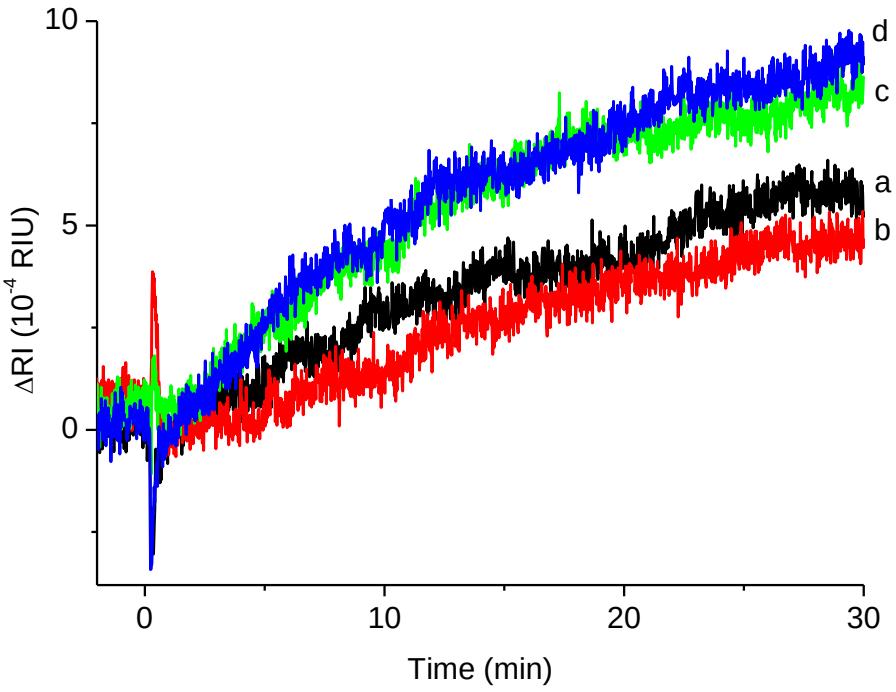

Figure 2.7. aBSA-BSA assay with [HSA] = 450 µM and varying [aBSA]; (a) 20 nM, (b) 30 nM, (c) 40 nM, and (d) 50 nM

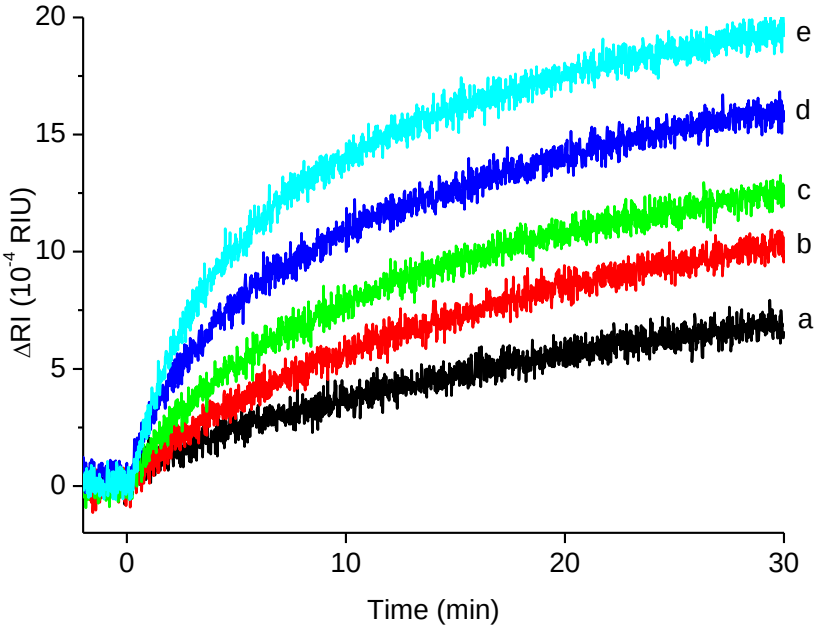

Figure 2.8. Immuno-kinetic aBSA-BSA assay in the presence of 150 mM KSCN, antibody concentrations; (a) 10 nM, (b) 20 nM, (c) 30 nM, (d) 40 nM, (e) 50 nM

The data from the reference channel presented in Figure 2.5 can be used to correct for the effect of high HSA concentration on the observed aBSA-BSA association rates shown in Figure 2.8. An empirical rational function efficiently describes the observed experimental dependence of $\vartheta_m k_a$ parameter on bulk refractive index change associated with HSA concentration in the sample. The empirical functional form is defined as:

$$[P] = \frac{a \times \left(\vartheta_m{}^{1st} k_a\right)}{1 - b\Delta_{bulk}} + c$$

$$[aBSA]/M = \frac{0.0135\left(\vartheta_m{}^{1st} k_a\right)}{1 - 115\ \Delta RI^*_{sample}} - 2.9\times10^{-9}$$

Equation 2.4

where a=0.0135, b=115 *and* c = -2.9 $\times$ 10^{-9} M are fitted parameters, c is a small offset parameter within the accuracy of the measurements. Consequently, with this correction the aBSA concentration may be derived with an accuracy of 10-15% for all samples containing HSA in 0-450 μM concentration range. The *a*, *b* and *c* parameters may be derived for a batch of slides produced and then used to calibrate each array slide, assuming consistent printing integrity.

There is a clear difference in the performance of the two plasmon platforms which may in part be explained by the differences in the plasmon field penetration of the continuous and nanoparticle gold surfaces. The plasmon field penetrates typically 300 nm from the gold surface of which only approximately 10 nm is occupied by the antibody assay. The majority of the field plasmon field is sensitive to large changes in the bulk refractive index which in the presence of the large HSA concentration and the chaotrope is significant. In the two-channel SensiQ platform the specific binding contributions to the signal are derived from a subtraction of the large refractive index changes associated with HSA and the chaotrope. The subtraction produces the change associated with the binding, both specific and nonspecific to the surface, an effect occurring in less than 10% of the continuous surface plasmon field. This is based on the assumption that the assay layer is approximately 20 nm thick including all of the ligand molecules and proteins. However, the particle platform performs the same subtraction over a number of control spots on the array to observe the change assay in the volume which occupies nearer 50% of the plasmon field, where similar assumptions have been made about the thickness of the assay layer and a particle plasmon field penetration depth of 50 – 60 nm.

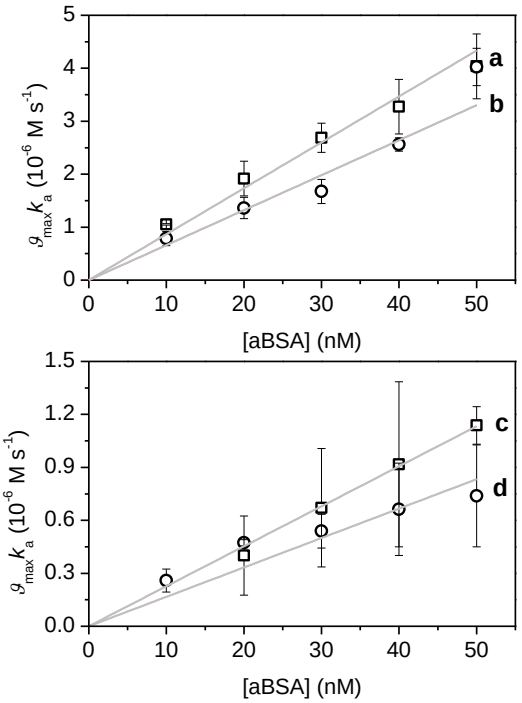

Figure 2.9. Variation of $\vartheta_m k_a$ *vs* antibody concentration for the immuno-kinetic aBSA-BSA assays with different analyte buffer composition; (a) KSCN and HSA-free PBS buffer (r^2 = 0.93); (b) PBS, 150 mM KSCN (r^2 = 0.95); (c) PBS, 450µM HSA (r^2 = 0.99); (d) PBS, 450 µM HSA, 150 mM KSCN (r^2 = 0.72)

Calibration curves may be constructed for the Liscar platforms from which variation of $\vartheta_m k_a$ against aBSA concentration may be seen in Figure 2.9. There is a significant difference in sensitivity of the assay in PBS, 84 ± 3 RIU s^{-1} M^{-1}, compared with the 23 ± 2 RIU s^{-1} M^{-1} for the assay at physiological HSA concentration. The detection limit and accuracy for the aBSA in PBS is 760 ± 160 pM (120 ± 25 ng ml^{-1}) whereas in physiological HSA it is 2.5 ± 0.7 nM (380 ± 100 ng ml^{-1}). The challenge for the measurement of antibodies in real serum samples with varying HSA concentrations is to provide a robust estimate of the effect of the HSA to enable to the concentration to be observed.

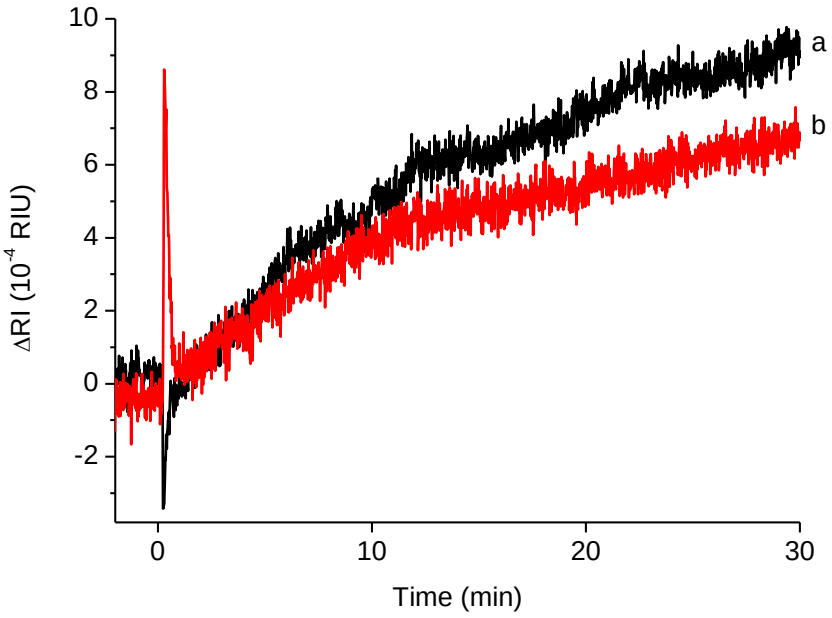

Figure 2.10. The effect of chaotrope on antibody binding from samples containing 50 nM aBSA and 450 µM HSA; (a) without chaotrope and (b) with 150 mM KSCN

The effect of the chaotrope is also clear from the original trace in Figure 2.10 and the calibration curve in Figure 2.9 with a sensitivity and accuracy of 66 ± 3 RIU s^{-1} nM^{-1} in 150 mM KSCN and PBS. The kinetic trace in Figure 2.10 is slower in rate when the chaotrope is present and does not reach the same ϑ_m during the course of the experiment. However, the quality of the exponential curve is better, resulting in an improved fit to the data. There is also a large increase in the refractive index of the sample with the added chaotrope and this causes a number of subtraction artefacts in the traces notably in the SPR surface but not as much in the particle plasmon surfaces. The chaotrope does however, improve the accuracy of the aBSA assay in the presence of 450 µM HSA ensuring the calibration is linear with a sensitivity of 2 × 10^{-8} M^{-1} s^{-1} whereas the calibration for the aBSA with HSA without the chaotrope is not linear (seen from the r^2 value for the line in Figure 2.9(d)). The detection limit for both assays is 2.5 ± 0.7 nM (380 ± 100 ng ml^{-1}) in PBS and 2.9 ± 0.5 nM (440 ± 80 ng ml^{-1}) in the chaotrope augmented PBS.

The KSCN behaves as a chaotrope by surrounding the proteins in the solution with a small-molecule, charged layer to each of the proteins in the solution causing a change in the protein-protein interactions but not so as to denature them. There are both ionic and non-ionic chaotropes such as KSCN and urea respectively, as well as kosmotropes such as CO_3^{2-} which affect the interactions between proteins and their solubility in solution [118]. The current mechanism of action [118] suggests polarisation of the salvation shell around large molecules such as proteins as well as hydrophobic, surface tension and direct binding mechanisms.

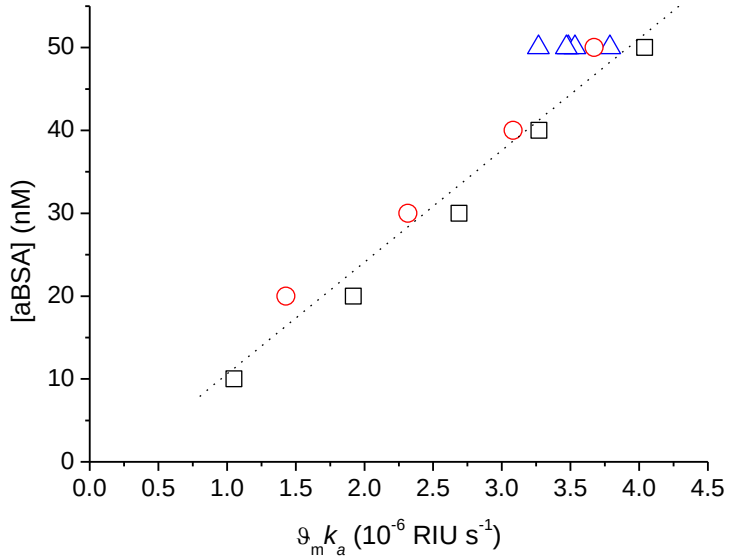

Figure 2.11. Empirical correction of the immuno-kinetic assay for the variation of bulk [HSA] using Equation 2.4. □, experimental series A; Δ, series B; ○, series C. r^2 = 0.96.

2.5 Conclusion

We have demonstrated the albumin interference affect on the immuno-kinetic assay for aBSA in analytes with varying concentrations of HSA. The total RI can be used as a simple measure of the HSA concentration thus allowing an empirical correction to immuno-kinetic assay for aBSA under varying HSA conditions. While testing complex analytes with large HSA content, there is a clear particle plasmon detection advantage on the Liscar platform compared with the continuous gold surface and addition of the KSCN chaotrope somewhat improves the integrity and accuracy of the assay although there is a slight reduction in the detection limit. Since

albumin interference with assays in blood serum is well known and there are propriety reagents which have been added to serum solutions to improve the integrity of a number of assays [97; 119], a novel set of reagents with some of the advantageous characteristics of KSCN will need to be developed specifically for the immuno-kinetic assays based on continuous surface and particle-based SPR techniques. It is also apparent that a different analytical approach is needed to determine the competition between nonspecific and specific analytes. Although this investigation contained complex samples where antibodies and albumin were allowed to compete for reaction sites, a development of this would be to investigate the competition between these species when one is already present on the surface. This is therefore addressed in the following chapter.

Chapter 3

Mathematical Model for Competitive Binding between Low and High Affinity Species on Biosensor Surfaces

3.1 Introduction

Nonspecific binding presents real problems to label-free, plasmon-based biosensors as shown in Chapter 2. Relative to the target analyte, the presence of abundant interfering components (with both high and low affinity for the sensor surface) affects the sensor's ability to detect the target species, and creates uncertainties regarding the reaction mechanisms normally used to analyse the data. At present this is a weakness of label-free biosensors, with most investigators avoiding the problem altogether by performing experiments with clean, analyte-only solutions. This is a reasonable strategy for standard protein-protein interaction research, but it poses a significant challenge if label-free biosensors are to succeed as a diagnostic tool, screening for biomarkers from real samples at the point-of-care. Owing to the complexity of real biological samples, and therefore the uncertainty surrounding the reaction mechanisms involved, kinetic SPR data become difficult to interpret as the favoured 1:1 interaction model [12; 46; 47] is no longer the correct description of the true set of reactions. Surface chemistry advances [120] have, to some extent, reduced the amount of nonspecific protein interference on the sensor surface and therefore also improved the specific signal produced. Nevertheless, it is unlikely that any advances in surface chemistry, however good, will ever completely eliminate the effect of nonspecific proteins interfering with the interaction between the immobilised ligand and the target analyte.

The nonspecific binding problem is accentuated further if we consider the complexity of real biological samples, the medium within which diagnostic tests are performed. For example, human plasma contains 289 known proteins [121] spanning a concentration range of over 11 orders of magnitude. In theory, affinity constants could be determined for all plasma protein-protein interactions, and the results presented in an extremely large model, tailored for a particular target analyte. However this is well beyond the scope of this investigation, and the field of label-free protein interaction analysis as it stands. Such a model would not just be dependent on the number of proteins present, but also their concentrations and relative affinities, which will vary depending on the target assay species and the disease state of the patient – a potentially insurmountable problem.

Many excellent SPR investigations [11; 12; 122] employing low-ligand surface coverage and low-analyte concentrations have yielded well-determined kinetic parameters for the interaction between proteins using the 1:1 interaction model, and thus the value of the 1:1 model should not be under-estimated. Nevertheless, its applicability to real biological samples analysis is questionable, as there are a number of additional factors to consider which contradicts some of the assumptions of a 1:1 interaction model, Section 1.2.3. For the 1:1 model to be employed with real biological samples, significant dilution of the sample is required to satisfy the non-interacting assumptions of the 1:1 interaction model. This has obvious detrimental effects for assay sensitivity and accuracy, and is therefore not appropriate for low-concentration analytes. Where investigations have used real biological samples, a number of techniques have been employed to obtain acceptable results. The simplest implementation to correct for any unwanted nonspecific binding is the introduction of control channels, present in almost all SPR-based studies to subtract the non-specific contributions from specific binding interactions. This involves functionalising one of the sensor surface channels with a protein that will not bind with the target analyte, and therefore it acts as a negative control for the interaction of interest.

Alterations to sensor surface chemistries have focussed around creating hydrophilic surfaces that limit interactions with any nonspecific proteins present in the sample. The most successful of these surface functionalisations have implemented poly-ethylene glycol (PEG) [123; 124] molecules of varying sizes and surface coverage. Furthermore, 'blocking' steps, whereby nonspecific proteins are bound to all sensor channels, followed by washing with regeneration buffers, have been introduced to binding protocols in order to stabilise the immobilised ligand [12] and cover any remaining immobilisation sites. Additionally, preconditioning of real biological samples has included delipidation [125], heat treatment [43], dilution [40; 41] and addition of chaotrope species [126; 127] prior to analysis. All these measures have been employed to investigate their effects on nonspecific binding in an attempt to minimise its effects.

In addition to advances in surface chemistries and sample preparation, analysis of complex samples also needs to evolve to accommodate the ever-present sample complexity, especially the high abundance of nonspecific proteins relative to the target analyte. Association and dissociation rates must be considered for the individual components in the complex media, and competitive displacement of 'low affinity' proteins by 'high affinity' species should be measured. Several studies [12; 46; 128] have successfully presented global analysis of kinetic binding data whereby all the binding curves for different analyte concentrations are fitted with a single set of parameters.

3.1.1 Aims and Objectives

The investigation presented in this Chapter aims to address the simplicity of the 1:1 single analyte binding model by developing a model for the analysis of complex analyte mixtures which contain a 'high affinity' target analyte in low concentration, an antibody, and a high concentration of a 'low affinity' background protein, Human Serum Albumin (HSA). A first-order kinetic model will be developed for a complex set of reactions by interrogating each

individual reaction subset that forms part of a system, and present the results in a global kinetic analysis model. Binding kinetics of the two competing analytes, with low and high affinity for the target ligand, will be studied separately, followed by a study where both analytes are allowed to compete for the surface ligand. This final set of conditions is therefore analogous to real blood where, for example, and antibody has to compete with a large background of nonspecific proteins (such as albumin) to locate and bind its respective antigen.

The investigation will be conducted using the Liscar (Light Scattering Array Reader) instrument discussed in detail in Chapter 2, which relies on optical scattering by gold nanoparticles. The robust nature of the Liscar instrument allows samples of very high protein concentrations to be screened. The data is fitted globally to a 1:1 interaction model, and then the model is expanded to include additional reactions to account for the complexity of the assay sample, explicitly considering the competition between low and high affinity species.

Model Nomenclature

The molecules used to model the reaction are chosen for their respective masses and affinities. Anti-BSA (aBSA), the '*high affinity*' analyte, is larger than the Human Serum Albumin (HSA), serving as the '*low affinity*' analyte. As the low affinity molecule is also of lower mass than the high affinity molecule, the study has minimised the nonspecific Vroman effect [89; 90; 91; 92], reducing the complexity of the model. Additionally, HSA does not interact with aBSA which serves to further simplify the model.

3.2 The Binding Models

A simple 1:1 model allows for the rate of adsorption to a surface to be proportional directly to the number of vacant sites on the surface, but its principal limiting assumption for protein binding studies is the lack of interaction between species as they bind to the sensor surface. A competitive binding model will allow for these co-operative binding interactions and additional reactions to occur at the sensor surface. This investigation identifies and analyses the

individual reactions that comprise a complex set of reactions forming a mechanism for the interaction of high affinity and low affinity species at a biosensor surface, Figure 3.1.

Firstly, the well-known [125; 127] interaction between aBSA (analyte A) and BSA (the surface ligand, S) is studied, followed by the nonspecific interaction between HSA (analyte B) and BSA. The reaction sets will be combined to monitor the displacement of HSA from the surface by aBSA. The first two datasets are analysed separately and the parameters obtained used to model the data from an experiment where both analytes A and B are allowed to interact with S, Figure 3.1. Additional reactions will be added to the reaction mechanism model as required.

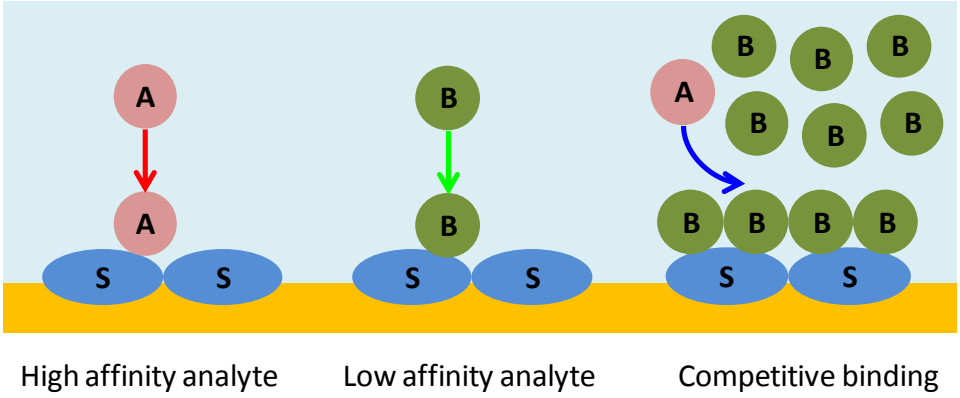

Figure 3.1. Schematic diagram of the three reaction-sets studied: A = High affinity analyte. B = Low affinity analyte. S = Surface ligand, with high affinity for analyte A only. In each reaction-set the concentration of the analyte in solution is varied, detailed in Table 3.1.

Figure 3.1 illustrates the three reactions that comprise this study. The high and low affinity analyte experiments are both performed with only the target analytes present in buffer, however the competitive binding experiment monitors the competition between A and B for S, with B already present on the surface before the introduction of the analyte solution which contains a low concentration of A against a large background concentration of B. A comparison with physiological conditions is possible, where antibodies (analyte A) in the blood in low concentration compete to bind with their respective antigens (the surface ligand, S) against a vast background of nonspecific protein concentrations such as albumin (analyte B).

3.3 Materials and Methods

The method used to collect the data for this experiment has been described in detail in Chapter 2 and elsewhere [86; 125], and will be discussed again briefly here.

The Liscar configuration is duplicated as per Sections 2.2.1 and 2.2.3, the only difference being the protein functionalization setup, Figure 3.2. A schematic diagram for the Liscar can be seen in Figure 2.3. A gold nanoparticle array is produced by chemical growing of small, ca. 3-4 nm, nanoparticles spotted onto a glass substrate in a 12×8 array format. The grown nanoparticles are in the shape of truncated polyhedra, approximately 130 nm in size [86]. The surface is then functionalised with a ligand according to the array key in Figure 3.2.

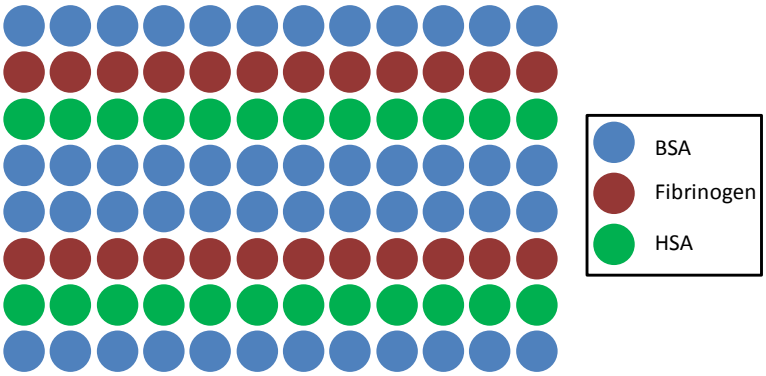

Figure 3.2. Surface ligand functionalisation key. A 12×8 array of gold nanoparticle spots was functionalised with three different surface ligand proteins as indicated.

A flow cell is fitted over the array to allow protein-protein interactions to be measured in real time by imaging the sensor array. The scattering properties of the nanoparticles depend on the local RI around the nanoparticle, which changes when proteins (RI = 1.36-1.55 RIU [22]) displace water (RIU = 1.33 [21]) in the immediate vicinity of the nanoparticles, which is detected by the photo camera and generates the signal. The scattered light intensity changes in time to provide real-time kinetic traces for individual array elements, which may be averaged together for a particular surface ligand channel.

The surface is blocked using a solution of BSA in PBS (1 mg/ml), and the surface is cleaned using a regeneration buffer, 10 mM HCl. After obtaining a stable baseline with a particular

running buffer, the sample containing analyte is injected over the ligand-functionalised surface at a flow rate of 100 µl/min to ensure concentration-limited kinetics [125]. Table 3.1 contains a complete list of running buffers and analytes relating to each experiment set. In addition to the analyte channels, surface control array spots functionalised with fibrinogen were used to act as a negative control for the specific aBSA-BSA interaction, thermal variations in refractive index (RI) and light output intensity variations of the LED. The fibrinogen negative control was subtracted from BSA-channel traces in experiment sets 1 and 3 to produce a target ligand specific kinetic trace. The nonspecific nature of experiment set 2 meant such a subtraction was not possible, and therefore the unprocessed data was used. Furthermore, an additional HSA channel monitored the interaction between HSA and aBSA in experiment set 1 to report any interaction that may take place between the two species in solution in experiment set 3.

Table 3.1. Detailed experimental conditions for the three experiment series

Reaction Set	**1: High Affinity Binding**	**2: Low Affinity Binding**	**3: Competitive Binding**
Surface Ligand	BSA	BSA	Immobilised BSA covered in HSA from running buffer
Running Buffer	PBS	PBS	100 µM HSA in PBS
Injected Analyte	aBSA (10 nM, 20 nM, 40 nM)	HSA (2 µM, 20 µM, 50 µM, 100 µM)	aBSA (10 nM, 20 nM, 40 nM) + 100 µM HSA
Association Time	15 minutes	10 minutes	15 minutes
Dissociation Time	25 minutes	6 minutes 40 seconds	25 minutes
Figure 3.4 Trace Colour	Red	Green	Blue

The absolute response from each set of surface ligand spots was calibrated by measuring the change in response between PBS and double-concentrated PBS, which corresponds to a refractive index change (ΔRI) of 1.53×10^{-3} refractive index units (RIU). All data presented in this investigation are in Response Units (RU), which corresponds to 10^{-6} RIU.

3.3.1 Chemicals

Bovine serum albumin (BSA) (98%), human fibrinogen (60%, with 40% buffer salts; the protein content is >80% clottable FBR), and human serum albumin (HSA) (>96%) were obtained from Sigma-Aldrich; sheep polyclonal antibodies to BSA (aBSA, 23mg/ml, IgG fraction) were supplied by AbD Serotec UK; all solutions where prepared in 18 MΩ cm^{-1} deionised water and protein solutions were prepared in standard phosphate buffered saline (PBS, 137 mM NaCl, 2.7 mM KCl, 10 mM Na_2HPO_4, and 1.5 mM, KH_2PO_4, pH 7.3) unless otherwise stated.

3.3.2 Sensor Surface Preparation

The array format sensors were functionalized with proteins by printing 1 mg/ml HSA, BSA, fibrinogen, and transferrin solutions in PBS directly over the nanoparticle containing array spots, according to the key in Figure 3.2. After a 2 hour incubation period the slides were washed with PBS and stored dry at 4^{o}C before installation into the Liscar.

3.3.3 Experiment List

Three sets of reaction experiments were performed separately in order to interrogate individual parts of a complex set of reactions to determine rate constants. The experiments were:

1: High affinity binding – this is the clean antibody-antigen binding experiment (high affinity reaction) using PBS as buffer, varying the concentrations of aBSA binding to BSA. As a control, the signal from the fibrinogen channel is subtracted.

2: Low affinity binding– the low affinity reaction, this experiment measures the binding of HSA at several different concentrations to the BSA surface from PBS buffer.

3: Competitive binding – the competition reaction requires the surface ligand binding sites to be occupied with HSA before the high affinity binding reaction of interest can occur. Therefore PBS containing 100 μM HSA is used as the running buffer. The HSA from the running buffer is allowed to bind to the ligand first before the analyte solution, containing varying concentrations of aBSA in the same running buffer (100 μM HSA in PBS) is introduced to the surface. Once again the signal from the fibrinogen channel acts as a negative control and is subtracted from the BSA channel.

The reactions sets, with their respective running buffers, surface ligands, analytes and injection times are summarised in Table 3.1.

3.4 Results

Three sets of protein-protein binding reactions were performed using the Liscar platform, employing the experimental setup detailed in Table 3.1.

Firstly, to confirm that there was no interaction between HSA and aBSA in solution during experiment set 3, unprocessed data from the HSA control channel in experiment set 1 can be seen in Figure 3.3 compared with the unprocessed data from the BSA channel. It clearly shows the aBSA binding to the BSA channel, but shows no binding between HSA and aBSA. Therefore it can be assumed that the interaction between aBSA and HSA in experiment set 3 is negligible for the purposes of the model presented here.

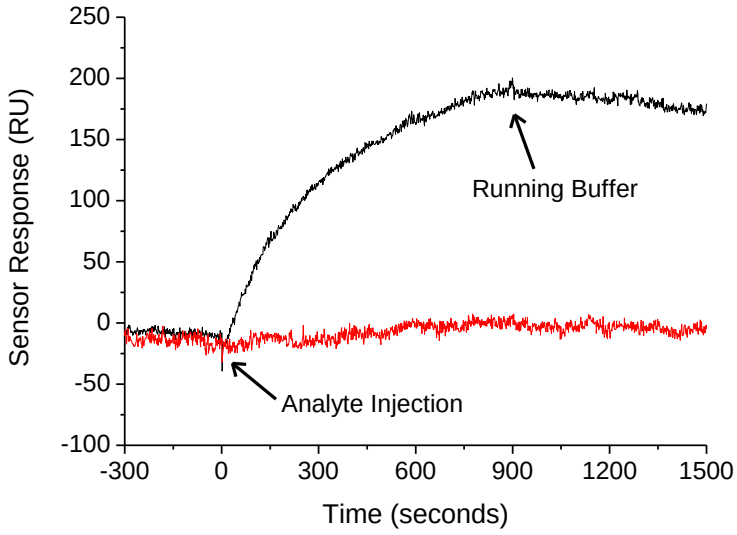

Figure 3.3. Binding traces for 40nM aBSA injected over BSA-functionalised spots (black) and HSA-functionalised spots (red). Switches between running buffer (PBS) and the analyte solution are also indicated.

As seen in Figure 3.4, red, kinetic traces were obtained for aBSA-BSA binding reactions (high affinity binding, reaction set 1) at aBSA concentrations of 10 nM, 20 nM and 40 nM in PBS buffer. The low affinity binding experiment (reaction set 2) was performed by injecting HSA in PBS buffer at concentrations of 2 µM, 20 µM, 50 µM and 100 µM, as is seen in Figure 3.4, green. An initial large jump is seen in the signal, especially for the higher concentrations, owing to the ΔRI between the running buffer and the analyte solution. The sum of the ΔRI between the running buffer and analyte solution plus the HSA binding to the surface causes an increased total sensor response.

Finally, the experiment for reaction set 3 was conducted to measure competitive binding between aBSA and HSA (high and low affinity analytes respectively), Figure 3.4, blue. The running buffer was changed to PBS + 100 µM HSA, and after the HSA was allowed to equilibrate on the sensor surface and the scattered light intensity had stabilised, analyte solutions containing aBSA at concentrations of 10 nM, 20 nM and 40 nM in PBS + 100 µM HSA were injected over the surface. A binding reaction can be seen for all three concentrations of aBSA.

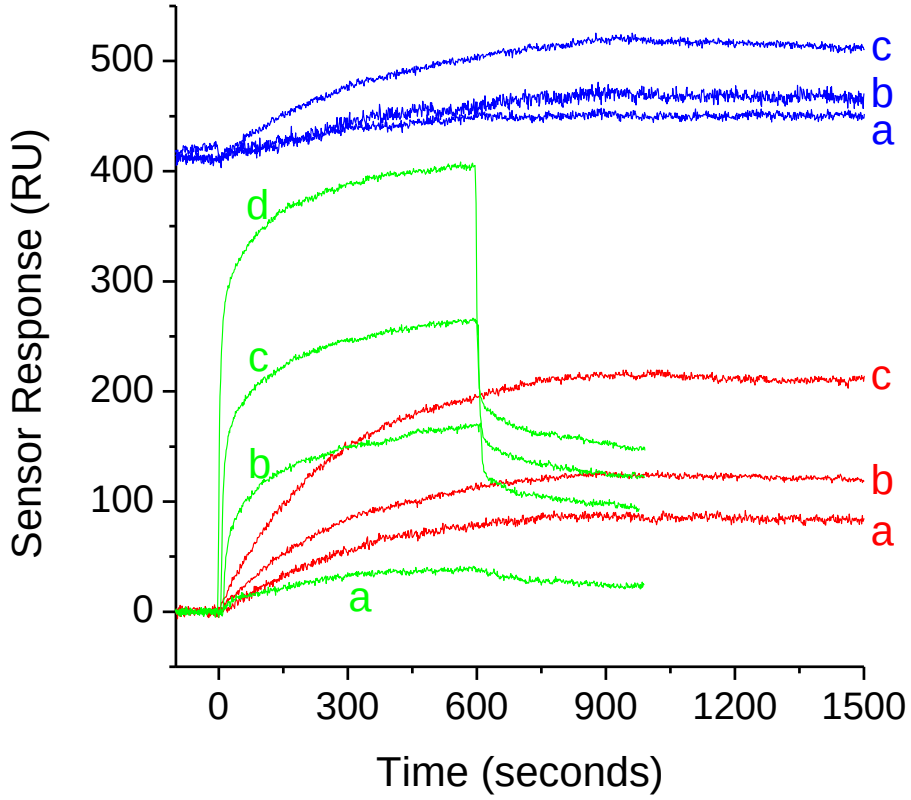

Figure 3.4. Kinetic binding traces for three sets of reactions: High affinity binding, red (a = 10nM aBSA, b = 20nM aBSA, c = 40nM aBSA); Low affinity binding, green (a = 2µM HSA, b = 20µM HSA, c = 50µM HSA, d = 100µM HSA); and Competitive binding, blue (a = 10nM aBSA in 100µM HSA, b = 20nM aBSA in 100µM HSA, c = 40nM aBSA in 100µM HSA). The baseline for the competitive binding data is offset to represent the refractive index difference and equilibrium HSA surface coverage due to the high concentration of HSA present in the running buffer. Owing to the specific nature of aBSA binding to the BSA surface ligand, the high affinity binding and competitive binding traces were produced by subtraction of the signal from the negative control channel, fibrinogen. However the nonspecific nature of the low affinity binding reaction meant the raw data was used, as the signal was approximately equal over all channels.

Each of the traces for the individual binding experiments produce sequentially increasing signal responses with increasing concentrations, as is expected. The high affinity reaction, Figure 3.4, red shows nearly no dissociation after switching back to the running buffer at 900 seconds, indicating a strong interaction between analyte and surface ligand. The low affinity reaction set, Figure 3.4, green, is comprised of a refractive index change (ΔRI) in the early part of the injection time, plus the binding of HSA to the sensor surface. The signal produced by the competitive binding reaction, Figure 3.4, blue, is therefore a sum of the ΔRI for 100 µM HSA

from pure PBS, plus the binding of HSA to the surface, plus the additional signal from the competitive binding reaction.

A large wash-off is seen for the traces in the low affinity binding experiment, Figure 3.4, green. This is largely due to the change in bulk refractive index of the analyte and the running buffer, especially the initial drop. After the initial drop, it also shows a greater wash-off than either of the other two experiments, giving some indication towards the low affinity this molecule has for the surface ligand.

It should be noted here that all traces shown in Figure 3.4 are averaged from three repeated binding traces at each concentration for a particular experiment set.

3.5 Discussion

The 1:1 interaction model for kinetic analysis of protein-protein interactions is used widely in the field as the first choice of model since it produces readily interpretable constants such as the association constant, k_a, dissociation constant, k_d and the affinity constant, k_a/k_d or K_D, for nearly all simple binding experiments [46; 86; 122]. However the 1:1 model has immediate obvious limitations when the target analyte is part of a complex medium such as serum, plasma or urine. The 1:1 interaction assumptions that binding is limited to one monolayer only, all binding sites are equivalent, and binding to a particular site is independent of any occupancy of neighbouring sites [129] are difficult to satisfy within such a complex analyte solution. The high concentration of nonspecific proteins means the specific interaction between the target analyte and the surface ligand is unlikely to remain uninfluenced by species adjacent to binding sites. The nonspecific proteins are likely to interact with the surface as a whole (binding sites or free space) and therefore this will have an effect on the analyte's ability to access the surface ligand, and in turn its ability to bind.

Alternative models, so-called Parallel, Competitive and Two State models, have been compared with the 1:1 interaction model [130] with an improvement of a factor of 5 in the

goodness of fit. However, even this investigation only dealt with simple solutions, containing just the analyte in buffer. The study concluded that the experimental data were not conclusive and could be interpreted in several ways. In light of this, it is also stressed that the model presented in this study is constructed from the individual reaction sub-sets step-wise including additional reactions when it is clear the model does not fit the experimental data well.

It is not possible to assign with statistical confidence the reactions to a particular analyte binding mechanism, but nevertheless this investigation aims to obtain meaningful parameters from three sets of reactions designed to give further insight into the possible binding and competition mechanisms present in real biological fluids. This is done by separating the individual components and monitoring their binding to the surface ligand, and then a competitive reaction is observed whereby the low affinity analyte obstructs the high affinity analyte for its binding reaction with the surface ligand. However, it is possible to assess the goodness of fit for a particular model, and thus to assess the chosen model based on its improvements from our starting point; the 1:1 interaction model in relation to complex media.

3.5.1 High Affinity Binding (aBSA-BSA binding only)

Initial analysis of the high affinity binding reaction used a 1:1 interaction model as characterised by the equations with rate constants k_1 and k_{-1} in Figure 3.5. The experimental data were fitted using a nonlinear least-square regression method employing the 'ode23' differential equation solver in Matlab. The association and dissociation phases were treated separately with different starting conditions in the differential equation solver – ca. 20 seconds of data bridging the point where the association phase is stopped is not included in order to be certain that no overlap between fitting of the association and dissociation phase occurs with the data from the opposing phase. The global fit to the simple 1:1 model shows a poor fit to the data, with a χ^2 value of 50.3. The χ^2 value indicates a poor model for the experimental data, however it must be compared with alternative models in order to assess the worth of an

alternative model. Additionally, the χ^2 value should be scrutinised with regard to increasing the number of parameters in the model for marginal improvement in χ^2 at the expense of an overly complex reaction mechanism. Therefore the χ^2 value should merely be considered a comparison metric for the models postulated herein, and is accompanied by the standard deviation of the residual which can also be compared between models.

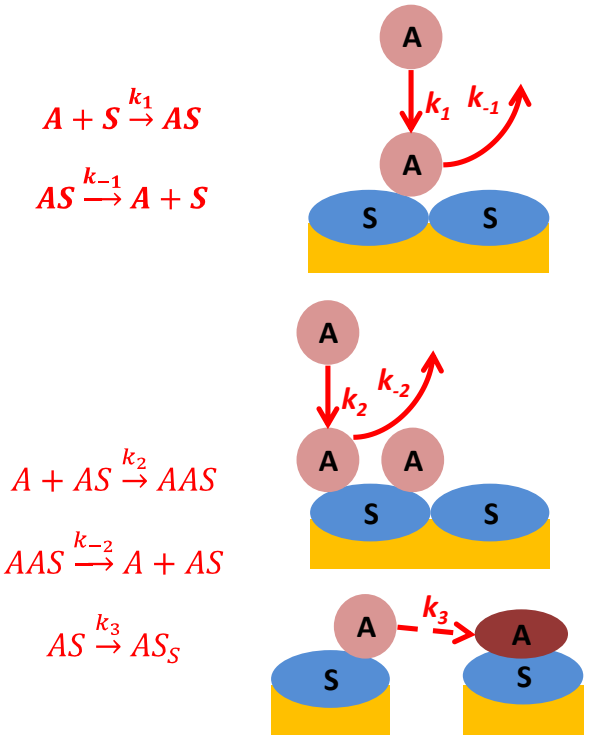

Figure 3.5. Schematic showing the reactions and mechanisms used in the model for the high affinity binding reaction set. The reactions in bold form the initial model, Figure 3.6, and the three extra reactions are added to refine it later, Figure 3.7.

It should also be noted that the absolute χ^2 value is not of particular use in this instance to determine the goodness of fit, as it can be seen from the residual plots in Figure 3.6 and Figure 3.7 that there is still a systematic error in the model, evidenced by the linear rising trend in the residual. However χ^2 is included for the purpose of evaluating the models employed within this study. The 1:1 model therefore needs further refinement, as the experimental data is not well defined by the 1:1 interaction model. It seems that the model consistently underestimates the initial association rate, but over estimates the maximum surface coverage (ϑ_{max}) of the analyte, and deviates especially in the latter parts of the association phase, Figure 3.6. This gives some

indication towards the unsuitability of the 1:1 interaction model, in that it suggests that there is some interaction between molecules on the surface, which will have an effect on both the rate and ϑ_{max} of the high affinity association reaction. Models have been altered before to allow the fitting of a heterogenous model in favour of the 1:1 [22].

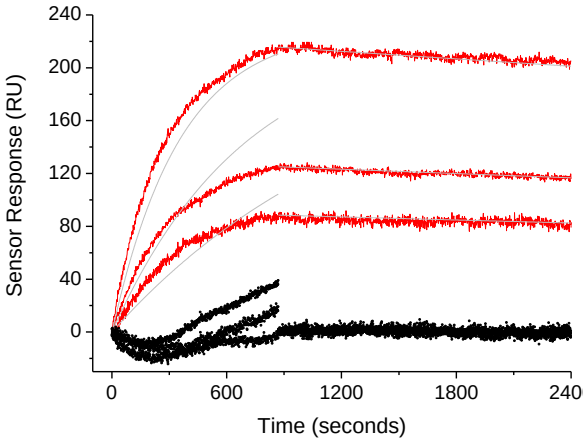

Figure 3.6. High affinity binding reaction (aBSA, red, a = 10 nM, b = 20 nM, c = 40 nM) fit to a 1:1 interaction model (grey), using the equations characterised by k1 and k-1. The residual between the fit and the raw data is shown in black.

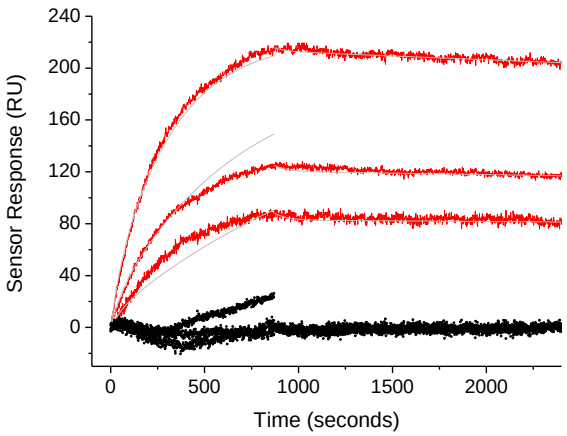

Figure 3.7. High affinity binding reaction (aBSA, red, a = 10 nM, b = 20 nM, c = 40 nM) fit using the model shown schematically in Figure 3.5, employing the reactions characterised by k1, k-1, k2, k-2 and k3 (grey). The residual between the fit and the raw data is shown in black.

The first refinement of the model adds two further reactions to the reaction set: a co-operative binding mechanism characterised by the rate constants k_2 and k_{-2}, and a further analyte-ligand complex stabilisation mechanism characterised by rate constant k_3, Figure 3.5. The reactions characterised by k_2 and k_{-2} allow for co-operative interactions between the analyte species on the surface, which will affect its binding to the surface, and therefore also its dissociation from it. This addresses the third assumption in the 1:1 model that species on adjacent binding sites do not interact with each other, which is highly unlikely in this scenario. The k_3 reaction captures the concept of a stabilisation reaction at the surface which may be explained by the avidity of the antibody, whereby the aBSA analyte has two binding sites, allowing it to form a stronger bond to the surface as a single molecule. With the introduction of these reaction mechanisms, the global fit yielded an average χ^2 value of 21.9, Figure 3.7, improving the fit by a factor of 2.3 from the initial 1:1 model.

The inclusion of the three extra reactions is empirical, and the mechanisms are postulated and not fully evidence-based from our experiments, however, it is needed to improve the goodness-of-fit to the data, and therefore the overall model. The justification for the inclusion of the extra mechanisms is explained below. The avidity of IgG, containing two Fab regions that can bind to the surface bound antigen, means that it can form a much more permanent bond to the surface, as can been seen experimentally by looking at the dissociation part of the binding trace in Figure 3.4, red. This provides justification for the addition of the reaction characterised by k_3, where the high affinity species is bound pseudo-permanently, and is modelled with no dissociation constant. Another postulated reaction is that, if one high affinity species binds close to another one of these molecules, they will have some effect on each other. This is not present in the simple 1:1 model, however it is unlikely that this is the case in such a concentrated protein solution, and therefore the inclusion of this reaction may be justified. This reaction is therefore treated separately and characterised by the constants k_2 and k_{-2}.

The extended model for the high affinity binding reaction is a better description of the experimental data, as evidenced by the χ^2 value above. Although it still overestimates the true ϑ_{max} for the reaction, it provides a much better estimate of the initial rate of reaction. Additionally, the standard deviation of the residual (during the association phase only) for the 1:1 interaction model is 13.4, compared with 8.6 in the alternative model. The extended model is only a reasonable description of the experimental data, and it suggests yet further complex mechanisms present at the surface, however expanding the model even more is unnecessary.

Assessing the quality of fit of the model

The model constructed herein attempts to present an undoubtedly highly complicated web of reaction mechanisms by a simple set of mechanisms, with specific focus on avoiding unnecessary over complication. The final model evolves from initial assumptions based on the

1:1 reaction model. Therefore any quantitative analysis of the goodness of fit only indicates the improvement of the model throughout its evolution. Thus, χ^2 and the SD of the residual is only used to compare the initial (1:1 interaction) model and the final model based on an expanded set of reaction mechanisms.

3.5.2 Low Affinity HSA-BSA Binding

They key difference between the analytes A and B used in this experiment is their respective affinities for the surface ligand, S, evidenced later by the difference in their affinity constants, K_D, Table 3.3. The concept of avidity allows for A to form a much stronger bond to S, and therefore it is referred to as the high affinity analyte, and B the low affinity analyte.

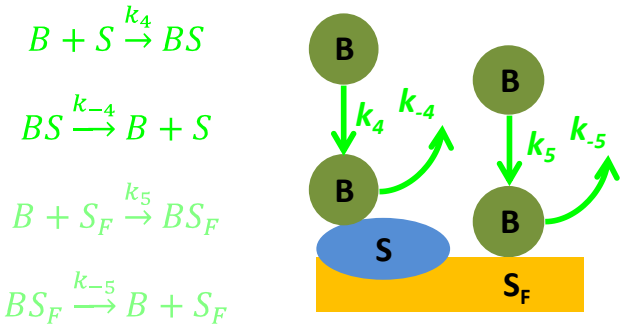

Figure 3.8. Schematic showing the reactions used in the model for the low affinity binding part of the investigation. The reactions in bold form the initial model, and the two extra reactions are added later for further refinement, where it is suggested that HSA may bind to additional binding sites (compared with aBSA) on the surface.

As with the high affinity binding reaction set, binding of HSA to the sensor surface, was initially fitted using a 1:1 interaction model as the starting point for the global fit using the reactions characterised by k_4 and k_{-4}, Figure 3.8. The global fit using a 1:1 interaction model yielded a χ^2 value of 64.3, and as can also be seen visually in Figure 3.10, the 1:1 interaction model is a very poor description of the experimental data. Once again the ϑ_{max} is underestimated, as is the initial rate of association.

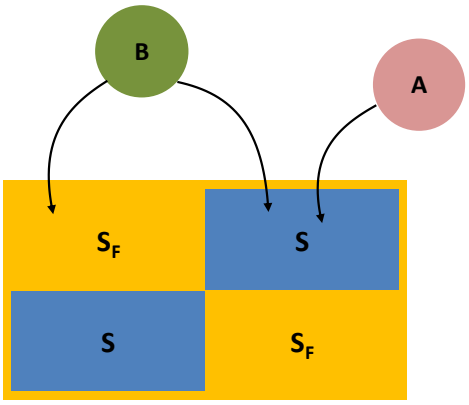

Figure 3.9 Schematic showing the differential binding for the high affinity IgG (A) to the surface ligand site (S) only, whereas the low affinity HSA molecule (B) can bind to both the surface ligand sites (S) and any available free surface sites (S_F).

It is suggested that unlike aBSA, which is restricted to binding only to exposed BSA epitopes on the surface, HSA can also bind to free parts of the surface (S_F) due to its nonspecific nature and, importantly, its large concentration in excess over the aBSA. The association reactions characterised by k_4 and k_5, (and their respective dissociation reactions, k_{-4} and k_{-5}, Figure 3.8) indicate nonspecific adsorption of HSA onto two different types of binding sites on the surface. As there are large differences in analyte concentrations in this experiment, it is crucial to treat the species separately in the model, as shown in Figure 3.9.

Justification for the binding of HSA to two different types of surface sites can be explained by considering the different maximum surface coverages (ϑ_{max}) achieved by the nonspecific and specific analytes. The ϑ_{max} achieved by the aBSA was 234 RU, compared with 195 RU for HSA (after subtraction of ΔRI contribution by bulk HSA from PBS), which yields a surface coverage ratio of 1.23. Considering that the mass ratio between aBSA (IgG) and HSA is 2.24 (150kDa/67kDa), it suggests that there are fewer binding sites available for aBSA than for HSA. Comparison between the surface coverage ratio and the mass ratio shows that aBSA can bind only to 55% of the surface available for HSA (1.23/2.24). This is also intuitive, as the sites available for aBSA binding are only where the surface BSA ligand is present and its specific

epitopes are exposed. Conversely the nonspecific nature of HSA means that it can bind to other free surface sites as well as surface ligand sites. This is shown schematically in Figure 3.9.

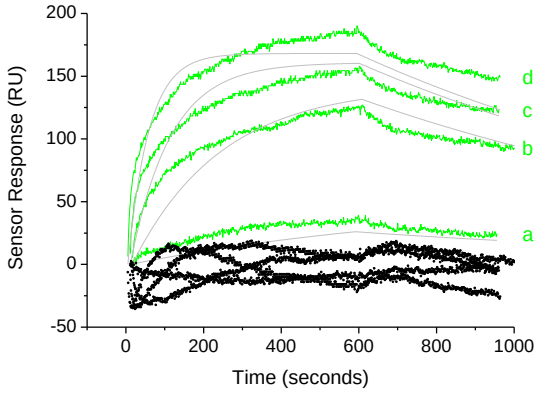

Figure 3.10. Low affinity binding reaction (HSA, green, a = 2µM, b = 20µM, c = 50µM, d = 100µM) fitted to a 1:1 interaction model (grey), using the equations characterised by k4 and k-4. The residual between the fit and the raw data is shown in black.

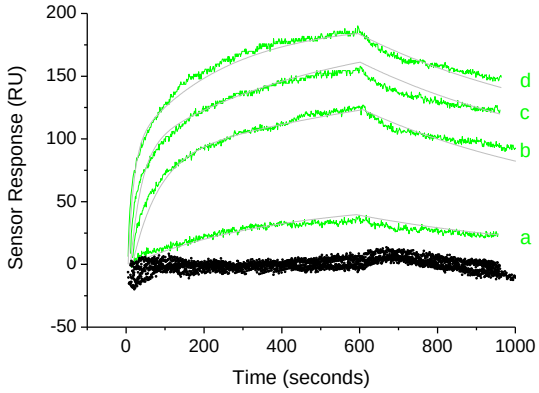

Figure 3.11. Low affinity binding reaction (HSA, green, a = 2µM, b = 20µM, c = 50µM, d = 100µM) fitted to an alternative model (grey), using the equations characterised by k4, k-4, k5 and k-5 to take account of HSA binding to two different surfaces as shown in Figure 3.8 and Figure 3.9. The residual between the fit and the raw data is shown in black.

As a result the model using the reactions characterised by k_4, k_{-4}, k_5 and k_{-5} was fitted to the low affinity binding data, yielding a χ^2 value of 5.48, Figure 3.11, improving on the 1:1 model by a factor of 11.7. Additionally, from the residuals traces in Figure 3.10 and Figure 3.11 it can clearly be seen that the introduction of the concept of different surface sites for HSA binding improves the fit considerably. For the association phase, the standard deviation of the residual was 12.1 for the 1:1 interaction model, *cf.* 4.0 for the alternative, free surface model, improving the fit by a factor of 3. Although the surface is blocked before any binding reactions are monitored, it would appear that nonspecific adsorption to the surface will take place regardless, and must therefore be considered in the model.

Table 3.2. χ^2 values, mean residual and residual standard deviation (SD) for the different models applied to reaction sets 1 and 2. The average χ^2 values for the global fir analysis is also calculated, taking into account the different association phase times between the low and high affinity analytes.

High Affinity Binding		
Analyte Concentration (nM)	χ^2 values for 1:1 Interaction fit	χ^2 values for fit using additional reactions
10	14.3	13.0
20	124	51.2
40	11.8	1.51
Average	*50.3*	*21.9*
SD of Average Residual	*13.4*	*8.6*
Low Affinity Binding		
Analyte Concentration (µM)	χ^2 values for 1:1 Interaction fit	χ^2 values for free surface reactions fit
2	41.5	3.25
20	83.4	7.76
50	79.4	3.38
100	52.9	7.51
Average	*64.3*	*5.48*
Average χ^2 for Global Fit	*56.3*	*14.8*
SD of Residual	*12.1*	*4.0*

3.5.3 Competitive Binding: HSA interference with aBSA-BSA binding

One of the objectives of this experiment was to produce a mathematical model characterising the reaction mechanisms involved in a surface ligand-specific analyte binding from a complex solution containing 100 µM HSA, which acts as a representation of physiological conditions. Once the sensor surface was refreshed with a regeneration buffer following the low affinity binding reaction set, the running buffer was changed to PBS containing 100 µM HSA and the

signal was allowed to stabilise. Then analyte solutions containing varying concentrations of aBSA in the presence of 100 µM HSA were injected over the surface and the signal recorded, Figure 3.4 and Figure 3.12, blue.

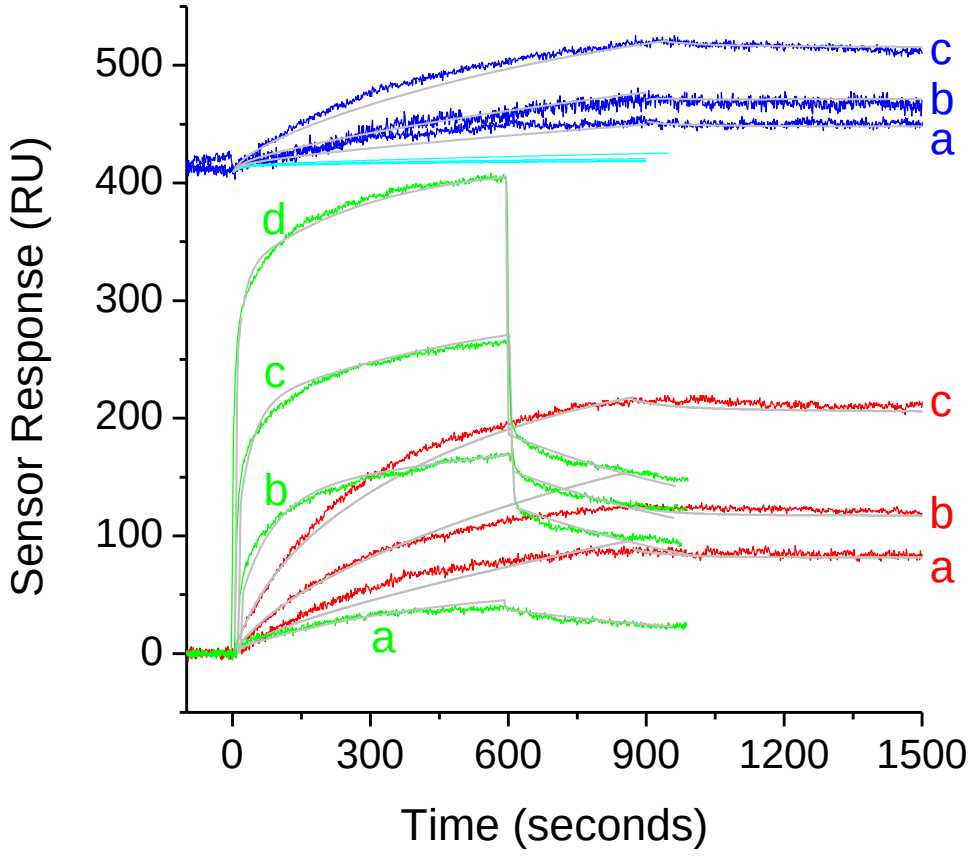

Figure 3.12. Kinetic traces for each set of reactions as seen in Figure 3.4: High affinity binding, red (a = 10nM aBSA, b = 20nM aBSA, c = 40nM aBSA); Low affinity binding, green (a = 2µM HSA, b = 20µM HSA, c = 50µM HSA, d = 100µM HSA); and Competitive binding, blue (a = 10nM aBSA in 100µM HSA, b = 20nM aBSA in 100µM HSA, c = 40nM aBSA in 100µM HSA). Included is the simulated model for competitive binding using parameters from High and Low affinity analysis only (light blue). Finally, after the introduction of a 'displacement' reaction to the model, k_6, a global fit for the data is achieved (grey).

Initial modelling of the competitive binding reactions used only the reactions from the high (Figure 3.7) and low affinity (Figure 3.11) reaction sets. Using the rate constants k_1, k_{-1}, k_2, k_{-2}, k_3, k_4, k_{-4}, k_5, and k_5 to model the data obtained from the competitive binding reaction set yielded the trace in Figure 3.12, light blue. Clearly, these reactions do not describe the experimental data, and therefore it could be concluded that using parameters derived from

high affinity and low affinity reactions in isolation are insufficient to model a competitive binding reaction between high and low affinity species.

As a positive increasing kinetic trace is observed in all three competitive binding traces (Figure 3.12, blue, a, b and c), it suggests the displacement of HSA by aBSA, as the positive change in signal is consistent with the difference in molecular mass (aBSA, 150 kDa > HSA, 67 kDa). Therefore it should also be noted that the signal change seen is not only aBSA binding to the surface, but rather the change in mass that comes with the displacement or replacement of the smaller molecule, HSA by the larger one, aBSA. The baseline for the competitive binding experiment is corrected for the bulk RI change and HSA binding to the sensor surface before the analyte is injected. This may be compared with Figure 3.4, green, d, where 100µM HSA was injected over a clean surface. It is therefore appropriate to include a further displacement reaction, as shown in Figure 3.13 and characterised by rate constant k_6.

$$A + BS \xrightarrow{k_6} AS + B$$

$$B + AS \xrightarrow{k_{-6}} BS + A$$

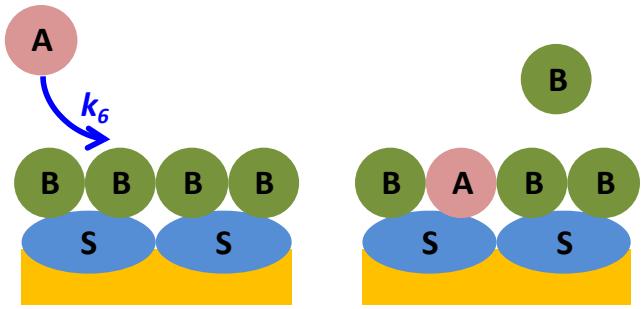

Figure 3.13. Schematic showing the 'competitive displacement' reaction of the Low affinity analyte by the high affinity analyte.

3.5.4 The Overall Global Fit – Competitive Binding Model

The competitive binding model including all of the mechanisms discussed previously can then be fitted to the global data set and is shown in Figure 3.12, grey, based on all the reactions in Figure 3.5, Figure 3.8, and Figure 3.13. These have been combined in Figure 3.15 for completion. The differential equations for the model are shown in Figure 4.14 and were solved numerically, globally for the complete reaction mechanism.

The model accurately reproduces the complete experimental data set with a χ^2 value of 1.16 for the entire fit, and 2.43 for the association phase only. The standard deviation of the entire fit was 4.70, and 4.05 for the association phase only.

$$\frac{d[AS]}{dt} = k_1[A][S] - k_{-1}[AS] - k_2[A][AS] + k_{-2}[AAS] - k_3[AS] + k_6[A][BS] - k_{-6}[B][AS]$$

$$\frac{d[S]}{dt} = -k_1[A][S] + k_{-1}[AS] - k_4[B][S] + k_{-4}[BS] - k_5[B][S_F] + k_{-5}[BS_F]$$

$$\frac{d[AAS]}{dt} = k_2[A][AS] - k_{-2}[AAS]$$

$$\frac{d[AS_s]}{dt} = k_3[AS]$$

$$\frac{d[BS]}{dt} = k_4[B][S] - k_{-4}[BS] + k_5[B][S_F] - k_{-5}[BS_F] - k_6[A][BS] + k_{-6}[B][AS]$$

Figure 3.14. Differential equations for each of the reactions used in the global fit model.

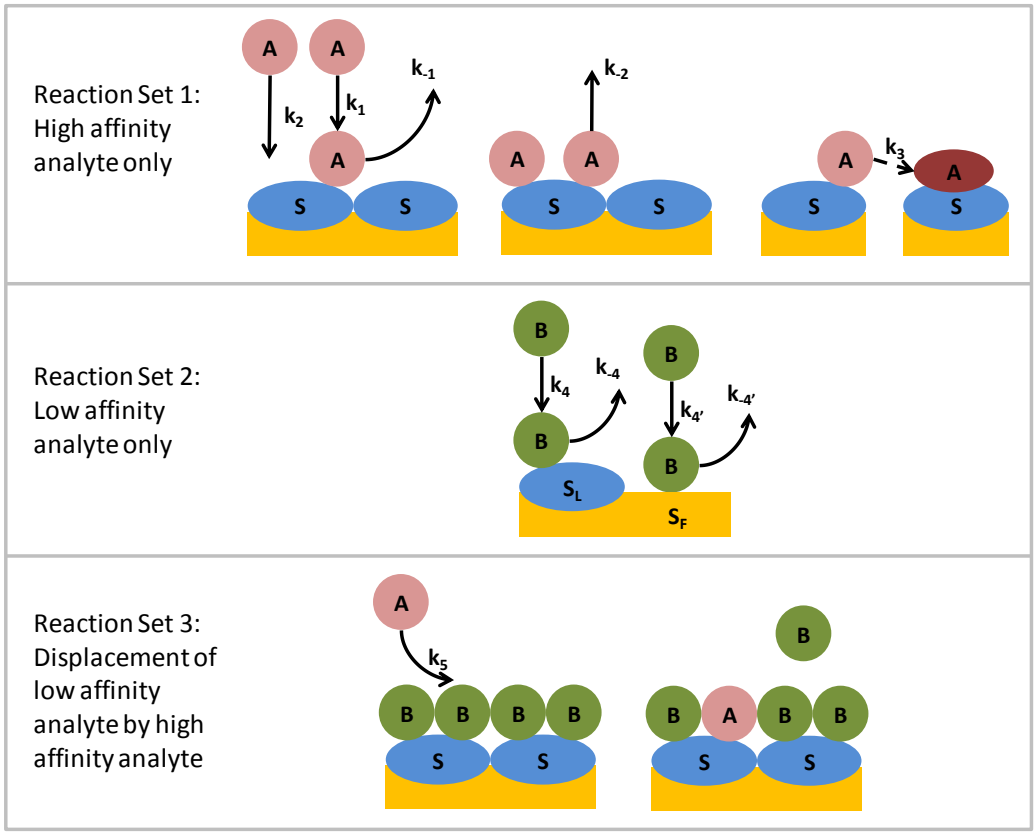

Figure 3.15. Combined reaction schematic outlining the reactions modelled for each of the reaction sets. The finalised, over all fit, Figure 3.12, is based on all of these reactions combined, with differential equations outlined in Figure 3.14.

The model comprises a simple set of postulated reactions consistent with observed experimental data for high and low affinity species binding competitively at a biosensor surface. The model has evolved by considering individual and competitive reactions separately, starting with the 1:1 interaction model and expanding on it.

Although there is no direct proof for the additional mechanisms in this model, there is some evidence of their existence in the literature. The reaction characterised by k_2 and k_{-2} can be described by cooperative binding [131], and justification for the surface stabilisation reaction, k_3, can be seen in Figure 3.12, red, c, where there is very limited wash-off when only PBS is reintroduced into the flow cell (after 900 seconds). Additionally, denaturation of proteins by the gold surface [132] may also explain the 'stabilisation' of molecule A onto the surface. The displacement reaction characterised by k_6 can to some extent be explained by the Vroman effect [133], however the additional affinity the antibody has for its antigen will also be a factor. The quality and assumptions in the model may now be considered.

Rate Constant Comparisons

The rate constants for the global kinetics model is presented below in Table 3.3.

Table 3.3. Kinetic rate constants for all reactions in the global kinetic model for all three reaction sets. Where possible, affinity constants (K_D) and the Gibbs free energy (ΔG) is also calculated.

Reaction Set	Reaction	Rate Constant	K_D (mol)	ΔG (kJ mol^{-1})
1: High Affinity Binding	k_1 (mol^{-1} s^{-1})	$(1.255 \pm 0.023)\cdot10^{5}$	$(6.51 \pm 0.32)\cdot10^{-8}$	40.73 ± 0.12
	k_{-1} (s^{-1})	$(8.17 \pm 0.37)\cdot10^{-3}$		
	k_2 (mol^{-1} s^{-1})	$(2.280 \pm 0.045)\cdot10^{4}$	$(1.00 \pm 0.12)\cdot10^{-9}$	50.57 ± 0.31
	k_{-2} (s^{-1})	$(2.29 \pm 0.28)\cdot10^{-5}$		
	k_3 (s^{-1})	$(5.838 \pm 0.091)\cdot10^{-3}$		
2: Low Affinity Binding	k_4 (mol^{-1} s^{-1})	$(5.961 \pm 0.053)\cdot10^{2}$	$(2.51 \pm 0.22)\cdot10^{-6}$	31.44 ± 0.23
	k_{-4} (s^{-1})	$(1.494 \pm 0.013)\cdot10^{-3}$		
	$k_{4'}$ (mol^{-1} s^{-1})	$(3.505 \pm 0.033)\cdot10^{1}$		
	$k_{-4'}$	Fixed at 0 (not defined)		
3: Competitive Binding	k_5 (mol^{-1} s^{-1})	$(6.41 \pm 0.12)\cdot10^{4}$		
	k_{-5}	Fixed at 0 (not defined)		

The mechanistic understanding following from the modelled set of reactions and rate constants focuses on comparisons between the low and high affinity reaction sets in order to determine the differences between them. Then a comparison is made between the high affinity and competitive binding experiment sets, as they both observe the binding of aBSA to BSA, albeit within a different environment.

As expected, the association rate constants for the specific, high affinity analyte (k_1 and k_2) are higher than the association rate constants for the nonspecific, low affinity analyte (k_4 and k_5).

The low affinity dissociation constant, k_{-5} was set to zero as it correlated highly with the other low affinity dissociation constant, k_{-4}. Therefore k_{-4} listed in Table 3.3 describes both dissociation processes of the low affinity analyte, and as the relative surface coverages of the reactions characterised by their respective association constants, k_4 and k_5, are in the ratio of 55:45, the true value of the dissociation constant k_{-5} is of the same order, 10^{-3} s^{-1}. This can be compared with the dissociation constants of the high affinity reaction set, of order 10^{-3} and 10^{5} suggesting a stronger interaction between the high affinity analyte and the surface than the low affinity analyte.

It is also interesting to observe the differences in K_D, (hence ΔG) between the high affinity binding and the low affinity binding reaction sets. The binding energy is approximately 1.5 times greater where the high affinity molecule is concerned, which is in line with expectations. Especially interesting in this comparison is the rates derived from k_1 and k_4 during the early part of the reaction, when the reaction characterised by k_2 cannot play a large part in the overall description of the reaction Table 3.4. At the concentrations used in the experiment, the rate of HSA adsorption onto the surface is much faster than aBSA, especially when 100 µM HSA is used, as in the case of the Competitive binding experiment. This places extra importance on the reaction characterised by k_6, as otherwise the sensor surface would be flooded by nonspecific proteins. This can be compared with physiological conditions, where the contrast in specific/nonspecific concentrations is even greater, as seen in Chapter 2.

The last reaction, with rate constant k_{-6}, illustrates the displacement of aBSA by HSA. This has been fixed at zero as the number could not be determined in the global fit. There could be a number of reasons for this, two suggested here. Firstly, the Vroman effect [89; 90; 91; 92] prohibits the reactions from taking place, as the mass of HSA is smaller than aBSA and it has a lower affinity for the BSA ligand. Secondly, from experimental observation we can see that in the competitive binding experiment, displacement of HSA by aBSA occurred in the presence of

a large concentration of HSA. This would suggest that the reverse reaction, HSA displacing aBSA is negligible at experimental conditions.

The most important observation about the model is the value of the rate constant k_6, which denotes HSA displacement by aBSA. More specifically, its magnitude in relation to k_1 is interesting, as it is only a factor of two smaller than the direct binding of aBSA onto the ligand, denoted by k_1. This suggests that, compared with no interference, when an antigen is surrounded by a large amount of albumin it takes approximately twice as long for a binding reaction to occur between the antibody and antigen. As already noted, the observed signal for the 'displacement' reaction is due to the change in mass between IgG and HSA, and not merely the arrival of IgG at the surface, which would yield a much greater signal. Also, as expected, we can see that the primary high affinity analyte association constant k_1, is over 200 times greater than the primary low affinity analyte association constant, k_4.

Initial Binding Rates

Further evidence for the existence of the displacement reaction characterised by k_6 can be seen from the comparison between the initial rates of the high affinity and low affinity binding reactions, specifically for 40 nM aBSA and 100 µM HSA, Table 3.4. At these concentrations, the initial rate of binding to the surface is a factor of 11.8 faster for HSA than aBSA. Therefore the experimental data should be expected to reflect this.

However, division of the kinetic trace for 40 nM aBSA in the high affinity binding reaction set, Figure 3.12, blue, (c), by the trace for 40 nM aBSA in the Competitive binding reaction set, Figure 3.12, red, (c), shows an initial ratio of ca. 8. This represents the upper limit of the ratio between the initial rates: firstly, as the signal from the Competitive binding is not all due to the arrival of the aBSA on the free surface ligands, HSA leaving the surface and aBSA taking its place results in signal proportional only to the aBSA-HSA mass difference rather than total

mass of aBSA. Secondly, only a fraction of the surface is freely available in the Competitive binding experiment. Therefore the observed faster-than-expected aBSA adsorption rate can be attributed to some other mechanism contributing to the model, here characterised by the exchange/replacement reaction with rate constant k_6.

Table 3.4. Comparison between association rates for the reactions characterised by k_1 and k_4, signifying specific and nonspecific adsorptions rates respectively at the given concentrations.

[aBSA] (nM)	[aBSA] × k_1 initial rate (10^{-3} s^{-1})
10	1.26
20	2.51
40	5.02

[HSA] (μM)	[HSA] × k_4 initial rate (10^{-3} s^{-1})
2	1.19
20	11.9
50	29.8
100	59.6

Correlation Matrix

A correlation matrix was calculated for each of the parameters used in the global competitive binding model. There are two pairs of relatively correlated rate constants; k_1 and k_{-1}, and k_1 and k_6. k_1 and k_6 are likely to be correlated because they describe similar processes – molecule A binding to S, even though the reaction described by k_6 also involves the displacement of molecule B before A can bind to S. k_1 and k_{-1} are likely to be correlated because they both contribute to the association phase for the high affinity binding reaction, however only k_{-1} is used to fit the dissociation reaction.

Table 3.5. Correlation matrix for all parameters used in the global analysis model. Correlated parameters are considered to be those > 0.8 and are indicated in red.

Correlation Matrix for all rate constants used in overall global fit model.									
	k_1	k_{-1}	k_2	k_{-2}	k_3	k_4	k_{-4}	k_5	k_6
k_1	**1.00**	0.84	-0.17	-0.62	-0.46	0.06	-0.15	0.01	0.83
k_{-1}	0.84	**1.00**	0.22	-0.71	-0.21	0.00	-0.21	0.03	0.65
k_2	-0.17	0.22	**1.00**	-0.18	0.13	0.01	-0.20	-0.08	-0.33
k_{-2}	-0.62	-0.71	-0.18	**1.00**	0.14	0.03	-0.42	-0.15	-0.46
k_3	-0.46	-0.21	0.13	0.14	**1.00**	-0.24	0.01	0.11	-0.71
k_4	0.06	0.00	0.01	0.03	-0.24	**1.00**	-0.04	-0.70	0.02
k_{-4}	-0.15	-0.21	-0.20	-0.42	0.01	-0.04	**1.00**	0.15	-0.06
k_5	0.01	0.03	-0.08	-0.15	0.11	-0.70	0.15	**1.00**	0.04
k_6	0.83	0.65	-0.33	-0.46	-0.71	0.02	-0.06	0.04	**1.00**

3.6 Conclusions

A 10-reaction competitive binding model is devised to describe the binding of a high affinity species against a large nonspecific low affinity species background. We have presented a global model for complex sample analysis employing individual high and low affinity reactions, and the displacement of the low affinity molecule by the high affinity molecule to simulate physiological conditions. Although the effect of albumin on antibody-antigen binding is notable, it is not major, which is expected and in line with biological considerations – for example if albumin had a notable effect on IgG binding to its respective antigen, the role of antibodies would be limited, especially given the high concentrations of albumin against individual IgG concentrations. Inclusion of additional postulated reaction sets has improved the model significantly. The correlation matrix shows only two out of a possible 18 correlation coefficients reaching ca 0.85, indicating that the model is not overcomplicated.

Our analysis shows that, even using complex samples, reliable and useful rate constants can still be extracted from kinetic analysis, and that the 1:1 interaction model should be expanded where complex samples are involved. This investigation shows the importance of a high affinity displacement reaction which has significance for all label free detection technologies screening complex samples. It provides a tool with which to analyse data from the Liscar where complex samples are analysed, and therefore has important implications for assay development on that platform.

Transferring immunoassays onto the Liscar platform is now a possibility, the major advance being the ability to screen complex samples with no pre-treatment. Once assays are developed on well established platforms they can be transferred onto the Liscar. The potential high-throughput capabilities of the Liscar instrument mean that we can interrogate an entire biological system by developing assays for the system constituents, thereby encouraging the introduction of multi-analyte biomarker panels. Such immunological systems could provide valuable information relating to patient recovery or overall state of health, which could prove valuable to clinicians. One such system-level profiling could be to interrogate the Complement cascade to profile the response of a patient to an immunological challenge rather than identify the challenge directly. The Liscar platform has the potential with the robust performance in the presence of high HSA levels to be a point-of-care device requiring limited sample preparation.

.

Chapter 4

Development of Electrochemiluminescent Assays for Complement Activation Products C3d, TCC and Bb

4.1 Introduction

The localised surface plasmon resonance (L-SPR) technique employed in Chapters 2 and 3 is capable of multi-analyte detection from a single sample. Ensuring the technique is optimised and validated for a chosen set of assays, a snapshot of a particular biological system can be taken from a sample at any given time from a single sample. The relative absolute concentrations between analytes can produce a profile of system activity at a given time, which may provide useful host-based diagnostic information valuable to a clinician caring for a patient. One such biological system is the Complement (C) System, introduced in Chapter 1 and outlined in Figure 4.1.

The C System, as part of the innate mammalian immune system, plays a key role in the immune response against pathogens [134]. The C system can be triggered by carbohydrate-recognising soluble factors, including mannose binding Lectin (MBL) and ficolins (Lectin pathway), microbial cell surfaces (Alternative pathway), or by antibodies bound to antigens in immune complexes (Classical pathway), Figure 4.1. Once triggered, the C system can trigger a number of responses including inflammation [57; 134; 135], chemoattraction of leukocytes [136], and lysis of pathogen membranes via the membrane attack complex (MAC) formed from the Terminal pathway [50; 57]. The C system is heavily self-regulated, with various mechanisms in place to ensure efficiency and prevent attack of host cells. Of particular interest is the fact that the C system is enzymatic, and does not require *de novo* production of system

components, as is required for CRP in the acute phase response. This means C can respond much faster when triggered, which has obvious advantages for monitoring patient recovery.

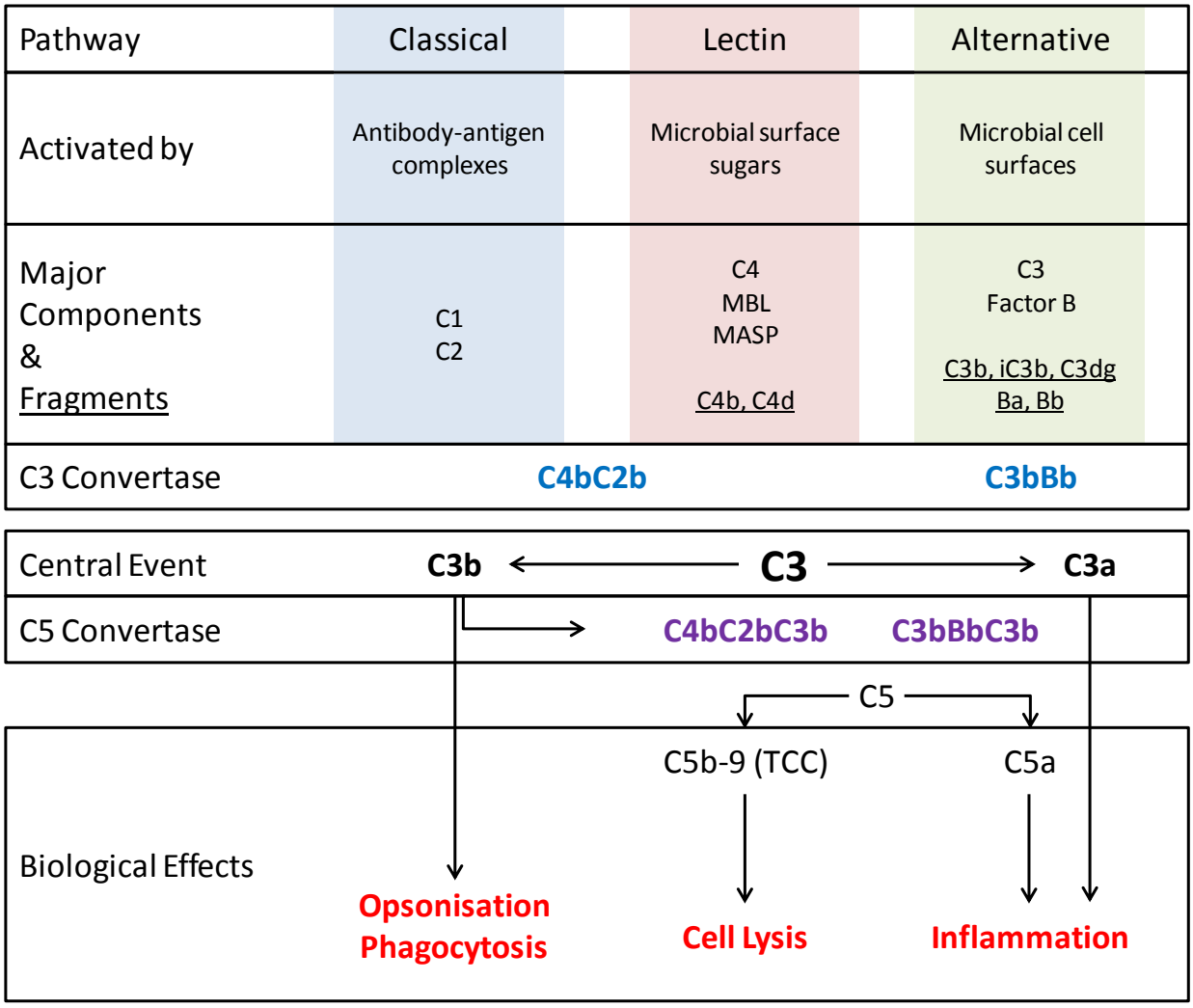

Figure 4.1. Outlay of the C system, with specific focus on activators, major components, fragments, C3 and C5 convertases, and the biological effects of the cascade.

Monitoring the C system response to an immune system challenge, for example inflammatory tissue damage [137] as a result of a surgical insult, can provide important information relating to immune system response and subsequent recovery. In principle, intimate perioperative monitoring of the developing state of a particular person's C system over the time course of recovery can provide a potential tool for presymptomatic diagnosis where pathogens activating C are involved. The idea being not to detect the pathogen itself but the response of the host's immune system to the pathogen challenge to produce a targeted diagnosis. This

approach is therefore applicable for monitoring both the effect of the surgical insult and also any C activation or consumption that may result from post-surgical secondary infections.

As mentioned, the C system has 4 distinct pathways [134], each with unique proteins that can act as a marker for activity in that particular pathway, Figure 4.2. The three triggering pathways may be activated separately, and therefore observation of activity in a particular pathway may be indicative of a trigger specific to that pathway, for example microbial cells triggering the Alternative pathway. The Terminal pathway can also be triggered independently by coagulation [138], so additional monitoring of this pathway is also crucial. It is with this aim and hypothesis that we have developed four assays to monitor the C system at key junctions, as they can be used to monitor complement activation at different points throughout the C system, which may lead to targeted diagnosis of disease based on relative pathway activity.

4.1.1 Previous Complement Activation Studies

Many C activation studies have been performed, where various combinations of fragments, C components and other activation products were used to establish C activation. A multi-analyte study was conducted which monitored levels and ratios of CRP, C3, C4, C9, TCC, C3a and C4d in pregnant women and in preeclampsia sufferers [139]. TCC and CRP was also used to monitor C activation following acute ischaemic stroke [140], and another study monitored the anaphylatoxins C3a and C5a, as well as C3, C4d and Factor B (fB) in emergency department patients with severe sepsis [141]. Two similar studies [142; 143] monitored C activation in cardiopulmonary bypass surgery, with both studies opting to monitor TCC, as it is an important and definite marker for overall C activation. However, the study by Hoedemaekers *et al* [143] also monitored the C3 convertase C3bBbP, and included the C3 and C4 fragments, C3bc and C4bc, as well as MBL and C1inh-C1rs. The other study, by Gu *et al* [142], monitored C3a, C4a, and the inflammatory marker Interleukin-6. Numerous investigations have shown C activation in Rheumatoid Arthritis (RA); one specifically monitored C3dg and TCC [144], and another

showed evidence for mediation of C activation by CRP [145]. A disease state firmly linked with C deficiencies is systemic lupus erythematosus (SLE) [146; 147], however C activation has also been monitored in patients with SLE using the anaphylatoxins C3a and C5a [148].

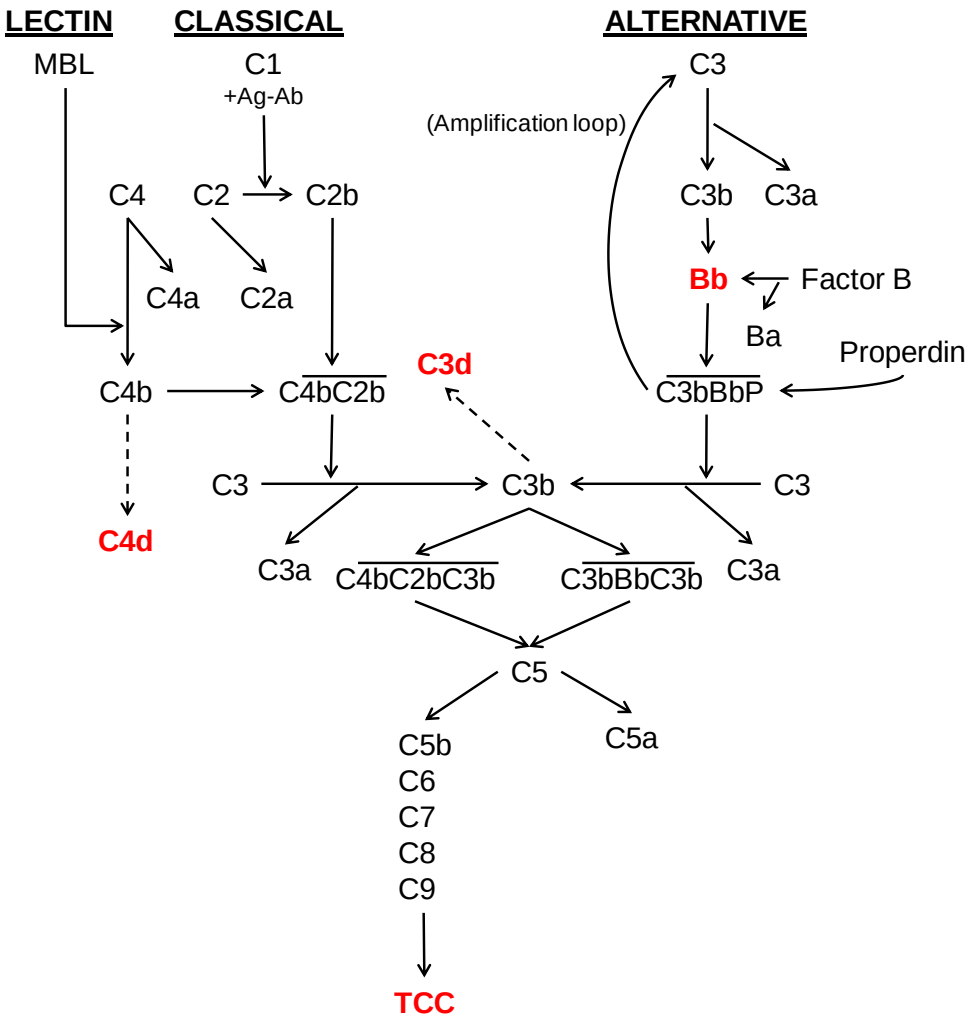

Figure 4.2. A schematic diagram showing the protein interactions of the three different C system pathways, leading to the formation of TCC. The selected assays are displayed in red. Ag-Ab denotes Antibody-Antigen complex

Considerable work has also been performed on *in vitro* C activation [147; 149], especially using Zymosan and Heat Aggregated IgG (HAIGG) to initiate C activation. Sample storage optimisation protocols have been developed [150; 151] so as to halt further *in vitro* C activation, thereby effectively freezing the C cascade at the time of sample collection. Some studies have focused on single pathway activation by removing key proteins in other pathways

[152], therefore halting C activation via that route, and another constructed the Alternative pathway using six isolated proteins, activating the pathway with erythrocytes [153].

C activation could also be monitored using urine samples, which contain several C activation products including the anaphylatoxins C3a and C5a. The kidney filtration cut-off (~45 kDa [121]) is larger than several of these C activation products, and therefore they will be found in the urine shortly after activation. Another study that focused on C5a and C3a in relation to SLE was conducted by Manzi *et al,* [154], where the analytes were measured in urine rather than plasma. Proteinuric patients were also monitored for C activation products, including TCC by Morita *et al* [155].

4.1.2 Aims and Objectives

This chapter explores the viability of developing immunoassays as biomarkers for Classical, Lectin, Alternative and Terminal pathway C activation. Specifically, electrochemiluminescence assays will be developed on the Meso Scale Discovery (MSD) platform for C3dg, TCC, Bb and C4d – all C activation markers. The development will also test the feasibility of using Activated Complement Serum (ACS) as a standard against which to measure C activation. Activation will be assessed *in vitro* using Zymosan and HAIGG as differential C activators, which will be a precursor for an *in vivo* C activation study in patients undergoing elective surgery in Chapter 6.

4.1.3 Proposed Complement Activation Study

This investigation aims to develop assays for C activation markers, with the explicit intention of combining the assays in a multiplex assay format later on, so that all the assays may be used together as a panel of biomarkers in a clinical trial to determine its use as a diagnostic test.

The set of biomarkers assays should provide a snapshot of the C system at a given time, and therefore the development of the C system throughout activation can be monitored from several snapshots over a given time course. The objective is dependent on the relationship between C activation and secondary infection. Given that this approach monitors the host

response (the C system) rather than the infection itself, its diagnostic value depends heavily on the implicit assumption that C activation correlates causatively with infection. It is important to make this distinction, and to appreciate that the detection of C activation would not necessarily mean the onset of a serious infection, but rather that it has responded to some immunological challenge, and therefore the patient's immune system has become alerted. Patients showing C activation could therefore be identified as 'at risk', and monitored more carefully for the event that the infection defeats the host's immunological defence mechanisms.

4.1.4 Differential Complement activation monitoring

The first hurdle to overcome in providing an assessment of C activation is to select the assays for the components that will indicate separate C activation at different key pathways of the C system, thereby providing information on a patient's C response profile, specifically the flux in each of the C pathways for that patient. The marker should ideally show a rapid response, and thus portray in 'real time' the developing state of the C system, and not suffer from the delayed reaction as with CRP. Finally and crucially, the protein should also be larger than the kidney filtration cut-off of ~45 kDa so that it remains present in the blood for a reasonable period of time and can therefore be detected in a blood sample.

Ultimately, the analysis may lead to the development of a model for the C system whereby, for example, the flux through the different pathways could be determined for a variety of activations. A similar study has been conducted with some success by Liu *et al*, [156] whereby time profiles of four C proteins and CRP were monitored during different activations. This study could be expanded to include many more C proteins, and a similar time profile analysis could be conducted for each individual pathway to assess the interaction between C proteins during activation. This would be a significant contribution to the fundamental understanding of the C system and its potential application as a tool for targeted disease diagnosis.

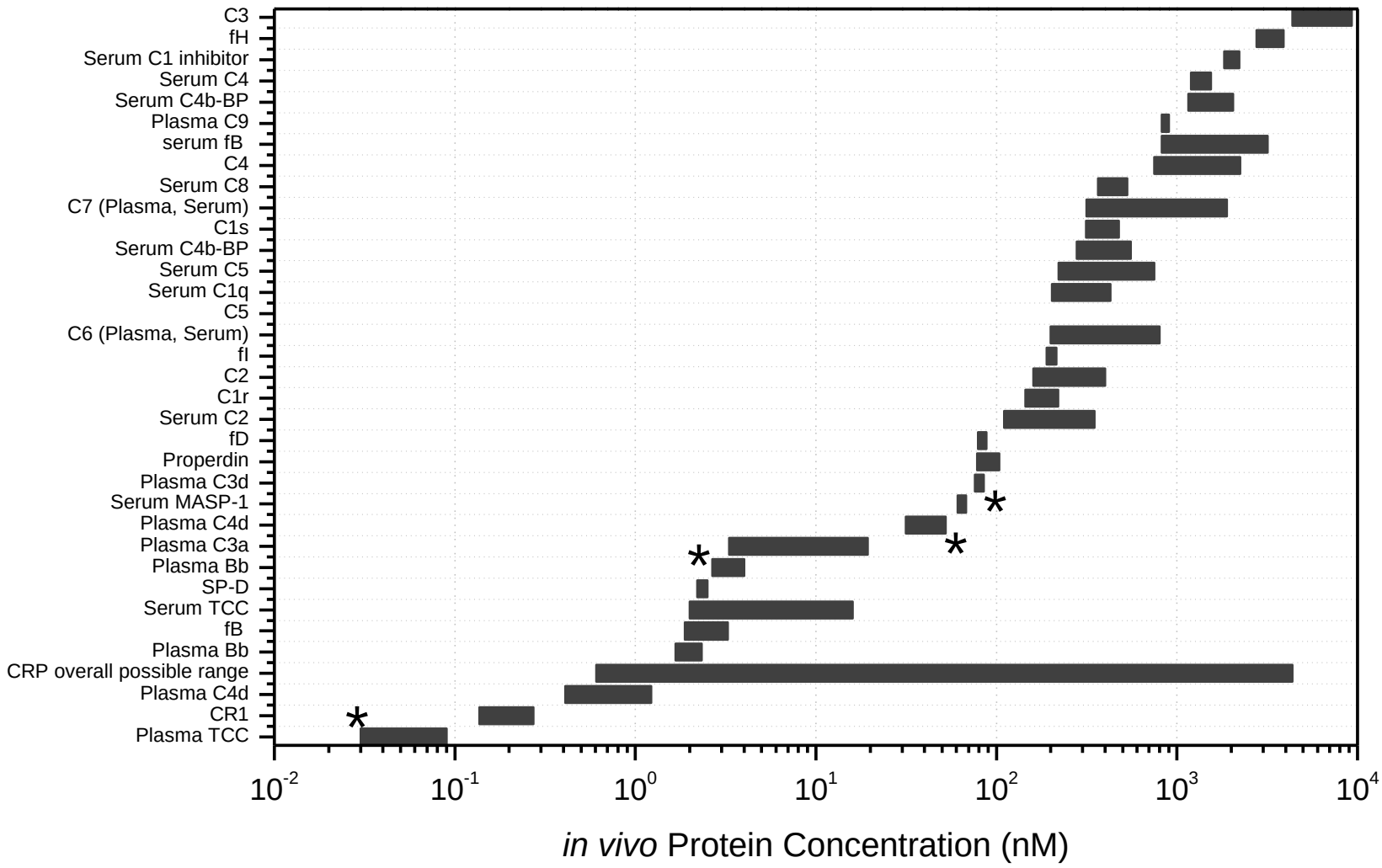

Figure 4.3. Molar range of 34 C system proteins and the overall possible range for CRP *in vivo*. Data collected from throughout the literature* denotes the target analytes of this study. Data collected from various references: [139; 157; 158; 159; 160; 161; 162; 163; 164]

4.1.5 in vitro Complement Activation

Many studies have been conducted to monitor Complement activation *in vitro* using Zymosan and HAIGG [147; 165; 166; 167; 168]. Kirschfink and Mollnes [166] point out that *in vitro* activation is useful for examining cross-species reactivity of an assay by activating the serum from a particular species using Zymosan, and comparing it with a non-activated control. Harboe *et al* used 'Zymosan activated serum' (the equivalent of 'Activated Complement Serum' in this study) as the standard for their TCC assay, which they defined as containing 1000 AU TCC/ml. It is important to consider that *in vitro* activation is not subject to the clearance and regulatory controls that would be present *in vivo*, but from the perspective of C fragment assay development it is a helpful way to monitor the progression of C activation, especially for the production of C fragments and activation products.

4.2 Target Activation Fragments

From the previous work done on C activation, discussed in section 4.1.1, it is clear that there is a wide range of potential C activation markers to screen in order to determine the best pathway-distinct markers for individual pathway flux through the system. There are several factors that can affect the performance of a particular marker as an indicator of pathway flux, for example clearance rates, intermediate complex formation, and activation rates, and these will determine the outcome of any investigation where a particular marker is interrogated. Figure 4.3 shows the concentration range of C cascade proteins in serum and plasma, which gives an indication about the target sensitivity for assay development

Biomarkers should be chosen and developed for clinical application and potential diagnostic use, and therefore should ideally be a good marker of activation *in vivo*. *in vitro* investigations can also be performed to validate the assays, yet the response from the target species will be different as activation fragments will not be cleared from the system. In light of the *in vivo* clearance of proteins, it is important to consider which fragments will be appropriate for a study to monitor *in vivo* C activation over a period of time. For such an investigation, plasma

samples are the only viable option as they can be taken at a specified time, and stabilised immediately with in EDTA. However, *in vivo,* due to the aforementioned clearance systems in place, it is possible to miss the increase in a particular protein concentration if activation and clearance occurs in between sampling points. For such a study timing will be as crucial as assay performance. However, if the window of opportunity for measuring increased analyte levels is indeed very small, the selected fragment may be unsuitable for *in vivo* C activation analysis.

With this in mind, the anaphylatoxins C3a and C5a may be less appropriate for such a study, as they will be cleared quickly through the kidney due to their small size, and although it is possible to detect these markers in urine [154; 155], it would be require a different sample collection protocol design. This also means that the other smaller fragments, C4a, C2a and Ba would be unsuitable. To interrogate the entire system, larger fragmentation products, unique to a particular pathway should be chosen so that distinct C activation can be established, thereby identifying the type of activating impulse.

We selected particular C target assays that would provide us with sufficient information to establish an overall C response. As is seen in Figure 4.2, C4d and Bb are fragments that are unique to the Alternative and Classical pathways respectively. C3d acts as an indicator for overall C activation, and TCC is the final component of the C system in the Lytic pathway. Thus, quantification of these four analytes over a given time course of patient samples will provide unique information about each pathway with regards to complement activation, and may lead to distinct diagnosis of disease, depending on the response obtained. Each target fragments chosen for this study is discussed individually below, with reference to their merits for selection.

4.2.1 Bb Fragment

The Alternative pathway protein Factor B, once bound to C3b, is enzymatically cleaved by Factor D to form the fragments Ba (33kDa) [169] and Bb (60kDa) [169], forming the unstable

C3 Alternative pathway convertase C3bBb, which can be further stabilised by 10-fold or more [170] by Properdin. The Alternative pathway can be triggered by various surface structures on foreign and apoptotic cells. This trigger not only supplements the spontaneous 'tick over' hydrolysis of C3 into its activation products C3a and C3b, but acts as a positive feedback amplification loop, significantly increasing C3 cleavage rate by formation of the active but unstable C3 convertase, C3bBb, as shown in Figure 4.4. Further binding of C3b to this convertase creates the C5 cleaving convertase, C3bBbC3b, leading to initiation of the Lytic pathway and eventual formation of TCC.

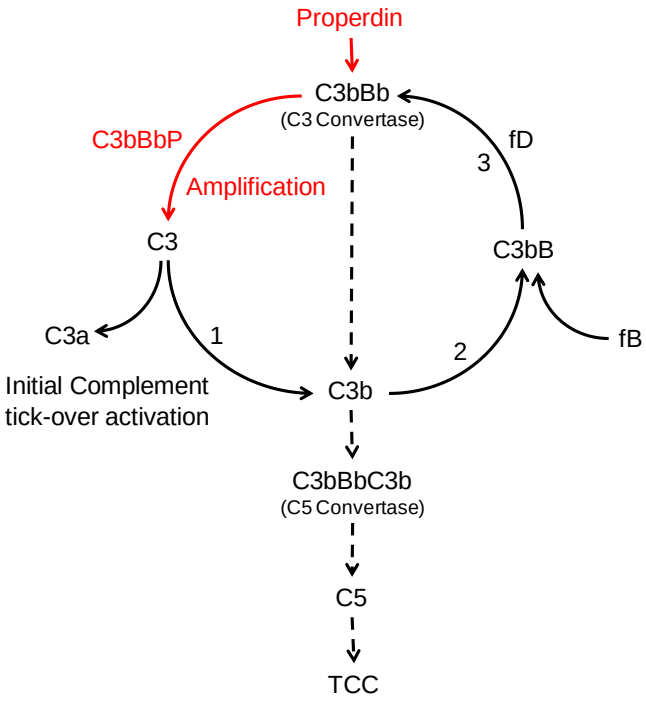

Figure 4.4. Schematic outlay of the Alternative pathway amplification loop. They key to this magnification in C activation is the ability of the intermediate end product, C3bBb to further activate the starting product, C3, causing it to fragment into C3a and C3b, the latter being the precursor for yet more C3 convertase formation. Additional intensification is provided by Properdin, which stabilises the C3 convertase, allowing it to activate even more C3 molecules.

As mentioned before, the Alternative pathway has been shown to be activated in a variety of diseases, including gram-positive and gram-negative bacterial infections [59; 171], viruses [172; 173], parasites [174; 175], cardiac bypass surgery [176]; and various dermatologic [177], renal [178] and hematologic diseases [179; 180]. Factor B and its fragments are unique to the

Alternative pathway, and therefore measuring activation of the Alternative pathway could be achieved by measuring Ba or Bb. A study by Wenish *et al*. [181] observed nearly a factor of three difference between C activated patients and healthy subjects. Commercial neoepitope antibodies exist for Bb, but not for Ba, and the molecular weight of Ba is below that of the kidney filtration cut-off (~45kDa) [121], which means it has a relatively short residence time in plasma. This suggests that Bb is the sensible option for monitoring the Alternative pathway.

Bb is therefore the best option to monitor Alternative pathway activation as it satisfies many of the practical requirements for a differential pathway activation marker; such as a molecular weight greater than the kidney filtration cut-off, available antibodies and assays for the fragment, and most importantly exclusivity to the Alternative pathway. It has a relatively low concentration in plasma (~20 µg/ml [139; 157]), and therefore it is important that the assay type chosen is sufficiently sensitive to detect the low concentrations of Bb. There have been many previous Alternative pathway activation studies that have used Bb as the target fragment [165; 182; 183; 184], both *in vivo* and *in vitro*, and it is the dominating choice of fragment for Alternative pathway activation in C literature. For these reasons, Bb will be used to monitor Alternative pathway C activation.

4.2.2 C3d Fragment

Evaluation of C3 fragmentation gives a good indication of general C activation as C3 is a key central component of the C system and is consumed by either of two C3 convertases, Figure 4.1. C3 can therefore be cleaved by activation of any of the upper cascade pathways, which is the first step in the production of our activation target. In the fragmentation process, C3dg is produced from a series of cleavages, as shown in Figure 4.5, that starts with cleavage of C3 (either by convertase or tick-over hydrolysis) into C3b (177kDa) [185] and C3a. C3b then associates with Factor B, which allows fD to cause enzymatic cleavage of Ba from the fB part of the C3bB complex, leaving C3bBb. C3bBb is a short lived [185] C3 convertase ($t_{1/2}$ = 90 seconds)

[186] that can be stabilised further by Properdin to form C3bBbP [158] to further stimulate the production of C3b, increasing C activation. C3bBb can then be dissociated into C3b and Bb by Factor H (which also acts as a cofactor to Factor I (fI) to degrade C3b into the inactive iC3b [187]) and finally C3dg (40kDa) [185] upon the cleavage of C3c [144; 185; 188], as shown schematically in Figure 4.5. *In vitro,* C3dg can be split into C3d and C3g [144; 189].

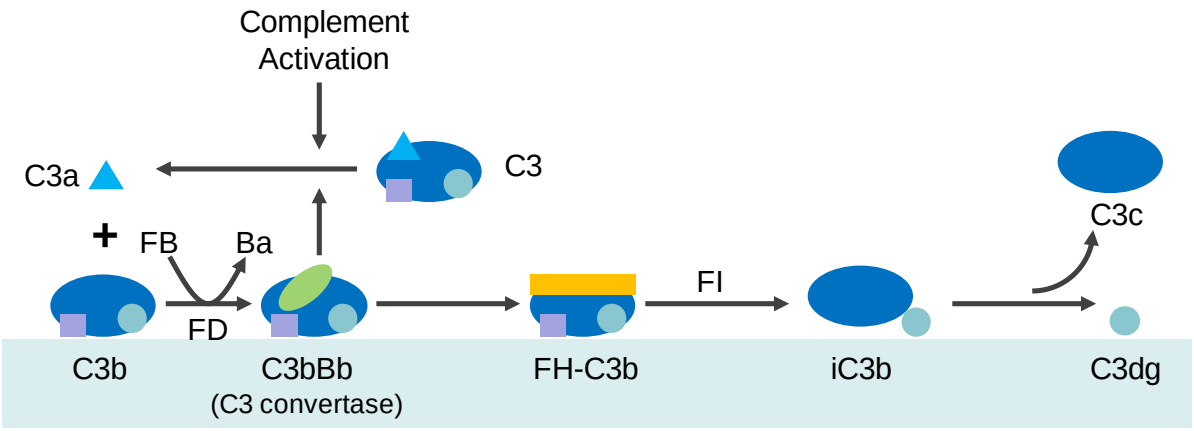

Figure 4.5 Detailed mechanism of C3dg formation from C3.

It should be noted here that as the antibody used to capture our target C3 activation products is specific to a neoepitope on C3d (and therefore detects all C3d-containing fragments, but not C3 itself [190]) the collection of C3 fragments assessed in this study (C3b/iC3b/C3dg) will be referred to collectively as 'C3d'. C3bBb could be detected but this is unlikely given its short serum half-life *in vivo* [185].

C3b, iC3b and C3dg have long been favourite markers of activation in the C community, [144; 190; 191; 192; 193] as C3 is such a central part of the C cascade. Commercial antibodies and assays exist for these fragments, and C3b and iC3b both have masses above (both 176 kDa [194]) the kidney filtration cut-off and are therefore present in circulation. Although the mass of C3dg is just below the kidney filtration cut-off, it still has a 'very long half-life' [195] which makes it a suitable target for this investigation. Therefore these fragments, collectively called 'C3d' will be the C3 fragmentation markers used in this proposed study.

4.2.3 C4d Fragment

An assay to determine the concentration of C4d in plasma will allow the observation of C activation via the Lectin and Classical pathways, Figure 4.2, as it is a fragment unique to this part of the cascade. The formation of C4d acts as a quasi-control on the C4bC2b C3 convertase formation as C4b is cleaved by Factor I and membrane co-factor protein (CD46) [196] into C4d – a catalytically inactive fragment [197]. Previous assessment of C activation by C4d measurement has included brain tissue of Alzheimer patients [198], and extensive assessment of organ allografts [197], particularly antibody-mediated rejection in human cardiac allografts [199], and capillary deposition of C4d in renal allografts [200]. The study by Wenish *et al*. [181] reported a concentration of C4d in C activated patients more than twice as big as the levels in healthy patients. Its molecular mass of 49 kDa [201] is also above the kidney filtration cut-off, which means it will remain in the blood supply for longer.

However, it must be said that comparatively there have been far fewer studies monitoring C activation using C4d than of any of the other markers discussed. This may be indicative of the difficulty associated with developing an assay for C4d. However, as it is unique to the Classical and Lectin side of the C cascade, it is crucial that an attempt be made to quantify the fragment for *in vivo* C activation analysis.

4.2.4 The Terminal Complement Complex (TCC)

TCC, also known as SC5b-9, is the final component in the complement system. The Lytic pathway concludes with the formation of TCC, either on the surface as the membrane attack complex (MAC) or in serum as SC5b-9, explained below.

Upon enzymatic cleavage by either the Classical or Alternative pathway C5 convertases (C4bC2bC3b or C3bBbC3b respectively), C5 splits into the anaphylatoxin C5a and C5b, the latter continuing the cascade as the basis for TCC formation. When C5b binds to C6 and C7, the

complex becomes inserted into the membrane and further associates with both C8 and several molecules of C9, forming the lytic pore. The nomenclature for this complex is therefore C5b-9. When activation occurs in the fluid phase, S protein binds to the complex rendering it nonlytic, and is referred to as SC5b-9, or TCC [61; 202]. Elevated levels of fluid phase TCC have been detected in patients with evidence of pathologic C activation, notably in cases of severe malaria [181] where plasma concentration of 1125.7 ± 496.9 µg/L TCC was observed, but also in kidney disease [203; 204; 205], inflammatory neurological disease [206; 207; 208], trauma and sepsis [209; 210; 211]. Therefore, serum TCC, SC5b-9, is the ideal target to measure C activation in the Lytic pathway and activity of the C5 convertases: its concentration is expected to rise with ongoing C activation *in vitro.* However, in the patient the surface-serum effects may be significant, making trends harder to observe especially given its low concentration in serum (~60 ng/ml), as shown in Figure 4.3. This requires the assay method employed to be sufficiently sensitive to detect such low concentrations of the TCC in order to establish its activation profile *in vivo.*

Nevertheless, TCC has also been an extensively assayed activation marker in the past, and several commercial assays exist for it. Especially encouraging is the existence of a neoepitope antibody, clone aE11, which is specific to TCC-bound C9. Furthermore, the fact that TCC is made up of several C proteins means that a range of sandwich antibodies could be trialled for use in the TCC assay. It also has a half-life of 50-60 minutes [212; 213], and is relatively stable *in vitro.* Additionally, an increase of a factor of 6 was observed for C activated patients compared with a healthy population [181].

4.2.5 Fragment-Specific Antibody Assays – Neoepitopes

The detection of C activation products is made possible by raising antibodies specifically to neoepitopes that are hidden in the native, un-fragmented component but become exposed on the surface of fragments formed during activation, Figure 4.6. This allows for the direct capture

of the activation fragment without interference from the respective parent C components. The development of specific monoclonal antibodies to the neoepitopes has generated new immunoassays to measure C activation specifically within the pathways of the cascade. These assays are a step forward from the older generation of C activation tests which concentrated on various separation and precipitation techniques [166].

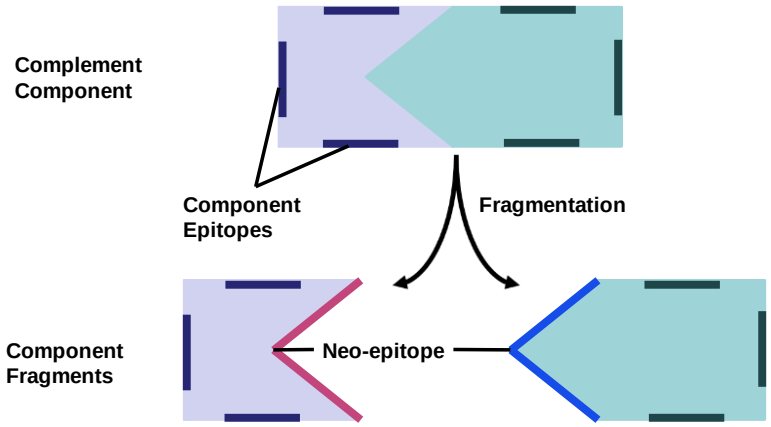

Figure 4.6. Schematic outlining the principle and origin of neoepitopes used to detect complement fragments.

A number of neopitope antibodies have been reported for the target fragments. Neoepitope detection principles have been reviewed recently by Mollnes *et al,* who describe the TCC neoepitope antibody [214], clone aE11. Three antibodies that each have an epitope on C9 are compared between EDTA-plasma and Zymosan activated serum. The first, polyclonal anti-C9 shows fast protein liquid chromatography (FPLC) fractions in both EDTA-plasma and Zymosan serum, for both TCC and C9, suggesting general specificity to both native C9 and TCC-bound C9. This would be expected from a polyclonal antibody batch. The second antibody, clone M1, presents C9 fractions in both EDTA-plasma and Zymosan serum, suggesting that this clone is specific to an epitope on native C9 only. The final antibody, clone aE11 shows a very small fraction for TCC in EDTA-plasma, and a large fraction for TCC in Zymosan activated serum, suggesting that clone aE11 is specific to the neoepitope on C9, exposed only when C9 is bound to TCC.

C activation products are generated rapidly *in vitro* [149], so it is essential to ensure that samples are collected and stored properly to avoid *in vitro* activation and therefore further generation of neoepitope containing fragments. Activation can be stopped by addition of Ethylenediaminetetraacetic acid (EDTA) at a final concentration of at least 10mM, after which the sample should be stored at -70^{o}C [166]. EDTA acts as a chelating agent that strongly binds Ca^{2+} and Mg^{2+}, both co-factors for complement activation.

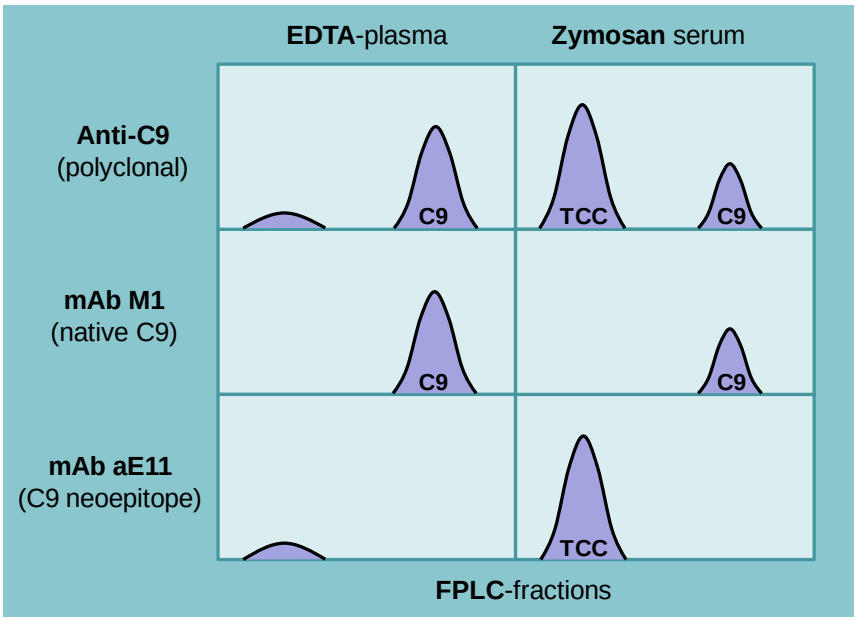

Figure 4.7. FPLC fractions of C components in normal EDTA plasma and C activated serum using Zymosan. C9 and TCC are detected using three different antibodies, displaying clearly the difference in epitope specificity: polyclonal anti-C9 reacting with a number of C9 epitopes, most activation independent; mAb M1 reacting with a native-restricted epitope exposed only on the native C9 component, and mAb aE11, reacting with a neoepitope created on C9 when bound into the C5b-9 complex (TCC). This is a key experiment to ensure the location of the epitope.

Epitope Access/Presentation

An important factor to consider when designing surface-mounted capture antibody assays is the position of the target epitopes on the analyte. If the detection antibody epitope is very close to the neoepitope used for capture, or if the binding of the neoepitope antibody to the fragment means that the epitope for the detection antibody is hidden, it is unlikely that the assay will perform well. Ideally the detection antibody should be specific to an epitope that

becomes presented when the neoepitope antibody binds to the fragment, shown schematically in Figure 4.8.

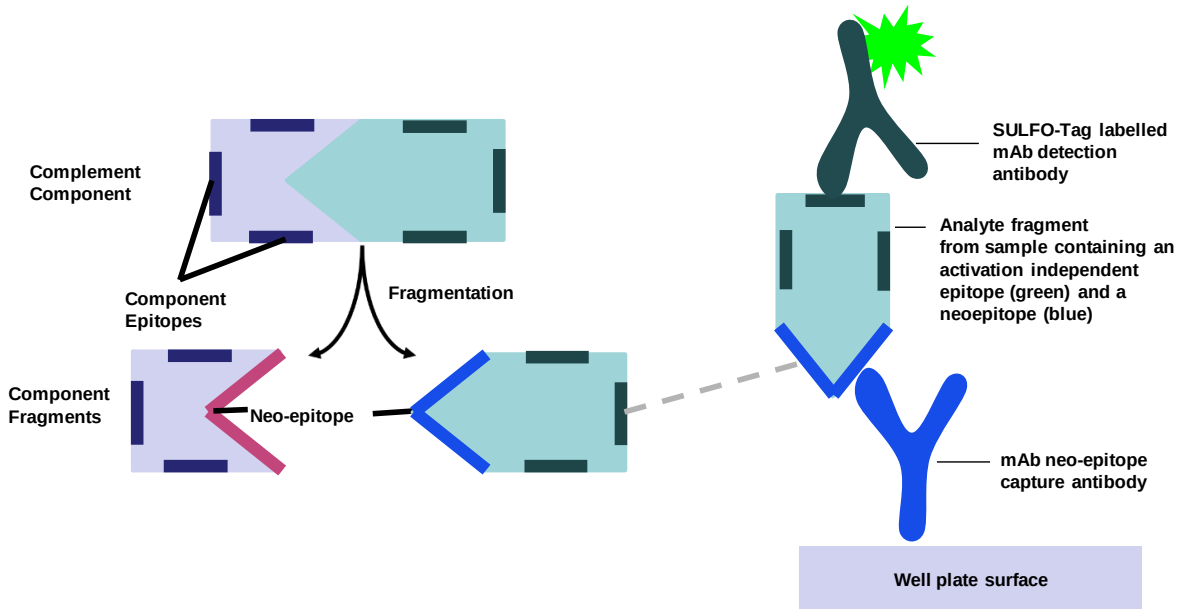

Figure 4.8 Schematic for a neoepitope fragment assay, detailing the neoepitope antibody specific to the neoepitope on the fragment, which can then be detected by a fluorescent antibody specific to an epitope elsewhere on the antibody.

4.3 Assay Method

Two different classes of electrochemiluminescence (ECL) assays are tested, one being a classical sandwich assay, the other employing a secondary species specific reporter antibody. Activated Complement Serum (ACS) is used as the calibration standard (supplied by Dr. Claire Harris, Cardiff, and stored at -80°C) in all ECL assays, and has itself been calibrated for TCC and Bb.

4.3.1 Electrochemiluminescence Assays

Thullier *et al* have performed ECL and ELISA comparison studies for ricin B chain and *Clostridium botulinum* type B neurotoxin [30; 31], using the same capture and detection antibodies for both targets. One of the studies [30] reported an 8 fold increase in sensitivity in the ECL format over the ELISA. Further, owing to the cost of the commercial ELISA kits for the C

fragment assays discussed above and the reported advantage in sensitivity via the ECL technique, this investigation aims to develop ECL assays for TCC, Bb, C3d and C4d.

The ECL platform used in this investigation is the Meso Scale Discovery (MSD) ECL instrument [30; 31]. The platform employs carbon electrodes in a 96-well plate format and, crucially, has the ability to perform multiplex assays, where each well can be functionalised with up to 10 carbon electrodes – each a different assay. Upon electrochemical excitation, the MSD instrument employs a CCD camera to detect light at 620nm, thereby eliminating problems with quenching. Additionally, assays with very low detection limits ($\leq 10^{-13}$M) [27] have been developed which is important from the perspective of this study, as the concentration of TCC in plasma is low ($<10^{-10}$ M), Figure 4.3.

We have chosen to develop ECL assays over ELISA or immunoturbidimetric assays because of the ability to multiplex the assays once developed. The performance of the assay in the clinical setting however needs to be assessed in a large scale clinical trial before it can be used as a diagnostic tool. The multiplexing capability of the MSD ECL instrument has significant economic implications for such a trial, which is a crucial advantage of this type of assay over ELISA or immunoturbidimetric assays.

4.4 Methods: Complement Activation Assay Development - TCC, Bb, C3d and C4d

4.4.1 Protocol for *in vitro* serum Complement Activation

This protocol has been adapted by combining protocols used previously by Bergseth *et al* [167] and Harboe *et al* [168], and tailoring it to suit a time course type study. Each of the referenced protocols focused on one end point, and therefore EDTA was added once to stop the cascade. Therefore our protocol was adapted so that the time course could be stopped for individual aliquots while the activation in the master batch could continue. The protocol in this study also had lower concentrations of the activating agents, as the focus of the time course study was to obtain several time points during the activation. Given that the protocol by Bergseth *et al*

produced near-complete activation of TCC after 1 hour, it was decided to lower the concentration of the Zymosan and HAIGG to slow down the activation. Also, in an attempt to show differential C activation, the activators were isolated, and two series of activations were performed, one with Zymosan, the other with HAIGG.

A stock of pooled human serum (Biochemed) was divided in two and temperature stabilised at 37^{o}C: to one half Zymosan (Sigma-Aldrich) was added to give a final concentration of 0.1 mg/ml; and to the second half HAIGG was added to make a final concentration of 0.1 mg/ml. Both activators were added to their respective stocks of serum simultaneously, at *t* = 0. 1 mL aliquots were taken 5 minutes prior to the addition of Zymosan and HAIGG as an initial value, and at several time points over a 24h period; in total at 0, 0.5, 1, 2, 4, 6, 10, 16 and 24 hours. Each sample was added to a concentrated solution of EDTA (Fluka) in PBS (Sigma-Aldrich) to make a final concentration of 10mM. The samples were centrifuged for 30 minutes in a Microfuge (Thermo Espresso Centrifuge) at 14400 RCF, after which two 300µL aliquots were taken from the top of the vial, leaving a Zymosan pellet. These aliquots were frozen immediately using liquid nitrogen and kept at -80^{o}C until the assays were performed. Due to the frequency of the sampling points and the time taken by the centrifuge step, at least two centrifuges are required initially to accommodate the incoming aliquots.

4.4.2 Polyclonal Secondary Antibody Assays

A neoepitope capture antibody against the target assay fragment is immobilised overnight at 4^{o}C onto the MSD high-bind plate surface (30µl, 1µg/ml in PBS). The surface is then blocked at room temperature for 1h using Blocker A (MSD) in PBS-T (PBS with 0.05% Tween-20), after which 25µl of the sample and assay standard, ACS (prepared in 10mM EDTA, 1% Blocker A PBS-T solution) is added to the surface for 2h at room temperature to bind any fragment present in the sample to the immobilised neoepitope capture antibody. The plate is then washed 3 times with 150 µl PBS-T, after which 25 µl of the polyclonal antisera (1/5000-1/1500 dilution.) is

added to the wells and left to incubate for 1h at room temperature. The plate is washed again as before, after which 25µl of the SULFO-TAG labelled secondary anti-species antibody is added to the well, and again incubated for 1h at room temperature. The plate is then washed a final time before 150µl of 1 × MSD Read Buffer is added to the wells before reading the plate using the MSD instrument. The assay structure is shown schematically in Figure 4.9.

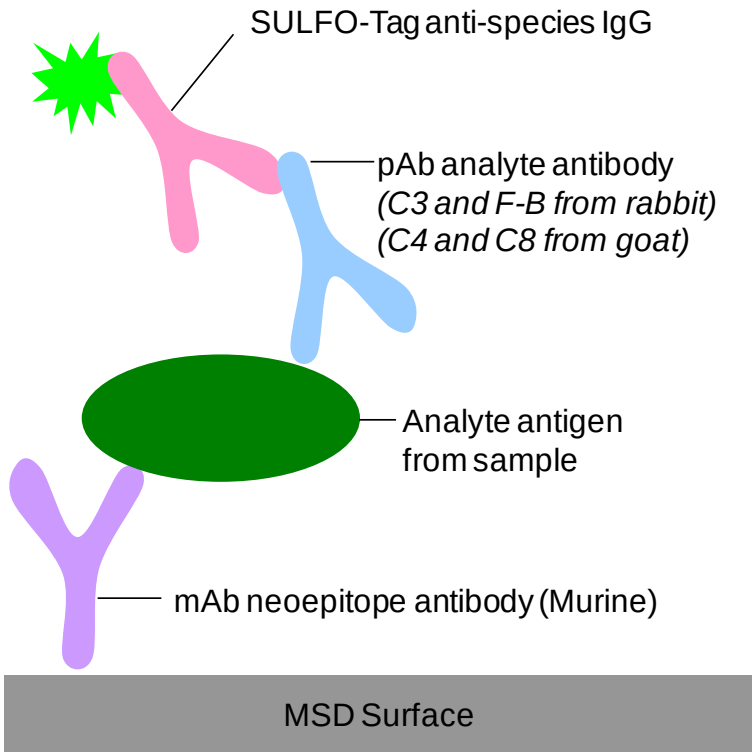

Figure 4.9. Schematic of Polyclonal Secondary Antibody Assay

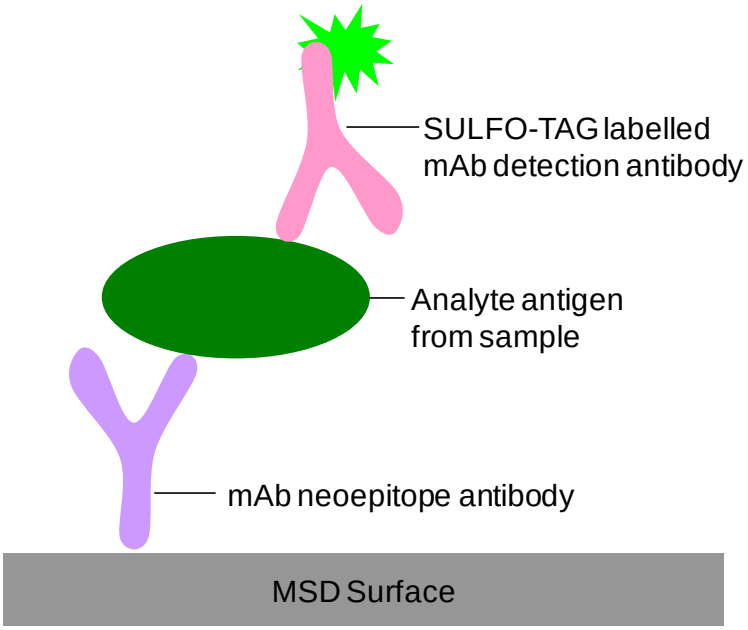

Figure 4.10. Schematic of SULFO-TAG labelled Monoclonal Antibody Assay

4.4.3 SULFO-TAG® labelled monoclonal antibody assays

A neoepitope antibody against the assay fragment is immobilised overnight at 4^{o}C onto the MSD high-bind plate surface (30 µl, 1µg/ml in PBS). The surface is then blocked at room temperature for 1h using MSD Blocker A in PBS-T (PBS with 0.05% Tween-20), after which 25 µl of the sample and assay standard, ACS (prepared in 10mM EDTA, 1% Blocker A PBS-T solution) is added to the surface for 2h at room temperature to bind any fragment present in the sample to the immobilised neoepitope antibody. The plate is then washed 3 times with 150 µl PBS-T, after which 25 µl of the SULFO-Tag labelled detection antibody (1/500 dilution) is added to the wells for 1h at room temperature. The plate is then washed a final time before 150 µl of 1× MSD Read Buffer is added to the wells before reading the plate using the MSD instrument. The outlay of this assay can be seen in Figure 4.10, and is based on a classical ELISA assay, developed with the help of Dr. Yvonne Clements (MSD).

The respective capture and detection antibodies for each assay are detailed below in Table 4.1, as well as the reported sensitivities and accuracies.

Table 4.1. Summary of all the monoclonal detection antibody electrochemiluminescence assays developed in this study.

Analyte	Capture Antibody	Detection Antibody (Labelled)	Detection Limit	Dynamic Range (orders of magnitude)	Intra-assay, Inter-assay Error	ACS Calibration Value
C3d	Anti C3d neo (Quidel), 1 µg/ml	Anti-C3b clone C3/30 (Dr. Claire Harris, Cardiff)	0.864 ACS Units	>3	8.8% 3.6%	C3bc in ACS ~1800 AU/ml [167]
Bb	Anti Bb neo (Quidel), 2 µg/ml	Anti-fB clone JC1 (Dr. Claire Harris, Cardiff)	995 ACS Units (54.7 ng/ml)	~1½	13.7% 3.9%	55 ± 6 µg/ml.
TCC	TCC mAb, clone aE11 (Hycult Biotech), 1 µg/ml	aC8 (Dr. Claire Harris, Cardiff)	1.11 ACS Units (2.32 ng/ml)	~3	18.2% 5.7%	2.10 ± 0.04 mg/ml
C4d	Anti C4d neo (Quidel), up to 4 µg/ml	Anti C4-1 (Dr. Diana Wouters), C4 mAb (Quidel)	N/A	<1	N/A	~18 µg/ml [167]

4.4.4 Labelling Detection Antibodies with MSD SULFO-TAG NHS Ester

The antibody labelling protocol is supplied by MSD, and is repeated here for completion. A 1-2 mg/ml solution of the antibody to be labelled is prepared in preservative-free PBS, pH 7.9. After equilibrating the antibody solution to room temperature, the MSD SULFO-TAG NHS ester (Figure 4.11) is reconstituted in water and immediately added to the antibody. The reaction vessel is incubated in the dark for 2 hours at room temperature, after which the free, unbound tag is removed from the reaction mixture by centrifuging three times at 1000 g for three minutes using a ZEBA Spin Desalting Column with a 40 kDa MW cut off at 4^{o}C. Once the unbound ester is removed, an optimal dilution of the antibody may be found for the respective assay.

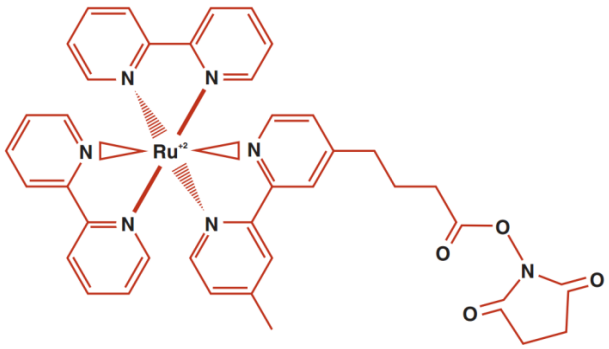

Figure 4.11. MSD SULFO-TAG® - Ruthenium (II) bi-pyridine, N-hydroxysuccinimide.

4.4.5 Assay Optimisation, Calibration and Controls

Two varieties of 96-well plates are available from MSD – standard bind and high bind (product numbers L11XA-6 and L11XB-6 respectively). Both were tested, yet the difference in assay performance between the plates was negligible. Therefore, the high bind plates were selected owing to the practical advantages: the high bind plates are hydrophilic as opposed to hydrophobic, and consequently initial filling of the well plate is easier; and incubation time for the capture antibody is also shorter. Concentrations of capture and detection antibodies were optimised by testing a variety of capture antibody and detection antibody concentrations, then

selecting the combination that yielded the greatest dynamic range. Consideration was also given to different dilution buffers at this stage.

Assay calibration vs ACS

All assays were calibrated using a stock solution of fully activated C serum (ACS) (prepared by Dr. Lana Hakobyan, Cardiff following the protocol set out by Mollnes *et al* [167]) that was quantified for TCC and Bb, and controls were performed for each test to determine assay degradation during the time it took to pipette all samples into the well plate. Every experiment included an ACS calibration channel employing 5-fold dilutions to obtain an ACS calibration curve, Figure 4.13, against which all assays were measured, with pure ACS being assigned a value of 10^6, and therefore values are reported relative to this.

ACS acts as a good calibrant against which to measure C activation as it contains high levels of activations products. If an absolute concentration can be determined for a particular activation product present in ACS, then subsequent measurement of an unknown concentration of analyte can be assigned an absolute concentration by comparison against the ACS calibration curve. ACS can be made cheaply, and in large quantities, so it is particularly well suited to large scale, multi centre studies. It can be made centrally, stabilised with EDTA, frozen and distributed to all the study participants.

4.5 Results

The results from this investigation comprise the rejection of the secondary antibody assay format, positive results from the tagged monoclonal assay, calibration values for TCC and Bb in ACS, and data from *in vitro* serum activation for all three assays, TCC, Bb and C3d.

4.5.1 Secondary Antibody Assays

Secondary antibody assays can be a useful format if monoclonal antibodies are not available to use as detection antibodies. Thus, a species specific antibody (pre-labelled by MSD) can be used to detect polyclonal antibodies specific to the analyte.

However, further development of secondary antibody assays was stopped owing to unacceptably high nonspecific background signal obtained from the whole antisera used in the assay, producing approx. 10^4 MSD counts. This high background level is most likely due to a high number of antibodies in the whole antisera having an affinity for the blocking solution used, Blocker A (MSD). Therefore, the labelled species specific antibody can bind to all these antibodies, as well as the specific antibody for the target analyte, as they are specific against all antibodies from a given species. This will then generate the large background signal from which any further increase in signal will be due to an increase in concentration of the analyte. However, as the upper limit for the MSD instrument is approx. 10^6 counts, the maximum obtainable dynamic range for this assay could only be two orders of magnitude, yet this was not attained as seen in Figure 4.12. This graph shows a typical secondary antibody assay, with a very high background signal and poor dynamic range – over one order of magnitude for TCC, but less than one for C4d.

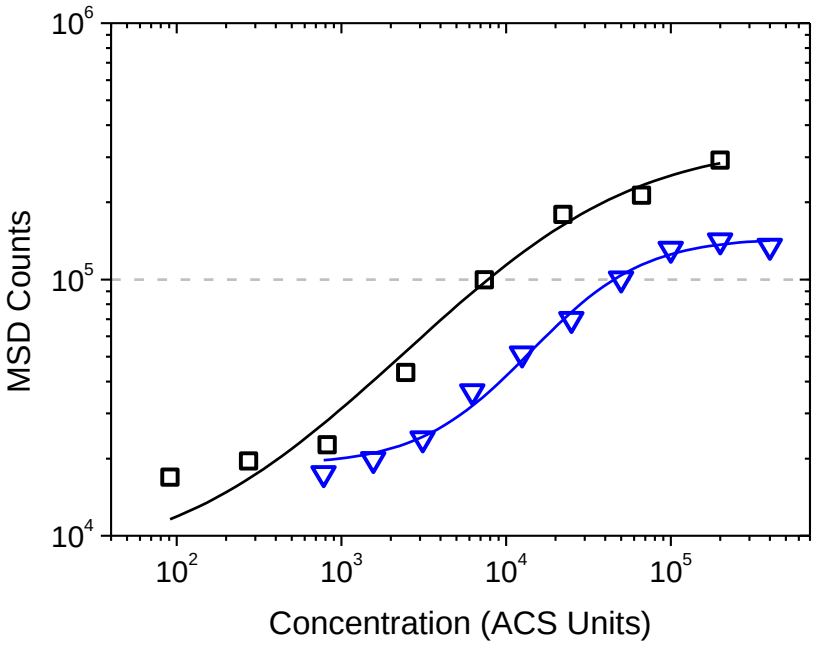

Figure 4.12. Typical ACS calibration curves for TCC (black) and C4d (blue) as secondary antibody assays. The high background (10^4 MSD Counts) and small dynamic range can be seen clearly. All data points are constructed from duplicate measurements.

This was therefore an insensitive assay, and any subsequent work to quantify the fragments in a given sample would be subject to substantial error. As a result any further work on this class of assay was halted. Nonspecific binding, its associated problems and possible solutions have been discussed in Chapter 2. Fortunately, the use of monoclonal antibodies in a traditional sandwich assay all but removed any background signal seen in the secondary antibody assay, as is shown below.

4.5.2 Tagged monoclonal assay development – TCC, Bb and C3d

All monoclonal assays had much lower background signals, approx. 10^2 counts, obtained by employing the protocol in Section 4.4.3. An anti-C8 antibody (supplied by Dr. Claire Harris, Cardiff) was used as a detection antibody for TCC, which consistently yielded a dynamic range of 3 orders of magnitude (Figure 4.13, black) and an assay sensitivity of 1.11 ACS Units (2.3 ng/ml). The anti Bb antibody, clone JC1 (supplied by Dr. Claire Harris) was used as a detection antibody in the Bb assay, and generally yielded a dynamic range of nearly 2 orders of magnitude (Figure 4.13, red) and a sensitivity of 995 ACS Units (54.7 ng/ml). The detection

antibody used in the C3d assay was the clone C3/30 (supplied by Dr. Claire Harris), which is specific to an epitope on C3b, from which C3d stems. This assay consistently yielded a dynamic range of nearly 3 orders of magnitude (Figure 4.13, green) and had a sensitivity of 0.864 ACS Units.

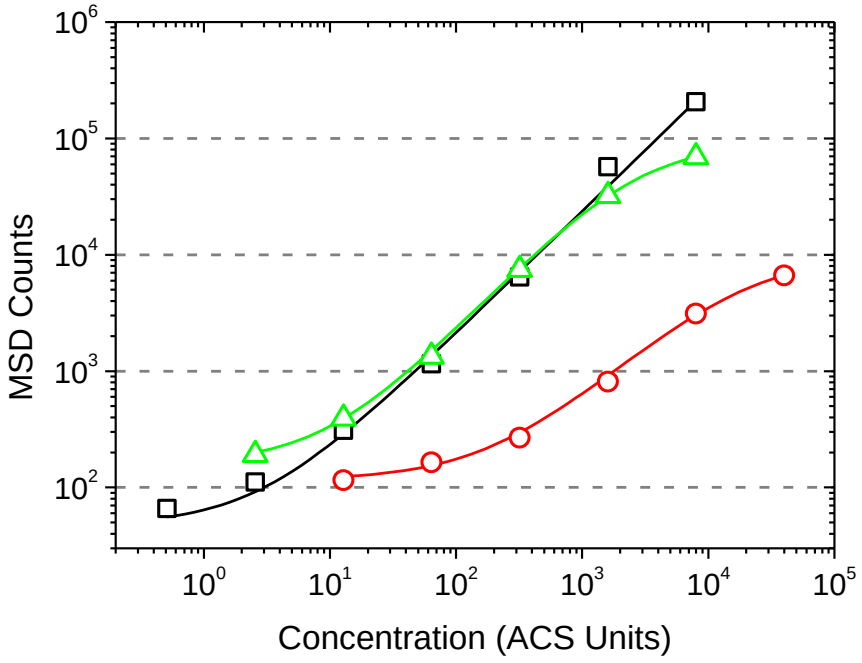

Figure 4.13. Typical ACS calibration curves for TCC (black), Bb, (red) and C3d (green). All data points are constructed from duplicate measurements.

All standard curves were fitted to the following expression by the MSD proprietary software, Equation 4.1,

$$y = b2 + \frac{b1 - b2}{1 + (x/b3)^{b4}}$$

Equation 4.1

where b1 and b2 defines the maximum and minimum of the curve respectively, b3 the midpoint and b4 the slope. Given there are 4 parameters in the curve it is important to have at least 4 points to fit within the dynamic range of the curve. All standard curves for all experiments fulfilled this requirement.

C4d Assay

We were unable to develop an ECL assay for C4d. The antibody combinations used yielded a dynamic range of less than one order of magnitude with little or no linearity. With such a poor dynamic range it was decided to reject C4d from the current activation analysis.

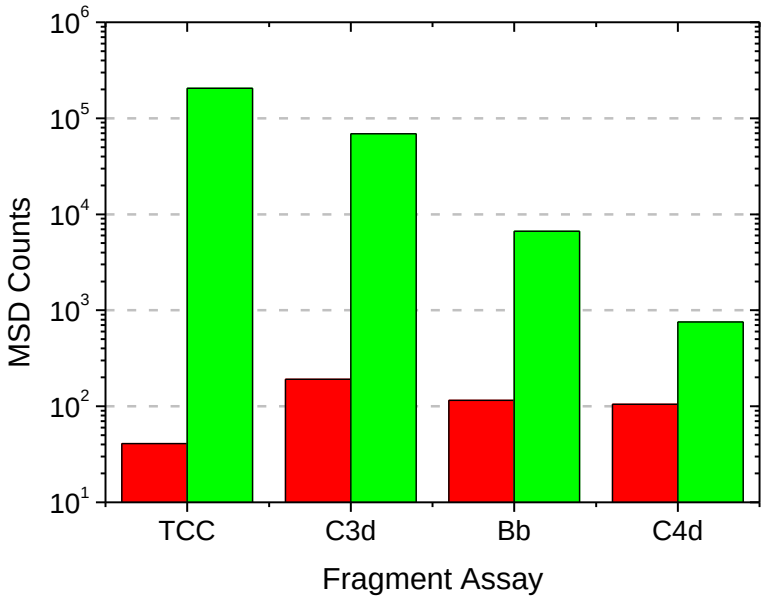

Figure 4.14. Typical upper (green) and lower (red) detection limits for all assays. Note C4d has a dynamic range of less than 1 order of magnitude.

4.5.3 Activated Complement Serum (ACS) Calibration– TCC and Bb Calibration

Both calibration experiments followed the same protocol as the tagged monoclonal antibody assays, Section 4.4.3, but for the dilution buffer.

ACS was calibrated for TCC, Figure 4.15, using purified TCC protein supplied by Dr. Claire Harris at Cardiff School of Medicine, Figure 4.15, black. Human plasma was used as the diluent throughout this experiment to maximise dilution invariance, but as a result the background signal associated with the assay also increased to ~10^3 MSD Counts, compared with <10^2 when using the standard PBS-T based buffer as in Figure 4.13. Serial dilutions of ACS were assayed against the purified TCC, after which a concentration was obtained for the ACS sample. This was then multiplied by the dilutions factor to obtain the data in Figure 4.15, blue. The consistent vertical correlation indicates a very conformity between all samples as to the

concentration of ACS. The concentration of TCC in the ACS calibration standard was determined as 2.10 ± 0.04 mg/mL.

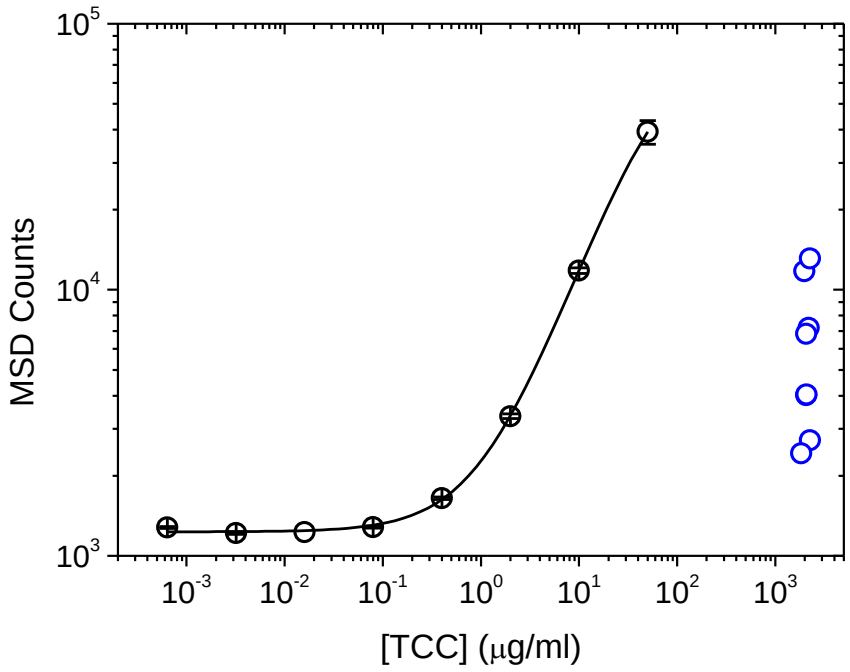

Figure 4.15. Calibration of ACS (blue) using purified TCC protein (black).

Similar ACS calibration experiments were performed for Bb, Figure 4.16, using a purified protein standard from Comptech, USA, Figure 4.16, black. The dilution buffer used in this experiment was human plasma, diluted 10 fold in PBS. Using pure plasma as the dilution buffer swamped the signal with high background noise, and using PBS only provided varying numbers depending on the level of ACS dilution. As for the ACS TCC calibration the separate dilutions of ACS assayed for Bb yielded consistent results, evidenced by the vertical line of blue circles in Figure 4.16. This experiment reported a Bb level in ACS of 55 ± 6 μg/mL.

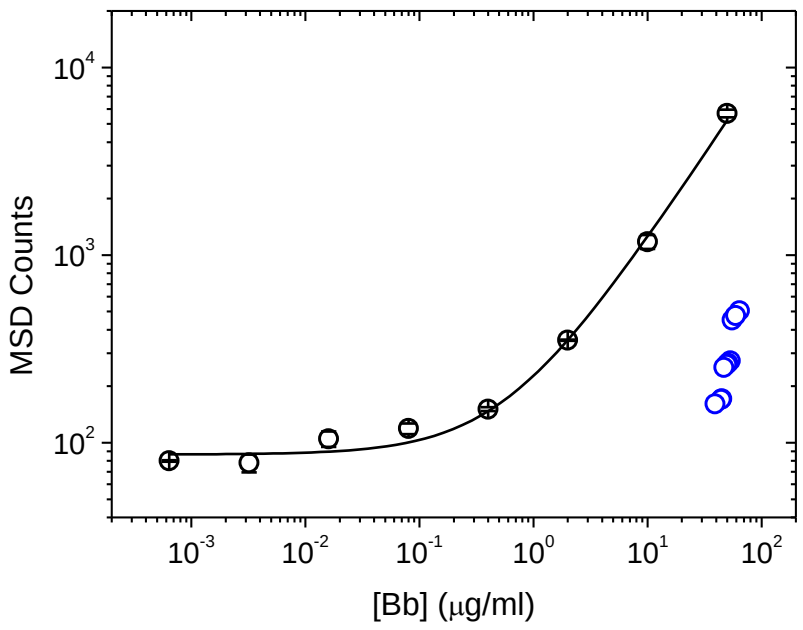

Figure 4.16. Calibration of ACS (blue) using recombinant Bb protein (black).

4.5.4 *in vitro* C activation assessment using Zymosan and HAIGG

The serum C activation, as detailed in section 4.4, was assayed for TCC, Bb and C3d over the measured time course. For TCC separate C activations were observed between Zymosan and HAIGG, as shown in Figure 4.17, whereas there was little difference between the Zymosan and HAIGG activations of both Bb, Figure 4.18, and C3d, Figure 4.19, and as a result the average of both responses was taken.

Comparison with the protocol and results from Bergseth *et al* [167], who observed near complete TCC formation after one hour using 10 mg/ml Zymosan and 1 mg/ml HAIGG, shows a slower rate of formation of TCC, continuing to rise up exponentially to 24, Figure 4.17. No activation is seen when HAIGG is used as an activator, the level of activation being within the error.

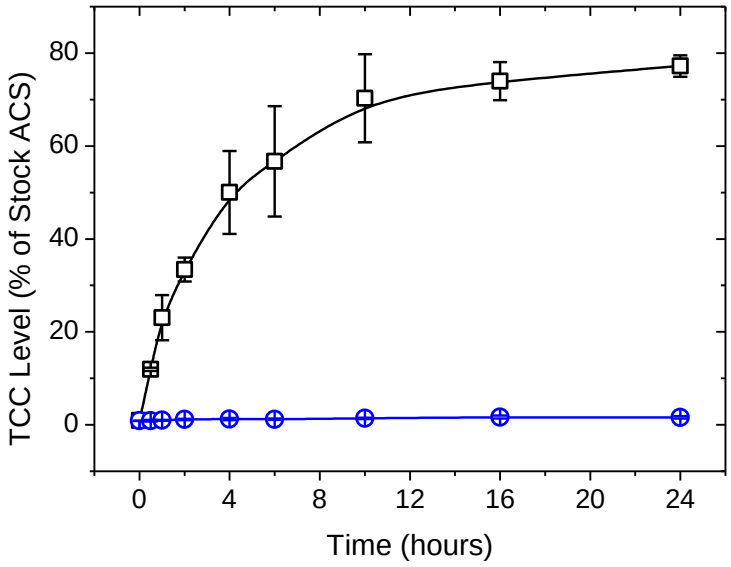

Figure 4.17. Zymosan (black) and HAIGG (blue) activation of TCC in human serum over a 24 hour period. Two repeats of both activations were performed, and the data shown is the mean ± standard deviation.

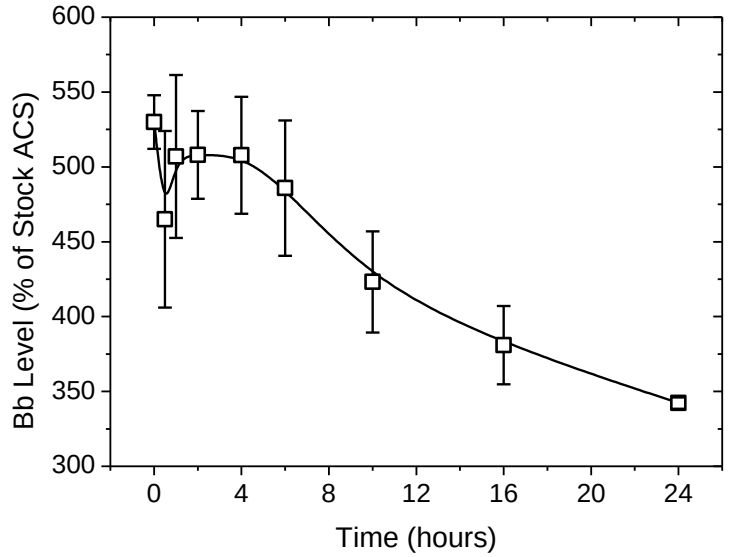

Figure 4.18. Activation of Bb in human serum over a 24 hour period. Two repeats of both activations were performed, and the data shown is the mean ± standard deviation. Zymosan and HAIGG activations yielded similar responses over time, so an average is shown of the data from both activations.

The variation of Bb with activation from both Zymosan and HAIGG is shown in Figure 4.18, with data from two activation experiments per activator presented. The concentration variation of the Bb fragment shows a complex behaviour up to 4 hours into the time course, after which it shows a steady decrease until 24 hours.

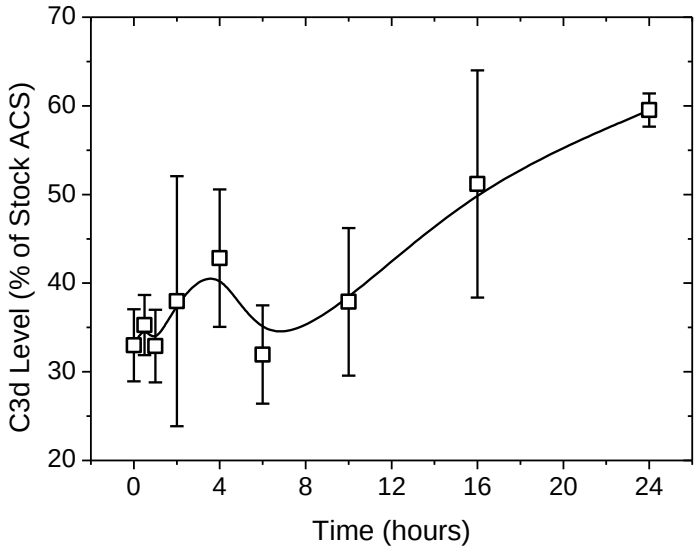

Figure 4.19. Activation of C3d in human serum over a 24 hour period. Two repeats of both activations were performed, and the data shown is the mean ± standard deviation. Zymosan and HAIGG activations yielded similar responses over time, so an average is shown of the data from both activations.

The activation time course profile for C3d concentration shows a complex behaviour over the first 4 hours, followed by a steady, monotonic, increase until 24 hours. Two replicated activation experiments were performed to generate the data.

Worth noting is the variation in the error bars – some points on the Bb and C3d time course seem well defined whereas others display a large error, which are likely to be due to experimental error -specifically the aliquot collection and activation halting part of the protocol.

The Zymosan and HAIGG activated serum was also tested for C3 and C4 for comparison using an automated immunoturbidimetric assay performed in the clinical chemistry laboratory at the RD&E Hospital. Samples were collected at the activation time points, frozen or transported to the laboratory using dry ice. Interestingly, with an associated error of 7.1% there was no change in the concentrations of both C3 and C4 at the level of accuracy of the assay.

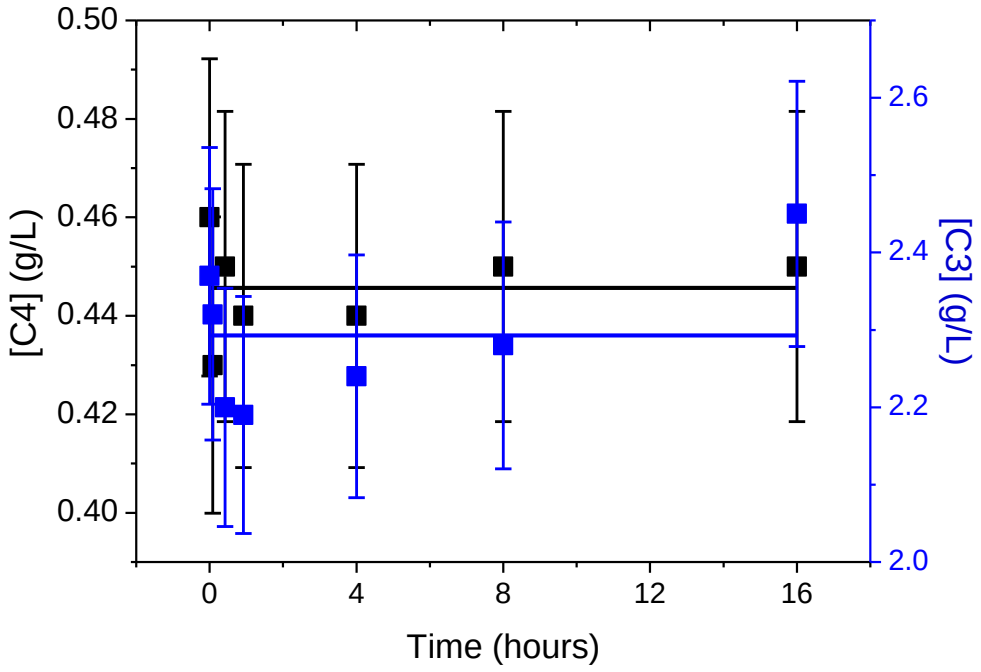

Figure 4.20. Levels of C3 and C4 were also measured over 16 hours of the activation. With an assay error of ±7% (2 SD), the levels of both proteins remain essentially constant.

4.6 Discussion

Many commercial assays exist for the assessment of C activation, such as the Hycult C5a, C3a and TCC ELISA kits. There are also Quidel Microvue EIA kits available for several fragments including Bb, C4d and TCC (SC5b-9). These kits are expensive and, crucially, cannot be multiplexed. Here we describe an ECL assay for the quantification of three C fragments, C3d, TCC and Bb. This technique has a unique advantage in that once developed, the assays can be 'multiplexed' whereby up to 10 assays can be performed in a single plate well. A comparison study for multiplex immunoassay platforms was performed by Fu *et al* [34] where it was determined that the MULTI-ARRAY assays supplied by MSD were the most suitable for biomarker analysis. Multiplexed assays will be a cheaper [35] alternative to screen for C activation in blood samples, which will enable large scale C activation monitoring trials to proceed.

Assay Performance and in vitro Activation

The TCC assay performed the best of the three assays, yielding a calibration curve with an excellent dynamic range (consistently greater than 3 orders of magnitude). The intra-assay accuracy was 18.2%, the inter-assay precision 5.7%, and the detection limit 1.11 ACS Units (2.32 ng/ml), Table 4.1. The intra assay accuracy gives an indication of the degradation of the antibody during the plate loading time for the analyte incubation, as this is the most time consuming part of the protocol. The inter assay precision shows the agreement between duplicate sample wells. Differential activation of TCC was shown, Figure 4.17, during *in vitro* activation using Zymosan and HAIGG, the former activation yielding an activation profile that reached a maximum of approximately 80% of the level present in ACS. For comparison, a recent experiment was conducted by Bergseth *et al.* [167] to establish ACS as an international complement standard. In their experiments the serum was activated with both HAIGG and Zymosan in tandem – the Zymosan having a concentration 100 times larger than that in our experiments and HAIGG 10 times greater. Their activation showed a rapid increase in TCC concentrations, reaching a maximum at 1h, then a slight decline at 4h which was stable until the final point at 24h. To observe the kinetic response, a lower 0.1 mg/ml concentration of Zymosan was used to obtain a profile of the production of TCC over a period of 24 hours with a greater sampling rate in the first 4 hours. The difference between the times to maximum TCC production between the two experiments suggests the kinetics of the TCC formation can be studied as a function of Zymosan concentration. That is an investigation that is outside the scope of this thesis, however the preliminary results show that this is possible, especially with comparison to the data presented by Bergseth and Mollnes [167].

The assay for Bb performed less well, with a dynamic range of typically one and a half orders of magnitude. The intra-assay accuracy was 13.7%, and inter-assay precision 3.9%, and detection limit 995 ACS Units (54.7 ng/ml), Table 4.1. The Zymosan and HAIGG activation showed little

differential activation for Bb, and the 'activation' actually showed a decrease in the Bb concentration in the serum by approximately 40% over the course of 24 hours. Regarding the comparison with Bergseth *et al*. [167], after an initial increase to approximately 90 µg/ml at 4 hours, the Bb fragment level also decreased to approximately 55 µg/ml at 24 hours, in agreement with our calibration measurement. It is unfortunate that this is the case, as ideally such a standard will have high concentrations of all activation markers, however further study into the rates of production and consumption during activation of a wide range of C proteins will provide a unique insight into the C system, especially in terms of pathway speeds and flux markers. Another comparative study by Opperman *et al* [165] monitored Bb production during Zymosan activation of C, and observed a response similar to TCC in this study. It is therefore suggested that the production profile for Bb is not fully understood, and therefore further study of its production as a function of Zymosan concentration is needed. Bb must remain the fragment of choice for Alternative pathway activation monitoring, as its mass allows it to remain in circulation, and it is the only unique marker for the Alternative pathway for which there are neoepitope antibodies commercially available.

The C3d assay performed well, consistently yielding a calibration curve of almost three orders of magnitude. The intra-assay accuracy was 8.8%, and inter-assay precision 3.6%, and sensitivity 0.864 ACS Units. Again, comparison with Bergseth *et al.* [167] is consistent, albeit with much lower concentrations of the activating substance. C3d steadily increases after 4h and 24h, however this time course study illustrates why closer examination is important, as a brief dip in C3d concentration is seen between 4 and 10 hours. As an isolated case this might not provide very enlightening insight into C system dynamics, however coupled with time course analysis of other C system proteins it can provide a telling insight into the relation between these proteins in this complex network.

in vitro C Activation: Protein Cascade Interactions

Differential activation was observed for TCC in the Zymosan activated serum, but not in the HAIGG activation. Zymosan, a glycan derived from yeast cell walls [215], activates the C system via the Alternative and Lectin pathways, whereas HAIGG initiates the Classical pathway [147]. This suggests the TCC (a lower C cascade activation marker, indicative of general C activation to completion) was formed from initiation of the Alternative or Lectin pathways, but not via the Classical pathway. The lack of activation via the Classical pathway suggests that the concentration of HAIGG was not high enough to warrant activation, or that the flux via that pathway is considerably slower than the Lectin or, more likely, the Alternative pathway. The alternative pathway has enormous potential for amplification via its amplification loop, and therefore once initiated can lead to rapid formation of C3 and C5 convertases, leading to the production of TCC.

More similar activation profiles were observed between the two activating experiments for C3d and Bb. This can be expected for C3d (a fragment common to all three activating pathways), but not Bb, especially given the differential production of TCC, most probably via the Alternative pathway. Experiments with varying concentrations of activators can be conducted to establish more firmly the role of Bb in the activating process, especially in relation to the formation of TCC, as Bb forms part of the C3 and C5 convertases, two quantities that the rate of TCC production is likely to be highly correlated with.

Epitope Presentation in the Assay

The difference in assay performance can be attributed to a number of factors, the most important of which is the choice of antibodies, and more specifically epitope access for those antibodies on the target analyte, explained schematically in Figure 4.21. Consider the well-performing TCC and C3d assays. In this case it is likely that the neoepitope capture antibody immobilises the fragment in such a way that the epitope for the detection antibody is well presented, unhindered by the binding between the neoepitope and the capture antibody.

Therefore the detection antibody can access and bind the analyte easily, allowing for a greater detection range. The situation may be slightly different for TCC, which is a very large molecule (1000 kDa) made up of several components, each of which can have antibodies raised against them. Therefore epitopes for capture and detection antibodies are unlikely to be physically adjacent. Comparing with the poorer performing Bb assay, it is possible that once immobilised, the Bb fragment does not present its respective detection antibody epitope as well as C3d and TCC, and therefore fewer detection antibodies can bind to the assay to generate the signal. Therefore Bb would suffer from a smaller detection range, as evidenced by the data. Unfortunately the location of the epitopes for each of the commercial antibodies is not available, and the location and proximity of the two epitopes cannot be determined easily. These two scenarios are displayed schematically in Figure 4.21.

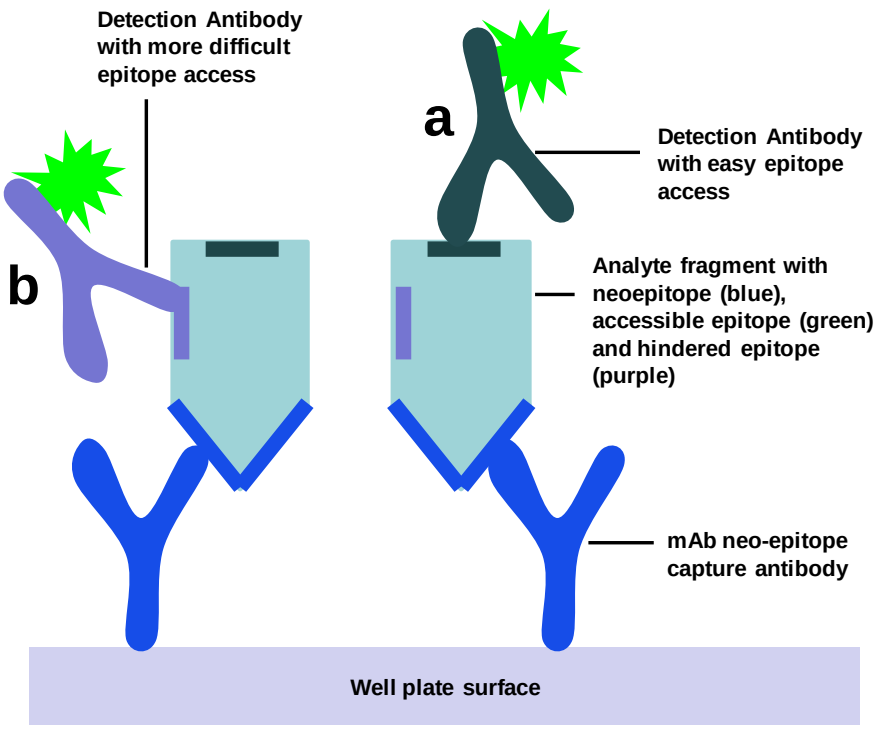

Figure 4.21. Schematic diagram showing the possible different detection antibody epitope layouts for the TCC and C3d assays (a), and the Bb assay (b).

Calibration of ACS Calibration

ACS was quantified for TCC and Bb using different dilution buffers for each calibration experiment. Calibration and stability of the ACS standard is critical to its adoption as an international standard for C activation studies. It was not possible to calibrate the ACS for the C3d assay because of the unknown mixture of individual fragments in the C3d group of analytes. As the ACS contained three fragments (C3b, iC3b and C3dg) that contained a C3d neoepitope it was not possible to determine their relative concentrations in ACS, and therefore an appropriate standard against which to calibrate ACS for C3d could not be made. As it was not possible to calibrate for C3d, consequently a value of 10^6 ACS Units was assigned to pure ACS, and all other values for all three assays were reported against this. If the levels of the fragments can be verified as stable in ACS when stored over a long period of time, ACS can become a useful international standard in C activation research, which is discussed below.

A representation of the C3d assay is made in Figure 4.22, illustrating why it cannot be calibrated. It shows the three analytes that make up the C3d group of fragments being captured onto the surface, followed by the selective binding of the C3-30 antibody to only C3b and iC3b. Therefore, as the proportion of C3b to iC3b in ACS cannot be distinguished using the antibodies available, calibration of the C3d fragment group in ACS is not possible.

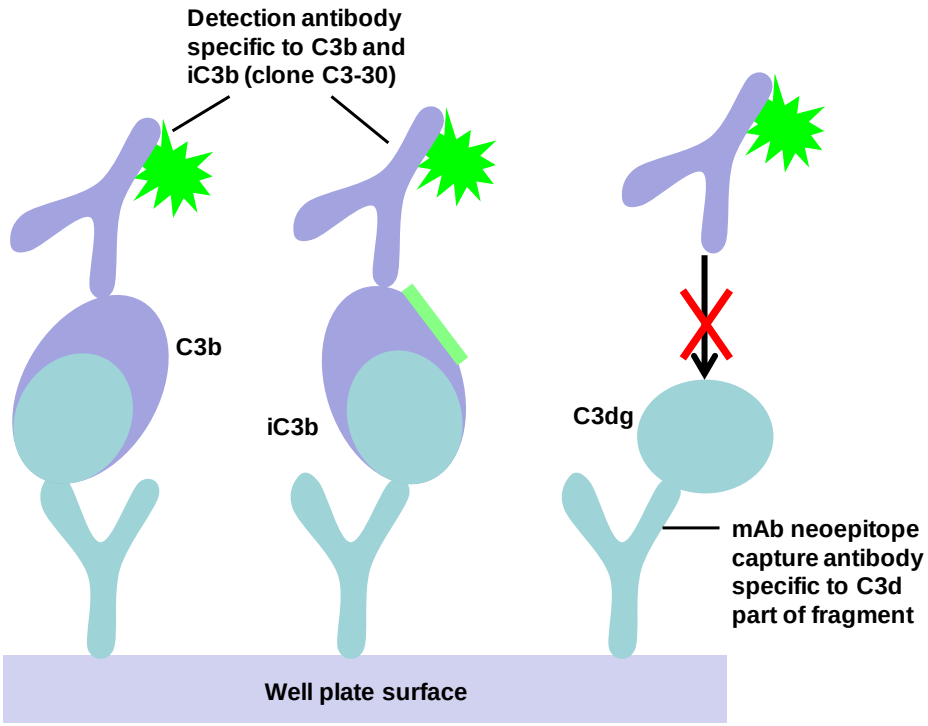

Figure 4.22. Illustration of antibody selectivity in C3d assay. Although the capture antibody can immobilise all three fragments, only two (iC3b and C3b) can be detected and reported by the detection antibody.

Comparison with C3 and C4

The constant level of C3 and C4 within the assay error during *in vitro* activation was not expected, especially considering the rise in C3d. The anticorrelation with C3d is consistent with data previously reported by Mollnes *et al* [144], but it is also potentially due to the specificity of the antibody used in the C3 assay. The antibody used is unlikely to be specific to C3 only, as the commonly used methods to detect C3 and C4 also detect their major soluble fragments, C3c and C4c [147], and therefore the signal is likely to be the sum of native C3 plus some C3 fragments. It would therefore follow that the level would stay constant, as the fragment concentration would increase with the decreasing native C3 concentration, yielding a constant level of protein that is specific to the antibody.

ACS as an International Complement Research Standard

Recently, an attempt was made by Bergseth *et al.* [167] to develop and establish an international standard against which to measure C activation, namely ACS, used as the calibration standard in this study. An assessment of its merit as such a standard is made here. In the same study the stability of ACS is shown as a function of a number of freeze/thaw cycles, Figure 4.24 and in time, Figure 4.23, – the only analyte to degrade being the C3 convertase C3bBbP. This is encouraging if you consider the practical implications for a clinical trial, or a multi-centre, standardised C activation investigation. The ACS can be made in bulk, aliquoted, frozen and transported with little impact on the stability of the components within the ACS.

Once the assays for C3d, Bb and TCC were developed, ACS was used as the standard for all activation experiments and the values obtained were reported in ACS units, with pure ACS being 10^6 ACS Units for each assay.

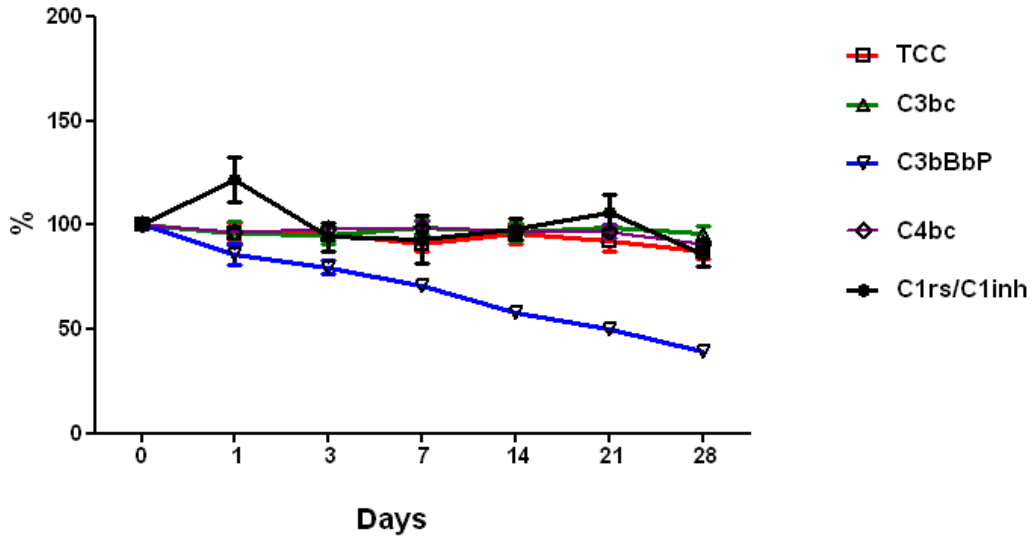

Figure 4.23. Reproduced with permission from conference poster by Bergseth *et al* [167] – Stability of C activation products over a period of 28 days when stored at 4°C. The only product to show notable degradation was the C3 convertase C3bBbP. The markers were assayed by ELISA, and the data are presented as the mean ± standard deviation. (*n*=6).

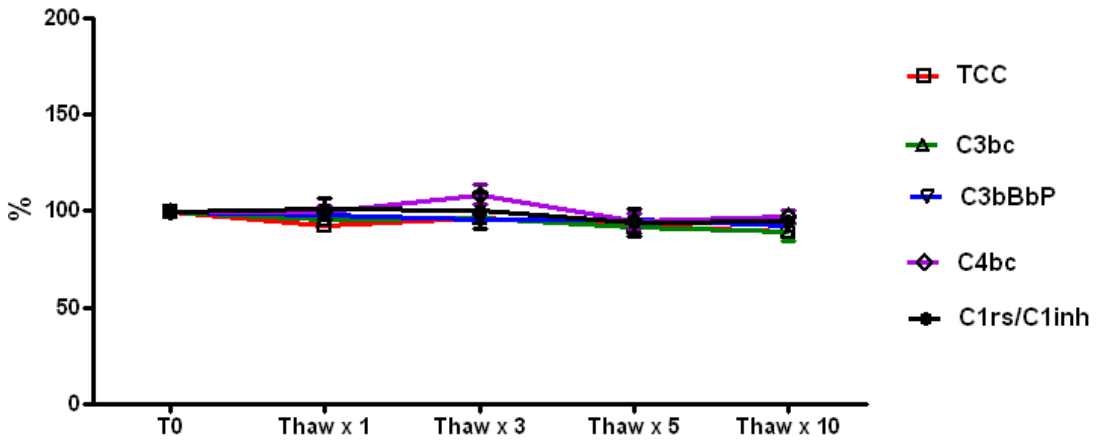

Figure 4.24. Reproduced with permission from conference poster by Bergseth *et al* [167] – Freeze/thaw cycles did not significantly degrade C activation products. The markers were assayed by ELISA, and the data are presented as the mean ± standard deviation. (*n*=6).

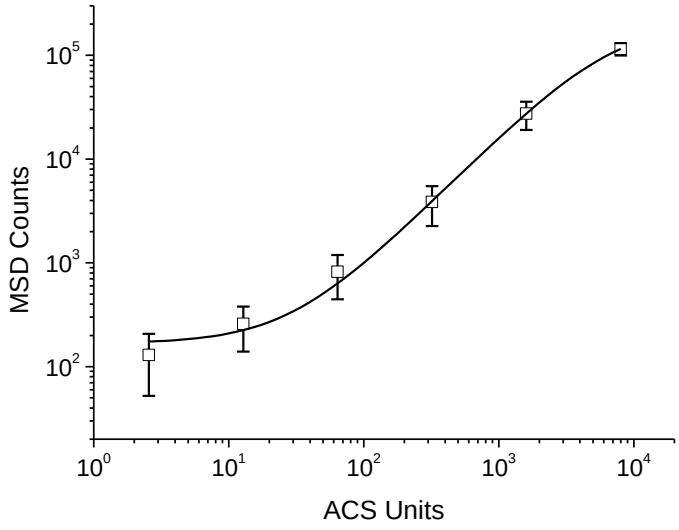

Figure 4.25. Graph showing an average standard curve for TCC using ACS for 10 experiments over a period of ~ 6 months. The errors shown are 95% confidence intervals (n=10).

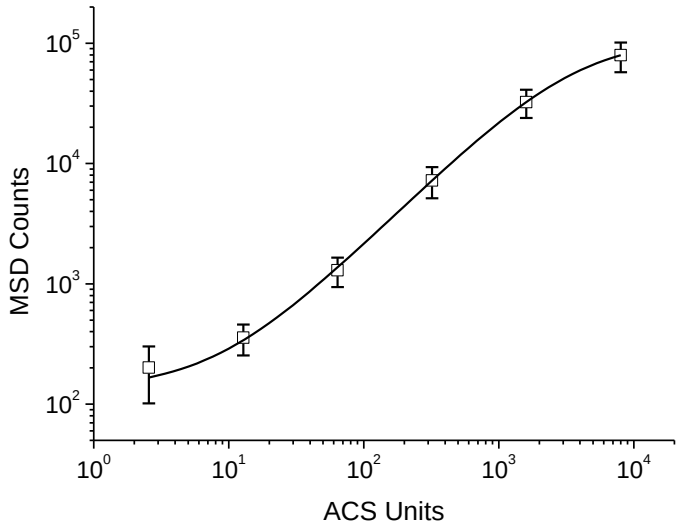

Figure 4.26. Graph showing an average standard curve for C3d using ACS for 10 experiments over a period of ~ 6 months. The errors shown are 95% confidence intervals (n=10).

Ten ACS calibration curves were measured over a period of 6 months, and the variability for each assay was determined using a 95% confidence limit as a percentage of the mean (Figure 4.25, TCC = 22.9%. Figure 4.26, C3d = 20.2% and Figure 4.27, Bb = 17.9%). The average value for the overall reproducibility of ACS was then determined to be 20.3% using data from all three assays. Coupled with the data from Bergseth *et al.* [167], as seen in Figure 4.23 and Figure 4.24, we can assume that the bulk of this variability is due to experimental inconsistency rather than degradation of ACS at -80°C, which was used with only one freeze/thaw cycle.

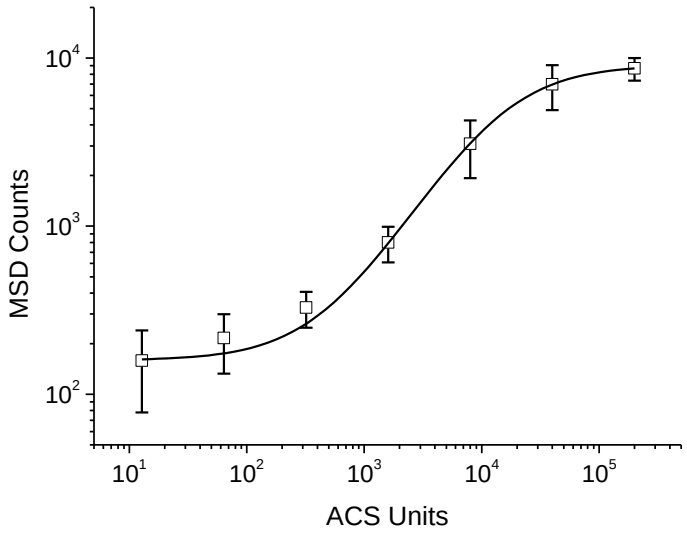

Figure 4.27. Graph showing an average standard curve for Bb using ACS for 10 experiments over a period of ~ 6 months. The errors shown are 95% confidence intervals (n=10).

It should be noted that the relative values of the fragments in this experiment compared with the stock solution of ACS was in the same general range (<90% for TCC, 35%-550% for Bb, and <60% for C3d), which gives an indication towards the possible variability associated with activating serum for C from different batches of serum. However, it should also be considered that the protocols differ greatly with regard to the concentrations of the activating substances, and therefore a strict formal comparison is not appropriate.

4.7 Conclusion

In this study, ECL assays were developed for C activation products C3d, TCC and Bb, which were subsequently assessed on a simple serum C activation experiment. The assays were optimised, discarding the use of the secondary antibody assay technique, and selecting monoclonal antibodies that yielded the greatest dynamic range for each assay. The combination of antibodies selected for the sandwich assay is key to ensure proper epitope presentation in the assay. The monoclonal antibody assay has a further advantage over the secondary antibody assay in that it takes one and a half hours less to complete. It is possible to

measure *in vitro* activation kinetics of the C cascade fragments, and in preliminary analysis C3d and TCC behaved as expected.

The standard for all experiments, ACS, was itself calibrated to quantify TCC and Bb, but unfortunately calibration for C3d was not possible. Given the stability of fragment components within ACS when it is stored over a long period of time, ACS can be used for further C activation studies as the standard against which activation is measured. We have developed two well performing electrochemiluminescence assays for C3d and TCC, an upper and lower cascade marker respectively. The assay for Bb performed less well, and we were unable to develop an assay for C4d that was deemed acceptable. The dynamic range of < 1 order of magnitude was not considered enough to proceed with further experiments using the assay. These monoclonal neoepitope antibody based ECL assays can be extended to other complement components and fragments, and once a particular set is optimised, a multiplex assay can be developed for multi-component (up to ten) screening from a single sample in a single plate well.

The assays for TCC, C3d and Bb can now be employed in an *in vivo* complement activation study. As with the *in vitro* activation experiment, a well established trigger of C activity is needed, such as surgical trauma [216]. This will allow a well defined initial time point from which the kinetic progression of the C fragments can be monitored. The effect of C activity regulation is an unknown parameter, is likely to affect the observed response *in vivo* cf. *in vitro.* Any subsequent immunological challenge activating the C system may also be observed by monitoring C activation postoperatively.

Chapter 5

The Complement System as a Surgical Procedure Outcome Predictor and Measure of Trauma

5.1 Introduction

Perioperative monitoring of hospital patients undergoing surgery, both clinically and biochemically, is an important facet of a given patient's road to recovery. Currently a range of clinical factors and biochemical tests can be used to monitor and adjust a patient's treatment, however a simple predictive test for the early onset of secondary complications could have significant effects on patient outcome, morbidity and mortality rates, length of stay and long-term survival.

Regular observations of temperature, blood pressure, full blood count and serum electrolytes are used together with C-Reactive Protein (CRP) as a routine set of tests and observations to monitor patients, especially post-operatively [63]. Post-operative complication rates following major abdominal surgery are reported to be as high as 27% [217] with potential for significant patient morbidity and mortality and the existing biomarkers, such as CRP, appear to be poor indicators of infection or complications especially in acute treatment scenarios [176].

Patients undergoing surgery are at their most vulnerable, and are especially prone to an immunological challenge via viral or bacterial infections, for example. If untreated, these infections can lead to the onset of sepsis or systemic inflammatory response syndrome (SIRS). In the UK, sepsis costs the NHS approximately £2.3 billion and is responsible for the deaths of 36,000 to 64,000 people every year [218]. Most notably, patients with severe sepsis use 46% of all intensive care unit bed days [218]. Therefore it is of significant interest to lower the rate of secondary infections, especially sepsis, which can be achieved by the concept of 'enhanced

recovery'. Recently, a large cohort study in Canada demonstrated that despite similar rates of complications, different organisations had marked variations in their 'in-hospital mortality rates'. The distinction came from the 'time to rescue' – the speed of recognition and management of complications [219]. Therefore, if a complication can be recognised early, before any signs of physical symptoms, the time to rescue could be reduced, thereby achieving lower mortality rates.

In order to recognise patients who are at risk of imminent complications, a biochemical marker is needed to monitor the patient's immune system to look for signs of activation upon immuno-compromise. An attempt has been made to predict shock and organ failure in septic surgical patients using so-called SMART (Systemic Mediator Associated Response Test) analysis, but unfortunately this relies on monitoring a number of factors including 'demographics, physiologic parameters, standard laboratory tests, and circulating markers of inflammation' [220]. Combining such a large number of factors has difficult practical implications for the time-pressed clinicians. The biomarker should be an intimate reflector of a patient's developing immunological state, and should be present systemically so that the assay can be performed on a routine blood sample.

The solution may be found with the Complement (C) system. The hypothesis is that under 'normal' conditions, the C system is 'idle', with stable levels of C components. Once the host is immunologically compromised, the C system becomes activated, evidenced by elevated C activation markers. In the context of a patient recovering from surgery, there will be an initial trauma associated with the procedure (reflected by C protein levels), however careful monitoring of the C system post operatively will identify when patients show C activity, and therefore a possible pathogenic invasion, for example. As this is the natural defence response, the patient's immune system may be able to deal effectively with the compromise itself, however these patients could be identified as 'at risk' and therefore be more carefully

monitored so that the 'time to rescue' (and therefore mortality rates) may be improved. There will undoubtedly be localised C activation at the site of the surgical trauma associated with inflammation, but monitoring the patient for systemic C activation is of particular interest as it is at this point that the host is responding to a general compromise, separate from the localised response due to surgery.

Our hypothesis states that consumption of the C proteins C3 and C4 is a general measure of surgical trauma for a typical broad cohort of major abdominal surgery and will provide significantly faster response than CRP. Further, the return of C3 and C4 pre-operative levels monitored over a serial time course can act as a personalised biomarker of recovery and secondary consumption events could indicate the potential onset of complications.

A number of classifications are used to assess the fitness of a patient for a particular procedure [221; 222; 223] and considerable technical advancement has occurred in the performance of surgical procedures, but recovery monitoring remains limited to clinical observations and a limited set of blood biomarkers dominated by C-reactive protein (CRP). The acute phase response triggered by, amongst others, production of the cytokines IL-6 and IL-1 and corticosteroids is monitored systemically and post-operatively by the production of CRP [63; 224]. CRP is a useful marker of the switch change in protein synthesis in the liver associated with the acute phase and can rise from typical healthy levels of (median) 0.8 mg/L in blood donors to up to 500 mg/L [63] during acute inflammatory events. After its production it is cleared with a constant plasma half-life of 19 hours under all health conditions [63]. There are an increasing number of studies however, pointing to limitations and diagnostic accuracy of CRP [225; 226].

CRP production is monitored by a cheap, reliable assay in the laboratory routinely with fairly low sensitivity typically 3 mg/L and it does not show a response during the 10 hours immediately post operatively. Thereafter its concentration continues to rise reaching a

maximum between 24 and 48 hours, after which the level falls as long as there is no further production stimulus, ie. inflammation resulting from infection. CRP is also a complex pentameric protein that requires considerable biosynthetic effort to produce.

The C cascade, however, is maintained homeostatically with sufficient levels of C3 and C4 to launch a C counter attack against a potential immunological challenge, with many control and regulatory proteins such as Factor H (fH) and Decay Accelerating Factor (DAF) present to ensure efficiency and rapid activation. These proteins form an enzymatic cascade which may be triggered by a number of challenges forming the innate immune response for an individual. This is a marked contrast with the *de novo* synthesis CRP in response to inflammation. Once the C cascade has responded the proteins will return to their normal concentrations, ready to be activated once more. The resetting to normal C component levels can therefore be monitored and considered as the return to health of a patient postoperatively.

The response of the cascade may then be considered a sensor system for all possible challenges including surgical trauma and secondary complications and infections, to name but a few. The enzyme-kinetic response is rapid resulting in the consumption of C3 and C4 proteins following the formation of the two key C3 convertases, C4b2b from the Lectin and Classical pathways and C3bBbP from the Alternative pathway, Figure 5.1. C3 consumption is then related to the number of the membrane-bound and serum C3-convertases resulting from surgical trauma, producing a rapid change of the serum C3 concentrations in minutes. This has the potential to provide information on the extent of trauma and the onset of recovery of the patient in the hours immediately post-operatively before CRP has responded. Further, the C3 and C4 levels will be reset during recovery to levels controlled by the patient's homeostasis indicating a healthy innate immune system – a personalised measure of recovery.

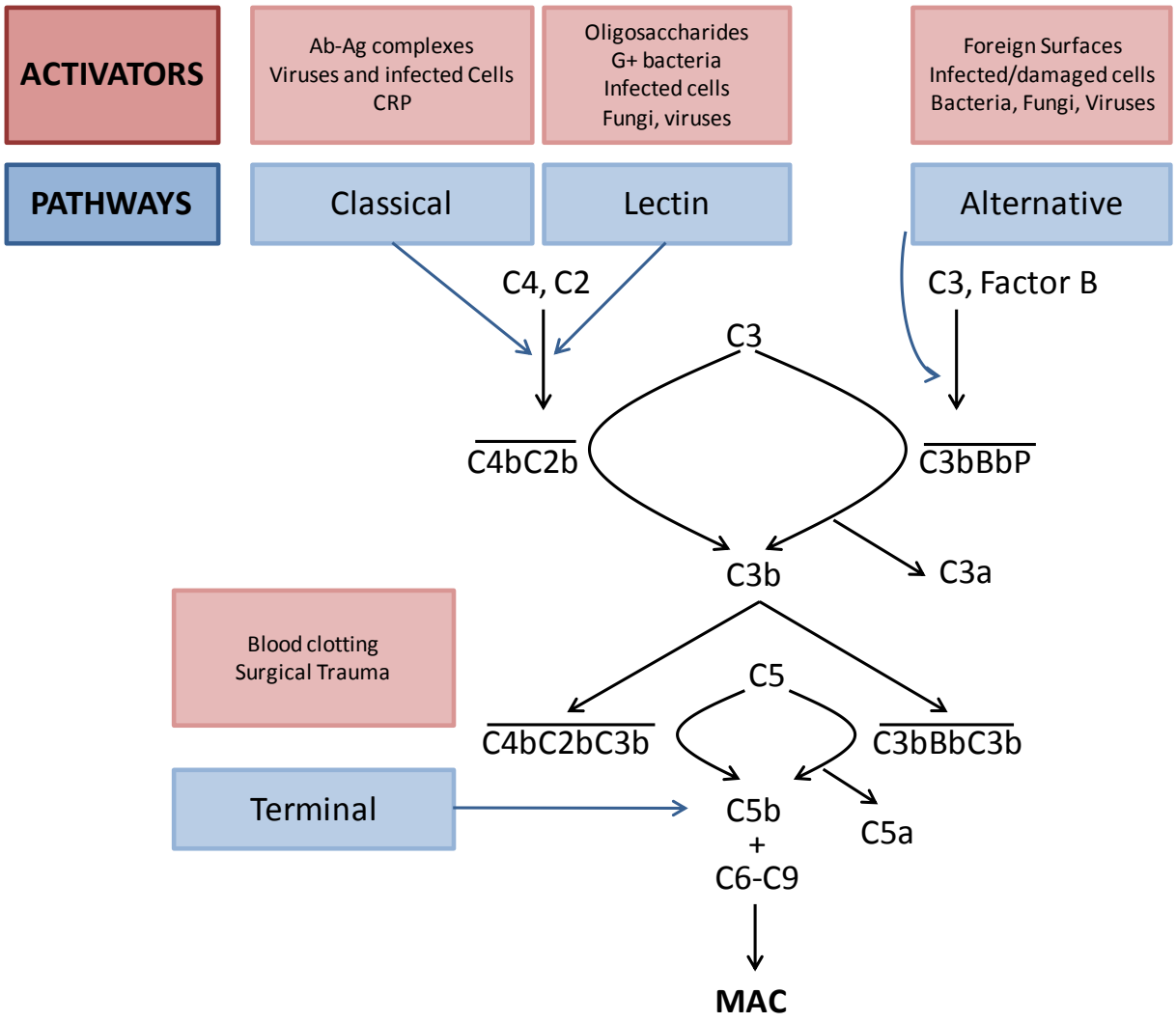

Figure 5.1. The Complement cascade showing the Classical, Lectin, Alternative pathways, the origin of C3 and C4 consumption, and Terminal Pathway. The C3 and C5 convertases are indicated with a bar above the text.

In order to evaluate the C system as a predictive test for secondary complication development and to monitor patient recovery post-operatively, a clinical trial was conducted at the Royal Devon and Exeter (RD&E) Hospital. 45 patients undergoing elective abdominal surgery were recruited and blood samples were taken from them during a time course before, during and after their operations. These samples were assayed for a range of C fragments (TCC, Bb and C3d), Chapter 6, and components (C3, C4) in order to gain an overview of overall C system activity in each patient. In addition the samples were assayed for CRP and IgG, and general routine tests ordered by the clinicians were added to the data set. This chapter aims to

interrogate the C system during the perioperative period as a diagnostic tool, and employs a number of parameters from a range of assays in order to do so.

5.2 CPOP Trial Protocol

The CPOP (Using **C**omplement as a **P**rocedural **O**utcome **P**redictor) trial was conducted at the RD&E Hospital, Devon between November 2010 and February 2011. 45 patients undergoing elective abdominal and pelvic surgery were recruited based on the following exclusion criteria: unable or unwilling to provide informed consent, pregnant women, patients under the age of 18, diabetics, patients with inflammatory bowel disorders, immuno-suppressed patients, or patients who underwent immuno-suppression or steroid treatment in the 12 months preceding their operation. The recruited patients were then monitored for C activation over a time course of typically 48-60 hours. The trial proposal received ethical approval from the LREC, South West Committee A, UK, REC, with reference number 10/H0107/66a.

Blood samples were taken from patients over a time course outlined in Table 5.1, with each sample coming from a fresh skin prick, or after 2mL blood had been discarded if a catheter was in place. Blood samples at each time point were split into clot samples and EDTA-stabilised plasma samples, the latter being split into 5 aliquots and frozen at -80^{o}C. The clot samples were used to perform C3, C4, CRP and IgG assays, and the EDTA samples were used to test for the C fragments – TCC, Bb and C3d – the focus of Chapter 6. It has been reported that further *in vitro* activation of C can occur, and therefore fragment analysis is performed in EDTA plasma so as to minimise C component degradation [191; 227; 228], effectively freezing the C cascade at the time of taking blood.

Table 5.1. Trial time course and samples

Time Point	**Time of Test**	**Trial Test**	**Trial Assays**	**Indicative Day Timings**
1 *t* = -1 hour	Pre-admission clinic **CONSENT**	ROUTINE	C3, C4, IgG, CRP	*t* =-1 day
2 *t* = 0	Pre-operatively Under anaesthesia	**Trial Sample NO.1**	C3, C4, IgG, CRP	9:30 hours
3 *t* =1 hour	Under anaesthesia	**Trial Sample NO.2**	C3, C4, IgG, CRP	10:30 hours
4 *t* = 2 - 4 hours	immediately post surgery	ROUTINE	C3, C4, IgG, CRP	13:30hours
5 *t* = 8 hours		**Trial Sample NO. 3**	C3, C4, IgG, CRP	17:30 hours
6 *t* = 12 hours		**Trial sample NO. 4**	C3, C4, IgG, CRP	21:30 hours
7 *t* = 24 hours		ROUTINE	C3, C4, IgG, CRP	09:30 hours
8 *t* = 36 hours		ROUTINE	C3, C4, IgG, CRP	21:30 hours
9 *t* = 48 hours	Some Patients Discharged Complications Develop	ROUTINE	C3, C4, IgG, CRP	
	t = *x*1	ROUTINE	CRP	
	t = *x*2	ROUTINE	CRP	
10	Discharge			

C components C3 and C4 are studied to monitor differential C consumption postoperatively. CRP is measured routinely and is currently a broad spectrum marker for the acute phase response and its subsequent development. The analysis of the C components will be compared with CRP to determine whether there may be any clinical advantages in using C3 and C4 to monitor patient recovery. Total IgG is also included in the study and acts as a control for any dilution that may occur during perioperative fluid administration.

Complement Component and Biomarker Assays

Assays for C3, C4, CRP and IgG were performed locally in the Clinical Chemistry Laboratory and Immunology laboratories. All assays were performed by Cobas® Immonoturbidimetric assays on Roche/Hitachi analysis platforms with the following accuracy and detection limits shown in brackets (percentage accuracy, detection limit): C3 (4.0%, 0.04 g/L), C4 (7.1%, 0.015 g/L), CRP (4.1%,0.3 mg/L) and IgG (3.7%,0.3 g/L). The general immunoturbidimetric technique has been described before, (Section 1.1.3) but briefly, antibodies against the target analyte are immobilised on latex beads that aggregate in the presence of the analyte as a result of antibody-antigen binding. The aggregation increases the turbidity of the solution in line with the analyte concentration, which can then be derived from measuring light absorption at a specified wavelength.

This is in contrast with the sandwich ECL C activation assays developed in Chapter 4, (and used in Chapter 6), where the capture antibody is immobilised. The immunoturbidimetric assays employed in this chapter are widely used, well established diagnostic assays, and therefore provide results with very good accuracies and precision. Just as in the ECL assays, a calibrant is used along with control samples to ensure quality control. The immunoturbidimetric assay relies on aggregation of antibody-immobilised latex particles, whereas the ECL assay employs an immobilised antibody raised against the target analyte, which can then be identified by binding to a second, labelled antibody that emits light upon electrochemical excitation.

To supplement the C analysis, complications were recorded where applicable using the Clavien-Dindo classification system, outlined below in section 5.3 [229].

5.3 General Trial Results

A total of 45 out of 52 approached patients were recruited into the trial, giving an 85% recruitment rate, and a further 96% retention (to time course completion) rate. 25 males and 20 females were recruited, with an average age of 64 years (inter quartile range 53-72 years). Blood samples were collected in 96% of the planned schedule, and the assay success rate for each sample was 92% for C3 assays, 92% for C4 assays and 91% for IgG assays. A total of 11,481 data points were collected from the 45 patient cohort. The average operation time was 154 minutes (inter-quartile range 105-205 minutes) and the average length of stay was 200 hours (inter-quartile range 94-199 hours). Eight operations were performed laparoscopically, the rest were open surgery in a cohort typical of an abdominal surgery list, included for completion in Table 5.2

Ten patients suffered complications (22%), of which two died, three developed sepsis (one of whom died) and 5 were re-admitted. The complications were reported in the patients' clinical notes along with their assigned Clavien Grades I – V [229]: Grade I, any deviation from the normal postoperative course without the need for pharmacological treatment; Grade II, requiring pharmacological treatment with drugs (blood transfusions and total parenteral nutrition are also included); Grade III, requiring surgical, endoscopic or radiological intervention; Grade IIIa, intervention not under general anaesthesia; Grade IIIb, intervention under general anaesthesia; Grade IV, life-threatening complication (including central nervous system complications) requiring intensive care management; Grade IVa, single organ dysfunction; Grade IVb, multiple organ dysfunction and Grave V, death. In this trial, the patient complications according to their respective Clavien grades were Grade I = 4, Grade II = 9, Grade IIIa = 1, Grade IIIb = 1, Grade IV = 1 and Grade V = 2. The results are summarised in Table 5.3

Table 5.2. List of surgical procedures carried out in the CPOP Clinical Trial supplied by Dr. Ian Daniel.

Major Pelvic Surgery	Stoma	Colonic Surgery
Laparoscopic sigmoid colectomy	Anterior resection	Right total nephrectomy
Laparoscopic total colectomy and ileostomy	Completion protetecomy, adhesionolysism, ileional J pouch defunctionaing loop ilesotomy	Laparoscopic nephrouretectomy
Elective laparoscopic right hemicolectomy	Abdominoperineal excision of rectum and end colostomy	Left open nephrourecterectomy
Laparoscopic sigmoid colectomy	Laparotomy, Protectomy, excision of anus	Left laparoscopic nephro-ureterectomy
Laparoscopic anterior resection	Male Pelvic Clearance	Partial nephrectomy
Laparoscopic hemicolectomy and bilateral salpineo-oophrectomy	Anterior Resection	Radical retropubic prostatectomy
Extended right hemicolectomy	Low Anterior Resection	Radical Prostatectomy
Subtotal colectomy and ileostomy	Proctectomy	Radical prostatectomy
Extended right hemi-colectomy and anastomosis of ileum to colon	Anterior Resection	Elective total right nephrectomy
Sigmoid colectomy and colostomy	Panproctocolectomy, Anastomosis of ileum to anus	Radical retropubic prostatectomy
Open right hemicolectomy	Reversal Hartmann's	Radical prostatectomy
Re-sighting of ileostomy	Anterior Resection +/- ileostomy	Radical retropubic prostatectomy
Closure ileostomy		Radical prostatectomy
Defunctioning colostomy		
Transverse colectomy		
Parastomal hernia repair		

It is appropriate here to give due attention to the small number of patients involved in this trial and its implications for statistical analysis. Given that a broad objective of the trial is to monitor C activation during post surgical complications, especially sepsis, any statistical data is hampered by the low number of complication outcomes (ten in this case, of which only three developed sepsis). It is therefore imperative that any conclusions drawn from this study be taken with caution, and considered only in light of the merits for conducting a larger trial to thoroughly test the conclusions drawn here. It is therefore important that the analysis herein remains largely descriptive and comparative, placing only limited emphasis on statistical analysis where it is used. This is especially important in light of the surgical procedures carried out. The scale of surgical trauma is broad, ranging from small laparoscopic procedures to large open surgery procedures. The trauma and subsequent recovery of each procedure differs, and this only adds to statistical uncertainty. However given this range of surgical procedures, it provides opportunity for extra observations regarding future trial design, as the type of surgery carried out should be considered.

Table 5.3. Trial demographics and biomarkers distributions

Property	November 2010 – February 2011			
Number of Patients	45		**Patients Approached** 52	Recruitment Rate 85% Retention Rate 96%
Males	25		**Females**	20
Number of Deaths CPOP0015, CPOP0028	2		**Death Rate**	4%
Number of Re-admissions CPOP0002, CPOP0010, CPOP0024, CPOP0048, CPOP0050	5		**Re-admission Rate**	11 %
Number of Sepsis Cases CPOP002, CPOP0015, CPOP0049	3		**Sepsis Rate**	7 %
Complications Rate	22 %		**Clavien Grade I** = 4 **Clavien Grade II** = 9 **Clavien Grade IIIa** = 1	**Clavien Grade IIIb** =1 **Clavien Grade IV** = 1 **Clavien Grade V** = 2
	Mean (SD)			**Mean (SD)**
Age of Participants (years)	64 (16)		**Length of Stay (hours)**	200 (195)
Surgery Duration (minutes)	154 (49)		**Max CRP (mg/L)**	134 (85)
Initial C3 (g /L)	1.42 (0.25)		**C3 Maximum Depletion (%)**	45% (15%)
Initial C4 (g/L)	0.27 (0.06)		**C4 Maximum Depletion (%)**	35% (13%)
Initial IgG (mg/L)	9.2 (2.4)			

Trial Overview Results

The CPOP clinical trial recruited 45 patients out of 52 patients approached at a recruitment rate of 85%. Two patients withdrew their consent for participation during the sampling time course, yielding a retention rate of 96%. The complications rate also compares well with the reported rate of 27% [217]. These are three important parameters to consider if a similar large scale trial is to be conducted, especially to manage resources and expectations. The initial C3 concentration in the cohort of patients fits within the reference range of 1-1.5 g/L [162], Figure 5.2A, whereas the initial C4 value observed in the trial is 0.26 ± 0.06 g/L, approximately half the reference value of ~0.6 g/L [162], Figure 5.2B. An important initial observation is the readmission rate of 11%. By monitoring a patient's postoperative recovery using the C system, it is anticipated that a predictive test can be developed as supporting evidence for discharging a patient, with the aim of reducing the number of readmitted patients.

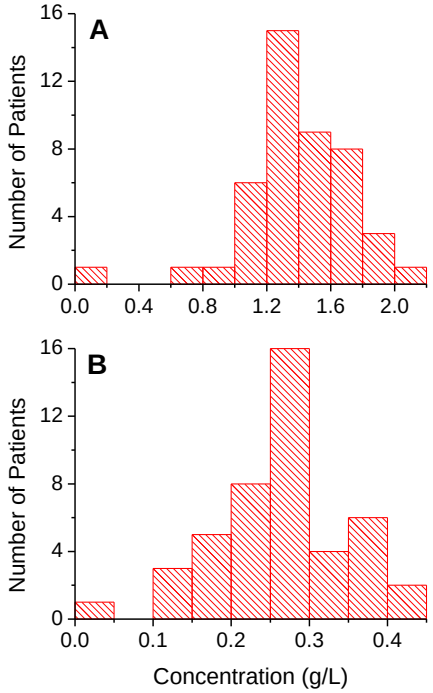

Figure 5.2. Distribution of C3 (A, bin = 0.2) and C4 (B, bin = 0.05) concentrations on admission across the patient cohort.

5.4 Results and Discussion

5.4.1 Time Course Data Analysis: Nomograms

The time course analysis of the data was descriptive given the small number of patients involved in the trial. All data points in the time course for each of C3, C4 and IgG were normalized by dividing by the C3, C4 and IgG values on admission, $C3_0$, $C4_0$, and IgG_0. CRP data were presented in the conventional units. Individual patient recoveries were plotted over the serial time course from admission to discharge. The evolution of the normalized analyte concentrations 'nC3', 'nC4' and 'nIgG' were plotted against the collection time precisely with the errors stated above. A linear interpolation was used between the data points to provide data points at consistent intervals between induction and discharge. The data at each interpolated point was then averaged over all 45 patients to produce the average recovery profile or 'nomogram', plotted as the mean of all values, Figure 5.3. The standard deviation (SD) was calculated from the sample at each time point from which the 95 % confidence limit was calculated ($1.96 \times SD \times (n)^{-1/2}$ where n=45). The resulting nomogram is therefore the perioperative average population response for each assay. Individual patient recoveries can be compared with the derived nomogram for nC3, nC4 and nIgG, Figure 5.4.

Furthermore, a stratification of nomograms for surgical procedure subclasses was created, Section 5.4.2. Nomograms were constructed for the group of patients that experienced complications, and the response was compared with patients who recovered without complication.

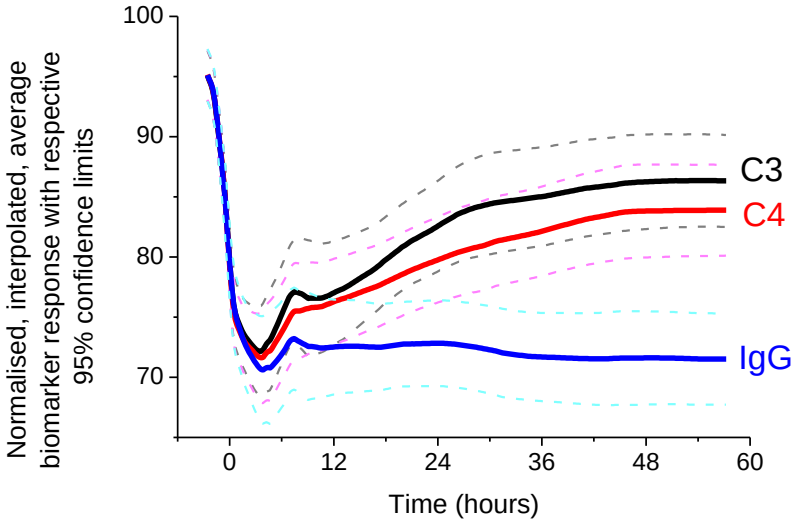

Figure 5.3 Consumption biomarker 'nomograms' for C3 (black, with dashed grey confidence intervals), C4 (red, with dashed pink confidence intervals) and total IgG (blue, with dashed light blue confidence intervals).

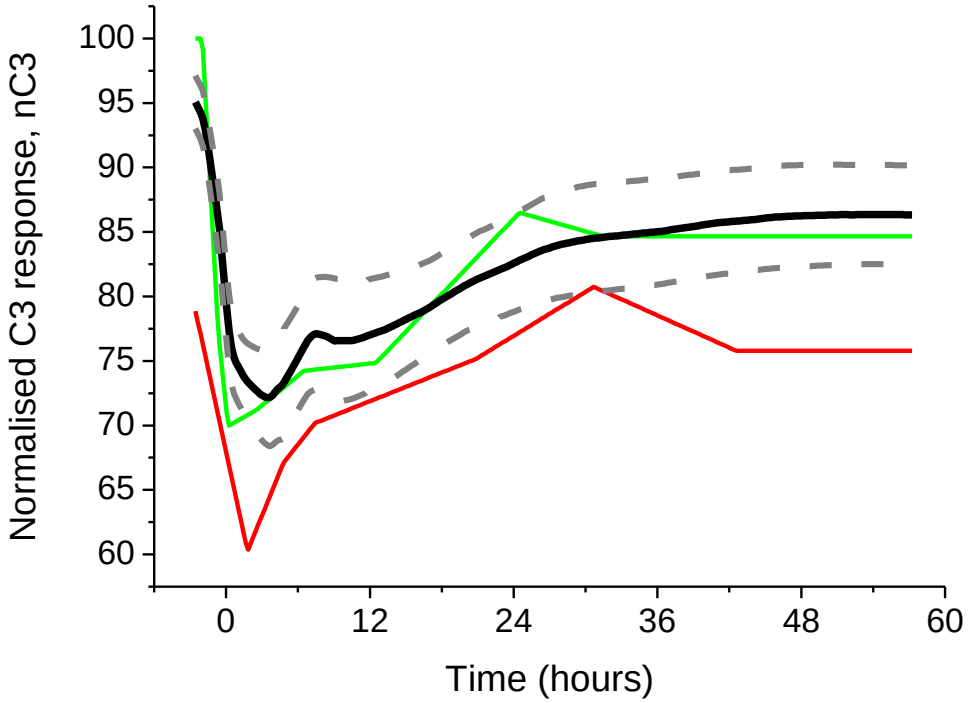

Figure 5.4. Normalised C3 consumption nomogram averaged over the 45 patient cohort; nC3, black; 95% confident limit, grey dashed; CPOP001 patient recovery pathway, green: Age: 63, Male, Radical Retropubic Prostatectomy, Duration of Operation 90 minutes and Length of Stay: 75 hours; and CPOP028 patient recovery pathway, red: Age 75, Male, Transverse colectomy, duration of operation 100 minutes and died at 192 hours.

Nomogram Observations

Observations are made about the time course nomogram profiles for all assays throughout the patient cohort. Both C3 and C4 nomogram profiles display similar behaviour, reaching a minimum and starting recovery within the first 10 hours after the knife-to-skin (KTS) time. C3 and C4 levels recover towards their pre admission values, whereas IgG remains diluted at the level to which it dropped immediately post operatively. The CRP assay does not show a response until approximately 10-12 hours, after which it increases considerably in a sigmoidal fashion before either decreasing reaching a plateau by 60 hours, see individual CRP profiles in Appendix 1. The contrast between C3 and C4 recovery and CRP production is stark, which may have important implications for recovery monitoring immediately post operatively. Some individual C3 and C4 time course profiles also show secondary consumption between 36 and 60 hours, indicating a potential secondary consumption event which may itself be indicative of some C activity.

Nomogram Discussion

The C cascade is an enzymatic pathway that leads to the rapid cleavage of a number of proteins starting at the two lead proteins for the Alternative and Classical/Lectin pathways, C3 and C4. The trigger is a rapid biochemical process with degradation of C3 and C4 occurring in minutes. This is in contrast to the delay in triggering the acute phase response in the liver and the *de novo* synthesis of the complex pentraxin CRP. Thus monitoring the consumption of C3 and C4 is a possible alternative measure of the activation of the C cascade observed for all patients in the prospective cohort of abdominal surgery. Conventional C activation focuses on the detection of activation fragments such as C3dg, C4d, Bb, C3a and C5a, however here we investigate whether the consumption of the parent components (C3, C4, Factor B) could also be used to determine C activity. Conventional C activation monitoring for the same patient cohort is performed in Chapter 6.

The nC3 and nC4 nomograms show an initial change in concentration by ~20% consistent with the fluid regimen given on anaesthetic induction. A similar comparative drop is seen in the concentrations of IgG, which remains permanently diluted during the 60 hours of the trial time course. There are two explanations for the observed dilution: the circulating volume is increased by ~20% or the mass circulation volume is maintained and there is a mass loss which is not replaced. Blood loss during the procedure is reported at ~300 mL, or a ~6% decrease. IgG levels show no recovery during the stay in hospital. Similar observations have been made previously and are attributed to insensible losses and haemodilution [230; 231]. The IgG observations indicate there is a permanent mass loss from the circulating volume during the surgical procedure with the circulating volume returning to near-normal on closure. Addition of saline to the closed circulating system volume results in kidney-lead homeostasis in 20 minutes to maintain the volume: the IgG appears to be lost to the patient for the duration of the trial time course.

One of the roles of the C cascade is to remove dead and ischemic tissue and as such should respond to the degree of surgical trauma. In this cohort study and representative selection of 45 procedures was undertaken with C consumption beyond dilution occurring in all but 5 cases. Intuitively, laparoscopic procedures would be expected to produce less surgical trauma compared with open procedures, although this will still depend critically on the comorbidities of the patients concerned. The C response to damaged tissue would predict, theoretically, that the surface area of the damaged tissue in the wound is responsible for C3 and C4 consumption with a larger surface area supporting a greater surface concentration of stable C3 convertases which causes further consumption of C3. Hence there is an expected correlation between the surface area of damaged tissue in the wound, surgical trauma, and C3 consumption. Within 10 hours from KTS the C3 levels are providing information on the degree of consumption and the C-compromised status of the patient.

The kinetic response of the cascade is fast showing a rapid decline in C3 and C4 concentrations within hours. Further, the minimum in C3 and C4 concentrations represents the balance in the rate of C consumption and the rate of *de novo* synthesis, predominantly in the liver [232; 233]. C3 and C4 start to return to admission levels much faster than the production of CRP in response to the surgical insult. The 10-hour window during which CRP synthesis is not observed with the conventional assays provided, C consumption and production provides information on the trauma from the procedure and the onset of recovery. The self-normalisation of C3 and C4 to the levels present in the patient on admission is important and these levels are set by the patient's homeostasis at a level that defines a patient-specific readiness of the innate immune system – a phenotype or personalised recovery metric. The normalisation allows the recovery of the entire cohort to be compared indicating the degree of C consumption and the time it takes to return to near pre-admission levels.

The C3 and C4 nomograms suggest the idea of a normal recovery, consisting of an average expected level of consumption as a result of the surgical trauma and an average rate of recovery associated with the production of C3. Surgical procedures that are minimally invasive should allow the patient to recovery faster than average and those with extensive trauma would expect to be slower based on the 10 hour minimum observation. The rate of return to normal depends on the health of the liver and the rate of synthesis with the slope of the increasing trend suggesting the return of the innate immune system to levels at which it should be able to mount a successful response to a challenge.

5.4.2 Complement Recovery Profiles: Stratified Nomograms

The comparison between nomograms of patients with normal recoveries and patients who suffered complications or were readmitted shows a clear difference, most notably in the rates at which C3 and C4 is produced after the initial trauma of surgery, Figure 5.5, Figure 5.7 and Figure 5.6, Figure 5.8, respectively. Unfortunately, given the low number of patients in the

study, and the discrepancy in time points for those patients (caused by varying induction times, surgical times and varying times of sample collection) there is a large error associated with perioperative C3 and C4 responses. This makes it difficult to distinguish patients with normal recoveries from patients with complications at this stage. Nevertheless as there is, on average, a definite difference in C3 and C4 recovery rates post operatively between normal recovery patients and patients with complications, it is relevant to consider the necessary implications of this result. In the scope of developing this study for a larger trial, analysis like this will be improved greatly by increased patient numbers.

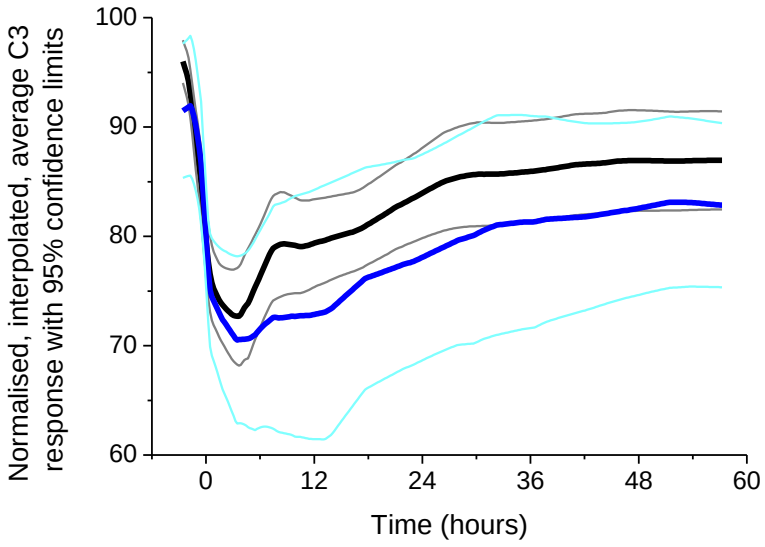

Figure 5.5 Two comparative C3 consumption nomograms for patients with normal recoveries (black, with grey 95% confidence intervals) and patients who suffered complications (blue, with light blue 95% confidence intervals, n=10).

Patients who develop complications appear to suffer a greater initial surgical trauma, evidenced by a greater early drop in concentration, followed by a slower recovery towards the analyte level on admission. In order to quantify this rate, the recovery section (after the initial analyte level drop) for both normal and complicated recovery patient groups was isolated and fitted to a 1-exponential model, and the rates of production compared. For C3, Figure 5.7, the initial rate at which the protein was produced in patients with normal recoveries was 2.46

times faster than in patients who suffered complications. For C4, Figure 5.8, the difference was a factor of 1.73, also faster in patients with uncomplicated recoveries.

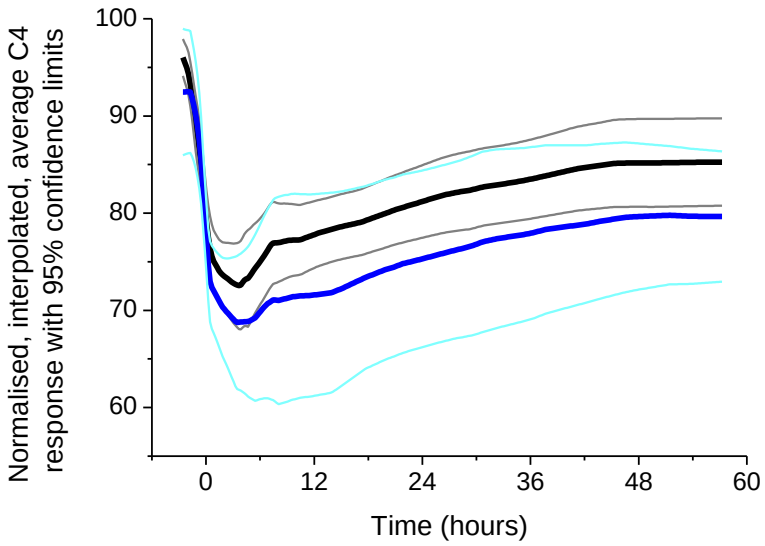

Figure 5.6 Two comparative C4 consumption nomograms for patients with normal recoveries (black, with grey 95% confidence intervals) and patients who suffered complications (blue, with light blue 95% confidence intervals, n=10).

A number of conclusions can be suggested here. Firstly, given the slower rate of C3 and C4 production (primarily synthesised in the liver [162]) in patients who developed complications, it may be suggested that this group of patients suffer from a slower homeostatic system, and therefore respond to immunological challenges slower than their normal recovery counterparts. The patients who recovered without complications may have faced similar immunological challenges, but their ability to combat the challenge was greater because of faster C3 and C4 production (and likely other proteins as well) and therefore they did not develop complications. The faster rate of synthesis may also give an indication of the state of the patient's liver (and possibly their wider health) as this is the primary synthesis site for C3 [162]. Secondly, the greater fall in C3 and C4 concentrations for patients who suffered complications, Figure 5.5 and Figure 5.6, suggests the trauma of surgery was worse for these

patients, which may also infer a likelyhood of developing secondary infections, as the trauma to the host was greater.

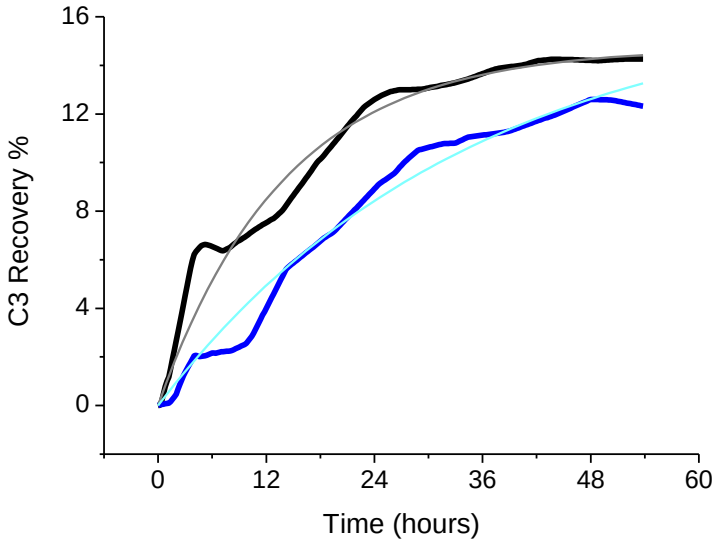

Figure 5.7 C3 replenishment profiles (taken from the tail end of the C3 consumption nomograms, after the initial fall in concentration) for patients with normal recoveries (black) and patients who suffered complications (blue). The respective 1-exponential fits can be seen in grey and light blue.

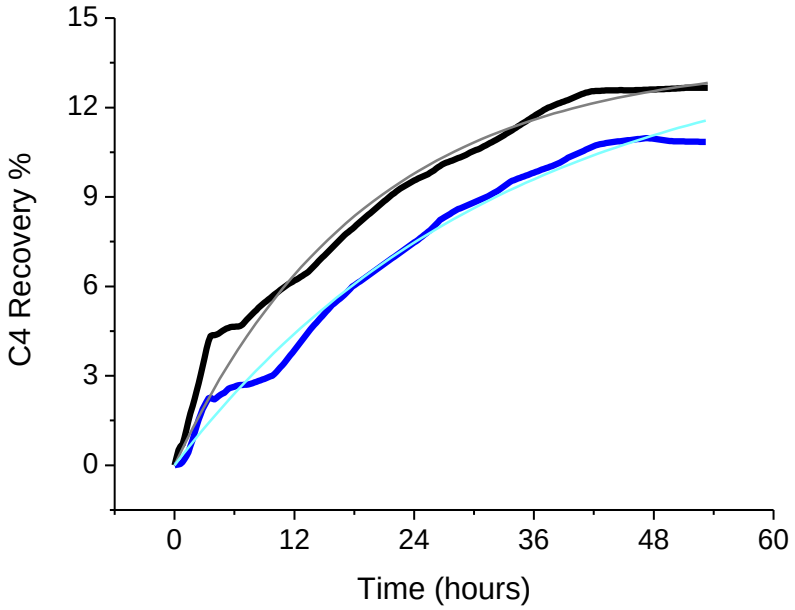

Figure 5.8 C4 replenishment profiles (taken from the tail end of the C4 consumption nomograms, after the initial fall in concentration) for patients with normal recoveries (black) and patients who suffered complications (blue). The respective 1-exponential fits can be seen in grey and light blue.

For comparison, very little difference can be seen in the comparative nomograms for IgG. Both sets of normal recovery patients and patients who suffered complications display very similar IgG response profiles, with both levels falling to nearly the same level, and remaining low for the duration of ~60 hours as is seen in Figure 5.9.

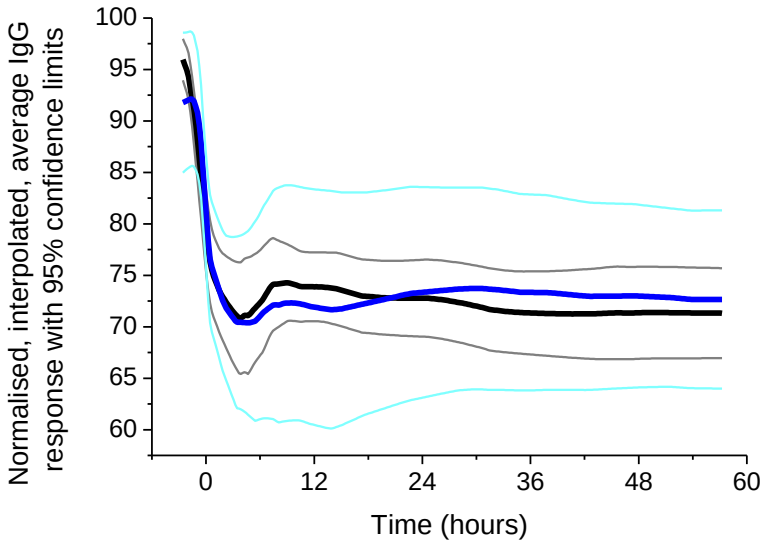

Figure 5.9 Two comparative IgG consumption nomograms for patients with normal recoveries (black, with grey 95% confidence intervals) and patients who suffered complications (blue, with light blue 95% confidence intervals).

The notion of a 'personalised recovery' may allow us to scrutinise this result appropriately. That is, every patient will have their own individual benchmark rate of healthy recovery, and therefore any actual post surgery recovery of an individual may be compared, especially the relative rates. The immediate practical limitations of this theory are obvious. If this can be a useful metric to measure an individual's recovery, an initial recovery profile should be obtained for each patient, against which their actual surgical recovery can be compared, which is unrealistic in the extreme. Therefore ideally, a biomarker (for example creatinine, which indicates healthy liver function) is needed that may give some indication as to what a particular patient's healthy recovery rate should be. This could then be compared with the

actual rate of C3 and C4 recovery post-operatively to determine whether a patient is likely to suffer complications.

Alternatively, it is suggested that an individual *in vitro* C activation profile may allow the investigator to assess the patient's C system response preoperatively, which may then be compared with postoperative recovery rate of C components C3 and C4. This personalised immunological screening may provide an insight into the biochemical ability of a patient to recover postoperatively or combat an immunological challenge, and therefore patients may be identified as high or low risk before admission.

Another hypothesis is that a patient's length of stay may be predicted from a patient's C recovery profile, possibly within 24 hours. It is shown that, on average, C3 and C4 levels recover to ~85% 60 hours postoperatively, and therefore a desired arbitrary percentage may be assigned by clinicians which can act as a biochemical marker that can support a clinician's decision to discharge a patient from hospital. With regard to length of stay, given that a 1-exponential growth model is assigned to C3 and C4 recovery, as few as three time points may be needed over a period of 12 hours post surgery to extrapolate the recovery profile and therefore predict when the level will recover to the desired percentage. Intuitively, such an arbitrary recovery measure may be linked with length of stay, and could form the basis of a hypothesis test for linking C3 and C4 recovery with fit-to-discharge criteria, which is currently a subjective decision for the on duty clinician.

5.4.3 Complement Component Consumption

The extent of C consumption across the cohort is shown in Figure 5.10 for the early-time minima in nC3 and nC4. Some patients show changes in C smaller than the indicated 20% dilution level and received only one unit of fluid on induction. All but 5 patients showed C consumption greater than the plasma dilution with similar nC3 and nC4 consumption minima, although there is some differential consumption between these two analytes.

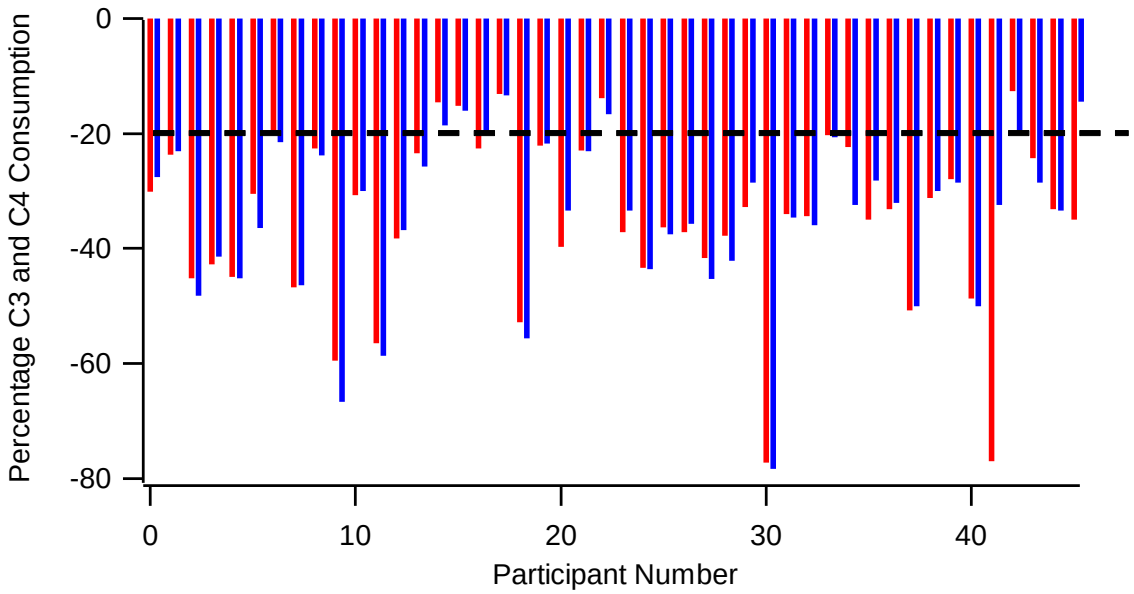

Figure 5.10. Normalised C3 (blue) and C4 (red) consumption minima for all patients in the cohort: the dotted line shows a 1L haemodilution level. 20% dilution level indicated.

Complement Consumption as a Measure of Surgical Trauma

Mr. Ian Daniels, the surgical consultant who performed many of the procedures as part of the CPOP trial, has classified all procedures into six subsections on the basis of ascending procedure severity, Table 5.4, determined qualitatively. C3 consumption (nC3 minimum) is plotted against each procedure subclass for all patients, Figure 5.11. A correlation is observed between increasing C3 consumption and procedure severity, R = 0.922.

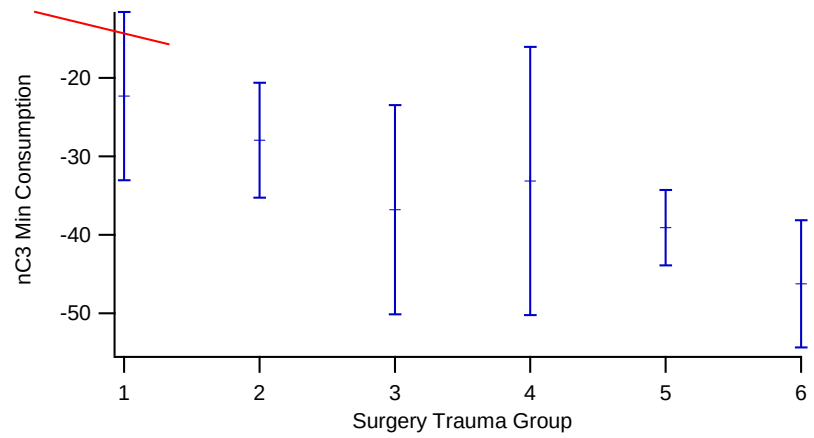

Figure 5.11. Stratified C3 consumption based on procedure severity based on a set of procedural classes outlined by Mr. Ian Daniels.

Table 5.4. Surgical procedure classification according to severity by Mr. Ian Daniels.

Class	Procedure
1	Sighting of ileostomy Closure ileostomy Defunctioning colostomy Transverse colectomy Parastomal hernia repair
2	Laparoscopic sigmoid colectomy Laparoscopic total colectomy and ileostomy Elective laparoscoping right hemicolectomy Laparoscopic sigmoid colectomy Laparoscopic anterior resection Laparoscopic hemicolectomy and bilateral salpineo-oophrectomy
3	Extended righ hemicolectomy Subtotal colectomy and ileostomy Extended right hemi-colectomy and anastomosis of ileum to colon Sigmoid colectomy and colostomy Open right hemicolectomy
4	Anterior resection Completion protetecomy, adhesionolysism, ileional J pouch defunctionaing loop ilesotomy Abdominoperineal excision of rectum and end colostomy Laparotomy, protectomy, excision of anus Male Pelvic Clearance Anterior Resection Low Anterior Resection Proctectomy Anterior Resection Panproctocolectomy, anastomosis of ileum to anus Reversal Hartmann's Anterior Resection +/- ileostomy
5	Nephrectomy Laparoscopic nephrouretectomy Left open nephrourecterectomy Left laparoscopic nephro-ureterectomy Radical retropubic prostatectomy Radical Prostatectomy Radical prostatectomy Partial nephrectomy Elective total right nephrectomy Radical retropubic prostatectomy Radical prostatectomy Radical retropubic prostatectomy Radical prostatectomy
6	Radical lystectomy, radical hysterectomy, left salpingo-oophrectomy Radical cystoprostatectomy ileal conduit formation and lymph node clearance Radical cyctectomy, ileal conduit, total abdominal hysterectomy, Bilateral salpingooophrectomy Abdominoplasty and epigastric hernia repair

The extent of C consumption could be therefore be indicative of the trauma suffered during surgery, and act as supporting evidence for the post surgical evaluation of the procedure. Once an average consumption value is established for a given procedure, an individual patient's C consumption may be compared to assess the biochemical effect on the patient by the operation. C consumption between different types of surgery, such as laparoscopic *vs.* open could be compared, and therefore further surgical advances that cause less trauma to patients can be proven to do so. Continued collaboration with clinicians is in place to properly evaluate the merits of C consumption as a measure of surgical trauma. Potential stratification of patients based on C consumption to identify risk patients is hypothesised, and may lead to more efficient management of complications by reducing the time to rescue, as these identified patients may be monitored more carefully.

5.4.4 Secondary Complement Consumption

The idea of secondary consumption of C3 and C4 is of interest when monitoring the host's response to infection following surgery. The initial fall in C3 and C4 concentration is probably entirely due to fluid administration under anaesthesia, however once concentrations have been replenished, any subsequent drop in concentrations may indicate cleavage of C3 and C4 and therefore C activation for some reason. It is this event, which can happen well before CRP has completed its response to the surgery-induced inflammation, which could indicate an immunological compromise of the host. Additionally, any sign of C fragment activation markers increasing in concentration before the end of the CRP response to surgery could indicate similar immune response action. The reason for such an apparent immune response may be unclear, however it should be enough to indicate that the host is under attack, which has important implications for post-operative patient care. Patients who show this response could be identified as 'at risk' and therefore monitored more carefully by clinicians and nurses. Secondary consumption was observed for a number of patients, and will be considered using individual case studies in conjunction with C activation in Chapter 6.

5.4.5 CRP vs C3 and C4 Consumption Nomograms

When compared with CRP production post surgical trauma, monitoring C3 and C4 gives a significant time advantage as it responds approximately 12-24 hours before CRP levels start to rise. Furthermore, this initial rise in CRP is in response to the initial surgery, and it is not until ~48 post surgery that the trauma-induced CRP response plateaus. CRP therefore has very little predictive clinical value in the immediate postoperative period, compared with C here and previously with Interleukin-6 [234; 235]. This is due to the initial rise in CRP being merely the 'background' signal related to the inflammation as a result of surgery, and due to its slow response, it will only be indicative of an infection well after the host is compromised. The time gap between C and CRP response is assessed using individual patient case studies in Chapter 6.

5.5 Conclusions

Complement activation during surgery has been observed previously associated with the effect of extra-corporal bypass circulation [176; 208; 236]. We have demonstrated C component consumption with all surgical procedures in our cohort which should produce C activation products. In addition, we have observed secondary consumption events which points to the potential for Complement to be a better marker of recovery than the conventional CRP levels which has been shown to correlate poorly with outcome in acute treatment scenarios in particular [237; 238]. The rapid response of C in the early 10 hour period immediately post operatively provides information of the degree of surgical trauma and the onset of recovery. We have also established that C components C3 and C4 recover slower in patients who go on to develop complications post surgery. C component recovery monitoring could provide an individual patient-normalised metric of recovery as supporting evidence for a clinician to discharge a particular patient. Recovery could be measured against the self-normalised innate system indicating a time at which the innate system has returned to an arbitrary percentage of its healthy levels indicating the patient is fit to discharge. Early recognition and potential identification of 'at risk' patients could reduce significantly the time to rescue which has been

shown to be beneficial in the management of the recovery in patients reducing in-hospital mortality rates. Furthermore the potential for predicting length of stay from early C recovery profiles could provide a valuable tool for hospital resource management.

The potential for the C system to be used as a health monitoring mechanism must also be considered in light of C activation products, which forms the second half of the CPOP investigation, Chapter 6.

Chapter 6

Complement Activation as a Biomarker of Secondary Complications in the Recovery of Patients from Abdominal Surgery

6.1 Introduction

Electrochemiluminescence assays for three Complement (C) activation markers, TCC, Bb and C3d, have been developed, Chapter 4. These assays can be used to measure overall C activation (C3d), Alternative (Bb) and Terminal pathway (TCC) activation. C components C3 and C4 have been shown to be consumed in the hours immediately following surgery, Chapter 5, after which the protein levels are replenished quickly; secondary consumption events and slower rates of recovery have been observed in patients presenting clinical complications.

The C activation assay development in Chapter 4 also measured *in vitro* activation of these three products over a given time period, and the same study has been proposed *in vivo*. *in vivo* and *in vitro* C activation profiles will clearly differ, as the homeostatic systems in place *in vivo* will alter the rates of activation marker production. For example, small activation products produced *in vitro* will remain in solution for much longer, as they are not be subject to filtration by the kidney as would be the case *in vivo*.

In order to evaluate C activation products as biomarkers for secondary complications in patients recovering from surgery, a clinical trial was conducted at the Royal Devon and Exeter (RD&E) Hospital. 45 patients undergoing elective abdominal surgery were recruited and blood samples taken over a perioperative time course. These samples were assayed for three C activation products, TCC, Bb and C3d, in order to monitor C activation intra and

postoperatively. These samples were also assayed for C3, C4, CRP and IgG for a separate C consumption and CRP-comparison investigation, Chapter 5. This chapter aims assess the potential for C activation to be a biomarker of secondary infection by monitoring C activation levels in patients undergoing abdominal surgery, with the hypothesis that C will react rapidly to any secondary complications, and therefore any activation postoperatively may be indicative of an immune system challenge. If successful, the C system can be used as a companion diagnostic for infections, or as a supporting evidence tool for clinicians to determine the immunological state of a patient.

6.1.1 Complement Consumtion vs Activation

Complement activation markers should, in theory, provide a much better indication of C activation activity, possibly even pathway specific activation because the background levels of the fragments should be small normally and activation should show a large rise. There are several C components that are individual to each pathway, and the enzymatic cleavage of these components upon activation can create large concentrations of cleavage products, or fragments or activation markers, very quickly. There are two main advantages to using C fragments, rather than the parent components. Firstly, during normal health, when the C system is idle, the fragments should be in a much lower concentration than when activated. This could provide a sensitive test for C activation, as the contrast between idle and activated fragment concentrations in the blood should be high. Secondly, the nature of the fragmentation process means neoepitopes are created, which can be used to isolate and detect fragmentation products only. These neoepitopes become exposed only when fragmentation occurs, as they are hidden on the native, parent component. Therefore specific assays can be developed for fragmentation products only.

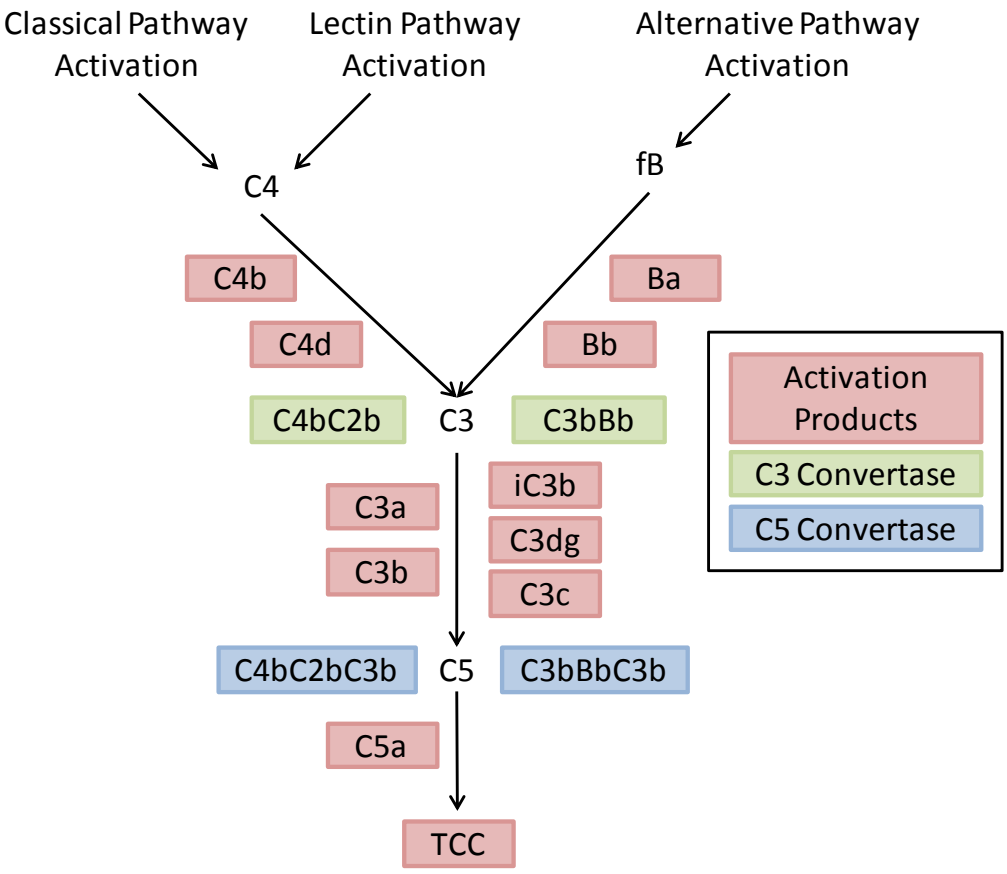

Figure 6.1. Simplified overview of the Complement system showing the three activating pathways, key C pathway components (black text), activation products (red boxes), C3 convertases (green boxes) and C5 convertases (blue boxes).

Many studies have been performed using C activation fragments as markers. TCC in particular has been used as C activation marker, [140; 142; 143; 239], and also the anaphylatoxins C5a and C3a [142; 239; 240]. Two of these investigations have even focused on C activation during and after surgery, particularly in cardiopulmonary bypass surgery looking at the effect of surfaces in the extra-corporeal circulation [142; 143]. Younger *et al.* concentrated on C activation in patients with severe sepsis, focusing on C components C3 and Factor B (fB), as well as fragments C5a, C3a and C4d [240]. They concluded that patients with community acquired sepsis show extensive C activation, particularly in the Alternative pathway. This is encouraging, and suggests that monitoring C system activation is a sensible metric to observe the development of sepsis post operatively. C activation has also been measured previously in relation to several other diseases including age-related macular degeneration [241], ischemic

heart disease [157], inflammatory disorders [242] and rheumatoid arthritis [144]. Figure 6.1 shows a simplified overview of the C system, indicating in red some of the most popular C activation products cited in the literature.

6.1.2 Detection of Complement Activation Markers

As briefly mentioned above, the exposure of neoepitopes on C fragments upon activation creates a good opportunity to detect, specifically, individual C activation products without interference from the whole parent component. This has already been discussed in detail in Chapter 4, but will be revisited here.

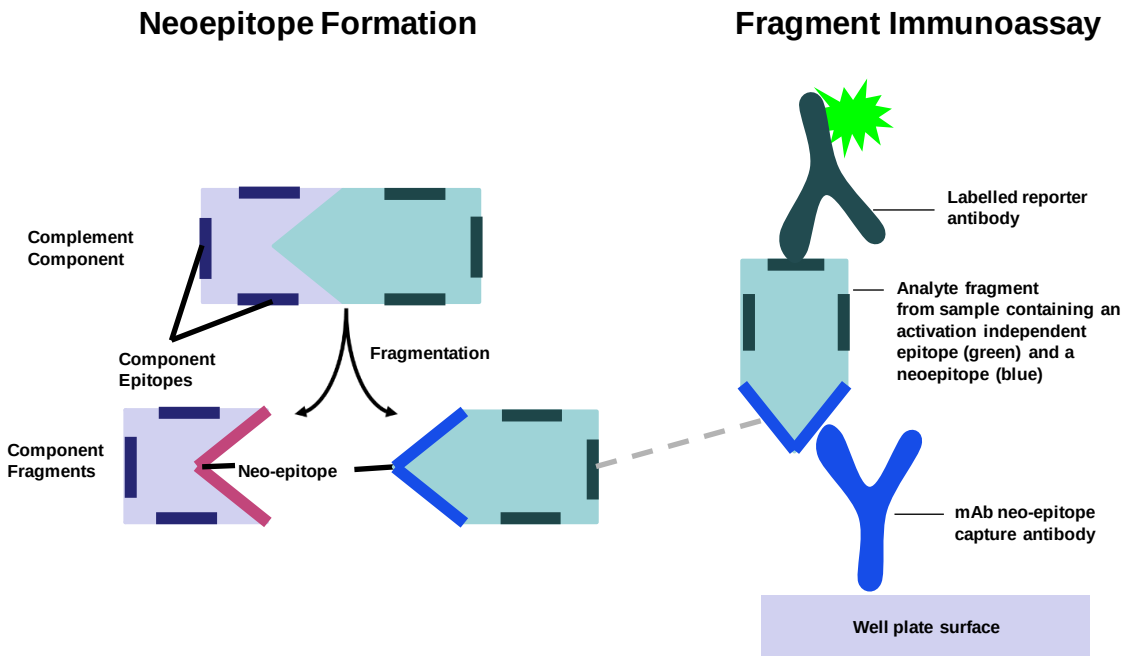

Figure 6.2. Schematic showing the origin of neoepitopes from parent components and the principle for a fragment immunoassay based on its neoepitope.

Antibodies can be raised against neoepitopes on C fragments, allowing the development of immunoassays against these fragments, Figure 6.2, whereby the neoepitope antibody captures the fragment and some other labelled reporter antibody is used to generate the signal.

Practically, it is very important that the fragmentation be stopped upon sample collection, as further *in vitro* activation of the C system has been shown to rapidly generate more

fragmentation products [149]. Therefore, to avoid post-sampling *in vitro* activation, it is important to collect blood samples directly into tubes containing EDTA at a final concentration of at least 10mM [147]. It is possible to measure C activation products C5a and C3a in urine [154; 155]. Both these fragments are excellent activation markers, and especially good candidates to measure from the urine as their masses are below the kidney filtration cut-off (45 kDa) [121], meaning they will be removed from the bloodstream into urine shortly after their production. However, urine samples would be unsuitable in a study looking for systemic complement activation during a given time course. Activation products in urine would mean a build-up of the target fragment over a given period of time, limited by the frequency of urination. Therefore, instead of obtaining a snapshot of C activation at a given time point, urine samples would only supply information regarding C activation over a given period of time. The level of activation over a given period of time will be determined, however given the rapidity of the C system it will not be possible to determine a well defined time course of fluctuating C fragment concentrations during activation.

6.1.3 Current Perioperative Patient Monitoring

Current patient monitoring post surgery is dominated by a range of simple clinical observations including heart rate, blood pressure and temperature, and a small list of biochemical markers such as C-Reactive Protein (CRP), creatinine, haemoglobin, white blood cell count and platelets [243; 244]. CRP and its limitations has already been explored in Chapter 5, and its continued use to monitor post operative well-being allows much room for improvement with regard to patient recovery monitoring, especially the early detection of the onset of sepsis [245]. A biochemical marker that could predict, presymptomatically, the development of secondary infection such as sepsis would be a significant improvement in post-operative patient monitoring and care. Effectively, it would create an presymptomatic early warning system for medical staff if a patient is likely to develop an imminent secondary infection, allowing them to take the necessary steps to treat the condition. Currently, an Early Warning Score (EWS)

system exists [246; 247; 248], and is based on monitoring a number of parameters including temperature, heart rate and blood pressure, producing a score from 0, normal, to 7, critical, based on the parameter output values and is presented in a simple chart. The score does not take account of any biochemical information and only triggers an intervention from a senior clinician. An example EWS sheet for a patient who developed sepsis is shown in Figure 6.3. It is suggested that an alternative EWS may be created that considers a range of interconnected biomarkers, and reports the developing state of a biological system within a patient, thereby monitoring and reporting on an individual's biochemistry.

It has been shown that a reduced 'time to rescue' [219] has significant implications for reduced 'in-hospital' mortality rates, so such an early warning system would be desirable within the medical community. Therefore a biochemical marker that can monitor the development of infection, or indeed the activation of the immune system in response to infection, will be a significant advance that will supply clinicians with a supporting tool to effectively monitor patients for either a healthy recovery or the development of complications.

The use of such a biochemical marker could be particularly useful in the early detection of systemic inflammatory response syndrome (SIRS) – a systemic inflammatory state diagnosed from the observation of at least two signs of inflammation [249] – or sepsis, diagnosed as such if a case of SIRS is coupled with a highly suspected infection [249]. Sepsis is extremely costly to the NHS, amounting to over £2 billion per year [218], and additionally causing the deaths of approximately 50,000 people.

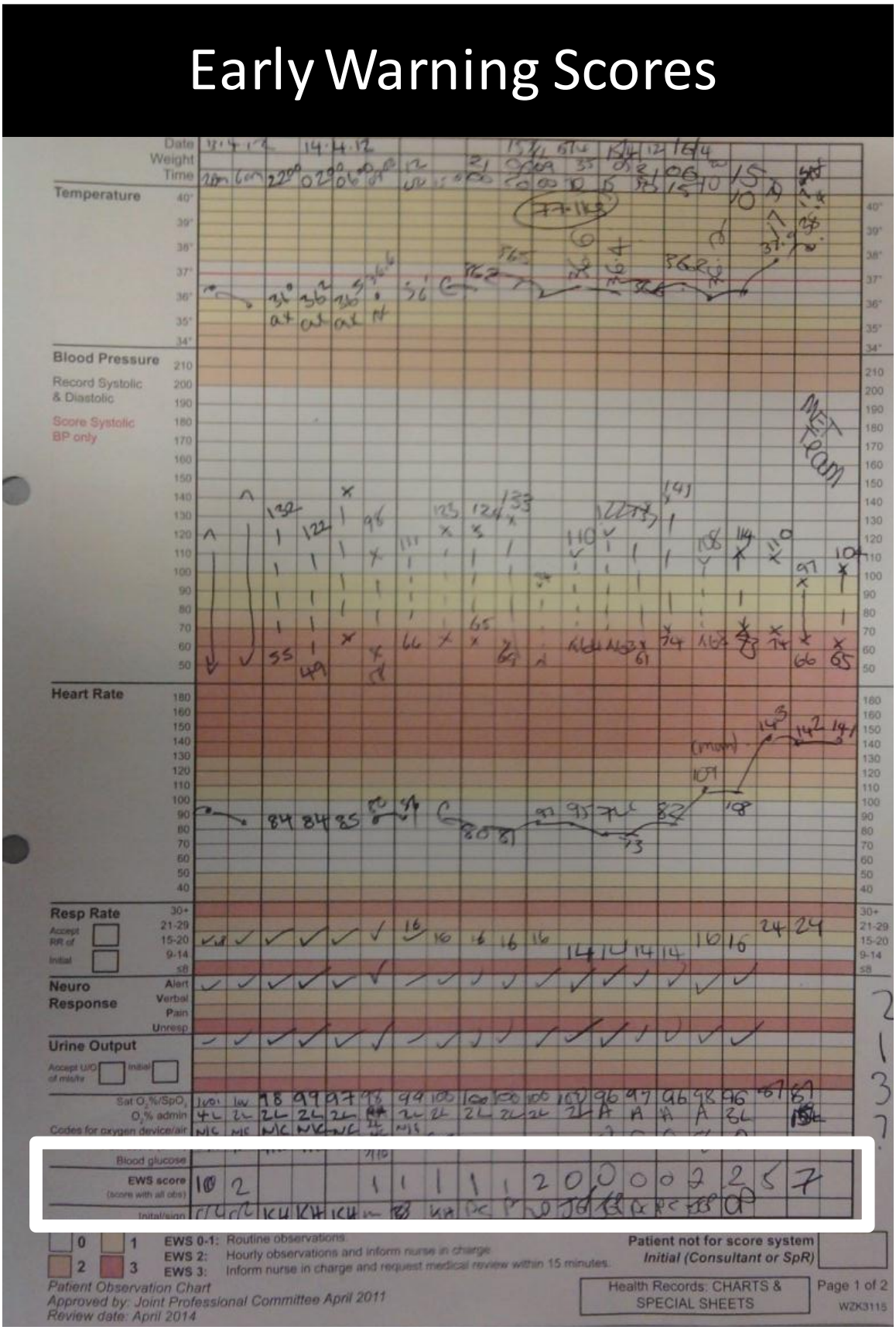

Figure 6.3. EWS sheet for a patient who developed postoperative sepsis. The EWS is indicated by the white box, and shows and rapid increase of their EWS from 0 to 7 towards the end.

6.1.4 Mechanisms for Complement Activation from Secondary Infections

The major advantage in using the C system as a tool with which to monitor the host's immune response is that it can be activated differentially. That is, different pathways can be activated by different immuno-compromising agents [57; 147; 228]. The Classical pathway is predominantly activated by antibody-antigen complexes, whereas the Alternative and Lectin pathways are mainly activated by microbial cell surfaces and microbial surface sugars respectively, as detailed previously in Chapters 4 and 1. Additionally the Terminal pathway may be activated by coagulation [138]. Therefore the ability to monitor *in vivo* C activation products unique to each pathway will provide information about differential C activity in each pathway, and will therefore allow the clinician to diagnose the response based on the known activators for that particular pathway. Figure 4.1 shows a simplified diagram of the C system, with specific focus on general pathway activators, major component, fragments, convertases and biological effects. There is a vast collection of C activators, which have been listed previously, Chapters 4 and 1, and will not be revisited here. However, the key assumption is that the C system can be activated differentially, and therefore the ability to detect individual C pathway activation may enable a clinician to make a differential diagnosis and determine the type of immuno-compromise to which the host is making a response.

If a patient develops an infection postoperatively, his or her C system will be activated to combat the compromise, causing C fragments to be produced quickly (within a matter of minutes) [250] and in large numbers. If this fragment production can be monitored, clinicians can be provided with more information regarding the recovery and well being of their patients post operatively.

6.1.5 Differential Complement Pathway Activation Markers

Previously, three assays have been developed for TCC, Bb and C3d with a view to monitoring differential C activation *in vivo*. Surgical trauma and potential consequent infection can be

used to activate the C system *in vivo*, and therefore a cohort trial involving elective surgery can be used as the platform with which to monitor C activation *in vivo*. The markers chosen to conduct this study have been chosen for their exclusivity to their respective pathways: Bb and TCC for the Alternative and Terminal pathways respectively and C3d to show overall C activation. All three chosen activation products and their respective merits are discussed in Chapter 4, but will be revisited here in the context of differential activation.

The collection of fragments referred to as 'C3d': C3b, iC3b and C3dg are all overall C activation markers, as they are fragments of the central C component, C3, Figure 4.1. Large quantities of C3 activation products (C3b) can be made quickly via the amplification loop along with Bb, a fragment from the Alternative pathway. However both these fragments together form the C3 convertase, C3bBb, which is the key contributor to the amplification loop in the Alternative pathway, especially if it is stabilised by Properdin. Therefore, with production and consumption processes in place for both markers, the success of these markers as biomarkers of activation may be dependent on the time at which blood samples are taken. It is not possible to know exactly when a peak in concentration is expected in either fragment before it is reduced by convertase formation. This is encapsulated in the concept of a C fragment 'avalanche', whereby the rise and fall of a C fragment may be over very quickly, especially within the initial pathways. Therefore an equally interesting observation from an *in vivo* C activation study will be the determination of a good time course from which to measure temporal activation.

Finally, TCC production indicates C activation to completion via initiation from any of the pathways, as it is the final activation product in the cascade to be produced. Therefore production of large amounts of TCC in patients post operatively could well indicate the development of bacterial or viral infections, the exact target it is designed to attack in the form of MAC. TCC may not be as vulnerable to the avalanche effect, as it is the final product to be

made in the C system, and is not subject to any additional clearance processes, other than normal homeostatic breakdown.

A review of previous C activation studies can be found in Section 4.1.1.

6.1.6 Aims and Objectives

This investigation aims to assess the potential for C activation as a biomarker of the early onset of complications during recovery following major abdominal surgery. A clinical trial was conducted at the Royal Devon and Exeter (RD&E) Hospital, from which 45 patients undergoing elective abdominal surgery were recruited and blood samples were taken from them during a time course before, during and after their operations – protocol and demographics presented in Chapter 5. These samples were assayed for three Complement activation markers; Bb for Alternative pathway activation, C3d for overall C activation, and TCC for activation in the Terminal pathway. Electrochemiluminescence assays were used to test the samples for the activation products, as developed in Chapter 4. C activation was then compared between patients who recovered normally and patients who suffered complications in order to establish whether C activation has potential to be a presymptomatic biomarker of secondary infections.

6.2 Methods

The CPOP trial, introduced in Chapter 5, included 45 patients undergoing elective abdominal and pelvic surgery. The blood samples collected were split into clot and EDTA stabilised plasma samples, the former being used to carry out the C consumption and CRP comparison investigation in Chapter 5. The EDTA-stabilised samples were collected in order to assay for C fragments. It has been reported that further *in vitro* activation of C can occur, and therefore fragment analysis is performed in EDTA plasma so as to minimise C component degradation [191; 227; 228], effectively freezing the C cascade at the time of taking blood. Bergseth *et al.* [167] have recently shown the effectiveness of EDTA in stopping the C cascade. They also

showed that it can be improved further by addition of Futhan, however the standard hospital collection protocol in the hospital only employs EDTA.

Samples were tested for C fragments TCC, Bb and C3d using the electrochemiluminescence assays developed in Chapter 4, using the protocol laid out in Section 4.4.3. Each assay is based on a classic immunoassay whereby a neoepitope antibody is used to capture the C fragment, Figure 6.2, and another antibody, labelled with SULFO-TAG (MSD), serves as the detection antibody that generates the signal. The antibody pairs, sensitivity, inter and intra-assay reproducibility for each assay is outlined in Table 6.1. Calibration values are also provided for each fragment in Activated Complement Serum (ACS), used as the standard for all assays throughout this investigation. Values are therefore reported in ACS Units, pure ACS itself being assigned 10^6 ACS Units for each fragment. ACS and has been quantified for Bb and TCC at 55 ± 6 µg/ml and 2.10 ± 0.04 mg/ml respectively, and its stability and suitability for its use in this study was review in Section 4.6.

Table 6.1. Summary of all assays employed to monitor C activation within the CPOP trial cohort. From Chapter 4.

Analyte	**Capture Antibody**	**Detection Antibody (Labelled)**	**Sensitivity ± Accuracy**	**Intra-assay, Inter-assay Error**	**ACS Calibration Value**
C3d	Anti C3d neo (Quidel)	Anti-C3b clone C3/30 (Dr. Claire Harris, Cardiff)	0.864 ACS Units	8.8% 3.6%	C3bc in ACS ~ 1800 AU/ml [167]
Bb	Anti Bb neo (Quidel)	Anti-fB clone JC1 (Dr. Claire Harris, Cardiff)	995 ACS Units (54.7 ng/ml)	13.7% 3.9%	55 ± 6 µg/ml.
TCC	TCC mAb, clone aE11 (Hycult Biotech)	aC8 (Dr. Claire Harris, Cardiff)	1.11 ACS Units (2.32 ng/ml)	18.2% 5.7%	2.10 ± 0.04 mg/ml

6.3 Results

The time course profiles for each of the three assays did not follow a general pattern, as with the C3 and C4 time course profiles in Chapter 5. Therefore a 'nomogram' analysis was not suitable for this investigation, and the results therefore remain largely descriptive and comparative. The results from each assay will be considered in turn. All time courses are complete for the C3d assay, although 8 entire time course profiles are missing for the TCC assay, as the values obtained fell below the detection limit. Of the remaining time course values, 96% were within the detection limit and remain in the overall time course. 98% of Bb time course values are intact, with the exception of a few individual time points which fell below the detection limit of the assay.

6.3.1 C3d Activation

The majority of observations regarding the fragment analysis was dominated by 'peak' analysis, after it was observed that many time course profiles contained at least one spike in fragment concentration, usually only for one time point. This is consistent with the 'cascade avalanche' theory, whereby the formation and subsequent consumption of a particular fragment may happen very quickly. A peak is defined as a value that is two times greater than the average time course value for a particular patient. For all time courses, 33 out of 45 patients displayed a peak during the time course, with 7 of the 33 having two points that classified as peaks. Seven out of the ten patients who developed complications show a peak in C3d. The average concentration of all C3d peaks was $8.1\times10^4 \pm 7.0\times10^4$ ACS Units, compared with the average concentration on admission of $2.0\times10^4 \pm 3.7\times10^4$ ACS Units.

Further investigation of the C3d activation events showed that there was some stratification regarding the peaks in C3d concentrations. Some patients displayed early peaks, either during or very shortly after the surgical procedures, and others much later – after 12 or even beyond 24 hours following the operation. Four patients showing typical early C3d peaks are shown in Figure 6.4 and similarly four typical time course profiles for late peaks are shown in Figure 6.5.

Three patients showed both early and late peaks. Four time course profiles with no C3d peaks are shown in Figure 6.6 (for comparison the time and concentration axes are consistent on all three graphs).

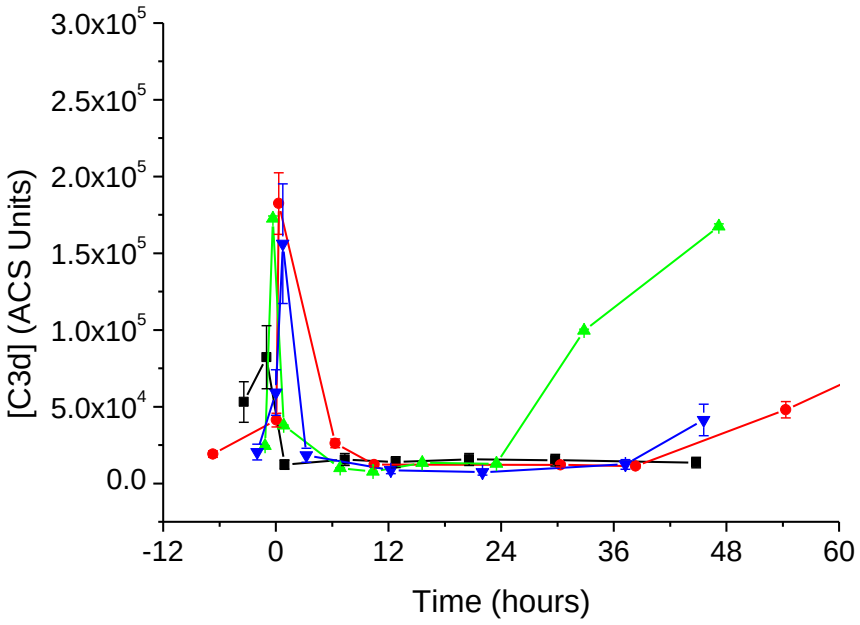

Figure 6.4. Graph showing early C3d peaks for patients CPOP0010 (black), CPOP0015 (red), CPOP0020 (green) and CPOP0035 (blue).

Figure 6.4 shows C3d activation profiles for 4 patients, all displaying early concentration spikes. CPOP0015, CPOP0020 also show secondary activation peaks after 36 and 24 hours respectively. Very noticeable is the quickness with which the C3d concentrations return to their respective preadmission levels, which indicates rapid clearance post production.

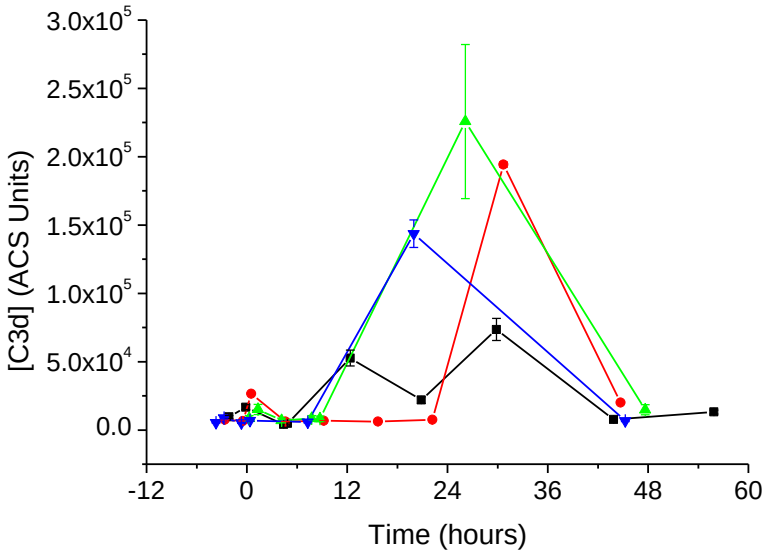

Figure 6.5. Graph showing late C3d peaks for patients CPOP0019 (black), CPOP0021 (red), CPOP0022 (green) and CPOP0042 (blue)

Figure 6.5 shows C3d activation profiles for 4 patients who did not present an initial concentration spike, but did show a peak in C3d concentrations after 12 hours, the latest peak recorded ~30 hours post operatively. Once again C3d concentrations return to their preadmission values after a concentration spike, however the timescales associated with this return to normal in this case may not be representative of the true situation due to the lower sampling frequency compared with the activation profiles in Figure 6.4.

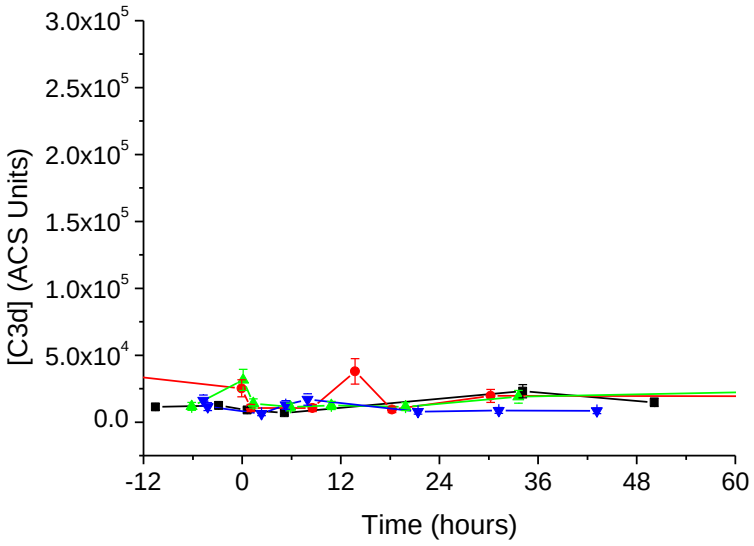

Figure 6.6. Graph showing no C3d peaks for patients CPOP0007 (black), CPOP0012 (red), CPOP0023 (green) and CPOP0028 (blue)

Figure 6.6 shows stable C3d levels for all patients, remaining constant throughout the time course of 60 hours, especially relative to the concentration peaks seen in Figure 6.4 and Figure 6.5 (note y-scale). In this instance it may have been possible that the spike in C3d concentrations occurred in between sampling points, and therefore it is not seen. Another explanation may be that these patients simply did not show C activation, and may be considered to have an inactive C system, possibly due to the absence of some cascade components.

All C3d peaks are collated and shown in Figure 6.7. It was expected that all patients would show C activation, however in this instance 73% of patients presented a peak in C3d. As seen from the rapid concentration spikes in Figure 6.4, it may be possible that the patients who did not present C3d peaks did so in between sampling points, and therefore the spike may not have been seen.

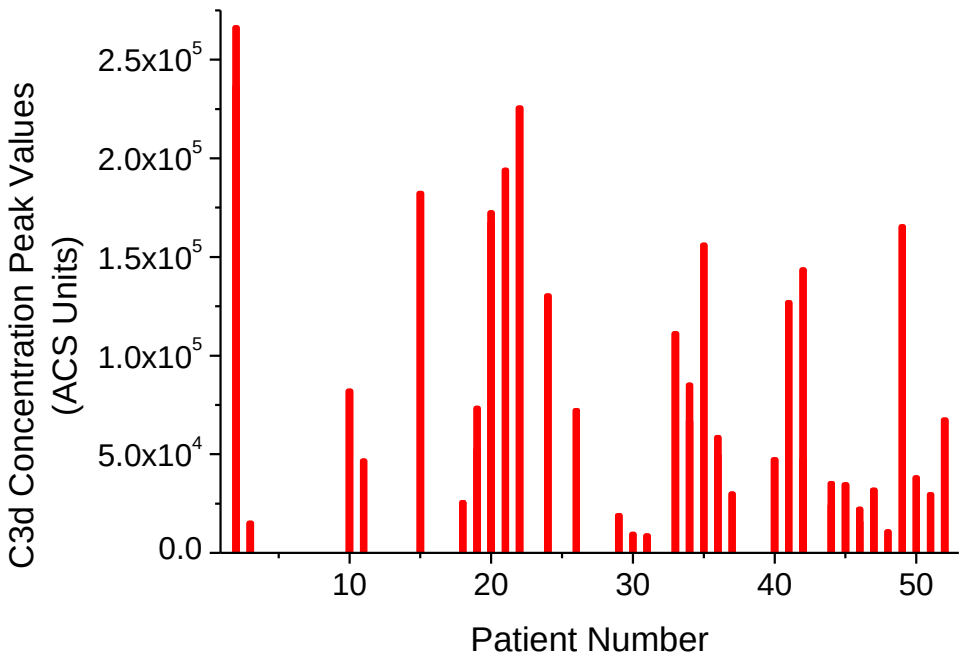

Figure 6.7. C3d concentration peaks for all 45 patients across the cohort. (Note 'Patient Number' does not correspond to the number of patients in the trial. It is the number assigned to patients as they were recruited)

6.3.2 TCC activation

TCC values for the majority of time course profiles remained relatively constant, with very few time course profiles displaying a significant rise or fall in analyte levels. The values were also low, often falling just above the detection limit for the assay. In total 9 patients displayed TCC peaks as in the C3d peak analysis, 20% of the cohort. The average relative ratio of the TCC concentration peaks to the values on admission was a factor of 9.1. Only one of these peaks correlated with a patient that developed a complication, CPOP0050.

6.3.3 Bb Activation

The concentration of Bb also remains fairly constant throughout the time courses for the majority of patients. For comparison only 10 patients (22%) display concentration peaks where values were greater than twice the average of the time course it is in. The same patient, CPOP0050 is the only one from those that developed complications that shows a peak in Bb.

6.4 Discussion

C activation assays were performed for C3d, TCC, and Bb on plasma samples from a 45-patient time course study. These markers are well documented in the literature as being good markers of C activation, and therefore they were implemented here. Samples were collected as EDTA-plasma, which has been well documented [57; 147; 149; 228] to stop the cascade and prevent any further *in vitro* formation of C activation products.

From the conclusions drawn in Chapter 4, the TCC and C3d assays worked well, yielding a dynamic range of ~3 orders of magnitude. With a dynamic range of <2 orders of magnitude, the Bb assay did not perform as well. These assays were employed to measure C activation among a cohort of patients undergoing elective abdominal surgery. Observed changes in TCC and Bb concentrations throughout the measured time course were small within individual time course profiles, with the absence of any regular pattern in biomarker behaviour. However a large range of concentrations was observed for both analytes on admission throughout the patient cohort: TCC, 505 ± 1078 ng/ml *cf*. 0.06 ± 0.03 µg/ml [157] and Bb, 0.429 ± 1.45 µg/ml *cf*. 0.20 ± 0.04 µg/ml [157], Figure 6.8. Absolute concentrations of C3d could not be determined, explained in detail in Section 4.5.3.

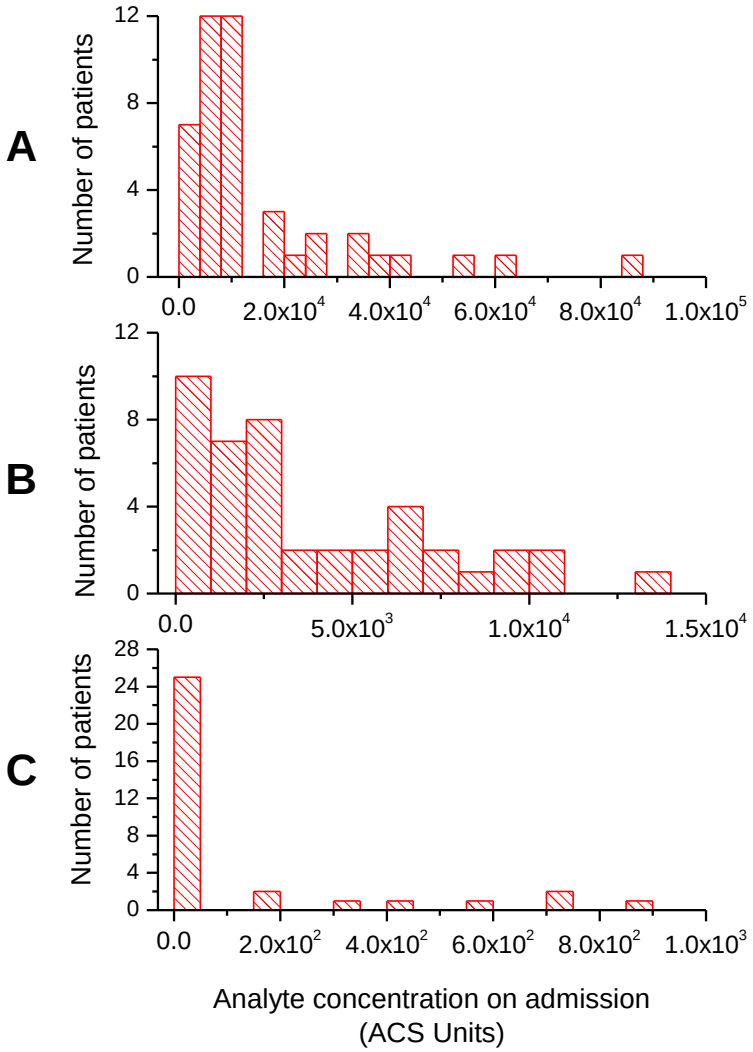

Figure 6.8. Concentration distributions (in ACS Units) of all three activation markers assayed; A, C3d, one value not shown (2.37×10^5), B, Bb, one value not shown (1.78×10^5) and C, TCC, two values not shown (1.82×10^3 and 2.27×10^3).

The concentration distribution profile of all three fragments is consistent with expected levels on admission. The C system should be idle in the majority of patients, however it is likely that some patients will exhibit an activated C system on admission, either due to the disease they are receiving surgery for, or another undiagnosed condition. Therefore a distribution that is shifted towards the lower concentration range is expected.

The low concentrations of both Bb and TCC in the samples, especially the latter, made it difficult to measure the analytes accurately, as they presented a low signal below the

calibration curve. Initial assessment suggests the low concentration of both of these analytes in plasma therefore has negative implications for their use as a predictive biomarker for C activation. However it should be stressed that the potential for TCC to be a C activation marker should not be easily dismissed.

TCC has a half-life in plasma of order 24 hours [251], and therefore systemic C activation leading to TCC formation may be detected by daily sampling. The time course designed for this clinical trial did not continue monitoring patients until they developed complications, which was days after the time course stopped in some cases. Once secondary infection develops postoperatively, a large increase in TCC levels will be observed, and may be detected systemically using daily routine blood samples. Therefore, in this case, the low native concentration of TCC in blood is in fact helpful, as any great increase in TCC levels will be indicative of systemic C activity. The surgical trauma almost certainly produced high amounts of TCC local to the surgical area, however no patients developed a systemic condition which would warrant the increase of TCC concentrations from their initial low levels after only 60 hours of monitoring. In a private communication with Prof. Tom Mollnes about the TCC activation data, it was suggested that noticeable increases in systemic TCC concentrations would not be seen unless the trauma of surgery was extremely large, for example major open heart surgery. This view is supported in several previous cardiopulmonary studies [252; 253; 254] and possibly explains why such little activation of TCC was observed here.

The C3d assay worked well as a C activation marker. Activation was observed in 33 out of 45 patients (73%), meaning that in the remaining 12 patients there was either no C activation, or the activation avalanche was missed with the time points of the samples taken. 7 out of 8 C3d time course profiles for laparoscopic procedures showed a peak in C3d, indicating that more minor procedures also cause C activation. The average C3d value on admission for all patients was 2.0×10^4 ACS Units, and the value of the observed peaks was more than a factor of 4

greater at 8.5×10^4 ACS Units. If C3d had been used as a predictor for complications in this study using the peak metric, it would have truly predicted 7/10 complications. However, it would also have identified a further 26 who did not develop complications – a high false positive rate.

Consideration should be given to the position of C3d and TCC within the C cascade. C3d is an upper cascade activation marker, whereas TCC is a lower cascade activation marker indicating C activation to completion. Therefore the lack of TCC activation may be indicative of the lack of activation conversion between C3d and TCC. In other words, a low fraction of patients converted upper cascade activation to complete C activation. All 9 of the TCC profiles that displayed a peak also showed a peak in C3d, as expected, however that means only 9 of the 33 C3d patients who showed C3d activation presented activation to completion by TCC formation. This suggests C3 fragmentation is required to cause TCC formation, as expected, however upper cascade activation does not necessarily lead to TCC formation, and therefore complete C activation. The long half-life of TCC [251] further indicates that the lack of TCC formation suggests lack of activation to completion rather than clearance in between sampling points.

Sample Collection Protocol

The collection of samples as EDTA-containing plasma is well advocated throughout the literature [147; 149; 166]. This investigation employed the same protocol, collecting blood samples directly into EDTA-containing tubes, and then centrifuging the blood samples to obtain EDTA-plasma. The absence of any unexpected concentration rises in any of the patient time course samples indicates that the collection protocol was suitable, and supporting evidence for EDTA-stabilisation of fragment concentrations can be seen in the study by Bergseth *et al.* [167]. Their study also demonstrates that the addition of Futhan increases fragment stability even further, however this is impractical for sample collection in a hospital ward, as the standard collection tubes contain EDTA only.

6.4.1 Complement Fragment Clearance

As mentioned before, many of the patient time course profiles did not present a peak in a certain analyte's level (11 time course profiles failed to show a peak in any of the fragment concentrations). There are two possible explanations for this. Firstly, given the short time span in which many of the peaks were observed, it is possible that for these patients the concentrations spike simply went undetected. That is, the concentration spikes possibly occurred in between blood sample time points, and therefore the event goes unnoticed. The second explanation could be that these patients have an idle, unresponsive C system, which may be indicative of a weak immune system. Again, the small number of patients involved in the trial means this inferred C inactivity cannot be proven, but it is an important consideration, especially if the trial is to be expanded to address further questions such as this.

Complement deficiencies must also be considered briefly, for if there are components of the cascade with low concentrations or missing completely, then the cascade function would be compromised. Many deficiencies in C components have been reported and have been linked with clinical disorders or accentuated susceptibility to infections [255; 256]. However such deficiencies are extremely rare, and therefore consideration of C deficiencies in a trial of this size should be limited.

6.4.2 Using the Complement System Clinically – CPOP Care

As the CPOP clinical trial yielded two parallel investigations, the C consumption (Chapter 5) and the C activation studies (Chapter 6), they will both be discussed here to address the question of whether monitoring the C system perioperatively has positive implications for patient recovery care. In addition to time course profile data for CRP, IgG, C3, C4, TCC, C3d and Bb, all other results from routine tests ordered were recorded and collated into a database, Appendix 1. This included a host of tests and observations that form part of regular patient monitoring perioperatively.

Monitoring Recovery

The starting point is that all patients will have an individual C activity measure, comprising initial component levels and C activation potential. The basis for the 'CPOP care' hypothesis is that all homeostatically controlled variables (in this case C component and fragment concentrations) must return to their preoperative values following complete recovery. Therefore the rate and status of recovery may be measured by monitoring a variety of measures, including immuno-components.

Currently the clinical standard for recovery monitoring is comprised of a list of clinician observations and checkpoints, with a limited role of biochemical markers mainly limited to creatinine and CRP. As we saw in Chapter 5, CRP is slow to respond to an immunological challenge, and therefore a more responsive marker would be preferred. The immediate postoperative synthesis of C3 and C4 could therefore provide a better indication of a patient's recovery status. It is not suggested that this should be a marker to replace the current status quo of patient monitoring, however it could be an additional test to supply the clinician with supporting evidence if they decide to discharge or keep a patient in hospital, for example.

Not only may it be a good addition for patient care, the initial rate of biochemical recovery, as measured by C3 and C4 levels returning to their preoperative levels, for example, may be of use in predicting a patient's length of stay postoperatively. Therefore stratification of patient recovery can also be attempted, whereby patients can be classified according to their initial rates of recovery postoperatively. This has significant implications for hospital ward management by optimising the use of the available resources. Early identification of patients who are at risk of developing infections will also help in this regard, as resources can be channelled more effectively.

Developing a Testable Hypothesis for further Investigation into CPOP Care.

There have been several unexpected results gained from the CPOP trial. Firstly, the consistent initial C3, C4 and IgG dilution was a surprise, however the additional C consumption was expected. The continued depletion of IgG levels was also not foreseen. The apparent C system inactivity in some patients, as evidenced by the lack of fragment peaks, also warrants further questioning, however it may be explained simply by a low frequency of sampling points, as activation could have occurred and been missed by the sampling regimen. The TCC assay performed very well, and although few patients presented with TCC peaks, the assay should be included in an expended study. TCC would be especially useful to monitor the levels of systemic TCC in patients with SIRS or sepsis by employing an extended time course, as TCC production would be expected from a severe systemic immunological challenge, as mentioned in the private communication with Prof. Tom Mollnes.

Crucially, to confirm or refute any of the hypotheses made in this study, any future trial will have to sample a far greater number of patients, all ideally undergoing a limited subset of procedures. Although the surgical procedures in this study are relatively comparable, further consistency with regard to the surgical procedures will remove some uncertainties, especially with regard to C consumption and subsequent recovery of the components. For example comparison between laparoscopic and open surgical procedures can introduce questions with regard to the degree of severity of the procedure, and therefore comparison between C consumption levels may not be valid. Although it was useful in this study to observe the difference between the two procedures, any future trial should employ a greater surgical procedure consistency in order to focus on stratified recovery profiles only. Although unknown variables such as co-morbidities cannot be controlled, experiment design can, and therefore known variables should be standardised as much as possible. A higher number of patients is required to obtain a meaningful number of patients who develop secondary infections so they

can be compared with the patients who recover normally. Comparing with the current size of the trial, to obtain data for 45 patients who develop complications would require a cohort of approximately 205 patients in a similar study with a similar complications rate. Ideally the number should be as high as possible to make the data obtained statistically significant.

6.4.3 Case Studies

Given the low number of participants in the prospective cohort, there is only a small group of patients who developed complications. It is appropriate to consider individual case studies, and compare their clinical data against surgery outcomes in light of all three fragments together, especially compared with their C3 and C4 time course profiles – a full C analysis. Where appropriate, comparison should also be made with the CRP response.

CPOP0015 – Secondary Complement Consumption, Figure 6.9

Figure 6.9 shows selected the clinical time course data for patient CPOP0015. Initial consumption of both C3 and C4 can be seen up to 12 hours, after which a partial recovery synthesis of both proteins is followed by a secondary consumption event from 38 hours, Figure 6.9A. Fragment data, Figure 6.9B shows an early spike in C3b concentrations followed by a rapid return to admission levels within 12 hours. After 36 hours a slower, smaller activation is observed up to 72 hours. The concentration of both other fragments, Bb and TCC, remain largely constant throughout the duration of the time course. Figure 6.9C shows the time course profiles for CRP and IgG, the latter displaying a large initial dilution, followed by a slight recovery up to 38 hours, after which another large drop in concentration is seen. CRP concentration rises as expected from an elevated initial value of 27 mg/L, but crucially, is then falls after 36 hours, indicating a decline of the acute phase response and therefore a return to normal health. The patient's basic observations of heart rate and temperate can be seen in Figure 6.9D, which forms a vital part of postoperative patient monitoring, and is two of the parameters monitored for the EWS. Note that the time scale for both these observations

continues well beyond the timescale for the other markers, up to approximately 170 hours. Heart rate shows a sharp initial rise associated with surgery, but then continues to display an elevated level for most of the continued time course. Temperature is normal for the majority of the time course, however the rise to ~38°C at 144 hours satisfies the temperature criteria for the definition of SIRS or sepsis [249].

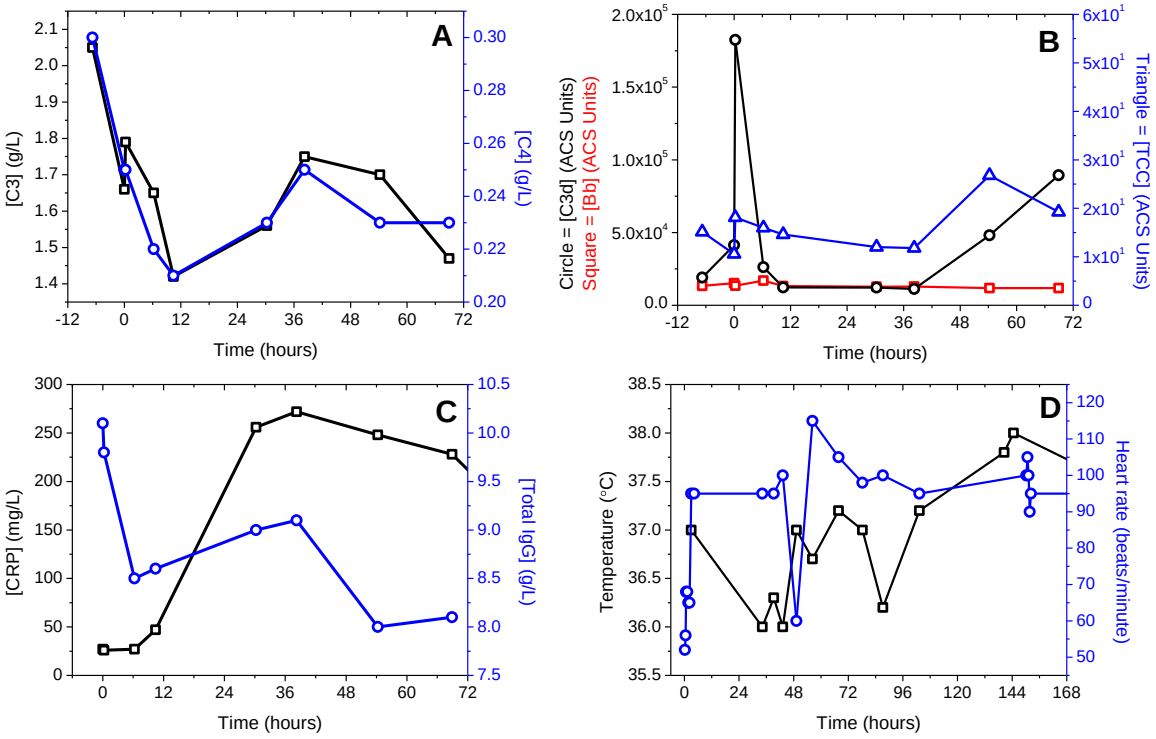

Figure 6.9. Clinical time course data for patient CPOP0015. A, concentrations of C3 (black) and C4 (blue). B, activation fragment time course profile for C3d (black), Bb (blue) and TCC (red). C, time course profiles for CRP (black) and Total IgG (blue). D, standard observations, temperature (black) and heart rate (blue).

Patient CPOP0015 was a 73 year old male who also received an anterior resection after being diagnosed with colorectal cancer. The patient's CRP level on admission was 27mg/L. Comparison between the C components C3 and C4, and CRP shows that C3 and C4 has responded to the initial trauma of surgery just as CRP begins its response, which does not conclude until 38 hours. After this time the concentration of all three analytes fall, indicating opposite outcomes. As mentioned, a reduction in CRP concentration suggests the recession of the acute phase response to the initial surgical trauma, and therefore suggests the patient is

returning to normal health. Conversely, C consumption may suggest complement activation, especially if coupled with the fragment C3d, which begins to rise after 36 hours. This patient went on to develop sepsis 6 days after surgery, consistent with the temperature rise to 38°C at 144 hours, and ultimately died a further 8 days later following additional complications. Therefore, for patient CPOP0015, C recovery and the secondary consumption event suggests that this patient had not returned to preadmission levels of health 72 hours postoperatively, and warranted heightened attention from medical staff. CRP concentrations continued to decline for three consecutive (third not shown) time points after 36 hours, which is not indicative of the imminent onset of sepsis that was to come. Crucially, the information provided by C recovery is observed considerably earlier than any of the other parameters available.

CPOP0003 – Complement Activation

Figure 6.10 shows the analyte concentration and basic observations time course data for patient CPOP0003. The patient experienced a large initial consumption of C3 and C4 levels, after which the levels replenished quickly, followed by some secondary consumption of both proteins from 8-12 hours, after which C recovery continued, Figure 6.10A. In terms of activation markers, CPOP0003 is exemplary with regard to what was expected from the C cascade activation markers. C3d and Bb, present earlier in the cascade than TCC, peak first – around 6 hours post induction, Figure 6.10B. Although TCC is seen to increase between 9 and 12 hours, it is not until 28 hours that a peak is seen in TCC, suggesting a lag period of 22h from initial C activation stimulus to cascade completion. This patient presented with elevated CRP levels on admission, which then continued to rise for 50 hours postoperatively, Figure 6.10C, and their IgG response profile was similar to C3 and C4, which is inconsistent with the rest of the patient cohort in this study. The patient's standard observations (temperature. heart rate)

were normal, with the exception of a slightly raised heart rate towards the end of her stay in hospital, Figure 6.10D.

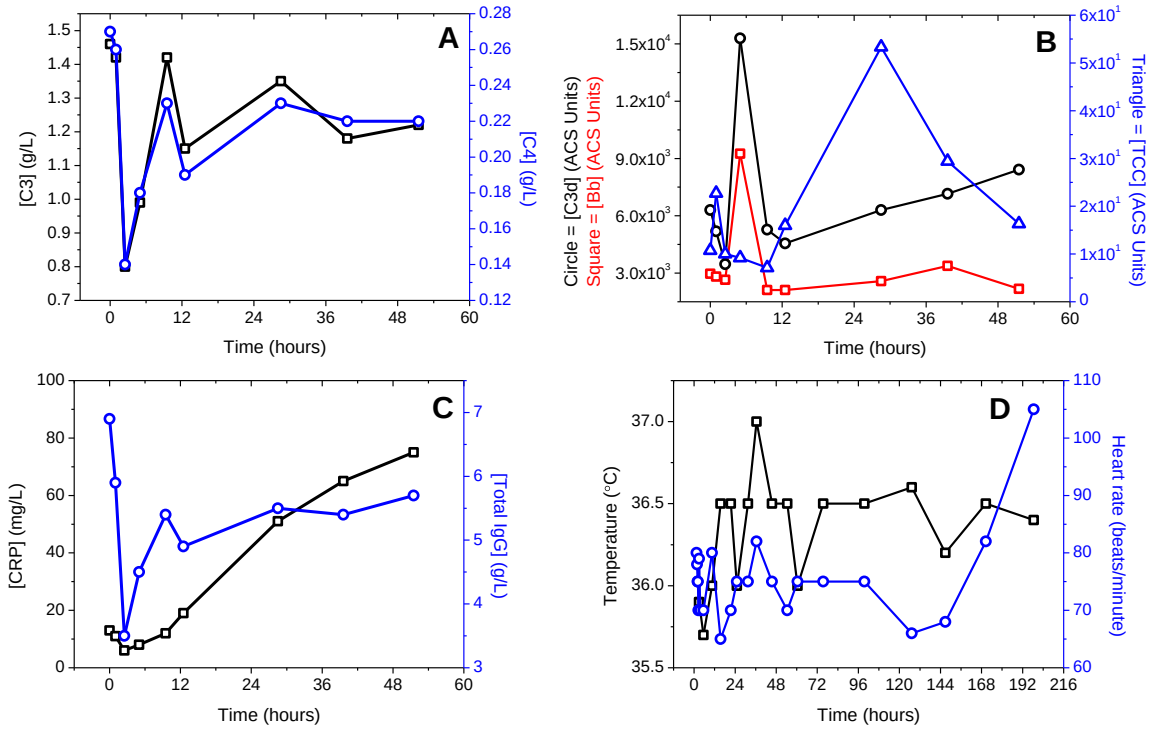

Figure 6.10. Clinical time course data for patient CPOP0003. A, concentrations of C3 (black) and C4 (blue). B, activation fragment time course profile for C3d (black), Bb (blue) and TCC (red). C, time course profiles for CRP (black) and Total IgG (blue). D, standard observations, temperature (black) and heart rate (blue).

Patient CPOP0003 was an 87 year old female who received an anterior resection after being diagnosed with colorectal cancer. The procedure severity was classified as Class 4 of 6 by Mr. Ian Daniels, the surgical consultant on the CPOP trial. Given the severity of this procedure classification by Mr. Daniels, it is expected that the physiological fingerprint evidenced by C3 and C4 consumption would be large. Indeed, a very large initial drop in C3 and C4 levels is observed, however the concentrations of these proteins are replenished rapidly, suggesting a fast recovery. The activation markers Bb and TCC reflect the consumption in C3 and C4, suggesting C activation as a result of surgical trauma in this instance, in particular Alternative and Lytic pathway activation. This patient suffered no complications and was discharged 8 days after surgery, a decision consistent with the C recovery of this patient.

CPOP0001 – Differential C3 and C4 recovery and comparison with IgG

Figure 6.11 shows the time course variations for C3, C4, IgG and CRP for patient CPOP0001. In the first ten hours the C3 and C4 levels decrease with an initial dilution consistent with the anaesthetic fluid regimen resulting in ~20% decrease in the circulating concentration of C3 and C4, Figure 6.11A. The C3 and C4 show a minimum after 2 hours from induction, where t=0. C3 and C4 synthesis starts immediately so that within the 60 hours of the trial time course their concentrations have returned towards the levels on admission, however C3 recovery at 50 hours is substantially lower than C4. The expected rise in CRP associated with the surgical incision trigger of the acute phase response is shown in Figure 6.11C. The *de novo* synthesis of C3, C4 and CRP may be contrasted with concentrations of total IgG, Figure 6.11C, blue, which shows an initial decrease associated with the 1 L fluid administration on induction and remain at or below the post-induction levels for the 60 hours of the trial time course. The time point for IgG at 34 hours is likely to be an anomaly. The basic observations of temperature and heart rate, Figure 6.11D are normal, aside from the low temperature early on, possibly associated with measurement error, and the initial spike in heart rate that can be attributed to the surgical procedure.

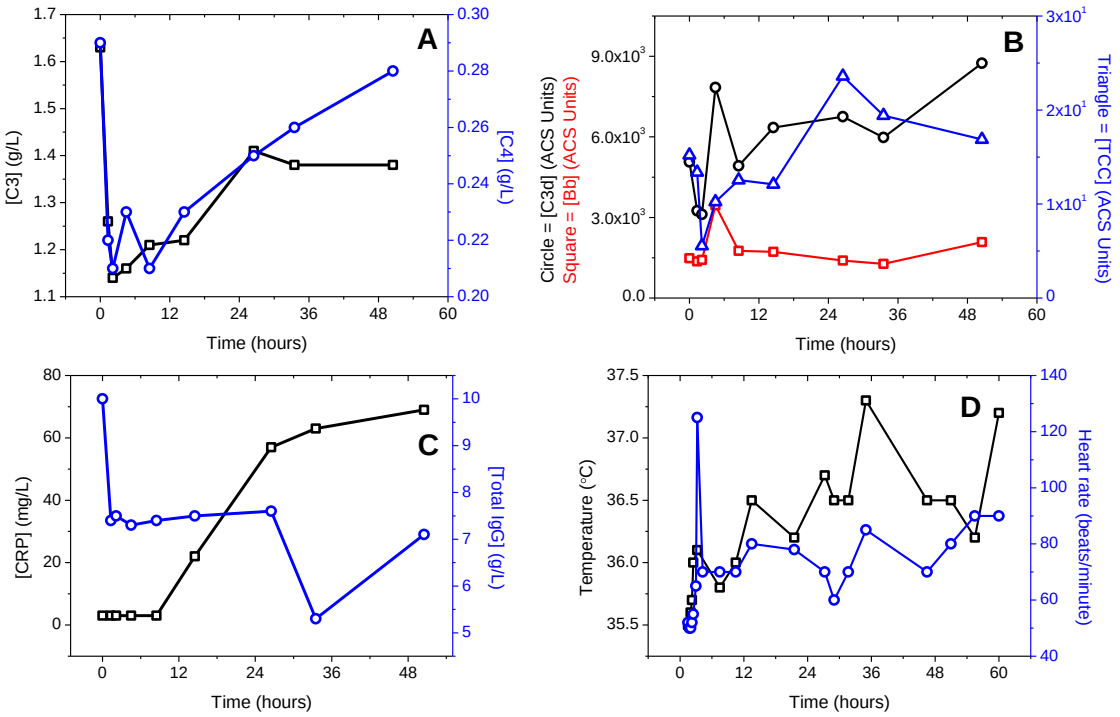

Figure 6.11. Clinical time course data for patient CPOP0001. A, concentrations of C3 (black) and C4 (blue). B, activation fragment time course profile for C3d (black), Bb (blue) and TCC (red). C, time course profiles for CRP (black) and Total IgG (blue). D, standard observations, temperature (black) and heart rate (blue).

An interesting observation is the difference between C3 and C4 recovery, Figure 6.11A. Apparent C3 consumption without C4 consumption may imply C activation via the Alternative pathway, which does not require C4, indicating the type of challenge the host is responding to. However very little C activation is shown by the C activation fragments for this patient to confirm activation. Although this patient recovered normally and was discharged after three days, cases of differential C3/C4 consumption pose interesting questions about individual C activity, as on average, both proteins respond the same across a patient cohort, meaning that differential C3/C4 activation for an individual patient is unusual. The contrast between C components and IgG is more typical of the patient cohort (bar the anomaly), as seen by the nomogram analysis in Chapter 5.

CPOP0025 and CPOP0039 – CRP vs Complement Response

The time course profiles of CRP, C3 and C4 are shown in Figure 6.12 for a laparoscopic procedure, Figure 6.12A, CPOP0039 and an open procedure Figure 6.12B, CPOP0025. In the less invasive laparoscopic procedure the patient shows a rapid return to near admission levels for C3 and C4 within 12 hours, whereas the CRP levels for this patient showed no significant change during this period. The concentration of CRP then increased to the comparatively low maximum of 28 mg/L before starting to decrease. The patient remained in hospital with near-normal levels of C before being discharged after 100 hours. CRP is an extensively studied marker for inflammation, and its relatively low maximum concentration in this case is likely to be related to a low amount of inflammation during surgery which is expected from the laparoscopic procedure [257; 258; 259]. However, the maximum in CRP is not reached until 24 hours, and a decrease is not seen until 34 hours, which indicates a reduction in inflammation. C component levels, on the other hand, are replenished in this case within 12 hours and provide a much earlier indication of the low trauma associated with this surgical procedure, as was the case with CPOP0003, Figure 6.10. Therefore C recovery profiles provide much faster information to the clinician with regard to patient recovery postoperatively.

Figure 6.12B shows a patient with a more complex procedure, (radical cystectomy, radical hysterectomy and left-salpingo-oophrectomy, lasting 190 minutes) which presented with greater than 50% C consumption within 10 hours of the procedure, indicating severe surgical trauma. The patient showed a slow but consistent recovery in C3 and C4 levels over the first 72 hours of their time course profile. The patient presented with a peak in CRP levels after 38 hours although the patient still showed significant C consumption. The CRP peak >80mg/L suggests a greater acute phase response compared with CPOP0039, as would be expected from the greater surgical trauma and tissue damage, which is also consistent with the large C consumption shown which reached a minimum before 10 hours. Thus, even in the largest C

consumption within the cohort, C consumption can still provide clinicians with recovery information well before CRP has finished its initial response, the offset in this case being ~24 hours.

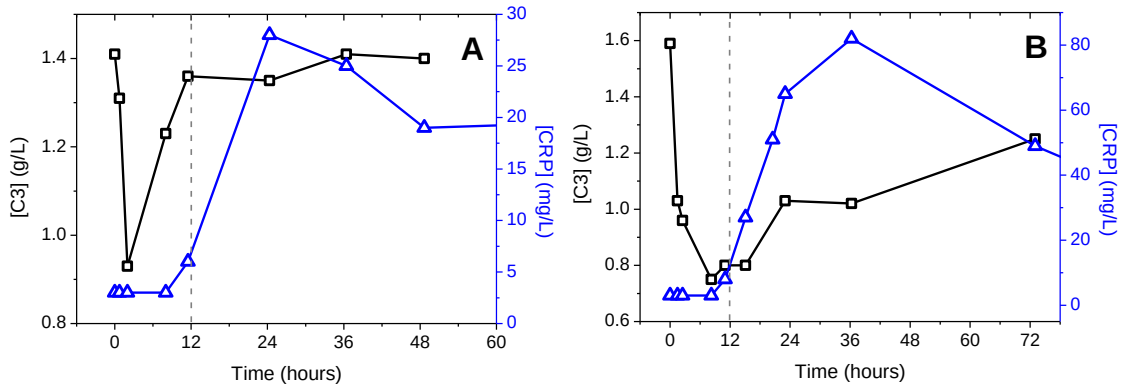

Figure 6.12. CRP and C3 time course profiles for two patients: A CPOP0039 Diagnosis colorectal cancer, Laparoscopic right hemicolectomy, Age 75, duration of surgery 115 minutes, length of stay 99 hours; B CPOP0025 Diagnosis of Bladder Cancer, radical cystectomy, radical hysterectomy and left-salpingo-oophrectomy, Age 83, duration of surgery 190 minutes, length of stay 386 hours. Recovery risks based on C3 consumption are indicated. CPOP0039 showed secondary CRP production 128 hours

6.5 Conclusions

The results from the initial, 45-patients CPOP clinical trial are promising, yielding a number of unexpected outcomes which warrant further investigation. The preliminary results from the C activation assays did not respond as expected, with the exception of C3d which showed both rapid and late C activation. The low TCC concentrations obtained is consistent with values previously reported in the literature, as shown in Figure 4.3.

Regarding the presymptomatic identification of patients who may be at risk by using C fragments, it is clear that a larger patient cohort is required to increase the numbers of patients suffering complications, and the surgical procedures can also be standardised. This will allow significant statistical analysis between patients who recover normally and patients who suffer complications. Furthermore, the usefulness of TCC as an indicator for SIRS or sepsis can be investigated by lengthening the time course over which blood samples are taken. Blood samples will need to be taken with relatively high frequency, as TCC can be generated quickly by the enzymatic cascade.

A study of possible C inactivity could also be designed, whereby blood samples are taken with a very high frequency early on in the time course, during and immediately following surgery. If some of the time course profiles in this study did indeed miss the C3d concentration spike, a study with a higher frequency of blood samples will stand a greater chance of detecting the peak. Such C inactivity may render an individual more vulnerable to an immunological attack, and therefore this inactivity may then be compared between patients who suffer complications and patients who follow a normal recovery.

6.5.1 CPOP Care Conclusions

C consumption and synthesis profiles of both C3 and C4 appear to be highly personalised markers of recovery, although a much larger patient cohort is required to test the hypothesis for statistical significance. There are a number of hypotheses which can be derived from the prospective cohort study. The degree of C3 consumption is correlated to an empirical classification of surgical trauma on the basis of severity – a successful trial here could prove C3 consumption to be a biomarker of surgical trauma. C response profiles are also considerably faster than CRP in reporting information regarding the patient's recovery postoperatively – C biomarkers may be better and more personalised measure of patient recovery. A combination of C metrics such as percentage consumption, postoperative synthesis rates and an arbitrary recovery percentage may be combined to assess their performance against the existing EWS system which may then be augmented by these markers to provide a biochemical element to the score. The C panel would then be a biomarker of infection or secondary complications. For all of these hypotheses however, a larger trial is required to assess significance and most importantly to establish clinical utility.

The combination of clinical observations and new C biomarkers has potential to change the biochemical monitoring of patient recovery. Simple correlations between rising parameters such as temperature and blood pressure may need to be analysed in a larger algorithm to

provide a significantly better informed clinical decision. Trends and significance tests of a systemic view of an individual's health appear very promising from the profile of C critically addressing a personalised recovery, perhaps leading to a more general stratification of outcomes against which healthcare resources can be marshalled. The multi-biomarker panel may provide pre-symptomatic diagnoses which will not be evident clinically and would require a change in the intervention strategy from clinicians if the full potential of CPOP care is to be achieved.

Chapter 7

Conclusions and Future Work

George Poste has written about the 'fragmented research on disease', and notes how although there are over 150,000 papers documenting thousands of different biomarkers for disease, only about 100 biomarkers are routinely used in the clinic [260]. He calls for the replacement of investigator-initiated research by a collaborative 'big-science' approach comprised of industry and multi-disciplinary scientific experts, including engineers, statisticians and experts in clinical trial design. From the point of view of the university researcher it is imperative to initiate collaboration, drawing together a range of expertise and consulting with scientific funding and governing bodies to bring potential biomarkers to the regulatory authorities such as NICE or the FDA for approval.

The cohort study marks the beginning of a long pathway to the validation of the Complement (C) system as a biomarker panel to be implemented as a companion diagnostic or a recovery monitoring tool. Monitoring of C activation in relation to disease states is well studied and has been discussed, with many infections and inflammatory disorders shown to stimulate the C system. The differential manner in which the C system is activated has promising potential for stratifying patients who present with C activation into different disease states, which has significant implications from the point of view of targeted disease diagnosis and treatment.

However, the current state of the field is that individual C components and fragments are monitored to establish activation, but it is suggested here that a panel of C system proteins are used to obtain a dynamic interaction profile between the components. This will provide a better understanding of C activation in relation to disease states, and may allow a more specific diagnosis of disease based on the C component interaction profile.

7.1 Thesis Conclusions

Complement

In this thesis, three working assays for C components TCC, Bb and C3d have been developed and employed to monitor C activation in a prospective cohort clinical trial for patients undergoing major abdominal surgery. Bb and TCC indicated low levels of C activation across the patient cohort, however a substantial rise in C3d concentrations indicated significant C activation in 73% of patients during the observed time course. Additionally, by monitoring levels of C3 and C4 it was demonstrated that consumption of the C system may be used to stratify surgical trauma and monitor subsequent recovery. Preliminary analysis was performed to establish hypotheses for testing stating that the initial rate of synthesis of C3 and C4 to pre-admission levels may identify patients at risk of developing complications. A slower synthesis rate could mean the patient's C system is compromised for longer, possibly leaving the host susceptible to a secondary immunological challenge.

C consumption appears to be a promising biomarker for surgical trauma that provides a response that is faster than CRP or other clinical observations. Stratification of patients based on this metric in relation to recovery monitoring looks interesting and may lead towards to new ways to manage clinical resources. Crucially, the assays are already in place and approved for clinical use. Additionally, normalised C3 and C4 recovery profiles may be used to predict a patient's length of stay, however an arbitrary percentage recovery threshold must first be established as an indicator of individual biochemical recovery. Interesting observations regarding secondary C consumption coupled with activation may lead to presymptomatic diagnosis of disease, which would allow the current Early Warning Score (EWS) system to be improved. Although surgical and drug advances for patient care have been large, postoperative patient monitoring has not enjoyed the same level of progression, and remains based around monitoring the vital signs of a patient.

The nature of conventional blood sample collection in hospitals means that detection of C system activity reflects the systemic health state of the patient, as activated C fragments present in plasma, for example, indicates systemic C activation. Therefore better and additional assays for C activation are needed to establish the full potential of the C system as a health monitoring tool.

Label-free Assay Development

In order to transfer established immunoassays, such as those developed to monitor C activation, onto label-free, kinetic binding measurement-type instruments such as the Liscar, the nonspecific interference effect of plasma proteins was investigated and demonstrated. In an effort to reduce nonspecific binding to the surface, addition of a chaotropic agent to the sample was also investigated. However, in an acknowledgement that nonspecific interference from real biological samples is unlikely to be completely removed, a mathematical model for data analysis was created based on a 10-reaction mechanism to account for specific binding, nonspecific binding and competitive binding between the analytes in solution. This can be used going forward, along with additional measures to improve label-free, kinetic binding signals in order to screen real biological samples for target analytes.

Efficient sample handling is a key aspect for point-of-care diagnostic technologies. The Liscar nanoparticle platform has many suitable properties in this regard – a robust sensing chip and fluid management system (possibly containing a chaotrope buffer if needed) has the potential to be a point-of-care technology capable of detecting up to ca. 20 biomarkers from a single blood sample. The investigation in Chapter 2 indicates that whole serum or plasma samples can be used. The concept is supported by the mathematical model which suggests there is a fundamental advantage in detecting a high-affinity molecule to a sensor surface. Currently, antibody-analyte solutions are preferred, employing the corresponding antigen as the surface

ligand, however recent screening of antigen-target analytes has been demonstrated by Tom Read.

7.2 Future Work

Complement

Going forward immediately, it is suggested that a detailed study of *in vitro* C activation is done to expand on the investigation carried out by Liu *et al.* [156]. Many different C components and fragments should be monitored with differing concentrations of Zymosan and Heat Aggregated IgG (HAIGG). The concentration dependence of the activation substance can then be determined, and the relative interactions of C system proteins studied mechanistically and mathematically. A high sampling rate during activation is important to observe fast, complex behaviour which is likely to be present. Preceding this investigation it would be useful to develop more C activation assays, ideally on the MSD electroluminescence platform so that the assays may be multiplexed and analysed in tandem. The activation markers should reflect the activity in each of the 4 C pathways so that differential activation may be observed. The range of activators could then be expanded to include gram-positive and gram-negative bacteria [141], for example. From a successful, complete *in vitro* activation analysis, the established assay set will be able to monitor the activation flux through all of the pathways which can then be tested *in vivo.* However, many unknown kinetic factors such as clearance rates and surface regulation alters the *in vivo* model drastically cf. *in vitro*. Additionally, the rapid kinetic response of the C cascade avalanche produces real practical problems for blood sampling time point selection.

Therefore, once the activation process is fully understood *in vitro,* it is suggested that a similar study to the CPOP trial be conducted to include C fragment screening in urine samples. Urine is not liable to many of the clearance and regulation factors present in blood, which can contribute to the rapid rise and fall in C fragment concentrations. If urine output could be

collected at recorded time points and assayed for C activation markers, the fragment concentration present in the urine sample could be integrated over the time in between sampling points, thereby producing a C activation profile over a given time period. Another important point is that this provides insight into the patient's immunological response over a given integrated time period, and not at a specific moment in time. This means the integrated signal is not subject to much of the fluctuations in C system protein concentrations. Additionally, C activation fragments such as C5a and C3a that have short half-lives in plasma can be detected easily in urine, which further increases the options for C activation monitoring fragments. Commercial ELISA assays exist for both C3a and C5a, and therefore this analysis would not be subject to a lengthy assay development stage along with its associated costs.

In order to test the hypothesis of differential postoperative C3 and C4 synthesis rates to identify patients at risk of developing complications, it is suggested that individual preoperative C activation screening is performed. The suggested experiment requires patients undergoing surgery to donate blood before their operation. Their blood can be clotted, and the serum activated using relatively low concentrations of Zymosan. The rate of TCC production, for example, could therefore be used as an individual C cascade calibration metric, against which their immediate postoperative C3 and C4 synthesis rates can be compared. This may give some indication of a particular patient's 'immuno-capacity'; that is, the ability of the patient's immune system to successfully combat an immunological challenge. The established immuno-capacity can be compared for differing demographics and age groups, supplying yet more information to surgeons preoperatively, allowing them to identify patients who may be at greater risk of surrendering to an immunological challenge.

Some further investigation regarding percentage C3 and C4 recovery as a supporting evidence metric to discharge patients can also be performed. This investigation requires input from a wide variety of surgeons to establish the recovery level at which they would discharge a

patient. This can be achieved by a blind investigation, whereby patients are monitored as standard by clinicians, and are discharged subjectively according to the clinicians criteria. A blood sample on admission and discharge can be assayed for C3 and C4 and compared to establish the average C recovery across all patients at time of discharge. A well-considered trial design is needed, as the time of discharge can be subject to considerable variation associated with the time gap between late night and early morning, when patients are unlikely to be discharged regardless of health state.

Alternatively, the study CPOP trial could be replicated in an animal model, which will have significant implications for the quality of results, as the experiment can be standardised, with known positive and negative controls put in place. Specific immunological challenges, and their effect on C activation can be studied. Individual pathways can be targeted using selected activators, which may confirm the best activation marker for a particular pathway for such an investigation. Assays for these activation markers could then be developed, combined, and multiplexed in order to create a single assay for overall C activation. From the data a multidimensional panel assay can be created, using the data in an algorithm to generate a C activation value.

Transfer of Assays to Label-free nanoparticle Based Platform, Liscar.

Once a panel of assays for C activation has been developed using well established, proven methodologies, the assays can be transferred to the Liscar platform. It has been shown that biomolecule detection from a complex sample is possible, and if an appropriate model is applied meaningful parameters can be obtained. The advantage is that potential high throughput screening capabilities of the Liscar instrument are enormous. Protein functionalised arrays can be produced to contain many ligands on a single chip against which a sample can be screened. In principle, this allows the detection of many different analytes from

a single sample, and therefore the ideology of a panel-assay from a single sample may be possible.

Furthermore, the cost, size and speed of the Liscar instrument may allow its widespread implementation as a point-of-care diagnostic device. Returning to the point made by Poste [260], this end point can only be facilitated if a big science approach – clinician led, multidisciplinary collaboration – is employed early on to ensure the C system, if truly warranted, is to become the monitoring system for disease diagnosis and recovery monitoring.

Publication

B. Jansen van Vuuren, T. Read, R.V. Olkhov, and A.M. Shaw, Human serum albumin interference on plasmon-based immunokinetic assay for antibody screening in model blood sera. Analytical Biochemistry 405 (2010) 114-120.

Bibliography

[1] H.C. Neu, The Crisis in Antibiotic Resistance. Science 257 (1992) 1064-1073.

[2] B.L. Stuart, The Challenge of Antibiotic Resistance, Nature Publishing Group, 1998.

[3] C. Schmidt, Challenges Ahead for Companion Diagnostics. Journal of the National Cancer Institute 104 (2012) 14-15.

[4] M. Pickl, E. Ruge, and M. Venturi, Predictive markers in early research and companion diagnostic developments in oncology. New Biotechnology (2012).

[5] H. Lilja, D. Ulmert, and A.J. Vickers, Prostate-specific antigen and prostate cancer: prediction, detection and monitoring. Nat Rev Cancer 8 (2008) 268-278.

[6] G. Aus, J.E. Damber, A. Khatami, H. Lilja, J. Stranne, and J. Hugosson, Individualized screening interval for prostate cancer based on prostate-specific antigen level: results of a prospective, randomized, population-based study. Arch Intern Med 165 (2005) 1857-61.

[7] J.L. Richens, E.A.M. Lunt, D. Sanger, G. McKenzie, and P. O'Shea, Avoiding Nonspecific Interactions in Studies of the Plasma Proteome: Practical Solutions to Prevention of Nonspecific Interactions for Label-Free Detection of Low-Abundance Plasma Proteins. Journal of Proteome Research 8 (2009) 5103-5110.

[8] D.J. Parekh, D. Pauler Ankerst, B.A. Higgins, J. Hernandez, E. Canby-Hagino, T. Brand, D.A. Troyer, R.J. Leach, and I.M. Thompson, External validation of the Prostate Cancer Prevention Trial risk calculator in a screened population. Urology 68 (2006) 1152-1155.

[9] F.R. Ueland, C.P. Desimone, L.G. Seamon, R.A. Miller, S. Goodrich, I. Podzielinski, L. Sokoll, A. Smith, J.R.J. van Nagell, and Z. Zhang, Effectiveness of a Multivariate Index Assay in the Preoperative Assessment of Ovarian Tumors. Obstetrics & Gynecology 117 (2011) 1289-1297 10.1097/AOG.0b013e31821b5118.

[10] P. Angenendt, Progress in protein and antibody microarray technology. Drug Discovery Today 10 (2005) 503-511.

[11] R.L. Rich, M.J. Cannon, J. Jenkins, P. Pandian, S. Sundaram, R. Magyar, J. Brockman, J. Lambert, and D.G. Myszka, Extracting kinetic rate constants from surface plasmon resonance array systems. Analytical Biochemistry 373 (2008) 112-120.

[12] P.S. Katsamba, I. Navratilova, M. Calderon-Cacia, L. Fan, K. Thornton, M. Zhu, T.V. Bos, C. Forte, D. Friend, I. Laird-Offringa, G. Tavares, J. Whatley, E. Shi, A. Widom, K.C. Lindquist, S. Klakamp, A. Drake, D. Bohmann, M. Roell, L. Rose, J. Dorocke, B. Roth, B. Luginbühl, and D.G. Myszka, Kinetic analysis of a high-affinity antibody/antigen

interaction performed by multiple Biacore users. Analytical Biochemistry 352 (2006) 208-221.

[13] M. Mecklenburg, J. Svitel, F. Winquist, J. Gang, K. Ornstein, E. Dey, X. Bin, E. Hedborg, R. Norrby, H. Arwin, I. Lundström, and B. Danielsson, Differentiation of human serum samples by surface plasmon resonance monitoring of the integral glycoprotein interaction with a lectin panel. Analytica Chimica Acta 459 (2002) 25-31.

[14] M.A. Cooper, and V.T. Singleton, A survey of the 2001 to 2005 quartz crystal microbalance biosensor literature: applications of acoustic physics to the analysis of biomolecular interactions. Journal of Molecular Recognition 20 (2007) 154-184.

[15] Z.-H. Wang, and G. Jin, Covalent immobilization of proteins for the biosensor based on imaging ellipsometry. Journal of Immunological Methods 285 (2004) 237-243.

[16] J. Xu, D. Suarez, and D. Gottfried, Detection of avian influenza virus using an interferometric biosensor. Analytical and Bioanalytical Chemistry 389 (2007) 1193-1199.

[17] J.M. Brockman, B.P. Nelson, and R.M. Corn, SURFACE PLASMON RESONANCE IMAGING MEASUREMENTS OF ULTRATHIN ORGANIC FILMS. Annual Review of Physical Chemistry 51 (2000) 41-63.

[18] P. Englebienne, A. van Hoonacker, and M. Verhas, Surface plasmon resonance: principles, methods and applications in biomedical sciences. Spectroscopy: An International Journal 17 (2003) 255-273.

[19] C. Pollock, Fundamentals of Optoelectronics, Richard D. Irwin, Chicago, 1995.

[20] R.V. Olkhov, J.D. Fowke, and A.M. Shaw, Whole serum BSA antibody screening using a label-free biophotonic nanoparticle array. Analytical Biochemistry 385 (2009) 234-241.

[21] I. Thormahlen, J. Straub, and U. Grigull, Refractive Index of Water and Its Dependence on Wavelength, Temperature, and Density. Journal of Physical and Chemical Reference Data 14 (1985) 933-945.

[22] J. Vörös, The Density and Refractive Index of Adsorbing Protein Layers. Biophysical Journal 87 (2004) 553-561.

[23] R.L. Rich, A.R. Miles, B.K. Gale, and D.G. Myszka, Detergent screening of a G-protein-coupled receptor using serial and array biosensor technologies. Analytical Biochemistry 386 (2009) 98-104.

[24] R.V. Olkhov, and A.M. Shaw, Label-free antibody–antigen binding detection by optical sensor array based on surface-synthesized gold nanoparticles. Biosensors and Bioelectronics 23 (2008) 1298-1302.

[25] E. Engvall, and P. Perlmann, Enzyme-Linked Immunosorbent Assay, Elisa. The Journal of Immunology 109 (1972) 129-135.

[26] M.M. Richter, Electrochemiluminescence (ECL). Chemical Reviews 104 (2004) 3003-3036.

[27] G.F. Blackburn, H.P. Shah, J.H. Kenten, J. Leland, R.A. Kamin, J. Link, J. Peterman, M.J. Powell, A. Shah, and D.B. Talley, Electrochemiluminescence detection for development of immunoassays and DNA probe assays for clinical diagnostics. Clinical Chemistry 37 (1991) 1534-9.

[28] L. Fang, Z. Lü, H. Wei, and E. Wang, Quantitative electrochemiluminescence detection of proteins: Avidin-based sensor and tris(2,2'-bipyridine) ruthenium(II) label. Biosensors and Bioelectronics 23 (2008) 1645-1651.

[29] H. Wei, and E. Wang, Electrochemiluminescence of tris(2,2’-bipyridyl)ruthenium and its applications in bioanalysis: a review. Luminescence 26 (2011) 77-85.

[30] V. Guglielmo-Viret, and P. Thullier, Comparison of an electrochemiluminescence assay in plate format over a colorimetric ELISA, for the detection of ricin B chain (RCA-B). Journal of Immunological Methods 328 (2007) 70-78.

[31] V. Guglielmo-Viret, O. Attrée, V. Blanco-Gros, and P. Thullier, Comparison of electrochemiluminescence assay and ELISA for the detection of Clostridium botulinum type B neurotoxin. Journal of Immunological Methods 301 (2005) 164-172.

[32] C. Holmes, C. Cunningham, E. Zotova, J. Woolford, C. Dean, S. Kerr, D. Culliford, and V.H. Perry, Systemic inflammation and disease progression in Alzheimer disease. Neurology 73 (2009) 768-774.

[33] E. Soon, A.M. Holmes, C.M. Treacy, N.J. Doughty, L. Southgate, R.D. Machado, R.C. Trembath, S. Jennings, L. Barker, P. Nicklin, C. Walker, D.C. Budd, J. Pepke-Zaba, and N.W. Morrell, Elevated Levels of Inflammatory Cytokines Predict Survival in Idiopathic and Familial Pulmonary Arterial Hypertension. Circulation 122 (2010) 920-927.

[34] Q. Fu, J. Zhu, and J.E. Van Eyk, Comparison of Multiplex Immunoassay Platforms. Clinical Chemistry 56 (2010) 314-318.

[35] S.X. Leng, J.E. McElhaney, J.D. Walston, D. Xie, N.S. Fedarko, and G.A. Kuchel, ELISA and Multiplex Technologies for Cytokine Measurement in Inflammation and Aging Research. The Journals of Gerontology Series A: Biological Sciences and Medical Sciences 63 (2008) 879-884.

[36] A. Hamano, M. Umeda, Y. Ueno, S. Tanaka, J. Mimuro, and Y. Sakata, Latex Immunoturbidimetric Assay for Soluble Fibrin Complex. Clinical Chemistry 51 (2005) 183-188.

[37] L. Borque, L. Bellod, A. Rus, M.L. Seco, and F. Galisteo-GonzÃ¡lez, Development and Validation of an Automated and Ultrasensitive Immunoturbidimetric Assay for C-Reactive Protein. Clinical Chemistry 46 (2000) 1839-1842.

[38] B. Mali, D. Armbruster, E. Serediak, and T. Ottenbreit, Comparison of immunoturbidimetric and immunonephelometric assays for specific proteins. Clinical Biochemistry 42 (2009) 1568-1571.

[39] M. Furuya, M. Haramura, and A. Tanaka, Reduction of nonspecific binding proteins to self-assembled monolayer on gold surface. Bioorganic & Medicinal Chemistry 14 (2006) 537-543.

[40] C. Campagnolo, K.J. Meyers, T. Ryan, R.C. Atkinson, Y.-T. Chen, M.J. Scanlan, G. Ritter, L.J. Old, and C.A. Batt, Real-Time, label-free monitoring of tumor antigen and serum antibody interactions. Journal of Biochemical and Biophysical Methods 61 (2004) 283-298.

[41] G.A. Canziani, S. Klakamp, and D.G. Myszka, Kinetic screening of antibodies from crude hybridoma samples using Biacore. Analytical Biochemistry 325 (2004) 301-307.

[42] N.L. Anderson, and N.G. Anderson, The Human Plasma Proteome: History, Character, and Diagnostic Prospects. Mol Cell Proteomics 1 (2002) 845-867.

[43] E. Hifumi, N. Kubota, Y. Niimi, K. Shimizu, N. Egashira, and T. Uda, Elimination of Ingredients Effect to Improve the Detection of Anti HIV-1 p24 Antibody in Human Serum Using SPR Apparatus. Analytical Sciences 18 (2002) 863-867.

[44] J.S. Wall, F.M. Ayoub, and P.S. O'Shea, A study of the interactions of an immunoglobulin light chain with artificial and B-lymphocyte membranes. Front Biosci 1 (1996) a46-58.

[45] J.S. Rees, and K.S. Lilley, Method for suppressing non-specific protein interactions observed with affinity resins. Methods 54 (2011) 407-412.

[46] D.G. Myszka, Kinetic analysis of macromolecular interactions using surface plasmon resonance biosensors. Current Opinion in Biotechnology 8 (1997) 50-57.

[47] D.G. Myszka, Analysis of small-molecule interactions using Biacore S51 technology. Analytical Biochemistry 329 (2004) 316-323.

[48] E.T. Fung, G.L. Wright, and E.A. Dalmasso, Proteomic strategies for biomarker identification: progress and challenges. Current opinion in molecular therapeutics 2 (2000) 643-50.

[49] T.H. Risby, Biomarkers of Disease: An Evidence-based Approach. Andrew K. Trull, Laurence M. Demers, David W. Holt, Atholl Johnston, J. Michael Tredger, and Christopher P. Price, eds. Cambridge: Cambridge University Press, 2002, 516 pp., $110.00, hardcover. ISBN 0-521-81102-3. Clinical Chemistry 49 (2003) 1233-1234.

[50] M.J. Walport, Complement. New England Journal of Medicine 344 (2001) 1058-1066.

[51] M.M. Frank, and L.F. Fries, The role of complement in inflammation and phagocytosis. Immunology Today 12 (1991) 322-326.

[52] C.A. Janeway, P. Travers, and MWalport, Immunobiology: The Immune System in Health and Disease, Garland Science, New York, 2001.

[53] C. Gaboriaud, N.M. Thielens, L.A. Gregory, V.r. Rossi, J.C. Fontecilla-Camps, and G.r.J. Arlaud, Structure and activation of the C1 complex of complement: unraveling the puzzle. Trends in Immunology 25 (2004) 368-373.

[54] R. Wallis, D.A. Mitchell, R. Schmid, W.J. Schwaeble, and A.H. Keeble, Paths reunited: Initiation of the classical and lectin pathways of complement activation. Immunobiology 215 (2009) 1-11.

[55] T.Y. Lin, and D.S. Fletcher, Activation of a complex of C1r and C1s subcomponents of human complement C1 by the third subcomponent C1q. Journal of Biological Chemistry 255 (1980) 7756-62.

[56] U. Kishore, C. Gaboriaud, P. Waters, A.K. Shrive, T.J. Greenhough, K.B.M. Reid, R.B. Sim, and G.J. Arlaud, C1q and tumor necrosis factor superfamily: modularity and versatility. Trends in Immunology 25 (2004) 551-561.

[57] D. Ricklin, G. Hajishengallis, K. Yang, and J.D. Lambris, Complement: a key system for immune surveillance and homeostasis. Nat Immunol 11 (2010) 785-797.

[58] D.E. Chenoweth, The properties of human C5a anaphylatoxin. The significance of C5a formation during hemodialysis. Contrib Nephrol 59 (1987) 51-71.

[59] J.A. Winkelstein, and A. Tomasz, Activation of the Alternative Complement Pathway by Pneumococcal Cell Wall Teichoic Acid. The Journal of Immunology 120 (1978) 174-178.

[60] J. Greenblatt, R.J. Boackle, and J.H. Schwab, Activation of the alternate complement pathway by peptidoglycan from streptococcal cell wall. Infection and Immunity 19 (1978) 296-303.

[61] C. Tegla, C. Cudrici, S. Patel, R. Trippe, V. Rus, F. Niculescu, and H. Rus, Membrane attack by complement: the assembly and biology of terminal complement complexes. Immunologic Research 51 (2011) 45-60.

[62] T.S. Halstensen, T.E. Mollnes, O. Fausa, and P. Brandtzaeg, Deposits of terminal complement complex (TCC) in muscularis mucosae and submucosal vessels in ulcerative colitis and Crohn's disease of the colon. Gut 30 (1989) 361-366.

[63] M.B. Pepys, and G.M. Hirschfield, C-reactive protein: a critical update. The Journal of clinical investigation 111 (2003) 1805-1812.

[64] J. Playfair, and G. Bancroft, Infection and Immunity, Oxford University Press, Oxford, 2008.

[65] S. Larsson, U. Thelander, and S. Friberg, C-reactive protein (CRP) levels after elective orthopedic surgery. Clinical orthopaedics and related research (1992) 237-42.

[66] I. Kushner, THE PHENOMENON OF THE ACUTE PHASE RESPONSE*. Annals of the New York Academy of Sciences 389 (1982) 39-48.

[67] D.M. van der Heijde, M.A. van 't Hof, P.L. van Riel, L.A. Theunisse, E.W. Lubberts, M.A. van Leeuwen, M.H. van Rijswijk, and L.B. van de Putte, Judging disease activity in clinical practice in rheumatoid arthritis: first step in the development of a disease activity score. Annals of the Rheumatic Diseases 49 (1990) 916-920.

[68] A.J. Szalai, M.A. McCrory, G.S. Cooper, J. Wu, and R.P. Kimberly, Association between baseline levels of C-reactive protein (CRP) and a dinucleotide repeat polymorphism in the intron of the CRP gene. Genes Immun 3 (2002) 14-19.

[69] D.E. Neal, T.D. Moon, S. Clejan, and D. Sarma, Prostate specific antigen and prostatitis I. Effect of prostatitis on serum psa in the human and nonhuman primate. The Prostate 20 (1992) 105-111.

[70] R.B. Nadler, P.A. Humphrey, D.S. Smith, W.J. Catalona, and T.L. Ratliff, Effect of Inflammation and Benign Prostatic Hyperplasia on Elevated Serum Prostate Specific Antigen Levels. The Journal of Urology 154 (1995) 407-413.

[71] I.M. Thompson, D.K. Pauler, P.J. Goodman, C.M. Tangen, M.S. Lucia, H.L. Parnes, L.M. Minasian, L.G. Ford, S.M. Lippman, E.D. Crawford, J.J. Crowley, and C.A. Coltman, Prevalence of Prostate Cancer among Men with a Prostate-Specific Antigen Level ≤4.0 ng per Milliliter. New England Journal of Medicine 350 (2004) 2239-2246.

[72] J.E. Adams, G.A. Sicard, B.T. Allen, K.H. Bridwell, L.G. Lenke, V.G. Davila-Roman, G.S. Bodor, J.H. Ladenson, and A.S. Jaffe, Diagnosis of Perioperative Myocardial Infarction

with Measurement of Cardiac Troponin I. New England Journal of Medicine 330 (1994) 670-674.

[73] S.J. MAYNARD, I.B.A. MENOWN, and A.A.J. ADGEY, Troponin T or troponin I as cardiac markers in ischaemic heart disease. Heart 83 (2000) 371-373.

[74] M. Galvani, F. Ottani, D. Ferrini, J.H. Ladenson, A. Destro, D. Baccos, F. Rusticali, and A.S. Jaffe, Prognostic Influence of Elevated Values of Cardiac Troponin I in Patients With Unstable Angina. Circulation 95 (1997) 2053-2059.

[75] D.P. Ankerst, J. Groskopf, J.R. Day, A. Blase, H. Rittenhouse, B.H. Pollock, C. Tangen, D. Parekh, R.J. Leach, and I. Thompson, Predicting Prostate Cancer Risk Through Incorporation of Prostate Cancer Gene 3. The Journal of Urology 180 (2008) 1303-1308.

[76] B.R. Kirkwood, and J.A.C. Sterne, Essential Medical Statistics, Blackwell Publishing Ltd., Oxford, 2003.

[77] K.H. Zou, A.J. Oâ€™Malley, and L. Mauri, Receiver-Operating Characteristic Analysis for Evaluating Diagnostic Tests and Predictive Models. Circulation 115 (2007) 654-657.

[78] D. Mesko, (Ed.), Differential Diagnosis by Laboratory Medicine, Springer-Verlag, Berlin, 2002.

[79] C. Gabay, and I. Kushner, Acute-Phase Proteins and Other Systemic Responses to Inflammation. New England Journal of Medicine 340 (1999) 448-454.

[80] H. Honda, A.R. Qureshi, O. Heimbürger, P. Barany, K. Wang, R. Pecoits-Filho, P. Stenvinkel, and B. Lindholm, Serum Albumin, C-Reactive Protein, Interleukin 6, and Fetuin A as Predictors of Malnutrition, Cardiovascular Disease, and Mortality in Patients With ESRD. American Journal of Kidney Diseases 47 (2006) 139-148.

[81] S.M. Graham, J.M. Baeten, B.A. Richardson, M.H. Wener, L. Lavreys, K. Mandaliya, J.O. Ndinya-Achola, J. Overbaugh, and R.S. McClelland, Short Communication: A Decrease in Albumin in Early HIV Type 1 Infection Predicts Subsequent Disease Progression. AIDS Research and Human Retroviruses 23 (2007) 1197-1200.

[82] B.W.M. Schalk, M. Visser, M.A. Bremmer, B.W.J.H. Penninx, L.M. Bouter, and D.J.H. Deeg, Change of Serum Albumin and Risk of Cardiovascular Disease and All-Cause Mortality. American Journal of Epidemiology 164 (2006) 969-977.

[83] D.T. Mytych, S. La, T. Barger, J. Ferbas, and S.J. Swanson, The development and validation of a sensitive, dual-flow cell, SPR-based biosensor immunoassay for the detection, semi-quantitation, and characterization of antibodies to darbepoetin alfa

and epoetin alfa in human serum. Journal of Pharmaceutical and Biomedical Analysis 49 (2009) 415-426.

[84] E. Hifumi, N. Kubota, Y. Niimi, K. Shimizu, N. Egashira, and T. Uda, Elimination of Ingredients Effect to Improve the Detection of Anti HIV-1 p24 Antibody in Human Serum Using SPR Apparatus. Analytical Sciences 18 (2002) 863-867.

[85] S. Scarano, M. Mascini, A.P.F. Turner, and M. Minunni, Surface plasmon resonance imaging for affinity-based biosensors. Biosensors and Bioelectronics 25 (2009) 957-966.

[86] R.V. Olkhov, and A.M. Shaw, Quantitative label-free screening for antibodies using scattering biophotonic microarray imaging. Analytical Biochemistry 396 (2009) 30-35.

[87] J.-F. Masson, T. Battaglia, J. Cramer, S. Beaudoin, M. Sierks, and K. Booksh, Reduction of nonspecific protein binding on surface plasmon resonance biosensors. Analytical and Bioanalytical Chemistry 386 (2006) 1951-1959.

[88] O.R. Bolduc, J.N. Pelletier, and J.-F.o. Masson, SPR Biosensing in Crude Serum Using Ultralow Fouling Binary Patterned Peptide SAM. Analytical Chemistry 82 (2010) 3699-3706.

[89] L. Vroman, and A.N.N. Lukosevicius, Ellipsometer Recordings of Changes in Optical Thickness of Adsorbed Films associated with Surface Activation of Blood Clotting. Nature 204 (1964) 701-703.

[90] L. Vroman, and A.L. Adams, Possible involvement of fibrinogen and proteolysis in surface activation. A study with the recording ellipsometer. Thromb Diath Haemorrh 18 (1967) 510-24.

[91] L. Vroman, and A.L. Adams, Identification of rapid changes at plasma-solid interfaces. J Biomed Mater Res 3 (1969) 43-67.

[92] L. Vroman, A. Adams, G. Fischer, and P. Munoz, Interaction of high molecular weight kininogen, factor XII, and fibrinogen in plasma at interfaces. Blood 55 (1980) 156-159.

[93] R.J. Green, M.C. Davies, C.J. Roberts, and S.J.B. Tendler, Competitive protein adsorption as observed by surface plasmon resonance. Biomaterials 20 (1999) 385-391.

[94] S. Choi, Y. Yang, and J. Chae, Surface plasmon resonance protein sensor using Vroman effect. Biosensors and Bioelectronics 24 (2008) 893-899.

[95] S.Y. Jung, S.M. Lim, F. Albertorio, G. Kim, M.C. Gurau, R.D. Yang, M.A. Holden, and P.S. Cremer, The Vroman Effect: A Molecular Level Description of Fibrinogen Displacement. J. Am. Chem. Soc. 125 (2003) 12782-12786.

[96] A. Krishnan, C.A. Siedlecki, and E.A. Vogler, Mixology of Protein Solutions and the Vroman Effect. Langmuir 20 (2004) 5071-5078.

[97] P. Eckersall, S. Duthie, S. Safi, D. Moffatt, N. Horadagoda, S. Doyle, R. Parton, D. Bennett, and J. Fitzpatrick, An automated biochemical assay for haptoglobin: Prevention of interference from albumin. Comparative Haematology International 9 (1999) 117-124.

[98] F. Frederix, K. Bonroy, G. Reekmans, W. Laureyn, A. Campitelli, M.A. Abramov, W. Dehaen, and G. Maes, Reduced nonspecific adsorption on covalently immobilized protein surfaces using poly(ethylene oxide) containing blocking agents. Journal of Biochemical and Biophysical Methods 58 (2004) 67-74.

[99] K.D. Pavey, and C.J. Olliff, SPR analysis of the total reduction of protein adsorption to surfaces coated with mixtures of long- and short-chain polyethylene oxide block copolymers. Biomaterials 20 (1999) 885-890.

[100] C.T. Mörner, Untersuchungen der Proteinsubstanzen in der lichtbrechenden Medien des Auges. Ztschr. physiol Chem. 18 (1894).

[101] T.P. Svedberg, K O, The Ultracentrifuge, Oxford University Press, London, 1940.

[102] H.A. Sober, and E.A. Peterson, Chromatography of Proteins on Cellulose Ion-Exchangers. Journal of the American Chemical Society 76 (1954) 1711-1712.

[103] E.A. Peterson, and H.A. Sober, Chromatography of Proteins. I. Cellulose Ion-exchange Adsorbents. Journal of the American Chemical Society 78 (1956) 751-755.

[104] I. Bjork, Studies on γ-crystallin from calf lens: I. Isolation by gel filtration. Experimental Eye Research 1 (1961) 145-IN21.

[105] A.M. Potts, Methods for Separation of Proteins. Investigative Ophthalmology & Visual Science 4 (1965) 531-538.

[106] M. Chaplin, Water's Hydrogen Bond Strength, 2007.

[107] S. Rao, and A.L. Zydney, High resolution protein separations using affinity ultrafiltration with small charged ligands. Journal of Membrane Science 280 (2006) 781-789.

[108] B. Yu, H. Cong, H. Liu, Y. Li, and F. Liu, Separation and detection of erythropoietin by CE and CE-MS. Trends in Analytical Chemistry 24 (2005) 350-357.

[109] A. Villa, L. Zecca, P. Fusi, S. Colombo, G. Tedeschi, and P. Tortora, Structural features responsible for kinetic thermal stability of a carboxypeptidase from the archaebacterium Sulfolobus solfataricus. Biochem J 295 (Pt 3) (1993) 827-31.

[110] D. Asthagiri, M.R. Schure, and A.M. Lenhoff, Calculation of Hydration Effects in the Binding of Anionic Ligands to Basic Proteins. The Journal of Physical Chemistry B 104 (2000) 8753-8761.

[111] S. Sheng, D. Chen, and J.E. Van Eyk, Multidimensional Liquid Chromatography Separation of Intact Proteins by Chromatographic Focusing and Reversed Phase of the Human Serum Proteome. Molecular & Cellular Proteomics 5 (2006) 26-34.

[112] Y. Qiu, T.H. Patwa, L. Xu, K. Shedden, D.E. Misek, M. Tuck, G. Jin, M.T. Ruffin, D.K. Turgeon, S. Synal, R. Bresalier, N. Marcon, D.E. Brenner, and D.M. Lubman, Plasma Glycoprotein Profiling for Colorectal Cancer Biomarker Identification by Lectin Glycoarray and Lectin Blot. Journal of Proteome Research 7 (2008) 1693-1703.

[113] P. Matt, Z. Fu, Q. Fu, and J.E. Van Eyk, Biomarker discovery: proteome fractionation and separation in biological samples. Physiological Genomics 33 (2008) 12-17.

[114] L. Lin, and J.T. Guthrie, Preparation and characterisation of novel, blood-plasma-separation membranes for use in biosensors. Journal of Membrane Science 173 (2000) 73-85.

[115] L.H. Chen, C.E. Price, A. Goerke, A.L. Lee, and P.A. DePhillips, A reversed phase HPLC assay for the simultaneous quantitation of non-ionic and ionic surfactants in bioprocess intermediates. Journal of Pharmaceutical and Biomedical Analysis 40 (2006) 964-970.

[116] N. Ahmed, and G.E. Rice, Strategies for revealing lower abundance proteins in two-dimensional protein maps. Journal of Chromatography B 815 (2005) 39-50.

[117] N.R. Jana, L. Gearheart, and C.J. Murphy, Wet chemical synthesis of high aspect ratio cylindrical gold nanorods. Journal of Physical Chemistry B 105 (2001) 4065-4067.

[118] Y. Zhang, S. Furyk, D.E. Bergbreiter, and P.S. Cremer, Specific Ion Effects on the Water Solubility of Macromolecules: PNIPAM and the Hofmeister Series. Journal of the American Chemical Society 127 (2005) 14505-14510.

[119] B.T. Doumas, W. Ard Watson, and H.G. Biggs, Albumin standards and the measurement of serum albumin with bromcresol green. Clinica Chimica Acta 258 (1997) 21-30.

[120] O.R. Bolduc, and J.-F.o. Masson, Monolayers of 3-Mercaptopropyl-amino Acid to Reduce the Nonspecific Adsorption of Serum Proteins on the Surface of Biosensors. Langmuir 24 (2008) 12085-12091.

[121] N.L. Anderson, and N.G. Anderson, The Human Plasma Proteome. Molecular & Cellular Proteomics 1 (2002) 845-867.

[122] D.G. Myszka, T.A. Morton, M.L. Doyle, and I.M. Chaiken, Kinetic analysis of a protein antigen-antibody interaction limited by mass transport on an optical biosensor. Biophysical Chemistry 64 (1997) 127-137.

[123] K. Uchida, H. Otsuka, M. Kaneko, K. Kataoka, and Y. Nagasaki, A Reactive Poly(ethylene glycol) Layer To Achieve Specific Surface Plasmon Resonance Sensing with a High S/N Ratio: The Substantial Role of a Short Underbrushed PEG Layer in Minimizing Nonspecific Adsorption. Analytical Chemistry 77 (2005) 1075-1080.

[124] D. Kozak, P. Surawski, K.M. Thoren, C.-Y. Lu, L. Marcon, and M. Trau, Improving the Signal-to-Noise Performance of Molecular Diagnostics with PEG-Lysine Copolymer Dendrons. Biomacromolecules 10 (2009) 360-365.

[125] R.V. Olkhov, J.D. Fowke, and A.M. Shaw, Whole serum BSA antibody screening using a label-free biophotonic nanoparticle array. Analytical Biochemistry 385 (2009) 234-241.

[126] M.D. Chapman, G. Keir, A. Petzold, and E.J. Thompson, Measurement of high affinity antibodies on antigen-immunoblots. Journal of Immunological Methods 310 (2006) 62-66.

[127] B. Jansen van Vuuren, T. Read, R.V. Olkhov, and A.M. Shaw, Human serum albumin interference on plasmon-based immunokinetic assay for antibody screening in model blood sera. Analytical Biochemistry 405 (2010) 114-120.

[128] K. Kourentzi, M. Srinivasan, S.J. Smith-Gill, and R.C. Willson, Conformational flexibility and kinetic complexity in antibody–antigen interactions. Journal of Molecular Recognition 21 (2008) 114-121.

[129] M. Yang, H.C.M. Yau, and H.L. Chan, Adsorption Kinetics and Ligand-Binding Properties of Thiol-Modified Double-Stranded DNA on a Gold Surface. Langmuir 14 (1998) 6121-6129.

[130] R. Karlsson, and A. Fält, Experimental design for kinetic analysis of protein-protein interactions with surface plasmon resonance biosensors. Journal of Immunological Methods 200 (1997) 121-133.

[131] J. Yang, C.P. Swaminathan, Y. Huang, R. Guan, S. Cho, M.C. Kieke, D.M. Kranz, R.A. Mariuzza, and E.J. Sundberg, Dissecting Cooperative and Additive Binding Energetics in the Affinity Maturation Pathway of a Protein-Protein Interface. Journal of Biological Chemistry 278 (2003) 50412-50421.

[132] H. Sota, Y. Hasegawa, and M. Iwakura, Detection of Conformational Changes in an Immobilized Protein Using Surface Plasmon Resonance. Analytical Chemistry 70 (1998) 2019-2024.

[133] P. Wojciechowski, P. Ten Hove, and J.L. Brash, Phenomenology and mechanism of the transient adsorption of fibrinogen from plasma (Vroman effect). Journal of Colloid and Interface Science 111 (1986) 455-465.

[134] J.R. Dunkelberger, and W.-C. Song, Complement and its role in innate and adaptive immune responses. Cell Res 20 (2009) 34-50.

[135] A. Klos, A.J. Tenner, K.-O. Johswich, R.R. Ager, E.S. Reis, and J. Köhl, The role of the anaphylatoxins in health and disease. Molecular Immunology 46 (2009) 2753-2766.

[136] S.-H. Li, P.E. Szmitko, R.D. Weisel, C.-H. Wang, P.W.M. Fedak, R.-K. Li, D.A.G. Mickle, and S. Verma, C-Reactive Protein Upregulates Complement-Inhibitory Factors in Endothelial Cells. Circulation 109 (2004) 833-836.

[137] T.E. Mollnes, W.-C. Song, and J.D. Lambris, Complement in inflammatory tissue damage and disease. Trends in Immunology 23 (2002) 61-64.

[138] U. Amara, D. Rittirsch, M. Flierl, U. Bruckner, A. Klos, F. Gebhard, J.D. Lambris, and M. Huber-Lang, Interaction Between the Coagulation and Complement System

Current Topics in Complement II, Springer US, 2008, pp. 68-76.

[139] Z. Derzsy, Z. Prohászka, J. Rigó Jr, G. Füst, and A. Molvarec, Activation of the complement system in normal pregnancy and preeclampsia. Molecular Immunology 47 (2010) 1500-1506.

[140] E.D. Pedersen, U. Waje-Andreassen, C.A. Vedeler, G. Aamodt, and T.E. Mollnes, Systemic complement activation following human acute ischaemic stroke. Clinical & Experimental Immunology 137 (2004) 117-122.

[141] G.-J. Wolbink, A.W.J. Bossink, A.B.J. Groeneveld, M.C.M.d. Groot, L.G. Thijs, and C.E. Hack, Complement Activation in Patients with Sepsis Is in Part Mediated by C-Reactive Protein. Journal of Infectious Diseases 177 (1998) 81-87.

[142] Y.J. Gu, M.A. Mariani, P.W. Boonstra, J.G. Grandjean, and W.v. Oeveren, Complement Activation in Coronary Artery Bypass Grafting Patients Without Cardiopulmonary Bypass. Chest 116 (1999) 892-898.

[143] C. Hoedemaekers, M. van Deuren, T. Sprong, P. Pickkers, T.-E. Mollnes, I. Klasen, and J. van der Hoeven, The Complement System Is Activated in a Biphasic Pattern After Coronary Artery Bypass Grafting. The Annals of Thoracic Surgery 89 (2010) 710-716.

[144] T.E. Mollnes, T. Lea, O.J. Mellbye, J. Pahle, Ø. Grand, and M. Harboe, Complement activation in rheumatoid arthritis evaluated by C3dg and the terminal complement complex. Arthritis & Rheumatism 29 (1986) 715-721.

[145] E.T.H. Molenaar, A.E. Voskuyl, A. Familian, G.J. van Mierlo, B.A.C. Dijkmans, and C.E. Hack, Complement activation in patients with rheumatoid arthritis mediated in part by C-reactive protein. Arthritis & Rheumatism 44 (2001) 997-1002.

[146] L. Truedsson, A.A. Bengtsson, and G. Sturfelt, Complement deficiencies and systemic lupus erythematosus. Autoimmunity 40 (2007) 560-566.

[147] T.E. Mollnes, T.S. Jokiranta, L. Truedsson, B. Nilsson, S. Rodriguez de Cordoba, and M. Kirschfink, Complement analysis in the 21st century. Molecular Immunology 44 (2007) 3838-3849.

[148] H.M. Belmont, P. Hopkins, H.S. Edelson, H.B. Kaplan, R. Ludewig, G. Weissmann, and S. Abramson, Complement activation during systemic lupus erythematosus: C3a and C5a anaphylatoxins circulate during exacerbations of disease. Arthritis & Rheumatism 29 (1986) 1085-1089.

[149] T.E. Mollnes, P. Garred, and G. Bergseth, Effect of time, temperature and anticoagulants on in vitro complement activation: consequences for collection and preservation of samples to be examined for complement activation. Clin Exp Immunol 73 (1988) 484-8.

[150] S. Stöve, A. Klos, W. Bautsch, and J. Köhl, Re-evaluation of the storage conditions for blood samples which are used for determination of complement activation. Journal of Immunological Methods 182 (1995) 1-5.

[151] P.H. Pfeifer, M.S. Kawahara, and T.E. Hugli, Possible Mechanism for in Vitro Complement Activation in Blood and Plasma Samples: Futhan/EDTA Controls in Vitro Complement Activation. Clinical Chemistry 45 (1999) 1190-1199.

[152] C.G. Stephens, R.C. Williams, Jr., and W.P. Reed, Classical and alternative complement pathway activation by pneumococci. Infect Immun 17 (1977) 296-302.

[153] R.D. Schreiber, M.K. Pangburn, P.H. Lesavre, and H.J. Müller-Eberhard, Initiation of the alternative pathway of complement: recognition of activators by bound C3b and assembly of the entire pathway from six isolated proteins. Proceedings of the National Academy of Sciences 75 (1978) 3948-3952.

[154] S. Manzi, J.E. Rairie, A.B. Carpenter, R.H. Kelly, S.P. Jagarlapudi, S.M. Sereika, T.A. Medsger, and R. Ramsey-Goldman, Sensitivity and specificity of plasma and urine complement split products as indicators of lupus disease activity. Arthritis & Rheumatism 39 (1996) 1178-1188.

[155] Y. Morita, H. Ikeguchi, J. Nakamura, N. Hotta, Y. Yuzawa, and S. Matsuo, Complement Activation Products in the Urine from Proteinuric Patients. Journal of the American Society of Nephrology 11 (2000) 700-707.

[156] B. Liu, J. Zhang, P.Y. Tan, D. Hsu, A.M. Blom, B. Leong, S. Sethi, B. Ho, J.L. Ding, and P.S. Thiagarajan, A Computational and Experimental Study of the Regulatory Mechanisms of the Complement System. PLoS Comput Biol 7 (2011) e1001059.

[157] M. Yasuda, K. Takeuchi, M. Hiruma, H. Iida, A. Tahara, H. Itagane, I. Toda, K. Akioka, M. Teragaki, and H. Oku, The complement system in ischemic heart disease. Circulation 81 (1990) 156-163.

[158] J.M. Weiler, M.R. Daha, K.F. Austen, and D.T. Fearon, Control of the amplification convertase of complement by the plasma protein beta1H. Proceedings of the National Academy of Sciences 73 (1976) 3268-3272.

[159] P. Horák, Z. Heřmanová, J. Zadražil, H. Ciferská, M. Ordeltová, L. Kusá, M. Žurek, and T. Tichý, C1q complement component and antibodies reflect SLE activity and kidney involvement. Clinical Rheumatology 25 (2006) 532-536.

[160] V. Marks, T. Cantor, D. Mesko, R. Pullmann, and G. Nosalova, Differential Diagnosis by Laboratory Medicine: A Quick Reference for Physicians, Springer, 2003.

[161] T.J. Oglesby, A. Ueda, and J.E. Volanakis, Radioassays for quantitation of intact complement proteins C2 and B in human serum. Journal of Immunological Methods 110 (1988) 55-62.

[162] B. Morley, and M.J. Walport, The Complement FactsBook, Academic Press, 1999.

[163] K.F. Nolan, S. Kaluz, J.M. Higgins, D. Goundis, and K.B. Reid, Characterization of the human properdin gene, 1992.

[164] I. Terai, K. Kobayashi, M. Matsushita, and T. Fujita, Human serum mannose-binding lectin (MBL)-associated serine protease-1 (MASP-1): determination of levels in body fluids and identification of two forms in serum. Clinical & Experimental Immunology 110 (1997) 317-323.

[165] M. Oppermann, U. Höpken, and O. Götze, Assessment of complement activation in vivo. Immunopharmacology 24 (1992) 119-134.

[166] M. Kirschfink, and T.E. Mollnes, Modern Complement Analysis, American Society for Microbiology, 2003.

[167] G. Bergseth, J.K. Ludviksen, P.C. Giclas, B. Nilsson, and T.E. Mollnes, Preparation of an International Complement Activation Standard. Part one: optimization of activation conditions., 13th European Meeting on Complement in Human Disease, Leiden, 2011.

[168] M. Harboe, G. Ulvund, L. Vien, M. Fung, and T.E. Mollnes, The quantitative role of alternative pathway amplification in classical pathway induced terminal complement activation. Clinical & Experimental Immunology 138 (2004) 439-446.

[169] R. Strohmeyer, Y. Shen, and J. Rogers, Detection of complement alternative pathway mRNA and proteins in the Alzheimer's disease brain. Molecular Brain Research 81 (2000) 7-18.

[170] D.T. Fearon, and K.F. Austen, Properdin: binding to C3b and stabilization of the C3b-dependent C3 convertase. The Journal of Experimental Medicine 142 (1975) 856-863.

[171] W.R. McCabe, Serum complement levels in bacteremia due to gram-negative organisms. N Engl J Med 288 (1973) 21-3.

[172] H.S. Ginsberg, L. Pillemer, and R.J. Wedgwood, The properdin system and immunity. VI. The inactivation of Newcastle disease virus by the properdin system. J Exp Med 104 (1956) 707-25.

[173] J.J. Mc Sharry, R.J. Pickering, and L.A. Caliguiri, Activation of the alternative complement pathway by enveloped viruses containing limited amounts of sialic acid. Virology 114 (1981) 507-515.

[174] N. Nogueira, C. Bianco, and Z. Cohn, Studies on the selective lysis and purification of Trypanosoma cruzi. J Exp Med 142 (1975) 224-9.

[175] W.D. Da Silva, and M.D. Kazatchkine, Schistosoma mansoni: Activation of the alternative pathway of human complement by schistosomula. Experimental Parasitology 50 (1980) 278-286.

[176] D.E. Chenoweth, S.W. Cooper, T.E. Hugli, R.W. Stewart, E.H. Blackstone, and J.W. Kirklin, Complement Activation during Cardiopulmonary Bypass. New England Journal of Medicine 304 (1981) 497-503.

[177] R.E. Jordon, Complement Activation in Bullous Skin Diseases. J Investig Dermatol 65 (1975) 162-169.

[178] J.B. Ziegler, F.S. Rosen, C.A. Alper, W. Grupe, and I.H. Lepow, Metabolism of properdin in normal subjects and patients with renal disease. J Clin Invest 56 (1975) 761-7.

[179] J.M. Corry, R.B. Polhill Jr, S.R. Edmonds, and R.B. Johnston Jr, Activity of the alternative complement pathway after splenectomy: Comparison to activity in sickle cell disease and hypogammaglobulinemia. The Journal of Pediatrics 95 (1979) 964-969.

[180] C.F. Hinz, Jr., W.S. Jordan, Jr., and L. Pillemer, The properdin system and immunity. IV. The hemolysis of erythrocytes from patients with paroxysmal nocturnal hemoglobinuria. J Clin Invest 35 (1956) 453-7.

[181] C. Wenisch, S. Spitzauer, K. Florris-Linau, H. Rumpold, S. Vannaphan, B. Parschalk, W. Graninger, and S. Looareesuwan, Complement Activation in Severe Plasmodium falciparum Malaria. Clinical Immunology and Immunopathology 85 (1997) 166-171.

[182] M. Oppermann, H. Baumgarten, E. Brandt, W. Gottsleben, C. Kurts, and O. Götze, Quantitation of components of the alternative pathway of complement (APC) by enzyme-linked immunosorbent assays. Journal of Immunological Methods 133 (1990) 181-190.

[183] A.M. Lynch, R.S. Gibbs, J.R. Murphy, T. Byers, M.C. Neville, P.C. Giclas, J.E. Salmon, T.M. Van Hecke, and V.M. Holers, Complement activation fragment Bb in early pregnancy and spontaneous preterm birth. American Journal of Obstetrics and Gynecology 199 (2008) 354.e1-354.e8.

[184] A. Aggarwal, A. Bhardwaj, S. Alam, and R. Misra, Evidence for activation of the alternate complement pathway in patients with juvenile rheumatoid arthritis. Rheumatology 39 (2000) 189-192.

[185] B.J.C. Janssen, E.G. Huizinga, H.C.A. Raaijmakers, A. Roos, M.R. Daha, K. Nilsson-Ekdahl, B. Nilsson, and P. Gros, Structures of complement component C3 provide insights into the function and evolution of immunity. Nature 437 (2005) 505-511.

[186] Z. Fishelson, M. Pangburn, and H. Muller-Eberhard, Characterization of the initial C3 convertase of the alternative pathway of human complement. The Journal of Immunology 132 (1984) 1430-1434.

[187] G.S. Pfrommer, S.M. Dickens, M.A. Wilson, B.J. Young, and T.R. Kozel, Accelerated decay of C3b to iC3b when C3b is bound to the Cryptococcus neoformans capsule. Infection and Immunity 61 (1993) 4360-4366.

[188] B.J.C. Janssen, A. Christodoulidou, A. McCarthy, J.D. Lambris, and P. Gros, Structure of C3b reveals conformational changes that underlie complement activity. Nature 444 (2006) 213-216.

[189] T. Seya, and S. Nagasawa, Limited Proteolysis of Complement Protein C3b by Regulatory Enzyme C3b Inactivator: Isolation and Characterization of a Biologically Active Fragment, C3d,g. Journal of Biochemistry 97 (1985) 373-382.

[190] J. Tamerius, M. Pangburn, and H. Muller-Eberhard, Detection of a neoantigen on human C3bi and C3d by monoclonal antibody. The Journal of Immunology 135 (1985) 2015-2019.

[191] M.J. Sinosich, B. Teisner, I. Brandslund, M. Fisher, and J.G. Grudzinskas, Influence of time, temperature and coagulation on the measurement of C3, C3 split products and C4. Journal of Immunological Methods 55 (1982) 107-114.

[192] J. van Beek, M. van Meurs, B.A. 't Hart, H.P.M. Brok, J.W. Neal, A. Chatagner, C.L. Harris, N. Omidvar, B.P. Morgan, J.D. Laman, and P. Gasque, Decay-Accelerating Factor (CD55) Is Expressed by Neurons in Response to Chronic but Not Acute Autoimmune Central Nervous System Inflammation Associated with Complement Activation. The Journal of Immunology 174 (2005) 2353-2365.

[193] K. Elward, M. Griffiths, M. Mizuno, C.L. Harris, J.W. Neal, B.P. Morgan, and P. Gasque, CD46 Plays a Key Role in Tailoring Innate Immune Recognition of Apoptotic and Necrotic Cells. Journal of Biological Chemistry 280 (2005) 36342-36354.

[194] B.J.C. Janssen, P. Gros, and J.D. Lambris, Conformational Complexity of Complement Component C3

Current Topics in Complement, Springer US, 2006, pp. 291-312.

[195] R. Reca, M. Wysoczynski, J. Yan, J.D. Lambris, and M.Z. Ratajczak, The Role of Third Complement Component (C3) in Homing of Hematopoietic Stem/Progenitor Cells into Bone Marrow

Current Topics in Complement, Springer US, 2006, pp. 35-51.

[196] M.L. Barilla-LaBarca, M.K. Liszewski, J.D. Lambris, D. Hourcade, and J.P. Atkinson, Role of Membrane Cofactor Protein (CD46) in Regulation of C4b and C3b Deposited on Cells. The Journal of Immunology 168 (2002) 6298-6304.

[197] J.L. Platt, C4d and the Fate of Organ Allografts. Journal of the American Society of Nephrology 13 (2002) 2417-2419.

[198] P.L. McGeer, H. Akiyama, S. Itagaki, and E.G. McGeer, Activation of the classical complement pathway in brain tissue of Alzheimer patients. Neuroscience Letters 107 (1989) 341-346.

[199] E.R. Rodriguez, D.V. Skojec, C.D. Tan, A.A. Zachary, E.K. Kasper, J.V. Conte, and W.M. Baldwin, Antibody-Mediated Rejection in Human Cardiac Allografts: Evaluation of Immunoglobulins and Complement Activation Products C4d and C3d as Markers. American Journal of Transplantation 5 (2005) 2778-2785.

[200] H. Regele, G.A. Böhmig, A. Habicht, D. Gollowitzer, M. Schillinger, S. Rockenschaub, B. Watschinger, D. Kerjaschki, and M. Exner, Capillary Deposition of Complement Split Product C4d in Renal Allografts is Associated with Basement Membrane Injury in

Peritubular and Glomerular Capillaries: A Contribution of Humoral Immunity to Chronic Allograft Rejection. Journal of the American Society of Nephrology 13 (2002) 2371-2380.

[201] M.K. Pangburn, R.D. Schreiber, and H.J. Muller-Eberhard, Human complement C3b inactivator: isolation, characterization, and demonstration of an absolute requirement for the serum protein beta1H for cleavage of C3b and C4b in solution. The Journal of Experimental Medicine 146 (1977) 257-270.

[202] J.D. Greenstein, P.W. Peake, and J.A. Charlesworth, The kinetics and distribution of C9 and SC5b-9 in vivo: effects of complement activation. Clinical & Experimental Immunology 100 (1995) 40-46.

[203] I. Horigome, J. Seino, K. Sudo, Y. Kinoshita, T. Saito, and K. Yoshinaga, Terminal complement complex in plasma from patients with systemic lupus erythematosus and other glomerular diseases. Clin Exp Immunol 70 (1987) 417-24.

[204] G. Nagy, M. Brózik, L. Varga, G. Füst, M. Kirschfink, E. Kiss, and P. Gergely, Usefulness of detection of complement activation products in evaluating SLE activity. Lupus 9 (2000) 19-25.

[205] R.J. Quigg, Complement and autoimmune glomerular diseases. Curr Dir Autoimmun 7 (2004) 165-80.

[206] E. Øvrum, E. Åm Holen, G. Tangen, M. Abdelnoor, M.A.L. Ringdal, R. Øystese, E. Fosse, T.E. Mollnes, and P. Venge, Complete heparin-coated cardiopulmonary bypass and low heparin dose reduce complement and granulocyte activation. European Journal of Cardio-Thoracic Surgery 10 (1996) 54-60.

[207] C. Baufreton, M. Moczar, L. Intrator, P.G. Jansen, H. te Velthuis, P. Le Besnerais, J.P. Farcet, C.R. Wildevuur, and D.Y. Loisance, Inflammatory response to cardiopulmonary bypass using two different types of heparin-coated extracorporeal circuits. Perfusion 13 (1998) 419-427.

[208] T.N. Hoel, V. Videm, T.E. Mollnes, K. Saatvedt, F. Brosstad, A.E. Fiane, E. Fosse, and J.L. Svennevig, Off-pump cardiac surgery abolishes complement activation. Perfusion 22 (2007) 251-256.

[209] T.E. Mollnes, H. Redl, K. Hogasen, A. Bengtsson, P. Garrhd, L. Speilberg, T. Lea, M. Oppermann, O. Gotze, and G. Schlag, Complement activation in septic baboons detected by neoepitope-specific assays for C3b/iC3b/C3c, C5a and the terminal C5b-9 complement complex (TCC). Clinical & Experimental Immunology 91 (1993) 295-300.

[210] T.E. Mollnes, and E. Fosse, The complement system in trauma-related and ischemic tissue damage: a brief review. Shock 2 (1994) 301-10.

[211] H. Schreiber, D. Rittirsch, M. Flierl, U. Brueckner, M. Schneider, M. Weiss, F. Gebhard, M. Huber-Lang, and J.D. Lambris, Complement Activation During Sepsis in Humans

Current Topics in Complement, Springer US, 2006, pp. 217-226.

[212] T.E. Mollnes, T. Lea, S.S. Froland, and M. Harboe, Quantification of the terminal complement complex in human plasma by an enzyme-linked immunosorbent assay based on monoclonal antibodies against a neoantigen of the complex. Scand J Immunol 22 (1985) 197-202.

[213] R. Deppisch, V. Schmitt, J. Bommer, G.M. Hansch, E. Ritz, and E.W. Rauterberg, Fluid phase generation of terminal complement complex as a novel index of bioincompatibility. Kidney Int 37 (1990) 696-706.

[214] M. Harboe, E.B. Thorgersen, and T.E. Mollnes, Advances in assay of complement function and activation. Advanced Drug Delivery Reviews 63 (2011) 976-987.

[215] E.C. Keystone, H.U. Schorlemmer, C. Pope, and A.C. Allison, Zymosan—Induced Arthritis. Arthritis & Rheumatism 20 (1977) 1396-1401.

[216] J. Jang, D. Liang, K. Kido, Y. Sun, D. Clark, and T. Brennan, Increased local concentration of complement C5a contributes to incisional pain in mice. Journal of Neuroinflammation 8 (2011) 80.

[217] J. Blumetti, M. Luu, G. Sarosi, K. Hartless, J. McFarlin, B. Parker, S. Dineen, S. Huerta, M. Asolati, E. Varela, and T. Anthony, Surgical site infections after colorectal surgery: Do risk factors vary depending on the type of infection considered? Surgery 142 (2007) 704-711.

[218] Sepsis II: Advancing biomarker use in sepsis management. in: T.S. Board, (Ed.), 2011.

[219] A.A. Ghaferi, J.D. Birkmeyer, and J.B. Dimick, Variation in Hospital Mortality Associated with Inpatient Surgery. New England Journal of Medicine 361 (2009) 1368-1375.

[220] G.J. Slotman, Prospectively validated predictions of shock and organ failure in individual septic surgical patients: the Systemic Mediator Associated Response Test. Crit Care 4 (2000) 319-26.

[221] M.E. Wilson, N.B. WIlliams, P.J. Baskett, J.A. Bennett, and A.M. Skene, Assessment of fitness for surgical procedures and the variability of anaesthetists' judgments. BMJ 280 (1980) 509-512.

[222] J.F. Nunn, J.S. Milledge, D. Chen, and C. Dore, Respiratory criteria of fitness for surgery and anaesthesia. Anaesthesia 43 (1988) 543-551.

[223] G.P. Copeland, D. Jones, and M. Walters, POSSUM: A scoring system for surgical audit. British Journal of Surgery 78 (1991) 355-360.

[224] R.S. Jawa, S. Anillo, K. Huntoon, H. Baumann, and M. Kulaylat, Analytic Review: Interleukin-6 in Surgery, Trauma, and Critical Care: Part I: Basic Science. Journal of Intensive Care Medicine 26 3-12.

[225] L. Corral, M.L. Carrió, J.L. Ventura, H. Torrado, C. Javierre, D. Rodriguez-Castro, E. Farrero, J. Valero, and D. Ortiz, Is C-Reactive Protein a Biomarker for Immediate Clinical Outcome After Cardiac Surgery? Journal of Cardiothoracic and Vascular Anesthesia 23 (2009) 166-169.

[226] H. Kørner, H. Nielsen, J. Søreide, B. Nedrebø, K. Søreide, and J. Knapp, Diagnostic Accuracy of C-reactive Protein for Intraabdominal Infections After Colorectal Resections. Journal of Gastrointestinal Surgery 13 (2009) 1599-1606.

[227] D.P. Fine, S.R. Marney, D.G. Colley, J.S. Sergent, and R.M. Des Prez, C3 Shunt Activation in Human Serum Chelated with EGTA. The Journal of Immunology 109 (1972) 807-809.

[228] M. Kirschfink, and T.E. Mollnes, Modern Complement Analysis. Clinical and Diagnostic Laboratory Immunology 10 (2003) 982-989.

[229] P.A. Clavien, J. Barkun, M.L. de Oliveira, J.N. Vauthey, D. Dindo, R.D. Schulick, E. de Santibanes, J. Pekolj, K. Slankamenac, C. Bassi, R. Graf, R. Vonlanthen, R. Padbury, J.L. Cameron, and M. Makuuchi, The Clavien-Dindo classification of surgical complications: five-year experience. Ann Surg 250 (2009) 187-96.

[230] L. Cagini, R. Capozzi, V. Tassi, C. Savignani, G. Quintaliani, G. Reboldi, and F. Puma, Fluid and electrolyte balance after major thoracic surgery by bioimpedance and endocrine evaluation. European Journal of Cardio-Thoracic Surgery 40 (2011) 71-76.

[231] P. Meyer, P. Pernet, G. Hejblum, J.L. Baudel, E. Maury, G. Offenstadt, and B. Guidet, Haemodilution induced by hydroxyethyl starches 130/0.4 is similar in septic and non-septic patients. Acta Anaesthesiologica Scandinavica 52 (2008) 229-235.

[232] C.A. Alper, A.M. Johnson, A.G. Birtch, and F.D. Moore, Human C'3: Evidence for the Liver as the Primary Site of Synthesis. Science 163 (1969) 286-288.

[233] B.J. Cox, and D.M. Robins, Tissue-specific variation in C4 and Slp gene regulation. Nucleic Acids Research 16 (1988) 6857-6870.

[234] R.J. Baigrie, P.M. Lamont, D. Kwiatkowski, M.J. Dallman, and P.J. Morris, Systemic cytokine response after major surgery. British Journal of Surgery 79 (1992) 757-760.

[235] D.C. Wirtz, K.D. Heller, O. Miltner, K.W. Zilkens, and J.M. Wolff, Interleukin-6: a potential inflammatory marker after total joint replacement. International Orthopaedics 24 (2000) 194-196.

[236] H. Segal, S. Sheikh, P. Kallis, S. Cottam, C. Beard, D. Potter, E. Townsend, B.P. Bidstrup, M. Yacoub, and B.J. Hunt, Complement activation during major surgery: The effect of extracorporeal circuits and high-dose aprotinin. Journal of Cardiothoracic and Vascular Anesthesia 12 (1998) 542-547.

[237] P.V. Giannoudis, M.R. Smith, R.T. Evans, M.C. Bellamy, and P.J. Guillou, Serum CRP and IL-6 levels after trauma: Not predictive of septic complications in 31 patients. Acta Orthopaedica 69 (1998) 184-188.

[238] L. Simon, F. Gauvin, D.K. Amre, P. Saint-Louis, and J. Lacroix, Serum Procalcitonin and C-Reactive Protein Levels as Markers of Bacterial Infection: A Systematic Review and Meta-analysis. Clinical Infectious Diseases 39 (2004) 206-217.

[239] Z. Derzsy, Z. Prohászka, J. Rigó Jr, G. Füst, and A. Molvarec, Activation of the complement system in normal pregnancy and preeclampsia. Molecular Immunology 47 (2010) 1500-1506.

[240] J.G. Younger, D.O. Bracho, H.M. Chung-Esaki, M. Lee, G.K. Rana, A. Sen, and A.E. Jones, Complement Activation in Emergency Department Patients With Severe Sepsis. Academic Emergency Medicine 17 (2010) 353-359.

[241] H.P.N. Scholl, P.C. Issa, M. Walier, S. Janzer, B. Pollok-Kopp, F. Börncke, L.G. Fritsche, N.V. Chong, R. Fimmers, T. Wienker, F.G. Holz, B.H.F. Weber, and M. Oppermann, Systemic Complement Activation in Age-Related Macular Degeneration. PLoS ONE 3 (2008) e2593.

[242] R.-F. Guo, and P.A. Ward, Role of C5a in Inflammatory Responses. Annual Review of Immunology 23 (2005) 821-852.

[243] C. Alberti, C. Brun-Buisson, S. Chevret, M. Antonelli, S.V. Goodman, C. Martin, R. Moreno, A.R. Ochagavia, M. Palazzo, K. Werdan, and J.R. Le Gall, Systemic Inflammatory Response and Progression to Severe Sepsis in Critically Ill Infected Patients. American Journal of Respiratory and Critical Care Medicine 171 (2005) 461-468.

[244] T. Calandra, and J. Cohen, The International Sepsis Forum Consensus Conference on Definitions of Infection in the Intensive Care Unit. Critical Care Medicine 33 (2005) 1538-1548.

[245] P. Povoa, C-reactive protein: a valuable marker of sepsis. Intensive Care Med 28 (2002) 235-43.

[246] C.P. Subbe, M. Kruger, P. Rutherford, and L. Gemmel, Validation of a modified Early Warning Score in medical admissions. QJM 94 (2001) 521-526.

[247] C. Stenhouse, S. Coates, M. Tivey, P. Allsop, and T. Parker, Prospective evaluation of a modified Early Warning Score to aid earlier detection of patients developing critical illness on a general surgical ward. British Journal of Anaesthesia 84 (2000) 663.

[248] J. Gardner-Thorpe, N. Love, J. Wrightson, S. Walsh, and N. Keeling, The value of Modified Early Warning Score (MEWS) in surgical in-patients: a prospective observational study. Annals of the Royal College of Surgeons of England 88 (2006) 571-5.

[249] R.C. Bone, Toward an epidemiology and natural history of sirs (systemic inflammatory response syndrome). JAMA: The Journal of the American Medical Association 268 (1992) 3452-3455.

[250] J. Szebeni, C.R. Alving, and F.M. Muggia, Complement Activation by Cremophor EL as a Possible Contributor to Hypersensitivity to Paclitaxel: an In Vitro Study. Journal of the National Cancer Institute 90 (1998) 300-306.

[251] J.D. Greenstein, P.W. Peake, and J.A. Charlesworth, The kinetics and distribution of C9 and SC5b-9 in vivo: effects of complement activation. Clin Exp Immunol 100 (1995) 40-6.

[252] M. Pekna, L. Hagman, E. Haldén, U.R. Nilsson, B. Nilsson, and S. Thelin, Complement activation during cardiopulmonary bypass: Effects of immobilized heparin. The Annals of Thoracic Surgery 58 (1994) 421-424.

[253] O. Moen, K. Høgåsen, E. Fosse, E. Dregelid, V. Brockmeier, P. Venge, M. Harboe, and T.E. Mollnes, Attenuation of Changes in Leukocyte Surface Markers and Complement Activation With Heparin-Coated Cardiopulmonary Bypass. The Annals of Thoracic Surgery 63 (1997) 105-111.

[254] V. Videm, T.E. Mollnes, K.r. Bergh, E. Fosse, B. Mohr, T.-A. Hagve, A.O. Aasen, and J.L. Svennevig, Heparin-coated cardiopulmonary bypass equipment. II. Mechanisms for reduced complement activation in vivo. The Journal of Thoracic and Cardiovascular Surgery 117 (1999) 803-809.

[255] H.D. Pettigrew, S.S. Teuber, and M.E. Gershwin, Clinical Significance of Complement Deficiencies. Annals of the New York Academy of Sciences 1173 (2009) 108-123.

[256] M. Botto, M. Kirschfink, P. Macor, M.C. Pickering, R. Würzner, and F. Tedesco, Complement in human diseases: Lessons from complement deficiencies. Molecular Immunology 46 (2009) 2774-2783.

[257] U. Hildebrandt, K. Kessler, T. Plusczyk, G. Pistorius, B. Vollmar, and M.D. Menger, Comparison of surgical stress between laparoscopic and open colonic resections. Surgical Endoscopy 17 (2003) 242-246.

[258] H. Miyake, G. Kawabata, A. Gotoh, M. Fujisawa, H. Okada, S. Arakawa, S. Kamidono, and I. Hara, Comparison of surgical stress between laparoscopy and open surgery in the field of urology by measurement of humoral mediators. International Journal of Urology 9 (2002) 329-333.

[259] A.J. Karayiannakis, G.G. Makri, A. Mantzioka, D. Karousos, and G. Karatzas, Systemic stress response after laparoscopic or open cholecystectomy: A randomized trial. British Journal of Surgery 84 (1997) 467-471.

[260] G. Poste, Bring on the biomarkers. Nature 469 (2011) 156-157.